



Faculty of Resource Science and Technology

**DISTRIBUTION OF GEOCHEMICAL BLOMARKERS IN
THE CORE SEDIMENTS OF SANTUBONG AND
SARAWAK RIVERS**

Bebe Norlita binti Mohamed

**Master of Science
2009**

Pusat Khidmat Maklumat Akademik
UNIVERSITI MALAYSIA SARAWAK

**DISTRIBUTION OF GEOCHEMICAL BIOMARKERS IN THE CORE
SEDIMENTS OF SANTUBONG AND SARAWAK RIVERS OF KUCHING,
SARAWAK**

P.KHIDMAT MAKLUMAT AKADEMIK

UNIMAS



1000246081

Bebe Norlita Bt. Mohamed

A thesis submitted in fulfillment of the requirement for
the degree of Master of Science
in Environmental Chemistry

Department of Chemistry
Faculty of Resource Science and Technology
UNIVERSITI MALAYSIA SARAWAK
2009

DECLARATION

I hereby declare that no portion of the work referred to in this thesis has been submitted in support of an application for another degree or qualification to this or any other university or institution of higher learning.



Bebe Norlita Binti Mohamed
05021185
May 2009

ACKNOWLEDGEMENTS

Firstly, I would like to express my greatest gratitude to Allah S.W.T. for giving me the opportunity to complete my study. Sincere thanks to my supervisor, Assoc. Prof Dr. Zaini B. Assim and Assoc. Prof Dr. Fasihuddin B. Ahmad for their guidance and encouragement throughout my research. I would like to gratefully acknowledge the Ministry of Science, Technology and Innovation (MOSTI), Malaysia for providing me with financial support in the form of postgraduate fellowship award. My appreciation to other lecturers and laboratory staffs especially Mr. Rajuna Tahir, Mr. Send Takuk, Mr. Jahina Bidi and Madam Dayang Fatimawati for their assistance and support in the field works and laboratory experiments. Also thanks to my colleagues, Rabuyah, Mohd. Razif, Norhasnan, Evayantie, Aisyaidil, Nuraqilah, Nurasyikin and Siti Muhainie for the experience shared throughout the duration of this study. Finally, my special appreciation to my beloved parents, siblings and family for their love, support, encouragement and understanding throughout the completion of my study.

ABSTRACT

The extent of pollution at Santubong and Sarawak Rivers was determined by analyzing the geochemical biomarkers in the core sediments. The distribution of aliphatic hydrocarbons and polycyclic aromatic hydrocarbons (PAHs) in the core sediments was determined qualitatively and quantitatively while the distribution of sterols, fatty acid methyl esters (FAMEs) and phthalates was determined qualitatively. The core sediments were Soxhlet extracted for 12 hours using dichloromethane to obtain the geolipids. Subsequently, the geolipids were fractionated into 5 fractions using activated silica gel column chromatography. The aliphatic and aromatic hydrocarbon fractions were analyzed on capillary gas chromatography/flame ionization detector (GC/FID) while polar fractions, FAMEs, phthalate esters and alcohols, were analyzed on gas chromatography/mass spectrometry (GC/MS). Total organic matter in the core sediments from Santubong and Sarawak rivers varied from 3.44 - 7.07 % and 2.03 - 6.55 %, respectively. Core sediments from both rivers showed the presence of unresolved complex mixture eluting between C₁₆ to C₃₄. The total n-alkanes in core sediments from Santubong and Sarawak rivers ranged from 10.8 - 101.1 µg/g dw and 7.3 - 61.7 µg/g dw, respectively. Pristane/C₁₇ and phytane/C₁₈ suggest low degradation of aliphatic hydrocarbons. Biomarker indices of total n-alkanes indicated a mixture of inputs from both biogenic and petrogenic sources. Total PAHs in core sediments from Santubong and Sarawak rivers ranged from 0.8 - 2.5 µg/g dw and 0.7 - 6.7 µg/g dw, respectively. The PAHs ratios including fluoranthene/pyrene and benzo[a]anthracene/chrysene showed the PAHs originated from pyrolytic inputs. Both Santubong and Sarawak Rivers are considered moderately polluted with n-alkanes and PAHs of anthropogenic natures. Domination of short chain FAMEs

($\leq C_{20}$) in core sediments from both rivers indicates planktonic sources of FAMES. Phthalate esters which are widely used as plasticizers were also detected in core sediments from both rivers. The core sediments from both rivers were also dominated by short chain alcohols and sterols ($\leq C_{22}$) that indicates inputs from unspecified marine, terrestrial and bacterial origins.

Keywords: Sediment, n-alkanes, polycyclic aromatic hydrocarbons, gas chromatography/flame ionization detector (GC/FID), gas chromatography/mass spectrometry (GC/MS), biomarker

ABSTRAK

Kadar pencemaran Sg. Santubong dan Sg. Sarawak ditentukan dengan menganalisis penanda biologi geokimia dalam enapan teras. Taburan hidrokarbon alifatik dan hidrokarbon aromatik polisiklik (PAHs) dalam enapan teras ditentukan secara kualitatif dan kuantitatif manakala taburan sterol, asid lemak metil ester (FAMES) dan ftalat dianalisis secara kualitatif. Enapan teras telah diekstrak menggunakan diklorometana dalam pengekstrak Soxhlet selama 12 jam untuk memperolehi geolipid. Geolipid seterusnya telah difraksikan pada kromatografi turus menggunakan gel silika teraktif dan menghasilkan 5 fraksi. Fraksi hidrokarbon alifatik dan aromatik telah dianalisis secara kromatografi gas/pengesan pengionan nyalaan, manakala fraksi polar iaitu FAMES, ester ftalat dan alkohol telah dianalisis secara kromatografi gas/spektrometri jisim. Kandungan bahan organik dalam enapan teras dari Sg. Santubong dan Sg. Sarawak adalah dalam julat 3.44 - 7.07% dan 2.03 - 6.55%, masing-masingnya. Enapan teras dari kedua-dua sungai juga menunjukkan kehadiran bahan kompleks tidak terlerai antara C_{16} hingga C_{34} . Jumlah *n*-alkana dalam enapan teras dari Sg. Santubong dan Sg. Sarawak adalah dalam julat 10.8 - 101.1 $\mu\text{g/g}$ berat kering dan 7.3 - 61.7 $\mu\text{g/g}$ berat kering, masing-masingnya. Nisbah pristana/ C_{17} dan fitana/ C_{18} mencadangkan hidrokarbon alifatik mengalami penguraian yang rendah. Indeks penanda biologi bagi *n*-alkana menunjukkan campuran input daripada sumber biogenik dan petrogenik. Jumlah PAHs dalam enapan teras dari Sg. Santubong dan Sg. Sarawak adalah dalam julat 0.8 - 2.5 $\mu\text{g/g}$ berat kering dan 0.7 - 6.7 $\mu\text{g/g}$ berat kering, masing-masingnya. Nisbah PAHs termasuk fluoranthena/pirena dan benzo[*a*]anthrasena/krisena menunjukkan sumber PAHs adalah daripada input pirolitik. Kedua-dua sungai boleh dianggap sebagai sederhana tercemar dengan *n*-alkana dan PAHs daripada

sumber antropogenik. FAMES rantai pendek ($\leq C_{20}$) yang dominan dalam enapan dari kedua-dua sungai menunjukkan bahawa FAMES adalah berasal dari sumber plankton. Ester ftalat yang digunakan secara meluas sebagai bahan plastik juga dikesan dalam enapan teras dari kedua-dua sungai. Enapan teras dari kedua-dua sungai juga didominasi oleh alkohol dan sterol rantai pendek ($\leq C_{22}$) yang menunjukkan sumber input dari hidupan marin, daratan dan bakteria.

Kata kunci: *Eenapan, n-alkana, hidrokarbon aromatik polisiklik (PAHs), kromatografi gas/pengesan pengionan nyalaan GC/FID), kromatografi gas/spektrometri jisim (GC/MS), penanda biologi*

TABLE OF CONTENTS

	Pages
DECLARATION	i
ACKNOWLEDGEMENTS	ii
ABSTRACT	iii
<i>ABSTRAK</i>	vi
LIST OF FIGURES	xi
LIST OF TABLES	xv
LIST OF ABBREVIATIONS	xviii
CHAPTER ONE	
INTRODUCTION	
1.1 Introduction	1
1.2 Objectives	5
1.3 Scope of the Study	6
CHAPTER TWO	
LITERATURE REVIEW	
2.1 Estuarine Environment	7
2.1.1 River-dominated Estuary	9
2.1.2 Partially-mixed Estuary	9
2.1.3 Vertically Homogenous Estuary	10

2.1.4	Tidal Effects Estuary	10
2.2	Sediments	11
2.3	Hydrocarbons in the Environment	12
2.3.1	Aliphatic Hydrocarbons	12
2.3.2	Hopanes (Terpanes) and Steranes	16
2.3.3	Polycyclic Aromatic Hydrocarbons	18
2.4	Fatty Acids	24
2.5	Phthalate Esters	26
2.6	Sterols	27
2.7	Biomarker Indices for Determination of Organic Matter Sources	30

CHAPTER THREE

MATERIALS AND METHODS

3.1	Core Sediment Samples	32
3.2	Determination of Total Organic Matter	34
3.3	Particle-size Analysis	35
3.4	Samples Extraction and Fractionation	36
3.4.1	Isolation of Geolipids	36
3.4.2	Fractionation of Geolipids	37
3.4.2.1	Removal of Elemental Sulfur	37
3.4.2.2	Sephadex Chromatography	38
3.5	Instrumental Analysis	38
3.5.1	Gas Chromatography/Flame Ionization Detector (GC/FID)	39
3.5.2	Gas Chromatography/Mass Spectrometry (GC/MS)	39
3.6	Gas Chromatographic Data Analysis	40

3.6.1	Concentration of Hydrocarbons in Sediment	40
3.6.2	Carbon Preference Index	42
3.7	Statistical Data Analysis	42
3.7.1	Correlation Coefficient	42
3.7.2	Principal Component Analysis (PCA)	43

CHAPTER FOUR

RESULTS AND DISCUSSION

4.1	Total Organic Matter	44
4.2	Particle Size	50
4.3	Aliphatic Hydrocarbons	53
4.3.1	Aliphatic Hydrocarbons Standard Mixture	53
4.3.2	Aliphatic Hydrocarbons in Sediment Samples	56
4.4	Polycyclic Aromatic Hydrocarbons	73
4.4.1	PAHs Standard Mixture	73
4.4.2	PAHs in Sediment Samples	75
4.5	Comparison of Hydrocarbons Data with Other Places	94
4.6	Fatty Acid Methyl Esters (FAMEs)	96
4.7	Phthalate Esters	102
4.8	Alcohols and Sterols	107
4.9	Relationships Between Organic Matter, Particle Sizes, n-Alkanes and PAHs	112
4.9.1	Correlation Coefficient	112
4.9.2	Principal Component Analysis (PCA)	121
4.10	Sources of Organic Matter in Sediments	124

CHAPTER FIVE

CONCLUSIONS AND RECOMMENDATIONS 131

REFERENCES 134

APPENDICES

- Appendix 1: GC/FID chromatograms of aliphatic fractions of core sediments from Santubong River and Sarawak River
- Appendix 2: Polycyclic aromatic hydrocarbons structures
- Appendix 3: GC/FID chromatograms of PAHs fractions of core sediments from Santubong River and Sarawak River
- Appendix 4: GC/MS chromatograms of FAMES fraction in core sediments from Sarawak River
- Appendix 5: Fatty acid methyl esters structures
- Appendix 6: GC/MS chromatograms of phthalate esters fractions in core sediments from Sarawak River
- Appendix 7: Phthalate esters structures
- Appendix 8: GC/MS chromatograms for alcohols fractions in core sediments from Sarawak River
- Appendix 9: Alcohols and sterols structures

LIST OF FIGURES

Figures	Titles	Pages
Figure 2.1	Schematic diagrams of four types of estuaries (Leeder, 1982).	8
Figure 3.1	Sampling area for sediment samples collection from Santubong River and Sarawak River.	33
Figure 4.1	The spatial distribution of TOM in the surface sediments from Santubong River	46
Figure 4.2	The spatial distribution of TOM in the surface sediments from Sarawak River	46
Figure 4.3	The vertical distribution of TOM in the core sediments from Santubong River	48
Figure 4.4	The vertical distribution of TOM in the core sediments from Sarawak River	48
Figure 4.5	Classification of sediment according to USDA soil textural triangle (Starr <i>et al.</i> , 2000)	51
Figure 4.6	Gas chromatogram from GC/FID analysis of n-alkanes in a standard mixture	53
Figure 4.7	GC/FID chromatograms of aliphatic hydrocarbon fractions in core sediments for SSTB01 at three different layers	58
Figure 4.8	GC/FID chromatograms of aliphatic hydrocarbon fractions in core sediments for SSWK01 at three different layers	59
Figure 4.9	The spatial distribution of the HMW n-alkanes ($>C_{23}$) in the surficial sediments from Santubong River	63
Figure 4.10	The spatial distribution of the HMW n-alkanes ($>C_{23}$) in the surficial sediments from Sarawak River	63
Figure 4.11	The vertical distribution of HMW n-alkanes ($>C_{23}$) in the core sediments from Santubong River	65
Figure 4.12	The vertical distribution of HMW n-alkanes ($>C_{23}$) in the core sediments from Sarawak River	65
Figure 4.13	The spatial distribution of the LMW n-alkanes ($\leq C_{23}$) in the surficial sediments from Santubong River	66

Figure 4.14	The spatial distribution of the LMW n-alkanes ($\leq C_{23}$) in the surficial sediments from Sarawak River	66
Figure 4.15	The vertical distribution of the LMW n-alkanes ($\leq C_{23}$) in the core sediments from Santubong River	68
Figure 4.16	The vertical distribution of the LMW n-alkanes ($\leq C_{23}$) in the core sediments from Sarawak River	68
Figure 4.17	The spatial distribution of the total n-alkanes in the surficial sediments from Santubong River	69
Figure 4.18	The spatial distribution of the total n-alkanes in the surficial sediments from Sarawak River	69
Figure 4.19	The vertical distribution of n-alkanes in the core sediments from Santubong River	71
Figure 4.20	The vertical distribution of n-alkanes in the core sediments from Sarawak River	71
Figure 4.21	Gas chromatogram from GC/FID analysis of PAHs in a standard mixture	73
Figure 4.22	GC/FID chromatograms for PAHs fractions in core sediments for SSTB01 at three different layers	76
Figure 4.23	GC/FID chromatograms for PAHs fractions in core sediments for SSWK01 at three different layers	77
Figure 4.24	The spatial distribution of the HPAHs in the surface sediments from Santubong River	82
Figure 4.25	The spatial distribution of the HPAHs in the surface sediments from Sarawak River	82
Figure 4.26	The vertical distribution of the HPAHs in core sediments from Santubong River	84
Figure 4.27	The vertical distribution of the HPAHs in core sediments from Sarawak River	84
Figure 4.28	The spatial distribution of the LPAHs in the surface sediments from Santubong River	85
Figure 4.29	The spatial distribution of the LPAHs in the surface sediments from Sarawak River	85
Figure 4.30	The vertical distribution of the LPAHs in core sediments from Santubong River	87

Figure 4.31	The vertical distribution of the LPAHs in core sediments from Sarawak River	87
Figure 4.32	The spatial distribution of the total PAHs in the surface sediments from Santubong River	89
Figure 4.33	The spatial distribution of the total PAHs in the surface sediments from Sarawak River	89
Figure 4.34	The vertical distribution of the total PAHs in core sediments from Santubong River	91
Figure 4.35	The vertical distribution of the total PAHs in core sediments from Sarawak River	91
Figure 4.36	GC/MS chromatograms for FAMEs fractions in core sediments of SSTB05 at three different layers (A, B and C)	97
Figure 4.37	GC/MS chromatograms for FAMEs fractions in core sediments of SSWK03 at three different layers (A, B and C)	98
Figure 4.38	GC/MS chromatograms for phthalate esters fractions in core sediments of SSTB05 at three different layers (A, B and C)	103
Figure 4.39	GC/MS chromatograms for phthalate esters fractions in core sediments of SSWK03 at three different layers (A, B and C)	104
Figure 4.40	GC/MS chromatograms for alcohols and sterols fractions in core sediments of SSTB05 at three different layers (A, B and C)	108
Figure 4.41	GC/MS chromatograms for alcohols and sterols fractions in core sediments of SSWK03 at three different layers (A, B and C)	109
Figure 4.42	The correlation between the percentages of TOM (%) and sand (%)	112
Figure 4.43	The correlation between the percentages of TOM (%) and clay (%)	113
Figure 4.44	The correlation between the percentages of TOM (%) and silt (%)	113
Figure 4.45	The correlation between the concentrations of total n-alkanes ($\mu\text{g/g dw}$) with percentages of TOM (%)	117

Figure 4.46	The correlation between the concentrations of total n-alkanes ($\mu\text{g/g dw}$) with percentages of sand (%)	115
Figure 4.47	The correlation between the concentrations of total n-alkanes ($\mu\text{g/g dw}$) with percentages of clay (%)	116
Figure 4.48	The correlation between the concentrations of total n-alkanes ($\mu\text{g/g dw}$) with percentages of silt (%)	116
Figure 4.49	The correlation between the concentrations of total PAHs ($\mu\text{g/g dw}$) with percentages of TOM (%)	117
Figure 4.50	The correlation between the concentrations of total PAHs ($\mu\text{g/g dw}$) with percentages of sand (%)	118
Figure 4.51	The correlation between the concentrations of total PAHs ($\mu\text{g/g dw}$) with percentages of clay (%)	119
Figure 4.52	The correlation between the concentrations of total PAHs ($\mu\text{g/g dw}$) with percentages of silt (%)	119
Figure 4.53	The correlation between the concentrations of total n-alkanes ($\mu\text{g/g dw}$) with concentrations of total PAHs ($\mu\text{g/g dw}$)	120
Figure 4.54	PCA score plot of first, second, third and fourth factors accounting for 89.267% of variance for core sediments from Santubong River and Sarawak River	123

LIST OF TABLES

Tables	Titles	Pages
Table 2.1	Hydrocarbon indices and the indicated sources of organic matter (Commendatore and Esteves, 2004; Gao <i>et al.</i> , 2007; Medeiros and Bicego, 2004; Wang <i>et al.</i> , 2006; Zhou and Maskaoui, 2007	31
Table 3.1	Location of five sampling stations in Santubong River and Sarawak River and its tributary (Kuap River)	34
Table 4.1	Total organic matter in core sediments from Santubong River (SSTB) and Sarawak River (SSWK)	45
Table 4.2	The percentages of TOM in sediments from marine environment in other countries and this study	49
Table 4.3	Particle size of core sediments from Santubong River and Sarawak River	50
Table 4.4	Retention times for n-alkanes (C ₁₂ -C ₃₂) and isoprenoid hydrocarbons (pristane and phytane)	54
Table 4.5	RF values for n-alkanes (C ₁₂ -C ₃₂) and isoprenoids hydrocarbons (pristane and phytane) using n-eicosene as internal standard	55
Table 4.6	Concentrations of n-alkanes in core sediments from Santubong River	60
Table 4.7	Concentrations of n-alkanes in core sediments from Sarawak River	61
Table 4.8	Retention times for 16 individual PAHs	74
Table 4.9	RF values for 16 individual PAHs using o-terphenyl as internal standard	74
Table 4.10	ERL and ERM guideline values for PAHs (ng/g dw) (Long and Morgan, 1990)	75
Table 4.11	Concentrations of PAHs in core sediments from Santubong River	78
Table 4.12	Concentrations of PAHs in core sediments from Sarawak River	79

Table 4.13	The concentrations of PAHs in core sediments from Santubong River and Sarawak River according to the number of rings	93
Table 4.14	The concentrations of total n-alkanes and PAHs in sediments from marine environment in other countries and this study	95
Table 4.15	Fatty acid methyl esters identified in Santubong River	99
Table 4.16	Fatty acid methyl esters identified in Sarawak River	100
Table 4.17	Phthalate esters identified in Santubong River	105
Table 4.18	Phthalate esters identified in Sarawak River	105
Table 4.19	Alcohols and sterols identified in Santubong River	110
Table 4.20	Alcohols and sterols identified in Sarawak River	110
Table 4.21	Pearson correlation matrices for type of sediments and TOM	114
Table 4.22	Pearson correlation matrices for TOM and total n-alkanes	115
Table 4.23	Pearson correlation matrices for type of sediments and total n-alkanes	117
Table 4.24	Pearson correlation matrices for TOM and PAHs	118
Table 4.25	Pearson correlation matrices for type of sediments and total PAHs	120
Table 4.26	Pearson correlation matrices for total n-alkanes and total PAHs	121
Table 4.27	Eigenvalues, percentage of variance and cumulative of variance in the factor analysis for core sediments from Santubong River and Sarawak River	122
Table 4.28	PCA loading of TOM, particle sizes, total n-alkanes, total PAHs and concentrations of LMW n-alkanes, HMW n-alkanes, LPAHs, HPAHs, pristane and phytane using varimax rotation.	123
Table 4.29	Hydrocarbon indices of core sediments from Santubong River	125
Table 4.30	Hydrocarbon indices of core sediments from Sarawak River	126

Table 4.31	PAHs ratios and total PAHs in the core sediments from Santubong River and Sarawak River	127
Table 4.32	Sources of organic matter as indicated by the bioindicators	130

LIST OF ABBREVIATIONS

AcP	Acenaphthene
AcPy	Acenaphthylene
An	Anthracene
BaA	Benzo[a]anthracene
BaP	Benzo[a]pyrene
BbF	Benzo[b]fluoranthene
BBP	Butylbenzyl phthalate
BghiP	Benzo[ghi]perylene
BkF	Benzo[k]fluoranthene
BOP	1,2-benzenedicarboxylic acid, butyl octyl ester
Chr	Chrysene
CPI	Carbon preference index
DBA	Dibenzo[a,h]anthracene
DBP	<i>n</i> -dibutylphthalate
DEHP	1,2-benzenedicarboxylic acid, bis (2-ethylhexyl) ester
DIBP	1,2-benzenedicarboxylic acid, bis (2-methylpropyl) ester
DIDP	1,2-benzenedicarboxylic acid, diisodecyl ester
dw	Dry weight
ERL	Effects-range low
ERM	Effects-range median
FAMEs	Fatty acid methyl esthers
Fl	Fluoranthene
Flu	Fluorene
GC	Gas chromatography
GC/FID	Gas chromatographic/flame ionization detector
GC/MS	Gas chromatographic/mass spectrometry
HMW	High molecular weight
HPAHs	High molecular weight PAHs
InD	Indeno[1,2,3-c,d]pyrene
ISTD	Internal standard
LMW	Low molecular weight
LPAHs	Low molecular weight PAHs
NaP	Naphthalene
PAHs	Polycyclic aromatic hydrocarbons
PCA	Principle component analysis
Ph	Phenanthrene
Phy	Phytane
Pri	Pristane
Py	Pyrene
R _f	Response factor
S ₈	Elemental Sulfur
TEL	Total extractable lipids
UCM	Unresolved complex mixture

CHAPTER ONE

INTRODUCTION

1.1 Introduction

Sarawak River was previously confluenced with Santubong River. However, after the construction of Bako Causeway, the flow of Sarawak River into Santubong River has been blocked. Santubong River runs through several villages including Santubong, Mangkisan and Rampangi villages. Santubong is a Malay fishing village, where most of those who live near the river still discharge their domestic wastes directly to Santubong River. Along Santubong River, land clearing can be observed at certain areas either for construction of new factories or other land development projects.

Sarawak River also confluent with Kuap River at downstream of Pending until further downstream at Muara Tebas, where it discharges to the South China Sea. Pending is an industrial area where several factories are situated including concrete, timber, furniture and ceramic factories. Several villages are situated near the Muara Tebas namely Muara Tebas, Goebilt, Senari and Sejingkat villages. There are shipping activities at the Senari Port which is not far from the estuary. In 1997, the first-ever barrage and ship lock in South East Asia was constructed through the Sejingkat Isthmus on the Sarawak River. This barrage helps to maintain a quite constant water level of the river and also preventing the intrusion of saltwater.

In recent years, the awareness towards contamination of coastal and marine environment caused by human activities has been increasing. In the aquatic

environment such as major rivers and estuaries, hydrocarbons including aliphatic and polycyclic aromatic hydrocarbons (PAHs) that are the ubiquitous organic contaminants have received much attention (Colombo *et al.*, 2005; Hostettler *et al.*, 1999; Wang *et al.*, 2006). The sources and levels of contaminants in the environmental compartments can be predicted using geochemical biomarkers (Colombo *et al.*, 2005). Biomarkers including aliphatic and polycyclic aromatic hydrocarbons, fatty acid methyl esters, phthalates and sterols were used in this study to identify the sources of organic matter and determine the extent of pollution at Santubong and Sarawak Rivers.

Complex organic compounds, which composed of carbon, hydrogen and other elements, found in geological deposits (including sediments, coals, crude oils and shale) are called biomarkers or geolipids. A geochemical molecule is considered to be a biomarker if its structure resembles the structural subunits of biological precursors, e.g. lipids, steroids or porphyrins, which occur commonly in possible source materials (Berthod *et al.*, 1998). As in living organisms, biomarkers show little or no change in structure from their parent organic molecules (Peng *et al.*, 2005; Peters and Moldowan, 1993). According to Peters and Moldowan (1993), there are three distinguishing characteristics of a biomarker: (a) it is a component in living organisms as indicated by its structure, (b) it is widely distributed as indicated by high concentration of the parent compound in the organisms and (c) it is highly stable chemically during sedimentation and early burial.

Since estuarine sediments serve as sinks of aliphatic hydrocarbons and PAHs, the geochemical history of estuarine or deltaic environments have been reconstructed in several studies using core sediments (Hostettler *et al.*, 1999).

Activities involving oil operation, petroleum transport and harbor activities are among the main contributors of anthropogenic hydrocarbons (i.e. petroleum and derived products) to the aquatic environment (Commendatore and Esteves, 2004). Petrogenic hydrocarbons pollution in the environment have been traced using chemical fingerprinting of terpanes, steranes, PAHs, isoprenoid hydrocarbons and evaluation of diagnostic ratios (Peng *et al.*, 2005).

Another major source of pollutants is sewage discharged into surface waters (Mudge and Duce, 2005). The widespread of waterborne diseases especially in Asia regions has also been related to sewage contamination (Peng *et al.*, 2002). In various environment compartments including sediments and water, sterols have been used as molecular tracers to indicate the sources of pollution (Peng *et al.*, 2002). One of the major fecal steroids is coprostanol which formed from cholesterol by bacteria hydrogenation in the small intestine. Coprostanol has been used to reconstruct the pollution history in sedimentary cores due to its stability especially once deposited in anoxic sediment.

Fatty acid biomarkers have been used to indicate the sources of organic matter and the transformation processes that affect organic matter in the marine environment (Gogou and Stephanou, 2004; Tolosa *et al.*, 2004a). The respective importance of inputs from bacteria, microalgae, marine fauna and continental higher plants can be evaluated using the relative abundances of individual fatty acids. Terrestrial higher plant organic matters are characterized by normal fatty acids with more than 22 carbon atoms, while organic matters of bacterial origins are indicated by branched fatty acid (C₁₅-C₁₉) meanwhile freshly biosynthesized autochthonous

material is indicated by monounsaturated fatty acids (MUFA) and polyunsaturated fatty acids (PUFA) (Tolosa *et al.*, 2004a).

Phthalates are industrial chemicals used in the manufacture of polyvinyl chloride (PVC), plasticizers for building materials and home furnishing, in food packaging and insect repellents. Losses during manufacturing processes, leaching from final products and volatilization from plastic products during their usage and disposal are among the pathways of phthalates inputs into the aquatic environment (Turner and Rawling, 2000; Fromme *et al.*, 2002). The levels of phthalates in the various environmental compartments are measurable and expected to reflect a constant and diffuse release into the environment due to their properties, high production volumes and widespread use (Peijnenburg and Struijs, 2006).

1.2 Objectives

The objectives of this project were:

- a. to isolate the geolipids from the core sediments of Santubong and Sarawak rivers of Kuching, Sarawak,
- b. to determine qualitatively and quantitatively the distribution of aliphatic hydrocarbons and polycyclic aromatic hydrocarbons in the core sediments of Santubong and Sarawak rivers,
- c. to determine qualitatively the distribution of sterols, fatty acids and phthalates in the core sediments of Santubong and Sarawak rivers,
- d. to evaluate the sources of organic matter in the sediments of Santubong and Sarawak rivers by carrying out statistical analysis using principal component analysis and Pearson correlation coefficient.

1.3 Scope of the Study

The scope of this study was to determine the extent of pollution at Santubong and Sarawak Rivers by analyzing the geochemical biomarkers in the core sediments. Soxhlet extraction, silica gel column chromatography fractionation, gas chromatography/flame ionization detector and gas chromatography/mass spectrometry were used to analyze the core sediments of both rivers for their organic compositions. This study focused on aliphatic and aromatic hydrocarbons of the core sediments, which had been analyzed qualitatively and quantitatively. These informations were used to determine the level of pollution and the sources of the organic matter in the core sediments. The sources of organic matter were also evaluated using n-alkanes indices, ratios of isoprenoid hydrocarbons and distribution of PAHs. Qualitative analysis on fatty acid methyl esters, phthalates and sterols were also performed. The hypothesis of this study is the sediments from Santubong and Sarawak Rivers are not polluted with hydrocarbons of anthropogenic natures.

CHAPTER TWO

LITERATURE REVIEW

2.1 Estuarine Environment

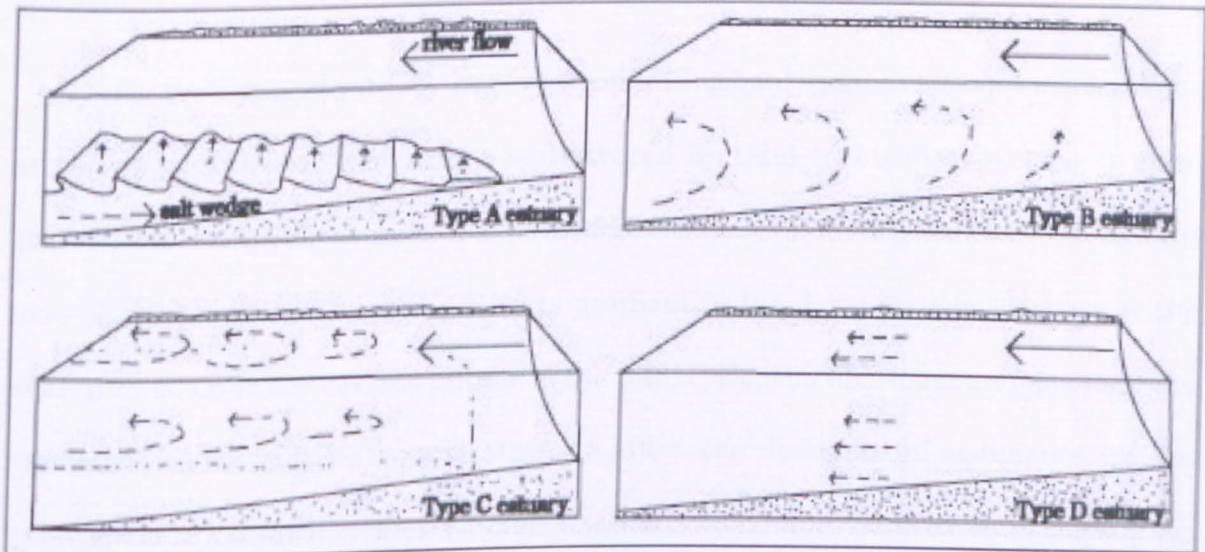
Estuary is defined as a semi-enclosed coastal water body that is connected freely to the open sea and within which fresh water of river origin measurably diluted the sea water (Leeder, 1982; Reineck and Singh, 1980). Due to the exchanges of water, contaminants and sediment between the estuaries and coastal seas, there is a global significance of estuaries to continental shelf and oceanic processes (Dyer, 1994). Continuous deposition, re-erosion and transport processes altered the grain-size distribution of the sediment during transport through the estuaries. Some fractions are transported into the sea, while others are trapped permanently. Fine particles, cohesive and prone to flocculate and organic rich are the characteristics of suspended sediments. Pollutants are transported with the sediment particles, as many of the sediments mobile in estuaries are fine-grained clay minerals, where contaminants absorbed on their surfaces (Dyer, 1994).

The mixing of river and sea water results in estuarine circulation due to density gradients, tidal movements and a highly differentiated development of water stratifications are the characteristics of an estuary (Leeder, 1982; Reineck and Singh, 1980). The relative magnitude of tidal, river and wave processes affect the dynamics of water and sediment in estuaries (Dyer, 1994; Leeder, 1982). The volume of water brought in by a tide, the volume of fresh-water and the form of estuary are the three essential factors that control estuarine circulation (Reineck and Singh, 1980). The salt-balance principle is the most fundamental way of considering the dynamics of

estuaries, whereby diffusion and advection are the two contrasting processes that caused the change of salinity in the estuaries (Leeder, 1982). The flux of salt by turbulent mixing is called diffusion, whilst circulation and internal breaking waves affect the mass flux of both water and salt in advection.

Different types of estuaries have varied patterns of sediment movement (Dyer, 1994). The residual or tidally averaged water flow affects the fine-grained material, which travels in suspension, while the coarser-grained particles, follow the highest velocity water flow, moving along the bed in the direction of the maximum current.

Estuary can be classified into four types, namely river dominated estuaries, partially mixed estuaries, vertically homogenous estuaries and tidal effects estuaries (Dyer, 1994; Leeder, 1982; Reineck and Singh, 1980) as shown in Figure 2.1.



Notes: Type A = River-dominated; Type B = Partially-mixed; Type C = Vertically homogenous and Type D = Tidal effects

Figure 2.1: Schematic diagrams of four types of estuaries (Leeder, 1982).

2.1.1 River-dominated Estuary

River-dominated estuary has minimum tidal and wave mixing processes. The fresh river water flows as a buoyant plume over an upstream tapering salt wedge dominated this system. Upward mixing of salt water with fresh water is limited but not vice versa due to the formation of internal waves at the sharp salt-wedge/river-water interface (advection). When sediment deposited from bedload in river and sea water, a prominent zone of shoaling at the tip of the salt wedge arises. Changes in river discharge and tidal oscillation cause the shifting of the deposition zone upstream and downstream. During high river stage, turbulent shear periodically flushed out fine bedload sediment deposit and flocculated suspended load from the system (Leeder, 1982).

2.1.2 Partially-mixed Estuary

Partially-mixed estuary involved both diffusional and advective mechanisms as the upper salt wedge interface is destroyed by tidal turbulence, forming a more gradual salinity gradient from bed to surface water. The mixing zone moves upward towards higher salinities as the salinity gradient in the down-estuary changes at the mixing zone. Over the various phases of the tidal cycle, the upstream and downstream movement of the salt water will strongly affect the dynamics of sediments. In the lower levels of estuarine water columns, turbidity maximum occurs due to the setting of the river sediment particles into the salt layer and subsequent transport by the net upstream tidal flow that cause the sediment particles to undergo various transport paths, usually of a 'closed loop' kind (Leeder, 1982).

2.1.3 Vertically Homogenous Estuary

Over the entire estuarine cross section, the salt-wedge/fresh-water interface was completely destroyed by strong tidal currents in vertically homogenous estuary. The system is dominated by longitudinal and lateral advection; and lateral diffusion processes. A steady downstream increase in overall salinity exists though there are no vertical salinity gradients. Strong tidal flow, with estuarine circulation gyres produced the lateral salinity gradient mainly affect the dynamics of sediment. In the inner reaches of some tidally-dominated estuaries, extremely high concentrations of suspended sediment may be found close to the bed. However, due to the highly effective tidal mixing process, the sediment traps caused by turbidity maxima and salt wedge effects should not exist (Leeder, 1982).

2.1.4 Tidal Effects Estuary

This system possesses both vertical and lateral salinity homogeneities. The salt lost by advective mixing is replaced through upstream diffusion of salt under equilibrium conditions. Tidal motions with no internal sediment trap entirely dominated the movement of sediment (Leeder, 1982). Depending upon the relative magnitude of river and tidal flow at particular times of the year, mixed river-dominated/partially-mixed or partially-mixed/vertically homogenous characteristics is shown by many estuaries. Most estuaries can be categorized into partially-mixed estuaries and hence possess high efficiency as sediment traps (Leeder, 1982).

2.2 Sediments

Weathering is the breakdown and alteration of rocks at the earth's surface i.e. the chemical decomposition of rocks (reaction between the rocks constituent minerals with water and air) and the non-chemical processes of rock fragmentation (Levin, 1985). Sediments are the altered and decomposed products of weathering, which are usually deposited in layers. After the formation of the weathering products from preexisting rocks, the products are then removed and transported by running water, moving ice and wind.

Solid particles of sediment and invisible dissolved salts can be carried effectively by water streams. The muddy bogs of estuaries and deltas, sandy beaches and silty floodplains may be formed from load of sediment deposited by sediment-laden streams flowing into lakes or the sea. The deposition of solid particles carried by water and wind occurred when there is insufficient energy to carry them further. After the sediment has been deposited, it experienced many changes i.e. compaction that caused distortion of the shapes of particles, removal of mineral grain through dissolution and additions of new mineral matter that caused growth of mineral grain. Some of the changes caused lithification, which is a process of converting sediment into sedimentary rock. Lithification of sediments occurred by three principal means namely cementation, compaction and crystallization.

2.3 Hydrocarbons in the Environment

Hydrocarbons are among the major components of the land-derived organic inputs (Medeiros and Bicego, 2004) and can be environmental polluting agents of risk to the ecosystems (Commendatore and Esteves, 2004). Various studies had been performed to determine the composition, levels, sources and fate of hydrocarbons using geochemical biomarkers including aliphatic hydrocarbons (normal and isoprenoid alkanes), petroleum biomarkers (terpanes and steranes) and polycyclic aromatic hydrocarbons.

2.3.1 Aliphatic Hydrocarbons

Aliphatic hydrocarbons that are widely used as source and maturity indicators of organic matter in geological deposits consist of n-alkanes, branched alkanes, isoprenoids and cyclic compounds. Aliphatic hydrocarbons originated from various sources such as pyrolytic sources (from incomplete combustion of fossil fuels), petrogenic sources (from petroleum and its by-products), diagenetic sources (from the post-depositional transformation of biogenic precursors) and biogenic sources (from terrestrial plant waxes, marine phytoplankton, volcanic eruptions, biomass combustion and natural oil seeps) (Tolosa *et al.*, 2004b; Medeiros and Bicego, 2004).

The spatial distribution and sources of aliphatic hydrocarbons in surface sediments from Coastal Caspian Sea were studied by Tolosa *et al.* (2004b). The aliphatic hydrocarbons investigated include n-alkanes (n-C₁₁ to n-C₃₅) and unresolved complex mixture (UCM) comprises a mixture of alicyclic compounds. The extent of degradation of hydrocarbons was estimated based on the ratio of unresolved to

resolved compounds (UCM/ n-alkanes). The aliphatic hydrocarbons and the biomarkers profiles have indicated that the shallow North Caspian Sea sediments had limited petrogenic contamination with a low total organic carbon (TOC), while the South Caspian Sea sediments (especially in the offshore oil fields) have moderate to high petrogenic contamination.

Wang *et al.* (2006) had studied the sources and distribution of n-alkanes and PAHs in the surface sediments from Jiaozhou Bay, Qingdao of China in order to provide a baseline for assessment of hydrocarbons contamination in those sediments. The sources of organic matter were determined using TOC, total nitrogen (TN), carbon/nitrogen (C/N) mole ratios and $\delta^{13}\text{C}$. The possible sources of n-alkanes were investigated using two hydrocarbon distribution indexes, which are the low molecular weight to high molecular weight ratio (LMW/HMW) and the carbon preference index (CPI). The total alkanes concentrations ranged from 0.5 to 8.2 $\mu\text{g/g}$ dry weight. The main source of n-alkanes was petroleum as indicated by LMW/HMW ratios that were greater than 2 and CPI values that were close to 1. Temporal and localized inputs of contamination sources were indicated to contribute to the great spatial variations of n-alkanes distribution in the sediments.

Marine biota and coastal sediments from four countries surrounding the Arabian Gulf were studied for their aliphatic hydrocarbons composition and spatial distribution by Tolosa *et al.* (2005). Total petroleum hydrocarbon (TPH) content, TOC, total hydrocarbon concentration (the sum of total aliphatic and total aromatic hydrocarbons) and UCM concentrations were determined in the sediments and biota to indicate the sources and level of contamination in the study areas. "Hot spots" (areas with high level of oil pollution) in the four countries were identified based on

the trends in both TPH and aliphatic hydrocarbons. Even though the Gulf region has approximately two-thirds of the world's oil production, only sediments collected near the BAPCO oil refinery in Bahrain can be categorized as chronically contaminated (with concentrations total petroleum hydrocarbon 779 $\mu\text{g/g}$) while other study areas have relatively low level of contamination compared to world-wide locations reported to be chronically contaminated by oil.

The lower course of the Chubut River (Argentina) was studied for their hydrocarbon levels based on the resolved aliphatic, UCM and total aliphatic hydrocarbons (TAH) (Commendatore and Esteves, 2004). Due to the high complexity of natural samples, the sources of anthropogenic or biogenic hydrocarbons were determined by analyzing various biomarker indices in addition to absolute concentration. Anthropogenic inputs of petroleum hydrocarbons to sediments can be indicated based on geochemical relationship, which is evaluated from the ratio of "trace-level" individual compounds or compound classes present at the ng/g (ppb) or $\mu\text{g/g}$ (ppm) level to a bulk parameter present at mg/g . Other biomarker indices include even/odd LMW/HMW, n-alkanes/n- C_{16} , pristane/phytane (pri/phy) ratios and CPI values. The total concentrations ranged from 0.07 to 460 $\mu\text{g/g}$ dry weight for resolved aliphatic hydrocarbons, 0.42 to 284 $\mu\text{g/g}$ dry weight for UCM and 0.55 to 741 $\mu\text{g/g}$ dry weight for aliphatic hydrocarbons. The sources of hydrocarbons in this study were categorized as terrigenous biogenic hydrocarbons (indicated by the presence of HMW odd hydrocarbons such as n- C_{23} , n- C_{25} , n- C_{27} , n- C_{29} and n- C_{31}), riverine biogenic hydrocarbons (indicated by the presence of LMW odd hydrocarbons such as n- C_{15} , n- C_{17} , n- C_{19} and n- C_{21}), mixture of terrigenous and riverine biogenic hydrocarbons (indicated by both LMW and HMW odd hydrocarbons) and also petrogenic

hydrocarbons (indicated by the presence of UCM and the homologous series of n-alkanes).

Nishigima *et al.* (2001) studied the aliphatic in sediments of Santos and Cananeia, Sao Paulo, Brazil to investigate the level of contamination by oil and also the biogenic contributions. The concentrations of total alkanes in sediments of Santos ranged from 1.05 to 4.29 $\mu\text{g/g}$. On the other hand, the concentrations of total alkanes in sediments of Cananeia were ranging from 4.37 to 157.90 $\mu\text{g/g}$. Evaluation on the biomarker indices (homogenous distribution between odd and even carbons) indicated that the hydrocarbons in sediments of Santos were mainly contributed by oil pollution and/or incomplete combustion. There were also high contributions from terrestrial plant in several sediments from mangrove areas but the presence of oil pollution was also observed. Evaluation on biomarker indices in sediments of Cananeia (predominance of the odd n-alkanes) indicated that hydrocarbons were originated from terrestrial plants with no indication of oil pollution and other anthropogenic activities.

Surficial sediments from the coastal environment of Egypt were studied for their lipid geochemistry in order to characterize their contents of biogenic and anthropogenic hydrocarbon inputs of organic matter (Aboul-Kassim and Simoneit, 1996). Sewage/industrial pollution and natural background sources were differentiated based on homologous long chain n-alkanes ($\text{C}_{15}\text{-C}_{38}$), CPI, UCM and biomarkers including pristane, phytane, terpanes and steranes. The hydrocarbon tracers were grouped based on their probable input sources and the sampling stations based on relative importance of each source contribution by means of multivariate statistical analyses including cluster analysis, factor analysis and linear

programming technique. The concentrations of total n-alkanes and UCM in the sediments ranged from 0.4 to 4.1 mg/g OC and 0.2 to 31 mg/g OC, respectively. Results from the statistical analyses (using both extended Q-mode factor analysis and linear programming technique) indicate that petrochemical represented 88.93% of the organic matter sources while 3.96% of the organic matter originated from terrestrial sources.

Coastal sediments of the Black Sea were studied by Readman *et al.* (2002) for their petroleum contamination. The concentrations of total petroleum hydrocarbons ranged from 2 to 300 µg/g dry weight. Contamination by degraded/weathered petroleum was indicated by UCM, which was the major component of the aliphatic hydrocarbons found in sediments of the Black Sea. The concentrations of total n-alkanes, $\Sigma n-C_{14}$ to $n-C_{34}$ (an indicator of "fresh" oil inputs) ranged from 0.1 to 3.4 µg/g dry weight, which was relatively low and comparable to uncontaminated areas on a worldwide basis.

2.3.2 Hopanes (Terpanes) and Steranes

Hopanes and steranes are branched cycloalkanes formed from multiple condensed five- or six-carbon rings and represent biomarkers with highly characteristic distributions of structural and stereochemical isomers in oils and sediments with mature organic matter (Peters and Moldowan, 1993). Hopanes and steranes exist as many stereoisomers with varied configurations of α/β and/or R/S, which have different thermodynamic stability (Gao *et al.*, 2007). Tricyclic terpanes ranging from $C_{19}H_{34}$ to $C_{45}H_{86}$ are important geochemical tracers that can be found in most crude oils. Tetracyclic terpanes are derivatives of the hopanes occur in fossil

fuels while pentacyclic triterpanes originated from petroleum. Steranes and diasteranes that can be found in fossil fuels are also useful geochemical tracers for petroleum contamination in urban coastal areas (Aboul-Kassim and Simoneit, 1996).

Surface sediments from the Galicia continental shelf (North West Spain) were studied by Franco *et al.* (2006) for the spatial distribution and ecotoxicity of petroleum hydrocarbons after the Prestige oil spill. Petrogenic molecular markers such as steranes and triterpanes were used to assess the presence of the Prestige oil in the sediments. The four most important parameters characterized the Prestige oil pollution were tetra and pentacyclic terpane indices (27Ts and 29 $\alpha\beta$) and the C-29 $\alpha\alpha$ S/R and $\beta\beta/\alpha\alpha$ sterane indices. The study on steranes and triterpanes in sediments concluded that a weathered petrogenic chronic pollution occurred in the shelf sediments but not of the Prestige oil.

Medeiros and Bicego (2004) investigated the natural and anthropogenic hydrocarbon inputs in sediments of Sao Sebastiao, Brazil using organic geochemical markers including petroleum biomarkers. The geochemical marker concentrations in the study area were greatly affected by the Petrobras Maritime Terminal (DTCS), Sao Sebastiao Harbor and sewage outfalls along the area. Tricyclic and tetracyclic terpanes, pentacyclic triterpanes or hopanes and steranes were among the petroleum biomarkers investigated. The total concentrations ranged from 51.1 to 422.0 ng/g for petroleum biomarkers. The presence of steranes and terpanes indicated that the sediments were impacted by petroleum or its derivatives.

Biomarker constituents in surface sediments and core sediments of San Francisco Bay were investigated for their spatial and historical input of

contamination (Hostettler *et al.*, 1999). The age of cores was determined using radioisotope profiles of fallout nuclides (^{137}Cs , $^{239,240}\text{Pu}$) and also ^{210}Pb and ^{234}Th . Petroleum biomarkers (hopanes and steranes) were determined to identify the sources of contaminants. It was reported that the surficial sediments of San Francisco Bay have anthropogenic petroliferous contaminant input as indicated by mature hopane and sterane biomarkers. For the core sediments, the lower sections of the cores show the dominance of biogenic input of hydrocarbons while the upper sections of the cores show the dominance of anthropogenic input. This observation corresponds to a transition from the pre-industrial to the industrial era in the San Francisco Bay area.

2.3.3 Polycyclic Aromatic Hydrocarbons

PAHs are organic compounds composed of three or more fused aromatic rings in various structural configurations. PAHs are known for their hazardous effects on human health, as PAHs possess mutagenic, teratogenic and carcinogenic properties (Kanaly and Harayama, 2000; Liu *et al.*, 2000) where two or three ring PAHs are less mutagenic than four to seven ring PAHs (Shi *et al.*, 2005). PAHs comprise of two to six fused aromatic rings are primarily products of incomplete combustion processes. A significant acute toxicity is found in low molecular weight PAHs (LPAHs) with two and three rings, while high molecular weight PAHs (HPAHs) with four, five and six rings are found to be carcinogenic.

The environmental fate of PAHs depends on the number of aromatic rings (the molecular size) and the pattern of ring linkage (Kanaly and Harayama, 2000). The hydrophobicity and electrochemical stability of PAHs that contribute to the

persistence of HMW PAHs in the environment are increased as the size and angularity of PAHs increase.

PAHs that are found in geological deposits including sediments originated from both natural and anthropogenic sources. LPAHs are produced from low temperature thermal alterations of organic matter as in formation of fossil fuels while HPAHs are produced from high temperature combustions (Readman *et al.*, 2002). There are also PAHs inputs from natural sources i.e. synthesis by organisms including bacteria, algae and fungi, but they are relatively low compared to PAHs of anthropogenic origins. Proximity of the contaminated site to the production source, the level of industrial development and the modes of PAH transports are among the factors that affect the concentrations of PAHs in the environment (Kanaly and Harayama, 2000).

Water, sediment and pore water of the Jiulong River Estuary and Western Xiamen Sea, China were investigated for their PAHs contamination by Maskaoui *et al.* (2002). The concentrations of PAHs and ratios of individual PAH concentrations i.e. Ph/An, Fl/Py and benzo[a]pyrene/benzo[ghi]perylene (BaP/BghiP) were used to assess the sources of PAHs in sediments. The relationship between dissolved contaminants and salinity were used to identify factors affecting PAH distribution in water and sediment. The concentrations of TPAHs ranged from 6.96 to 26.9 µg/L in water, 59 to 1177 ng/g dry weight in surficial sediments and 158 to 949 µg/L in pore water. Higher concentrations of dissolved organic carbon or colloids with which the hydrophobic pollutants were strongly associated may contribute to the higher levels of PAHs present in pore water compared to surface water. The PAHs distribution and PAHs ratios indicated that the PAHs were originated from anthropogenic sources

such as urban air deposition, discharges of crude oil and sewage and shipping activities. Distribution of PAHs in sediment and pore water indicated that no correlation was observed between sediment-associated PAHs and PAHs in pore water.

The concentrations, distribution between different phases, transition and sources of PAHs in the water, suspended particles and sediments from the middle and lower reaches of the Yellow River, China were assessed by Li *et al.* (2006). Water samples from all stations had similar relative proportions of PAHs. There was positive correlation between the concentrations of PAHs in suspended particles with the content of TOC, while a correlation between PAHs concentrations with grain size less than 0.01 mm instead of TOC was observed for surface sediments. Due to the low water solubility, more types of PAHs were detected in suspended particles than in water samples, and the proportion of higher molecular weight PAHs were higher in suspended particles than in water phase. As results of accumulation over time in different sections of the main river, levels of PAHs in sediments were not in proportion to those in suspended particles. The origins of PAHs in the Yellow River sediments were either from combustion of coal and wood or combustion of petroleum. It was also indicated that the transfer of PAHs in the water body was influenced by high sediment load as sediments may act as a sink for PAHs.

Shi *et al.* (2005) studied the PAHs contamination in the sediments, water and suspended particulate matter (SPM) of rivers in Tianjin, China. The spatial distribution of PAHs and concentrations of the individual PAHs were determined to track the contaminant source and indicate the fate and transport of PAHs in the environment. Naphthalene was the most dominant component in the sediments and water while in SPM, phenanthrene was the most dominant. Since small-size PAHs

are more labile and are expected to degrade faster than larger ones, the LMW PAHs predomination suggests either a local source of PAHs or a relatively recent introduction of these chemicals. It was also predicted that the main source of PAHs in the sediments, water and suspended particulate matter is from combustion of coals. The chemical profile of sediment PAHs is also very similar to the profile of the sum of dissolved phase and SPM associated phase PAHs, indicating no selective loss of PAHs via sedimentation. Due to the different aqueous transport capability, the chemical profiles of varied media changed during processes of transportation and transformation.

Sediments from several estuaries in China were studied by Yuan *et al.* (2001) for their persistent organic pollutants including PAH, polychlorinated biphenyl (PCB) and dichlorodiphenyltrichlorethan (DDT). The concentrations of total PAH, PCB and DDT were reported in the range of 400 to 1500 ng/g, 2 to 14 ng/g and 6 to 73 ng/g, respectively. The major sources of PAHs varied in the several estuaries, where Jiulongjian and Zhujiang Estuaries were mainly contaminated by PAHs from petroleum related sources (as indicated by high concentrations of alkylated PAHs and LMW PAHs); while pyrogenic PAHs (indicated by low concentrations of alkyl PAHs and high concentrations of HMW PAHs) were the primary contributor to Minjiang Estuary. Potential for biological effects was obtained based on the effects range low (ER-L) and effects range median (ER-M) designated by Long and Morgan (1990), where the ER-L and ER-M values for total PAHs are 4000 and 35000 ppb respectively, for PCBs are 50 and 400 ppb respectively and for total DDT are 3 and 350 ppb respectively.

Liu *et al.* (2000) investigated PAHs in core sediments from the Yangtze Estuary, China to identify their sources and determine their history of contamination. Approximate estimation of core sediment intervals from depth profile sediments were made based on dates calculated from the sediment rate (1.85cm/year) previously calculated by Xu *et al.* (1997) using ^{210}Pb measurements in tidal flat sediments along the Shanghai Coast. It was determined that the core sediments from Yangtze Estuary were dated from 1971 to 1996 (Liu *et al.*, 2000). The total PAHs concentrations in the core sediments were in the range of 0.08 to 11.74 $\mu\text{g/g}$. Specific target compound (including acenaphthene, indicator of a combustion-specific PAH), the ratio of Fl/Py, the fingerprint indices of PAHs (including isomeric compounds or substituted alkylated PAHs) and the ratio of alkylated PAH homologues to parent compounds i.e. alkylated naphthalene homologues to parent naphthalene indicated that the major sources of PAH were petrogenic and incorporation of atmospheric sources by pyrolysis/combustion.

Water and surface sediments from Daya Bay of China was studied for their PAHs distribution by Zhou and Maskoui (2003). Based on ratios of Ph/An, Fl/Py and BaP/BghiP it was indicated that the origins of PAHs in the sediments are of pyrolytic and petrogenic sources. The water samples were dominated by three ring PAHs while four ring PAHs mostly dominated the sediment samples. This may be due to the more dominant and widespread of petrogenic sources than pyrolytic ones, where water column receives direct PAH input from both sources, while sediment had only receives PAH that can survive down-column transport, which are likely to be HMW PAHs (more resistant to degradation processes). Effects range-low (ERL) and effects range-median (ERM) were also compared to the PAH levels in sediments to indicate the toxicity of sediments in Daya Bay. ERL and ERM are guideline values to define

chemical concentration ranges usually associated with adverse biological effects (Long and Morgan, 1990). It is concluded that Daya Bay sedimentary environment would not face immediate biological effects caused by PAHs alone, as only three individual PAHs i.e. acenaphthene, fluorine and chrysene at only one station exceeded their respective ERL values.

Mai *et al.* (2002) investigated the spatial distribution of chlorinated hydrocarbons and PAHs in the riverine sediments (Zhujiang, Shiziyang and Xijiang Rivers) and estuarine sediments (Lingding Bay and Macao Harbor) of Pearl River Delta, China. Possible sources of PAHs were identified based on the relative abundance of alkylated PAHs to parent PAHs and the composition of parent PAH compounds. The highest concentrations of PAHs were detected in the Zhujiang River sediments and Macao Harbor. Anthropogenic sources predominated the organic matter in the sediments as indicated by no correlation between the TOC content of sediments with the organic pollutant concentrations. The chlorinated hydrocarbons and PAHs were also compared to ERL and ERM where it is indicated that there is a potential source of concern for biological impairment in sediments of Pearl River Delta especially in sediments of Zhujiang River and Macao Harbor as most of their chlorinated hydrocarbons and PAH compositions had concentrations greater than ERL or ERM.

2.4 Fatty Acids

Fatty acids are cell membranes, fats and oils consist of esters of long-chain (mainly C₁₄, C₁₆ and C₁₈) carboxylic acids. Fatty acids that are large hydrophobic biomolecule families are usually defined by the physical operation, which are used to isolate them (Solomons and Fryhle, 2004). Most natural fatty acids consist of unbranched chains with even number of carbon atoms as they are synthesized from two carbon units. Unsaturated fatty acids consist of two or three double bonds, where the first double bond commonly occurs between C₉ and C₁₀ while the remaining double bonds usually begin with C₁₂ and C₁₅. Saturated fatty acids consist of single bond carbon chains which tend to be fully extended though they can adopt many conformations (Solomons and Fryhle, 2004).

A study on changes in composition of geochemical biomarkers in interfacial sediments of Laurentian Trough, Canada including fatty acids during early diagenesis had been conducted by Colombo *et al.* (1997). Fatty acids biomarkers provided information on the geographical and temporal trends observed in settling particles of the sediments. The depth distribution of bacterial fatty acids and coprostanol indicated the contrasted conditions of organic matter diagenesis resulting from the different rates of sedimentation, bioturbation and quality of organic matter inputs at each site. The concentrations of total fatty acids ranged from 3.2 to 11 mg/g OC in the interfacial sediments indicating a 46 to 93% loss relative to settling particles.

Tolosa *et al.* (2004a) studied the distribution of pigments and fatty acid biomarkers to determine the source and fate of organic matter in particulate matter from the frontal structure of the Alboran Sea of South West Mediterranean Sea. Four different classes of fatty acids were investigated including linear saturated fatty acids (C₁₄ to C₂₆), branched saturated fatty acids (*iso* and *anteiso* branched compounds for C₁₅-C₁₉), cyclopropane fatty acids (C₁₇) and two isoprenoids (4,8,12-trimethyltridecanoic acid) and 3,7,11,15-tetramethylhexadecanoic (phytanic acid). Sources and isotopic composition of the fatty acids, spatial distribution of phytoplankton and transport and transformation of particulate matter were also studied. Based on fatty acid distribution and compound specific isotope analysis of $\delta^{13}\text{C}$, it was indicated that the fatty acids originated from marine sources. Odd/branched chain fatty acids suggested that bacterial biomass was minimal and mainly associated with the planktonic biomarkers.

Muri *et al.* (2004) studied the distributions of lipid biomarkers in sediments of Lake Planina, a remote mountain lake in North West Slovenia. Concentration of organic carbon, C/N ratio, total lipid concentration and fatty acids (C₁₄-C₃₂) were determined in the surface and core sediments to evaluate the changes in organic matter delivery and preservation processes. Relative contribution of allochthonous vs. autochthonous components was assessed using ratios of longer chain to shorter chain lipids and it was indicated that the sources of organic matter are mainly from terrestrial origin as longer chain lipids predominated the Lake Planina sediments.

2.5 Phthalate Esters

Phthalate esters are esters of 1,2-benzenedicarboxylic acid usually found in the environment almost ubiquitously as it is one of the most commonly used classes of industrial synthetic chemicals. In aquatic systems, phthalate esters are susceptible to sorption onto the sediments or suspended particles due to their hydrophobicity (Preston, 1989). The most common phthalate esters detected in environmental samples are di-(2-ethylhexyl)phthalate (DEHP) and n-dibutylphthalate (DBP).

Peijnenburg and Struijs (2006) have studied the occurrence of phthalate esters in freshwater, marine water, sediment, fish, soil and vegetation and air of Netherlands by determining the levels of DBP and DEHP. The concentrations of DBP and DEHP in marine water and sediment were mostly below the limit of detection while the highest concentrations of DBP and DEHP were found in freshwater. The DBP levels in fish were often below limit of detection. Fugacities calculations based upon physicochemical properties of the phthalates investigated were used to indicate whether there is physical equilibrium with regard to phthalate concentrations detected. In the aquatic environment, sediment seems to be a sink for DEHP, where the rates of supply of DEHP (through sedimentation) and degradation affect DEHP concentrations in sediments.

The behaviour of DEHP in Beaulieu Estuary, Southern England was studied by Turner and Rawling (2000). Intertidal sediments, sea water and Beaulieu river water were analyzed to determine the relative solubility and sorptive behaviour of DEHP. It was concluded that the estuarine distribution of DEHP are unlikely to be affected by solubility effects alone and in salinity conditions, adsorption of DEHP is

more favourable. It was identified that salinity, particle concentration, particulate organic content and biodegradation of DEHP are the factors that control the distribution of DEHP in estuaries. A model to retain DEHP in estuaries was made based on these factors, which can be used as a guide for water quality purposes.

The occurrence of phthalates and bisphenol A and F in the Germany aquatic environment was investigated by Fromme *et al.* (2002). Surface water, sediments, sewage treatment plant effluents and other environmental compartments were analyzed for the level of butylbenzyl phthalate (BBP), DBP and DEHP. It was indicated that in the phthalate concentrations were dominated by DEHP, DBP was found in relatively lower concentrations, while low amounts of BBP were found only in a few samples. The results were also compared with eco-toxicological effect data using predicted no effect concentration (PNEC). 3 % of the samples have DEHP concentrations above the PNEC, while for DBP only one sample has the value exceeding the PNEC.

2.6 Sterols

Alcohols i.e. sterols are organic compounds consist of saturated carbon atom attached with a hydroxyl group (Solomons and Fryhle, 2004). Based on the degree of carbon substitution to which the hydroxyl group is directly attached, alcohols can be categorized into three groups which are primary, secondary and tertiary alcohols. Primary alcohol has only one carbon atom attached to the carbon that bears the hydroxyl group, while secondary and tertiary alcohols have two and three carbon atoms attached to the carbon with the hydroxyl group respectively.

In a study done by Peng *et al.* (2005), the impacts of anthropogenic activities on the Pearl River estuarine and marine environment of South China Sea were assessed by quantitative investigation of 5 β -coprostanol together with eight other sterols and UCMs for surficial sediments and surface waters. Concentrations of 5 β -coprostanol ranged from trace amounts to 53 $\mu\text{g/g}$ OC in surface sediments, 11 to 299 ng/L in waters, while the concentrations of UCM ranged from 215 to 10491 $\mu\text{g/g}$ OC in surface sediments and 2 to 26 $\mu\text{g/L}$ in waters. Based on a combination of coprostanol concentration, diagnostic indices, sterol profiles and UCM, it was indicated that the sources of organic matter were from anthropogenic activities such as sewage discharges, shipping and urban runoff. It was also reported that the submarine outfalls in Hong Kong represent important sources of anthropogenic contamination to the sediments as coprostanol and UCM accumulation are relatively higher in the sites close to the submarine outfalls. Fecal sterol biomarkers also indicated that dispersion of the sewage contamination from the Pearl River estuary to the open South China Sea did not occur.

The source, transport path and sinks of sewage derived organic matter from the Rio Formosa Lagoon, Portugal was studied by Mudge and Duce (2005). In this study, the sewage sources and effected deposition sites were identified using simple ratios between key biomarkers i.e. 5 β -coprostanol, cholesterol and epi-coprostanol, by quantifying sterol and fatty alcohol biomarkers in source materials, suspended sediments and settling matter from the lagoon. The total concentrations of sterols and n-alcohols (C₁₀-C₂₈) in the sinks ranged from 0.11 to 1654 $\mu\text{g/g}$ and 3.1 to 14617 $\mu\text{g/g}$, respectively. Cholesterol was used in the form of ratios with other sterols as its use as an independent biomarker is limited since cholesterol has various potential sources i.e. animals and sewage. Based on the long chain/short chain ratio of the fatty alcohol, the

sources of the sewage was ascribed, as principally, long chain compounds originated from terrestrial organic matter (possibly plant waxes). It was concluded that most samples had organic matter mainly from sewage and little contributions from terrigenous sources.

Distribution of coprostanol was also determined by Jeng *et al.* (1996) in a study of marine sediments from Southwestern Taiwan. The input of coprostanol over the past and the extent of both coprostanol addition and distribution were obtained by analyzing quantitatively the surface sediments and a core sediment of Southwestern Taiwan. The ratio of coprostanol to total sterols (percent coprostanol) was one of the indices used in this study, where the sum of coprostanol and biogenic sterols are defined as total sterols. By expressing coprostanol as percent coprostanol (relating it to total sterols), the grain size effect on coprostanol would be eliminated. It was reported that progressive seaward declines in concentrations were found for the coprostanol and the highest level of coprostanol was found around the river mouth. This may be due to dilution of coprostanol by biogenic sterols and degradation of coprostanol. It was also indicated that over the past 20 years, there was an increased input of coprostanol as a core sediment exhibits relatively higher level of coprostanol in the top 15 cm.

Jaffe *et al.* (2003) have assessed the sources and distribution pathways of contaminants in surface sediments from Montego Bay by analyzing the organic compounds and trace metals of anthropogenic origin. In order to evaluate different pollution sources to the bay, potential contaminants including various trace metals, and coprostanol were analyzed. There was a distribution of particle-associated pollutants along the Montego River plume and these pollutants were also transported

by the prevailing water currents to the south-western sections of the bay. High level of coprostanol indicated high concentrations of raw sewage, while Pb indicated the street runoff and industrial chemicals were indicated by levels of Zn, Pb and Cr.

The distribution of coprostanol in San Pedro Shelf bottom sediments was determined in order to obtain the fate of sewage from the adjacent sewage outfall (Maldonado *et al.*, 2000). Coprostanol was used as a molecular marker because the affinity of coprostanol for organic matter in the sediments to trace domestic inputs close to the source. Based on the ratios of coprostanol to other sterols and high concentration of coprostanol, which was 8.3 µg/g in sediments at the area nearest to the sewage outfall, it was indicated that the source of steroidal sewage markers originated from the wastewater discharge. It was also reported that the concentrations of coprostanol decreased as the distance from the sewage outfall increased for most of the sediments. The accumulation of coprostanol was observed in the bottom sediments due to the efficient trapping system of submarine canyons.

2.7 Biomarker Indices for Determination of Organic Matter Sources

In order to evaluate the sources of organic matter in the sediments of Santubong and Sarawak rivers, various biomarker indices of hydrocarbons had been used as summarized in Table 2.1.

Table 2.1: Hydrocarbon indices and the indicated sources of organic matter (Commendatore and Esteves, 2004; Gao *et al.*, 2007; Medeiros and Bicego, 2004; Wang *et al.*, 2006; Zhou and Maskaoui, 2007)

Type of Hydrocarbons	Hydrocarbons Indices	Values	Indication
Aliphatic Hydrocarbons	Pristane/phytane	Close to 1	Petrogenic sources
		1.4 to 6.7	Biogenic sources
	nC ₂₅ /nC ₁₅	< 0.8	Petrogenic sources
		> 0.8	Biogenic sources
	nC ₃₁ /nC ₁₉	> 0.4	Non-marine sources
		< 0.4	Marine sources
	CPI	Close to 1	Petrogenic sources
		3-6	Biogenic sources
	LMW/HMW	> 1	Petrogenic sources
		< 1	Biogenic sources
Even/odd	No predominance	Petrogenic sources	
	Predominance of odd numbered carbon (8 to 10 times)	Biogenic sources	
Total n-alkanes/nC ₁₆	< 15	Petrogenic sources	
	> 50	Biogenic sources	
Pristane/C ₁₇ and Phytane/C ₁₈	≤ 1	Low degradation of aliphatic hydrocarbons	
	> 1	High degradation of aliphatic hydrocarbons	
PAHs	Fluoranthene/pyrene	> 1	Pyrolytic sources
		< 1	Petrogenic sources
	Benzo[a]anthracene/chrysene	> 0.4	Pyrolytic sources
		≤ 0.4	Petrogenic sources
	ΣLPAHs/ΣHPAHs	< 1	Pyrolytic sources
> 1		Petrogenic sources	

As for more polar compounds, the presence of short chain FAMES ($\leq C_{20}$) indicates planktonic origins while terrestrial source is indicated by long chain FAMES ($> C_{20}$) (Colombo *et al.*, 1997). The presence of phthalate esters namely DIBP, DEHP and DIDP indicates organic matter of industrial origins. Short chain alcohols and sterols (≤ 22) indicate inputs from marine and bacterial origins while long chain alcohols and sterols (> 22) indicate terrestrial source (Mudge and Duce, 2005).

CHAPTER THREE

MATERIALS AND METHODS

3.1 Core Sediment Samples

The core sediment samples were collected from various locations along Santubong River, Sarawak River and its tributary, Kuap River. Sediment samples were collected from fourteen sampling sites as shown in Figure 3.1 while the location and position based on GPS reading are presented in Table 3.1. The core sediments were collected using a gravity core sampler and sliced at 10 cm interval. The samples were taken at three locations within each site and then combined to obtain a composite sample. The sediments were then wrapped with aluminum foil and kept in cooler box during the sampling. The core sediment samples were collected from 0-20 cm to 0-60 cm depths, depending on the availability of the core sediments lengths as taken by the gravity core sampler. All sediment samples were then stored in cold room prior to the analysis. The field work for samples collection from Santubong River and Sarawak River were carried out in March and June 2006, respectively.

The core sediments were analyzed for the vertical distribution at three different depths, while the spatial distribution was investigated based on the surficial sediment (upper layer of core sediment) from each sampling site. The total organic matter (TOM) and the particle sizes of the core sediments were determined. The geolipids in the core sediments were isolated using Soxhlet extraction before fractionated into five fractions using column chromatography. Elemental sulfur from F1 fractions were removed while F2 fractions were

purified prior to gas chromatography analyses. Detailed on each procedure were described in section 3.2 to 3.7.

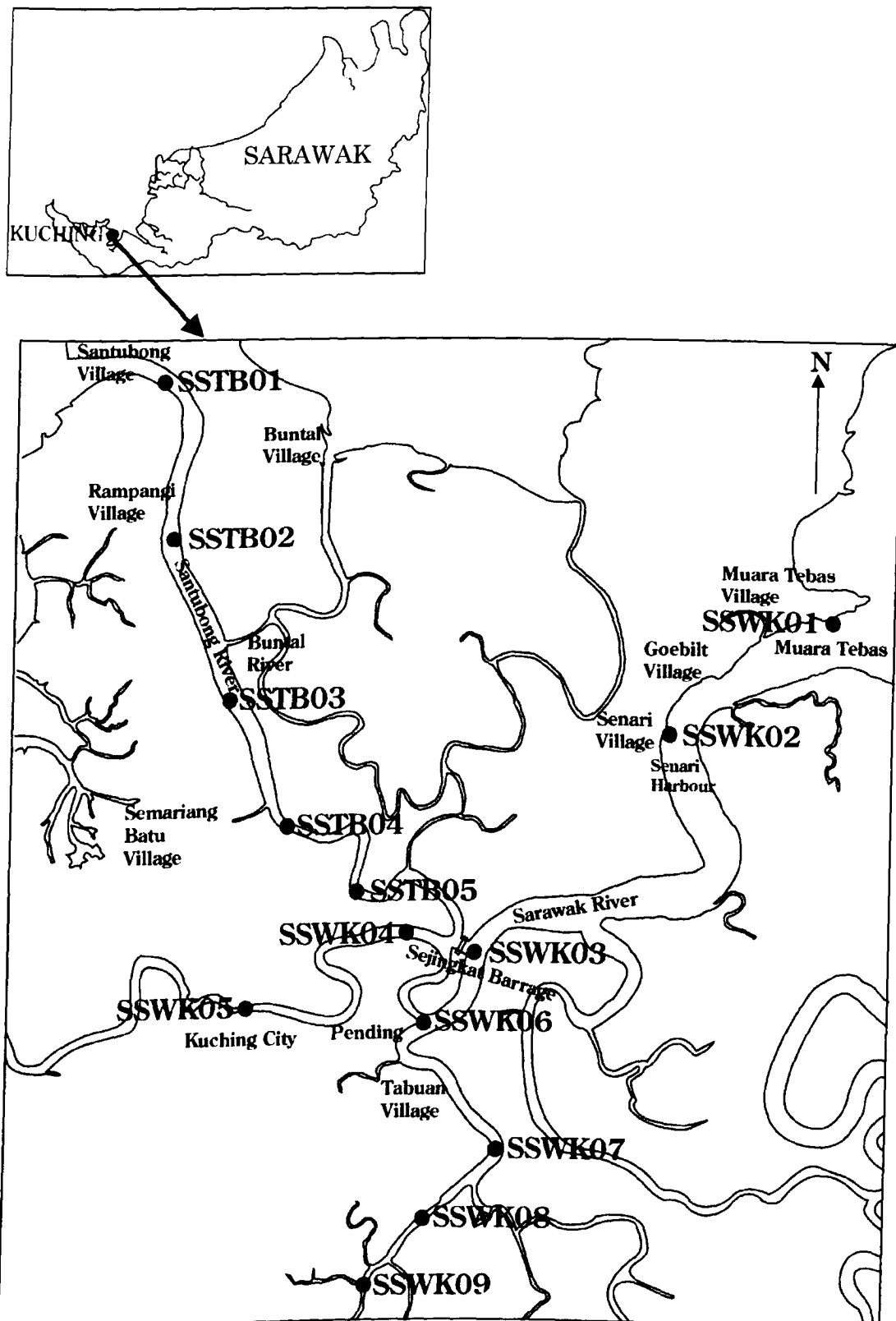


Figure 3.1: Sampling area for sediment samples collection from Santubong River and Sarawak River.

Table 3.1: Location of fourteen (14) sampling stations in Santubong River and Sarawak River and its tributary (Kuap River)

Station	Location	Position based on GPS reading
SSTB01	Santubong estuary	01° 42' 41.3" N 110°, 20' 04.6" E
SSTB02	Santubong Bridge	01° 40' 28.0" N 110°, 20' 23.4" E
SSTB03	Semariang New Town	01° 38' 15.9" N 110°, 21' 02.5" E
SSTB04	Demak Laut Village	01° 36' 15.7" N 110°, 21' 56.5" E
SSTB05	Bako Causeway	01° 35' 13.1" N 110°, 22' 59.4" E
SSWK01	Muara Tebas	01° 38' 47.0" N, 110° 29' 19.0" E
SSWK02	Senari Port	01° 37' 10.9" N, 110° 26' 56.6" E
SSWK03	Sejingkat Barrage	01° 34' 22.4" N, 110° 24' 44.5" E
SSWK04	Marine Police Base	01° 34' 34.0" N, 110° 23' 48.5" E
SSWK05	Kuching City	01° 33' 33.0" N, 110° 21' 03.1" E
SSWK06	Kuching Port	01° 33' 11.3" N, 110° 23' 50.0" E
SSWK07	Samajaya Industrial Zone	01° 31' 30.9" N, 110° 24' 46.3" E
SSWK08	Kuap Bridge	01° 29' 56.0" N, 110° 23' 28.2" E
SSWK09	Stampin Resettlement Village	01° 29' 13.7" N, 110° 22' 58.0" E

3.2 Determination of Total Organic Matter

The TOM in the core sediments was determined according to the loss on ignition method as used by Commendatore and Esteves (2004). Approximately 5 g of sediments were dried in the oven at 60°C for 24 hours to obtain the dry weight. The sediments were then heated in the furnace at 450°C for 2 hours, where three replicates were performed for each sample.

The TOM was determined using the equation 3.1 below.

$$\text{TOM (\%)} = [(M_1 - M_2) / M_1] \times 100\% \quad \text{eq 3.1}$$

where,

M_1 = weight of sediments after heated at 60 °C for 24 hours

M_2 = weight of sediments after heated at 450 °C for 2 hours

3.3 Particle-size Analysis

Analysis of particle-size was performed using the Pipette Method as described by Starr *et al.* (2000) in three replicates for each sample. The sediment samples were air dried at room temperature. Approximately 10 g of sediments were mixed with 150 mL of water in a 250 mL conical flask and then the mixture was shaken on the biospin shaker overnight. The dispersed sediment suspension was then transferred through a 0.050 mm sieve into a 1 L measuring cylinder by placing a large funnel below the sieve to channel all the suspension and subsequent washings into the cylinder. The particles on the sieve were then carefully washed until all fine particles are washed through into the cylinder. The fraction remaining in the sieve is the sand fraction > 0.05 mm. The entire sand fraction on the sieve was transferred into an evaporating dish by rinsing with water. The evaporating dish was placed in an oven set at 105 °C and left to dry until constant weight (weight of sand fraction > 0.05 mm after cooling = A g). The suspension and washings in the 1 L measuring cylinder were made up to 1000 mL with distilled water.

The suspension was stirred thoroughly with a special hand plunger using an up-and-down movement. The plunger was then removed and after the swirling motion stopped, 20 mL of the suspension was pipette from 6 cm depth and transferred into an evaporating dish and heated in the oven until constant weight (weight of 0 - 0.05 mm fraction = B g). Stirring as above was repeated, 20 mL of suspension was pipette from 10 cm depth at 4 minutes after stirring, transferred into an evaporating dish and heated in the oven until constant weight (weight of 0 - 0.02 mm fraction = C g). Stirring as above was repeated, 20 mL of suspension was pipette from 10 cm depth at 6 hours after stirring, transferred into an evaporating dish and heated in the oven until constant weight (weight < 0.002 mm fraction = D g). The particle size was determined using the equations 3.2 -3.5 below.

$$\% \text{ sand fraction } > 0.05 \text{ mm} = (A / 10) \times 100 \quad \text{eq. 3.2}$$

$$\% \text{ clay fraction } < 0.002 \text{ mm} = [(D / 20) \times 1000 / 10] \times 100 \quad \text{eq. 3.3}$$

$$\% \text{ (silt + clay) fraction } < 0.05 \text{ mm} = [(B / 20) \times 1000 / 10] \times 100 \quad \text{eq. 3.4}$$

$$\% \text{ silt fraction} = \{(B - D) / 20\} \times 1000 / 10 \times 100 \quad \text{eq. 3.5}$$

3.4 Samples Extraction and Fractionation

3.4.1 Isolation of Geolipids

The extraction and fractionation of sediment samples were carried out using the method described by Tolosa *et al.* (2004b) in three replicates for each sample. Approximately 10 g of sediment sample was Soxhlet extracted using 250 mL of dichloromethane for 12 hours. Prior to Soxhlet extraction, the sediment

sample was spiked with 50 μL of 50 ppm mixture of internal standards containing eicosene and o-terphenyl. Eicosene is the internal standard for aliphatic hydrocarbons, while o-terphenyl is the internal standard for PAHs. The crude extract was then evaporated to dryness using vacuum rotary evaporator. The total crude extract obtained from Soxhlet extraction is considered as geolipid.

3.4.2 Fractionation of Geolipids

Geolipid was separated into five fractions on silica gel (230-400 mesh) column chromatography by elution with the following solvent systems: (1) 40 mL n-hexane (F1 fraction; total aliphatic hydrocarbons), (2) 40 mL mixture of toluene and n-hexane (1:3; v:v) (F2 fraction; polycyclic aromatic hydrocarbons), (3) 20 mL mixture of toluene and n-hexane (1:1; v:v) followed by 20 mL mixture of ethyl acetate and n-hexane (1:19; v:v) (F3 fraction; alkenones and fatty acid methyl esters), (4) 40 mL ethyl acetate in n-hexane (1:9; v:v) (F4 fraction; phthalates), and (5) 20 mL ethyl acetate in n-hexane (3:17; v:v) followed by 20 mL mixture of ethyl acetate and n-hexane (1:4; v:v) (F5 fraction; alcohols and sterols).

3.4.2.1 Removal of Elemental Sulfur

Elemental sulfur (S_8) co-extracted from sediment samples may interfere with gas chromatographic/flame ionization detector (GC/FID) analysis of individual aliphatic hydrocarbons in the F1 fractions. Prior to GC/FID or GC/MS analysis, elemental sulfur was removed from the F1 fraction using activated copper column (Blumer, 1957). A bed (~3 cm high) of copper powder (~40 mesh)

packed dry into a glass chromatographic column was used to treat the TAH fraction. The TAH fraction was dissolved in 1 mL dichloromethane and transferred to the activated copper column. The sample was then allowed to elute slowly through the column with 25 mL dichloromethane.

3.4.2.2 Sephadex Chromatography

F2 fraction was enriched with PAHs by using the Sephadex LH-20 (25-100 μm particle size) column chromatography. According to Giger and Blumer (1974), the non-PAH components in F2 fraction including polyunsaturated hydrocarbons (e.g. heneicosahexene, squalene) must be separated from the PAHs in order to achieve enrichment. 1 g of Sephadex LH-20 was added with 30 mL mixture of benzene-methanol (1:1; v/v) and poured into a chromatographic column. The F2 fraction was redissolved in 1 mL mixture of benzene-methanol (1:1; v/v) and transferred to the top of the Sephadex column. The first fraction (F2_S1), which contained the non-PAH components of the F2 fraction was eluted with 20 mL mixture of benzene-methanol (1:1; v/v) while the second fraction (F2_S2) that contained the PAH components was eluted with 30 mL mixture of benzene-methanol (1:1; v/v).

3.5 Instrumental Analysis

Gas chromatography analyses were performed to determine qualitatively and quantitatively the distribution of aliphatic hydrocarbons and polycyclic aromatic hydrocarbons in the core sediments of Santubong and Sarawak rivers. The gas chromatography/flame ionization detector (GC/FID) and gas

chromatography/ mass spectrometry (GC/MS) were used for the instrumental analysis.

3.5.1 Gas Chromatography/Flame Ionization Detector (GC/FID)

GC/FID analysis was carried out on a Shimadzu 17A 5890 Series III equipped Class GC-10 data system and a fused silica capillary column (BP-1, 30 m x 0.25 mm i.d x 0.50 μ m film thickness). Nitrogen was used as carrier gas. 1 μ L of sample was introduced into a column by a splitless injection mode. The injector and detector temperature were maintained at 280°C and 300°C, respectively. Initially, the gas chromatograph oven was programmed at 50°C for 2 minutes and subsequently ramped to 300°C at the rate of 6.5 °C/min. Final temperature was maintained for 10 minutes.

3.5.2 Gas Chromatography/Mass Spectrometry (GC/MS)

GC/MS analysis was performed on a Shimadzu QP5000 GC/MS equipped with a quadrupole mass spectrometer. A fused silica capillary column (25 m x 0.25 mm i.d) coated with DB-5 (film thickness 0.25 μ m) was used. The temperature program used was similar to that of GC/FID analysis. Mass spectrum was obtained by using linear scanning (m/z 45-450, cycle time of 1.0 second) and electron impacts (70 eV) ionization. Helium at the flow rates of 1.2 mL/ min was used as the carrier gas. Temperature of the injector and the transfer line to the mass spectrometer were maintained at 280 °C.

GC/MS analysis of FAMES, phthalate esters and alcohols and sterols in core sediments was performed on all layers of three core sediments from Santubong namely SSTB01, SSTB03 and SSTB05. However, only surficial sediment of core sediments from SSTB02 and SSTB04 were analyzed. All the core sediments from Sarawak River were analyzed qualitatively for FAMES. Phthalate esters and alcohols and sterols..

3.6 Gas Chromatographic Data Analysis

3.6.1 Concentration of Hydrocarbons in Sediment

The aliphatic hydrocarbon fractions are expected to contain aliphatic hydrocarbons including straight-chained alkanes, branched alkanes and alkenes. However, only n-alkanes ranging from n-dodecane ($C_{12}H_{26}$) to n-tetratricontane ($C_{34}H_{70}$) were considered for quantitative analysis in this thesis. There are 16 individual PAHs considered in this study that consist of LPAHs and HPAHs. LPAHs include naphthalene (NaP), acenaphthylene (AcPy), acenaphthene (AcP), fluorene (Flu), phenanthrene (Ph) and anthracene (An) while HPAHs include fluoranthene (Fl), pyrene (Py), benzo[a]anthracene (BaA), chrysene (Chr), benzo[b]fluoranthene (BbF), benzo[k]fluoranthene (BkF), benzo[a]pyrene (BaP), indeno[1,2,3-c,d]pyrene (InD), dibenzo[a,h]anthracene (DBA) and benzo[g,h,i]perylene (BghiP) (Zhou and Maskaoui, 2003). N-alkanes in aliphatic fractions and PAHs compounds from sediment samples were identified by comparing retention times obtained from GC/FID analysis with retention times of n-alkanes and PAHs standards, respectively.

The internal standardization method was used to determine the concentration of hydrocarbons in sediment samples using eicosene (C₂₀H₄₀) and o-terphenyl as the internal standards for aliphatic and PAHs fractions, respectively (Peters and Moldowan, 1993). The concentration of each hydrocarbon in the sediment samples was calculated using the following equations:

$$C_X = \frac{RF \times A_X \times C_{I.S} \times \text{dilution factor}}{A_{I.S}} \quad \text{eq 3.6}$$

where, C_X = concentration of hydrocarbon X,

RF = response factor

A_X = peak area of gas chromatogram for hydrocarbon X

C_{I.S} = concentration of internal standard

A_{I.S} = peak area of gas chromatogram for internal standard

$$RF = \frac{C_{X,STD} \times A_{I.S}}{A_{X,STD} \times C_{I.S}} \quad \text{eq 3.7}$$

where, C_{X,STD} = concentration of hydrocarbon X

A_{X,STD} = peak area of gas chromatogram for hydrocarbon X

The response factors of individual n-alkanes and isoprenoid hydrocarbons were determined by analyzing 50 µg/mL mixtures of n-alkanes (C₁₂ to C₃₄). The response factors for pristane and phytane were estimated using the average response factors of C₁₇ and C₁₈, and of C₁₈ and C₁₉, respectively (Peters and Moldowan, 1993).

3.6.2 Carbon Preference Index

Carbon preference index (CPI) was calculated using the formula proposed by Bray and Evans (1961) as shown by equation below:

$$\text{CPI} = \frac{1}{2} \left[\frac{C_{25} + C_{27} + C_{29} + C_{31} + C_{33}}{C_{26} + C_{28} + C_{30} + C_{32} + C_{34}} + \frac{C_{25} + C_{27} + C_{29} + C_{31} + C_{33}}{C_{24} + C_{26} + C_{28} + C_{30} + C_{32}} \right] \quad \text{eq 3.8}$$

where, C_n = alkane with n number carbons

3.7 Statistical Data Analysis

In order to determine any significant environmental variations, data for organic matter, particle size, aliphatic and aromatic hydrocarbons were examined statistically using correlation coefficient and principal component analysis (PCA). All statistical analyses were performed using SPSS 13.0 software program.

3.7.1 Correlation Coefficient

The existence of correlation between hydrocarbon concentrations and organic matter contents in the sediments can be determined based on the Pearson's correlation coefficients (Shao *et al.*, 2003). The strength of a relationship between variables can be measured using correlation coefficient study. The degree of rarity of a certain result is represented by significance.

Significance less than 0.05 means that there is less than 5% chance that this relationship occurred by chance.

3.7.2 Principal Component Analysis (PCA)

The data was analyzed statistically using principal component analysis (PCA). The PCA was conducted on the samples as a single data set. The data was investigated using the proportion data (to remove the concentration effect) and after log-ratio transformation in order to normalize the results, hence removing the “closure” effect and the co-dependence of values (Mudge and Duce, 2005). Prior to PCA analysis, all the data was mean centered to unit variance. TOM, particle sizes, total n-alkanes, total PAHs and concentrations of LMW n-alkanes, HMW n-alkanes, LPAHs, HPAHs, pristane and phytane were the parameters involved in the PCA analysis.

CHAPTER FOUR

RESULTS AND DISCUSSION

4.1 Total Organic Matter

Table 4.1 presents the percentage of total organic matter in core sediments from Santubong River and Sarawak River. The spatial distribution of organic matter was assessed using the data obtained for the upper layer of core sediments. Figures 4.1 and 4.2 show the spatial distribution trends of TOM for the surface sediment from Santubong River and Sarawak River, respectively while Figures 4.3 and 4.4 present the vertical distribution trend of core sediments from Santubong River and Sarawak River, respectively. Correlations between total organic matter with the particle sizes, total n-alkanes and total PAHs were determined based on Pearson correlation and further discussed in section 4.7.1.

Organic matter is an organic compound whose molecular structures and distributions can be significantly altered by various geochemical and biochemical processes (Muri *et al.*, 2004). Organic matter belongs to the most dynamic components of sediment and it is subjected to extensive early diagenetic alteration and loss.

Table 4.1: Total organic matter in core sediments from Santubong River (SSTB) and Sarawak River (SSWK).

River	Samples	Depth (cm)	Total Organic Matter (%)
Santubong	SSTB01	0-10	6.71 ± 0.01
		20-30	5.66 ± 0.01
		30-40	4.70 ± 0.04
	SSTB02	0-10	5.19 ± 0.02
		20-30	4.70 ± 0.03
		30-40	3.44 ± 0.01
	SSTB03	0-10	6.87 ± 0.04
		30-40	6.14 ± 0.04
		50-60	5.25 ± 0.01
	SSTB04	0-10	6.92 ± 0.03
		20-30	6.33 ± 0.01
		40-50	6.09 ± 0.01
	SSTB05	0-10	7.07 ± 0.01
		20-30	6.40 ± 0.01
		30-40	6.04 ± 0.02
Sarawak	SSWK01	0-10	4.90 ± 0.05
		20-30	3.38 ± 0.02
		40-50	3.27 ± 0.03
	SSWK02	0-10	6.55 ± 0.01
		20-30	4.52 ± 0.01
		30-40	4.00 ± 0.02
	SSWK03	0-10	5.99 ± 0.03
		20-30	5.71 ± 0.01
		30-40	5.33 ± 0.02
	SSWK04	0-10	4.60 ± 0.03
		10-20	3.96 ± 0.04
	SSWK05	0-10	5.15 ± 0.02
		10-20	3.09 ± 0.01
		20-30	2.03 ± 0.01
	SSWK06	0-10	5.36 ± 0.01
		10-20	4.27 ± 0.01
	SSWK07	0-10	5.24 ± 0.02
		10-20	5.07 ± 0.03
SSWK08	0-10	5.20 ± 0.04	
	10-20	4.79 ± 0.02	
SSWK09	0-10	4.74 ± 0.03	
	10-20	4.52 ± 0.02	

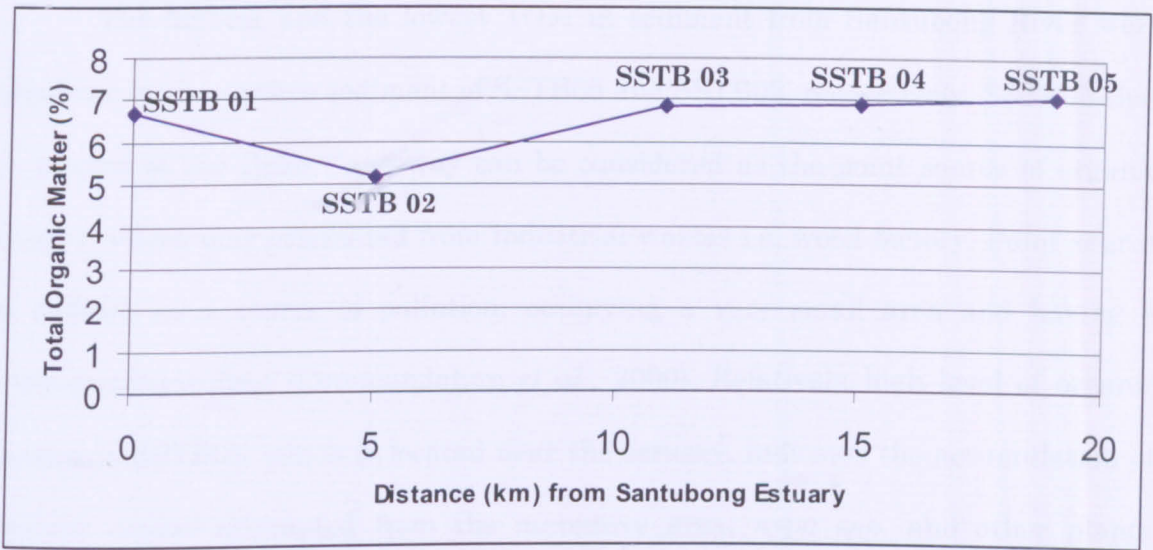


Figure 4.1: The spatial distribution of TOM in the surface sediments from Santubong River

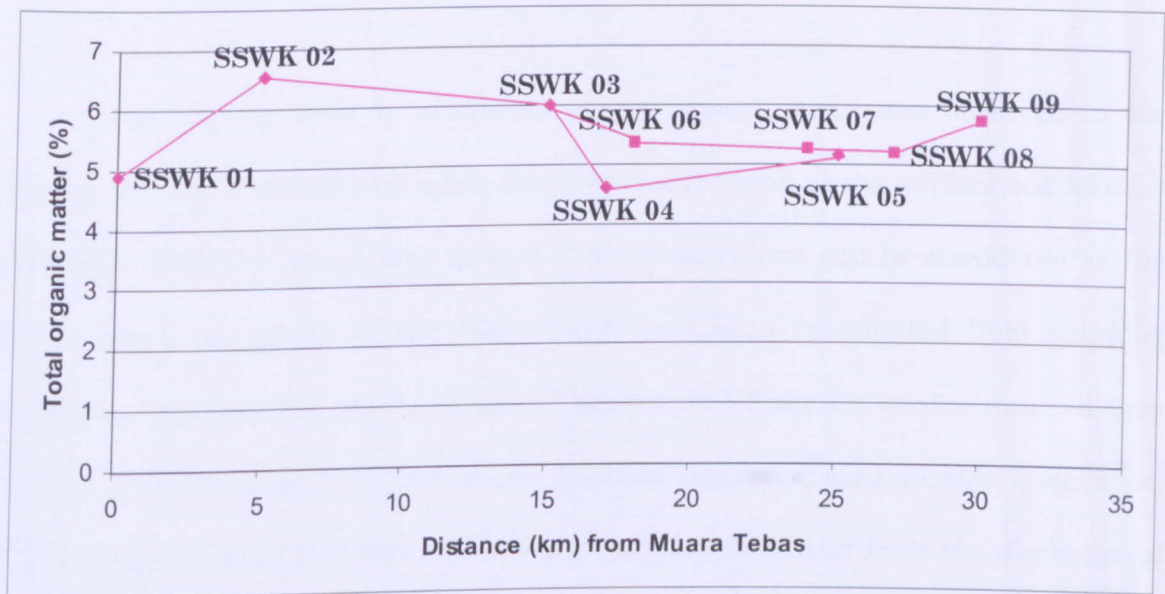


Figure 4.2: The spatial distribution of TOM in the surface sediments from Sarawak River

The highest and the lowest TOM in sediment from Santubong River were observed in the surface sediment of SSTB05 and SSTB02, respectively. SSTB05 that is located at the Bako Causeway can be considered as the point source of organic matter, which may originated from industrial wastes i.e. wood factory. Point source is defined as a source of pollution, occupying a very small area and having a concentrated output (Commendatore *et al.*, 2000). Relatively high level of organic matter in SSTB01, which is located near the estuary, indicates the accumulation of organic matter originated from the mangrove area, *nypa spp.* and other plants growing along the river and also from the discharge of domestic wastes. This is also supported by the aliphatic hydrocarbon biomarker indices that indicate contribution of biogenic contribution to the organic matter.

The highest TOM in sediments from Sarawak River was observed in the surface sediment of SSWK02 while the lowest was found in the surface sediment of SSWK04. SSWK02, which was located at the Senari Port can be considered as the point source of organic matter that might have been contributed from shipping activities, coal-powered plant, industrial wastes and domestic wastes from villages nearby. SSWK05 that is located at the Kuching city has a considerable quantity of TOM compared with SSWK04 due to inputs of organic matter from the discharge of urban waste. A considerable amount of TOM was also observed for the surface sediments of SSWK09 at the Stampin Resettlement Village. Domestic and industrial wastes can be considered as the sources of TOM in this station. Evidence of the aliphatic hydrocarbon indices also indicates the anthropogenic inputs of the organic matter. The TOM was gradually reduced in sediment collected from the sites toward downstream of river.

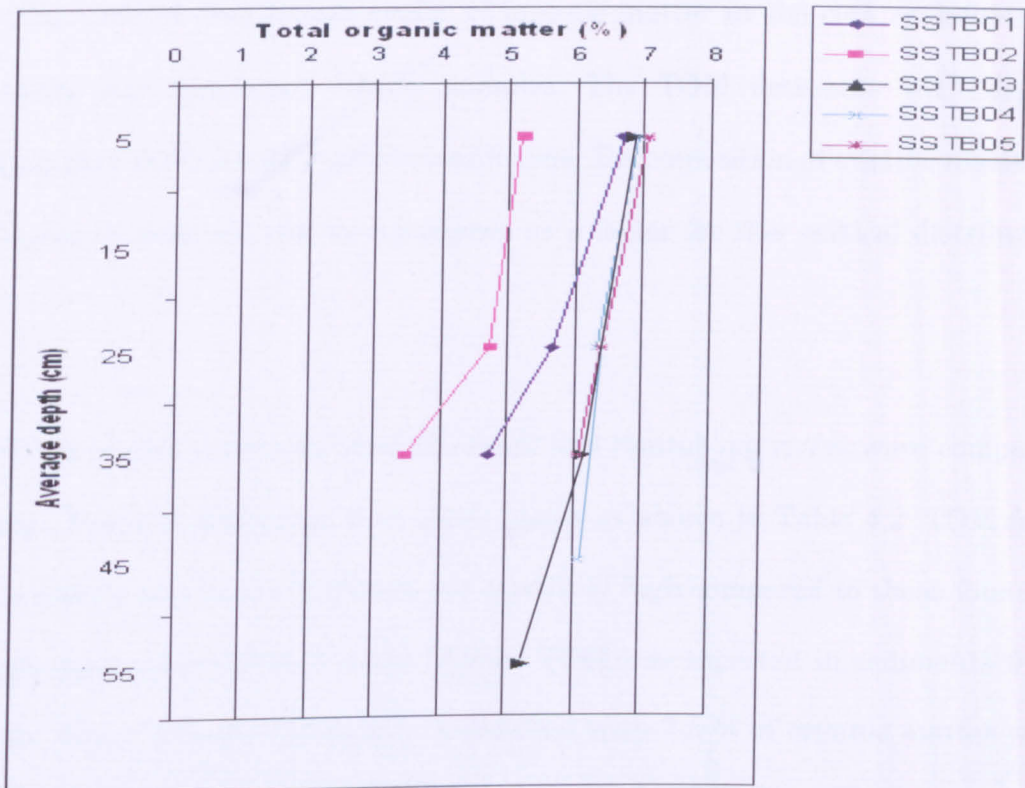


Figure 4.3: The vertical distribution of TOM in the core sediments from Santubong River

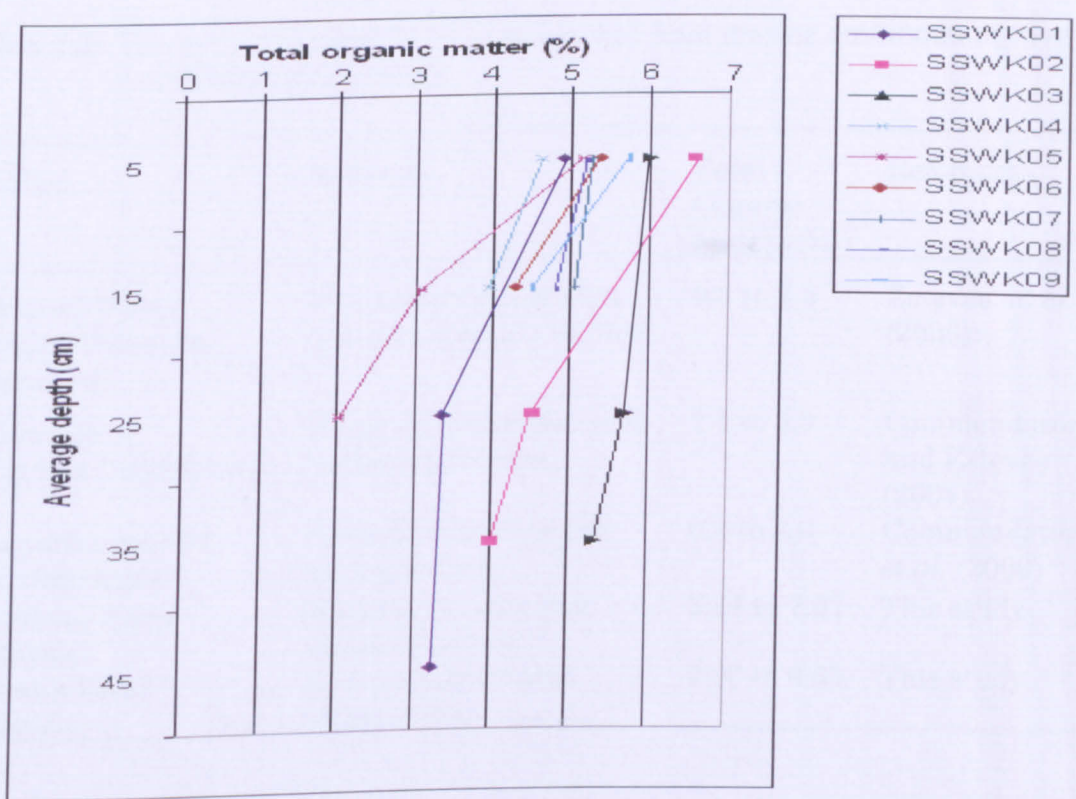


Figure 4.4: The vertical distribution of TOM in the core sediments from Sarawak River

The vertical distribution profile of organic matter in the core sediments for both rivers was consistent for all samples. The TOM decreases with depths indicating that TOM inputs decreases with time. Decomposition of organic matter at lower layers of sediment can be considered as a factor for this vertical distribution trend.

TOM in core sediments from Sarawak and Santubong rivers were compared with those found in sediments from other places as shown in Table 4.2. TOM from both Santubong and Sarawak Rivers are relatively high compared to those found in sediments from other places but the highest TOM was reported in sediments from Tierra del Fuego Islands, Patagonia (Argentina) with 7.3 % of organic matter with the sources of organic matter originated from both biogenic and anthropogenic activities (Esteves *et al.*, 2006).

Table 4.2: The percentages of TOM in sediments from marine environment in other countries and this study.

Location	Activities	Total Organic Matter (%)	References
Tierra del Fuego Islands, Patagonia (Argentina)	Petroleum exploitation port and coastal seagrass	0.3 to 7.3	Esteves <i>et al.</i> (2006)
Chubut River, Patagonia (Argentina)	Crude oil production and harbour activities	1.1 to 3.9	Commendatore and Esteves (2004)
Patagonian coastal zone (Argentina)	Harbour activities and fishing vessels	0.4 to 3.6	Commendatore <i>et al.</i> (2000)
Santubong River (Malaysia)	Mangrove region and industrial areas	3.44 to 7.07	This study
Sarawak River (Malaysia)	Port, industrial and urban areas	2.03 to 6.55	This study

4.2 Particle Size

The particle size of core sediments from Santubong River and Sarawak River are shown in Table 4.3.

Table 4.3: Particle size of core sediments from Santubong River and Sarawak River

River	Samples	Depth (cm)	%Sand	%Clay	%Silt+Clay	%Silt	Type of sediment
Santubong	SSTB01	0-10	49.5	20.0	50.0	30.0	Loam
		20-30	39.1	15.0	60.0	45.0	Loam
		30-40	49.6	20.0	50.0	30.0	Loam
	SSTB02	0-10	47.0	20.0	50.0	30.0	Loam
		20-30	44.0	20.0	50.0	30.0	Loam
		30-40	41.5	15.0	50.0	35.0	Loam
	SSTB03	0-10	25.0	10.0	65.0	55.0	Silt loam
		30-40	26.1	15.0	70.0	55.0	Silt loam
		50-60	25.5	5.0	70.0	65.0	Silt loam
	SSTB04	0-10	29.5	15.0	70.0	55.0	Silt loam
		20-30	34.5	10.0	65.0	55.0	Silt loam
		40-50	28.7	5.0	60.0	55.0	Silt loam
	SSTB05	0-10	25.5	15.0	70.0	55.0	Silt loam
		20-30	24.8	10.0	75.0	65.0	Silt loam
		30-40	19.9	10.0	80.0	70.0	Silt loam
Sarawak	SSWK01	0-10	45.0	10.0	50.0	40.0	Loam
		20-30	55.8	5.0	35.0	30.0	Loam
		40-50	46.7	10.0	50.0	40.0	Loam
	SSWK02	0-10	26.3	10.0	70.0	60.0	Silt loam
		20-30	25.5	10.0	65.0	55.0	Silt loam
		30-40	25.0	10.0	65.0	55.0	Silt loam
	SSWK03	0-10	29.1	15.0	70.0	55.0	Silt loam
		20-30	25.1	15.0	70.0	55.0	Silt loam
		30-40	29.4	5.0	70.0	65.0	Silt loam
	SSWK04	0-10	34.9	10.0	65.0	55.0	Silt loam
		10-20	28.9	15.0	70.0	55.0	Silt loam
	SSWK05	0-10	34.5	10.0	65.0	55.0	Silt loam
		10-20	39.4	5.0	60.0	55.0	Silt loam
		20-30	19.1	20.0	80.0	60.0	Silt loam
	SSWK06	0-10	24.1	25.0	75.0	55.0	Silt loam
10-20		25.1	15.0	70.0	55.0	Silt loam	
SSWK07	0-10	25.3	15.0	70.0	55.0	Silt loam	
	10-20	19.4	20.0	80.0	60.0	Silt loam	
SSWK08	0-10	27.9	5.0	65.0	60.0	Silt loam	
	10-20	19.8	25.0	80.0	55.0	Silt loam	
SSWK09	0-10	19.3	25.0	80.0	55.0	Silt loam	
	10-20	26.8	5.0	70.0	65.0	Silt loam	

The types of sediments were determined based on the United States Department of Agriculture (USDA) soil textural triangle (Starr *et al.*, 2000), as simplified in Figure 4.5. Even though the core sediments analyzed do not have percentages of sand, silt and clay that define a single point on the triangle, the types of sediments can be determined based on the point that best fit the characteristics of sediments described by Brown (2003).

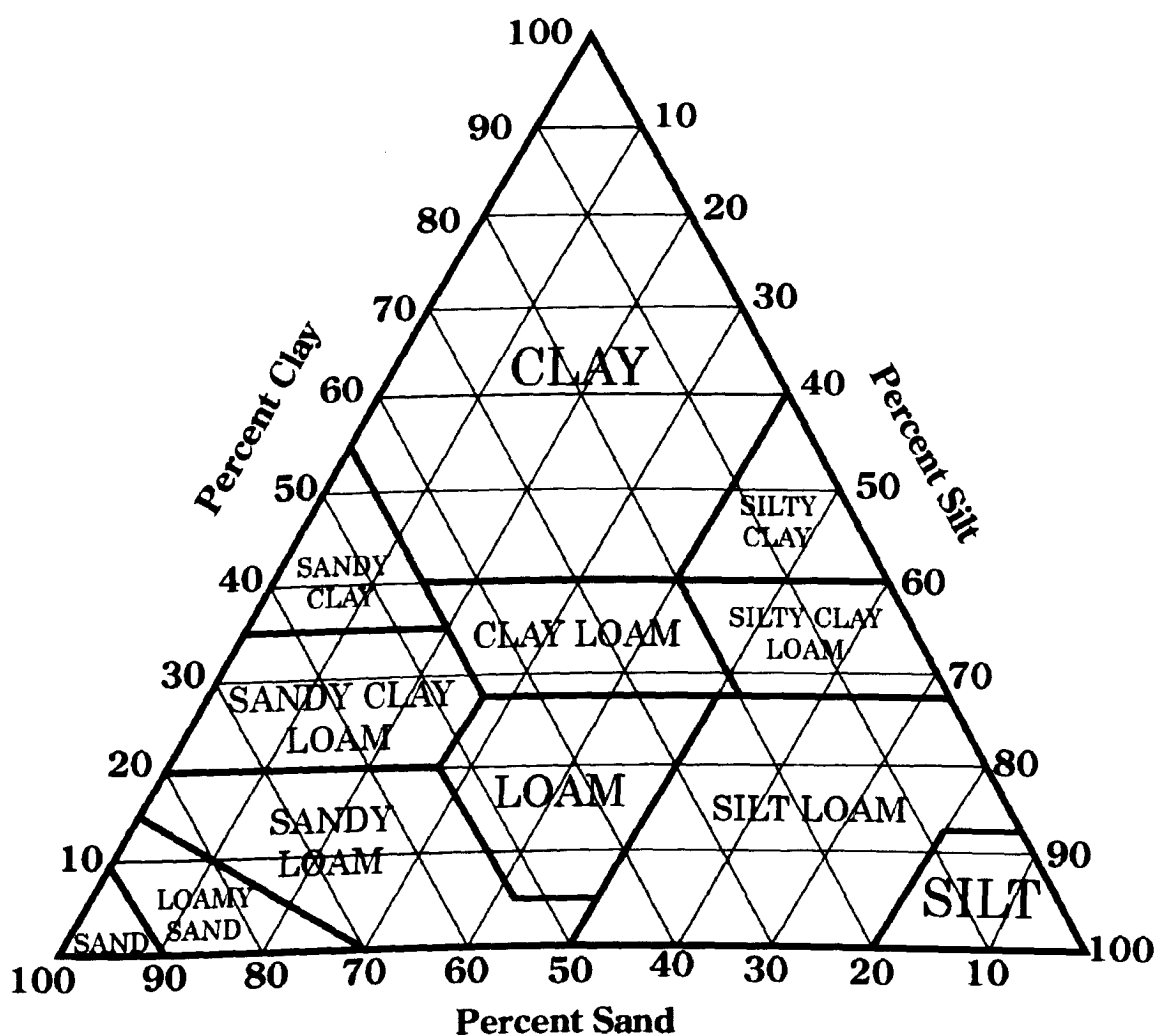


Figure 4.5: Classification of sediment according to USDA soil textural triangle (Starr *et al.*, 2000)

Estuarine sediments, which are SSTB01, SSTB02 and SSWK01 sediments are categorized as loam. Loam is a medium-texture soil material with relatively even mixture of sand, silt and clay. Even though the percentages of clay are relatively low in sediments from these three stations, loam can be considered as the best types of sediments that best fit the characteristics as loam tends to be rather soft and friable (Brown, 2003). Furthermore, clay exert a greater influence on soil properties than sand or silt due to the small size, high surface areas and high physical and chemical activities of the clay particles.

Other sediments collected from both rivers can be categorized as silt loam sediments. Silt loam consists mainly of silt and relatively smaller amounts of sand and clay. The silt loam is soft and smooth when moist and rather cloddy when dry (Brown, 2003).

The different depositional environments attributed to the different types of sediments observed in sediments collected from estuary of the rivers compared to those from other stations (Jeng *et al.*, 2003). The strength of water current towards the sea and vice versa for both rivers also influenced the deposition of sand, silt and clay in the study area.

4.3 Aliphatic Hydrocarbons

4.3.1 Aliphatic Hydrocarbons Standard Mixture

The chromatogram obtained from GC/FID analysis for a mixture of n-alkanes standard is shown in Figure 4.6 while the retention times for n-alkanes and isoprenoid hydrocarbons (pristane and phytane) is presented in Table 4.4.

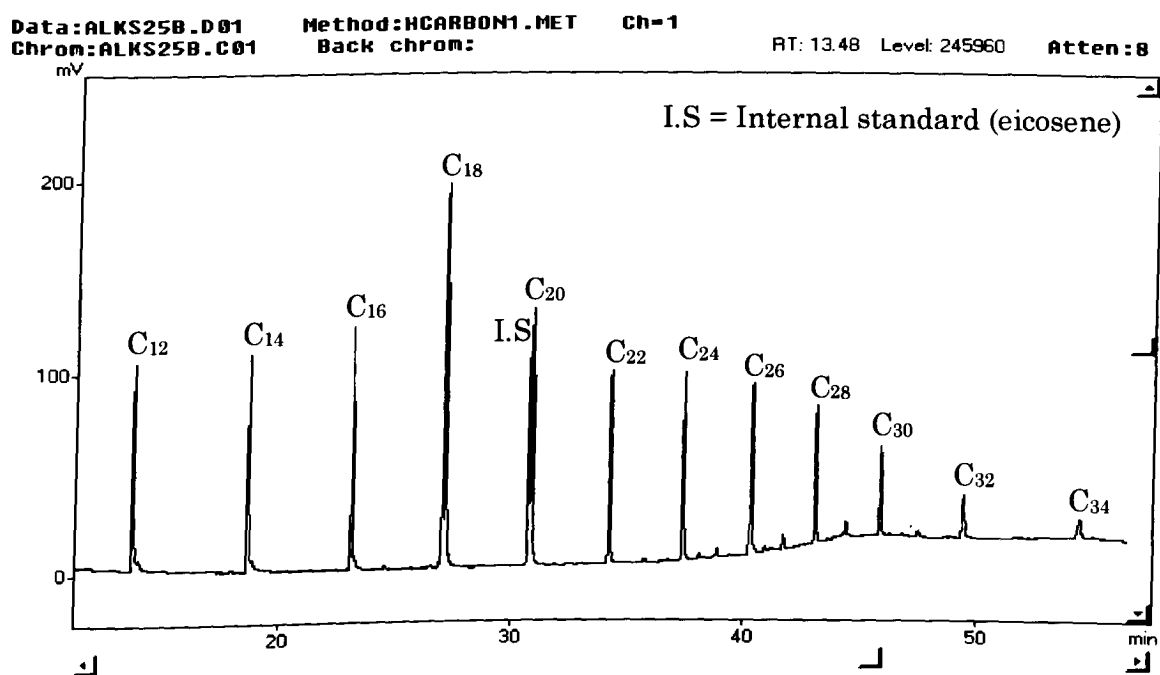


Figure 4.6: Gas chromatogram from GC/FID analysis of n-alkanes in a standard mixture

Table 4.4: Retention times for n-alkanes (C₁₂-C₃₂) and isoprenoid hydrocarbons (pristane and phytane)

Compounds	Molecular formula	Retention time (minutes) (n=3)	Determination of retention time
Dodecane	C ₁₂ H ₂₆	13.62 ± 0.01	GC analysis
Tridecane	C ₁₃ H ₂₈	16.10	Estimated
Tetradecane	C ₁₄ H ₃₀	18.58 ± 0.01	GC analysis
Pentadecane	C ₁₅ H ₃₂	20.81	Estimated
Hexadecane	C ₁₆ H ₃₄	23.05 ± 0.01	GC analysis
Heptadecane	C ₁₇ H ₃₆	25.08	Estimated
Pristane	C ₁₉ H ₄₀	26.09	Estimated (nearest to peak C ₁₇)
Octadecane	C ₁₈ H ₃₈	27.11 ± 0.01	GC analysis
Phytane	C ₂₀ H ₄₂	28.03	Estimated (nearest to peak C ₁₈)
Nonadecane	C ₁₉ H ₄₀	28.95	Estimated
Eicosene –	C ₂₀ H ₄₀	30.69 ± 0.02	GC analysis
Internal standard			
Eicosane	C ₂₀ H ₄₂	30.80 ± 0.01	GC analysis
Heneicosane	C ₂₁ H ₄₄	32.50	Estimated
Docosane	C ₂₂ H ₄₆	34.20 ± 0.02	GC analysis
Tricosane	C ₂₃ H ₄₈	35.78	Estimated
Tetracosane	C ₂₄ H ₅₀	37.37 ± 0.02	GC analysis
Pentacosane	C ₂₅ H ₅₂	38.84	Estimated
Hexacosane	C ₂₆ H ₅₄	40.31 ± 0.02	GC analysis
Heptacosane	C ₂₇ H ₅₆	41.69	Estimated
Octacosane	C ₂₈ H ₅₈	43.06 ± 0.02	GC analysis
Nonacosane	C ₂₉ H ₆₀	44.46	Estimated
Eicontane	C ₃₀ H ₆₂	45.86 ± 0.02	GC analysis
Henetricontane	C ₃₁ H ₆₄	47.64	Estimated
Dotricontane	C ₃₂ H ₆₆	49.43 ± 0.05	GC analysis
Tricontane	C ₃₃ H ₆₈	51.93	Estimated
Tetracontane	C ₃₄ H ₇₀	54.42 ± 0.08	GC analysis

Response factor (RF) can be defined as ratio of amount to signal magnitude for the compound of interest measured relative to that for the internal standard through external analysis of a standard solution (Blumer, 1957). Determination of response factor is very important as the analytical results of the hydrocarbons are strongly affected by the response factors. The response factor for n-alkanes (C₁₂ to C₃₂) and isoprenoid hydrocarbons (pristane and phytane) are shown in Table 4.5.

Table 4.5: RF values for n-alkanes (C₁₂-C₃₂) and isoprenoids hydrocarbons (pristane and phytane) using n-eicosene as internal standard

Compounds	RF value (n=3)
Dodecane (C ₁₂ H ₂₆)	0.67 ± 0.01
Tridecane (C ₁₃ H ₂₈)	0.76 ± 0.02
Tetradecane (C ₁₄ H ₃₀)	0.85 ± 0.02
Pentadecane (C ₁₅ H ₃₂)	0.97 ± 0.03
Hexadecane (C ₁₆ H ₃₄)	1.09 ± 0.03
Heptadecane (C ₁₇ H ₃₆)	1.28 ± 0.02
Pristane (C ₁₉ H ₄₀)	1.37 ± 0.02
Octadecane (C ₁₈ H ₃₈)	1.46 ± 0.02
Phytane (C ₂₀ H ₄₂)	1.67 ± 0.02
Nonadecane (C ₁₉ H ₄₀)	1.89 ± 0.01
Eicosane (C ₂₀ H ₄₂)	2.31 ± 0.01
Heneicosane (C ₂₁ H ₄₄)	3.43 ± 0.02
Docosane (C ₂₂ H ₄₆)	4.54 ± 0.05
Tricosane (C ₂₃ H ₄₈)	5.71 ± 0.08
Tetracosane (C ₂₄ H ₅₀)	6.88 ± 0.07
Pentacosane (C ₂₅ H ₅₂)	7.35 ± 0.09
Hexacosane (C ₂₆ H ₅₄)	7.82 ± 0.09
Heptacosane (C ₂₇ H ₅₆)	8.01 ± 0.08
Octacosane (C ₂₈ H ₅₈)	8.20 ± 0.09
Nonacosane (C ₂₉ H ₆₀)	9.45 ± 0.12
Eicontane (C ₃₀ H ₆₂)	10.70 ± 0.14
Henetricontane (C ₃₁ H ₆₄)	12.04 ± 0.15
Dotricontane (C ₃₂ H ₆₆)	13.38 ± 0.15
Tricontane (C ₃₃ H ₆₈)	16.46 ± 0.18
Tetracontane (C ₃₄ H ₇₀)	19.54 ± 0.22

4.3.2 Aliphatic Hydrocarbons in Sediment Samples

Gas chromatograms for aliphatic hydrocarbon fractions from SSTB01 core sediment samples are shown in Figure 4.7, while gas chromatograms for aliphatic hydrocarbon fractions from SSWK01 core sediments are shown in Figure 4.8. Gas chromatograms for aliphatic hydrocarbon fractions from other core sediments from Santubong River and Sarawak River are presented in Appendix A. The concentrations of n-alkanes and isoprenoid hydrocarbons in core sediment samples from Santubong River and Sarawak River are shown in Tables 4.6 and 4.7, respectively.

All samples showed a baseline elevation or hump that cannot be resolved by capillary GC column. This hump is due to unresolved complex mixture (UCM) which usually exists in the carbon number of 16-34 that indicates oil pollution (Nishigima *et al.*, 2001). According to Commendatore and Esteves (2004), overlapping elution of a complex mixture of petroleum hydrocarbons over the entire boiling point ranges caused the existence of UCM. Therefore, the presence of UCM in gas chromatograms can be used as petroleum indicators.

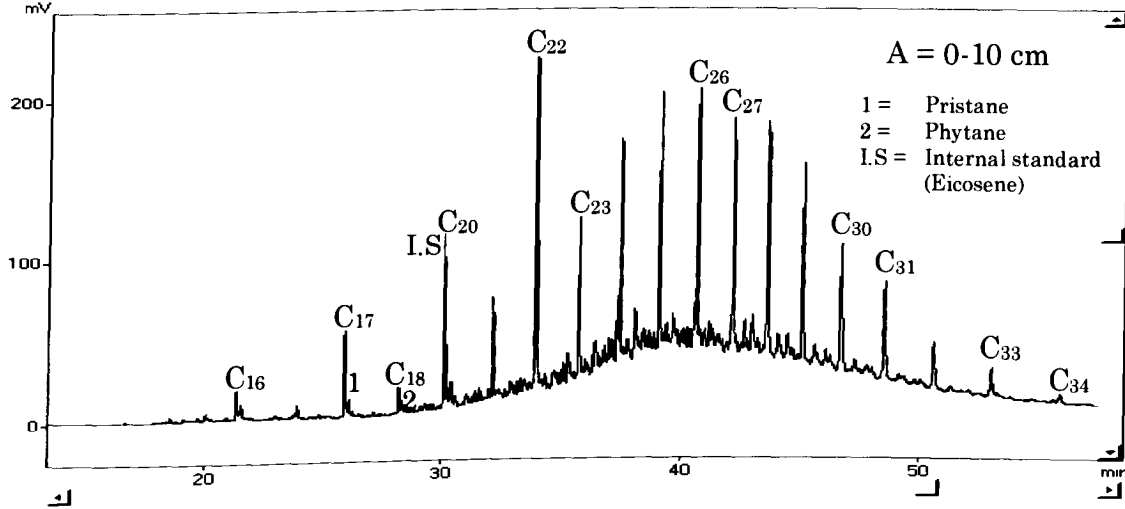
UCM, which consists of cyclic and branched alkanes, tends to remain in the environment after n-alkanes have degraded as UCM resist microbial degradation more effectively than n-alkanes (Jeng, 2006; Bouloubassi and Saliot, 1993). This is attributed to the "T-shaped" molecules of UCM as result of their linear carbon chains that are connected at branch points (Jeng *et al.*, 2003). Core sediments from SSWK04 to SSWK09 show prominent UCM suggesting high organic input from petroleum or biodegradation sources or from eroded hydrocarbons (Jeng *et al.*, 2003).

The prominent UCM in gas chromatogram of these core sediments are as a result of strong depletion of n-alkanes due to biodegradation as petroleum pollution enhanced microbial activity (Aboul-Kassim and Simoneit, 1996).

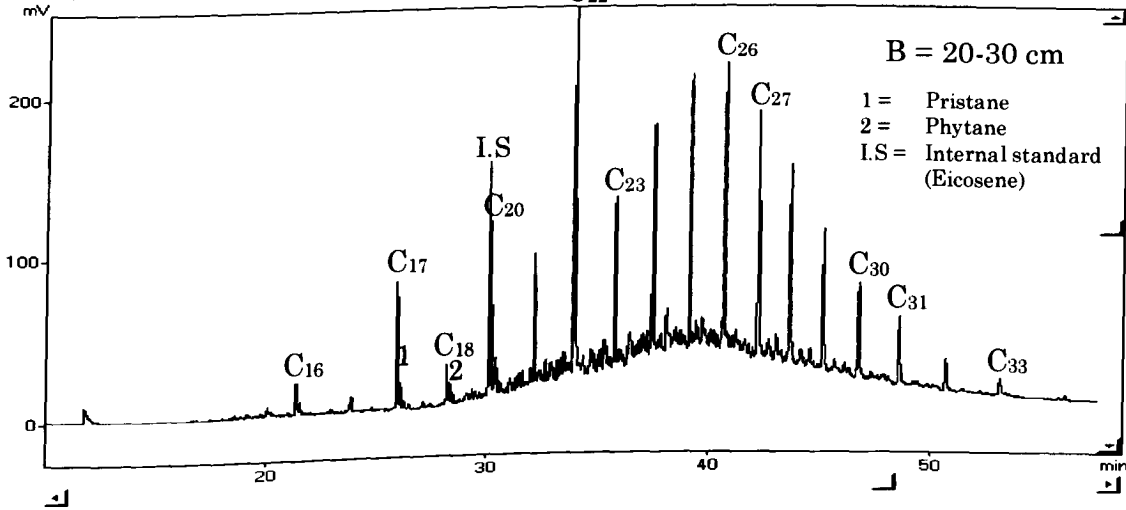
The sediment samples from both rivers were dominated by long-chain n-alkanes (>C₂₃) where the major hydrocarbons are C₂₃, C₂₅, C₂₇, C₂₉ and C₃₁ indicating the sources of n-alkanes are from vascular land plants. This observation can be attributed to the low susceptibility of long-chain n-alkanes to degradation due to association of long-chain terrestrial homologues with more refractory biopolymers (Muri *et al.*, 2004).

Short-chain hydrocarbons were detected in lower concentrations compared to long-chain hydrocarbons with C₂₂ or C₂₃ as the dominant hydrocarbons in core sediments from both rivers. Due to higher solubility of the short-chain n-alkanes (that probably aids their metabolism by microorganisms) compared to long-chain n-alkanes, the former are presumed to be more suitable substrates for microorganisms (Muri *et al.*, 2004). Thus, during the decomposition processes, short-chain n-alkanes are preferentially removed, attributing to the lower concentrations of short-chain n-alkanes.

Data: STB05A3.D01 Method: HCARBON1.MET Ch-1 RT: 8.93 Level: 233554 Atten: 8
 Chrom: STB05A3.C01 Back chrom:



Data: STB05A2.D01 Method: HCARBON1.MET Ch-1 RT: 10.97 Level: 249536 Atten: 8
 Chrom: STB05A2.C01 Back chrom:



Data: STB05A1.D01 Method: HCARBON1.MET Ch-1 RT: 6.75 Level: 446726 Atten: 9
 Chrom: STB05A1.C01 Back chrom:

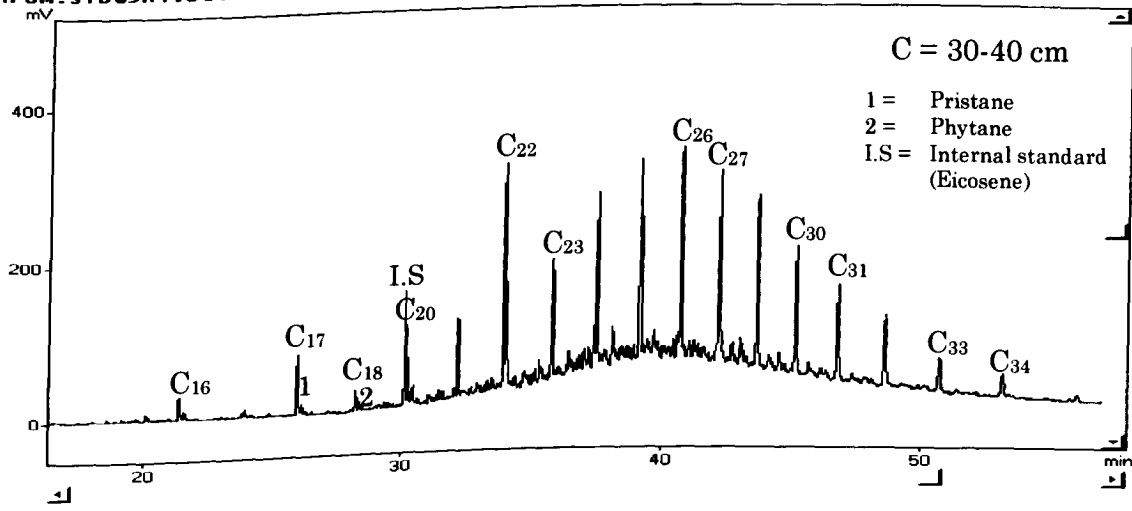
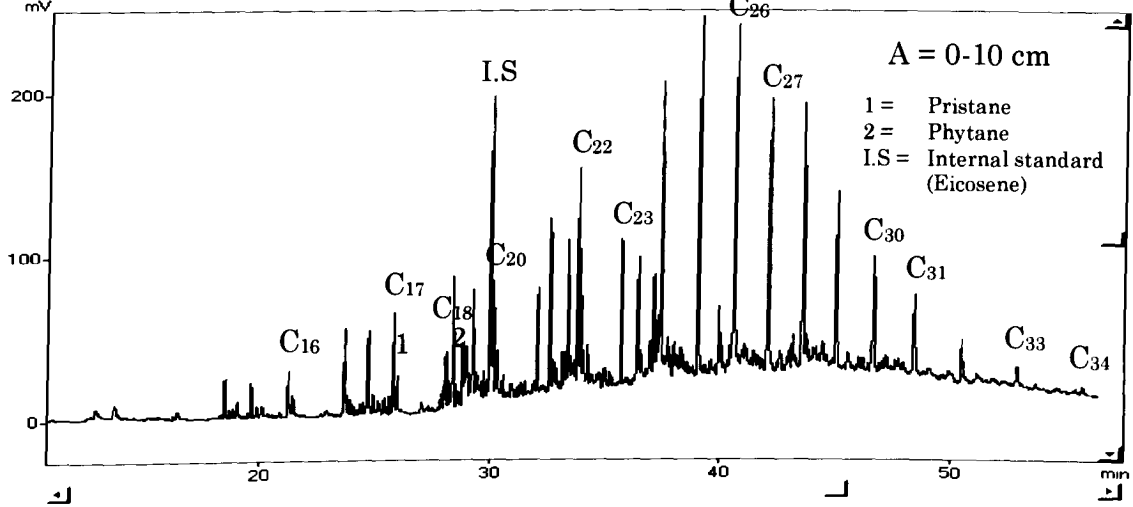
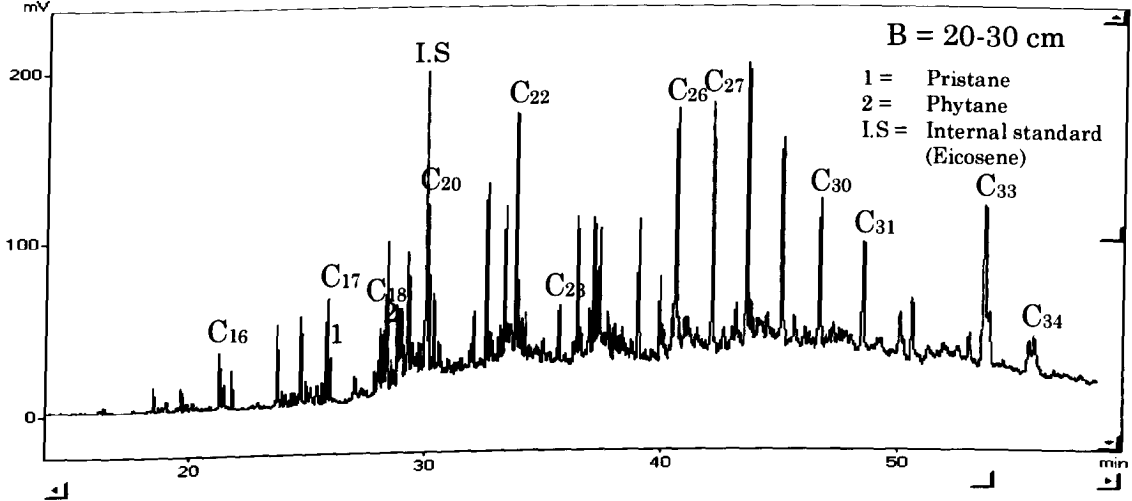


Figure 4.7: GC/FID chromatograms of aliphatic hydrocarbon fractions in core sediments from SSTB01 at three different layers

Data: MTB03A1.D01 Method: HCARBON1.MET Ch-1 RT: 12.99 Level: 243350 Atten: 8
 Chrom: MTB03A1.C01 Back chrom:



Data: MTB03A2.D01 Method: HCARBON1.MET Ch-1 RT: 13.91 Level: 220475 Atten: 8
 Chrom: MTB03A2.C01 Back chrom:



Data: MTB03A3.D01 Method: HCARBON1.MET Ch-1 RT: 19.20 Level: 253991 Atten: 8
 Chrom: MTB03A3.C01 Back chrom:

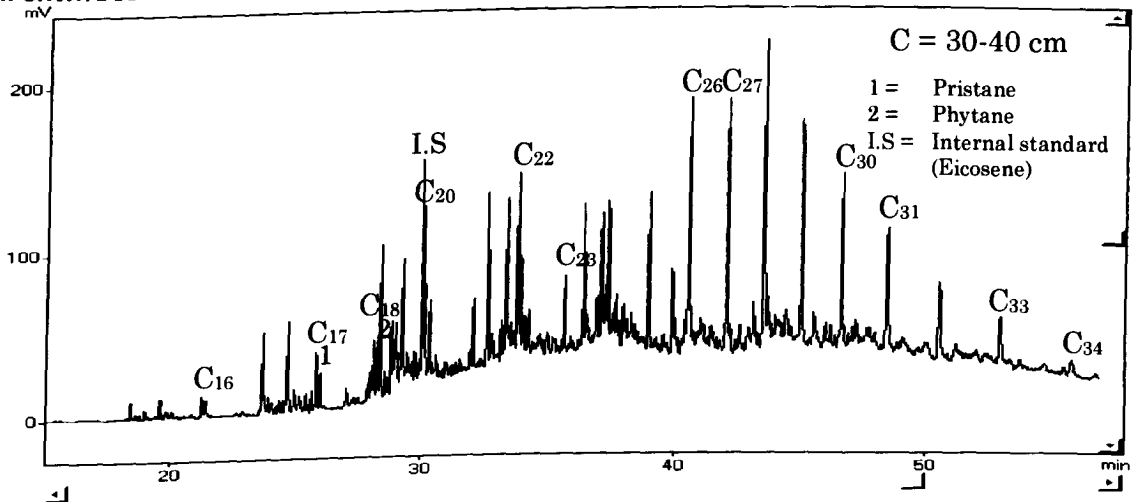


Figure 4.8: GC/FID chromatograms of aliphatic hydrocarbon fractions in core sediments from SSWK01 at three different layers

Table 4.6: Concentrations of n-alkanes in core sediments from Santubong River

n-alkane	Concentrations (ng/g dw)														
	SSTB01			SSTB02			SSTB03			SSTB04			SSTB05		
	A	C	D	A	C	D	A	D	F	A	C	E	A	C	D
C ₁₂	n.d	n.d	n.d	n.d	19	45	n.d	n.d	n.d	n.d	n.d	13	n.d	n.d	n.d
C ₁₃	n.d	n.d	n.d	n.d	7	12	n.d	n.d	n.d	n.d	n.d	13	n.d	n.d	n.d
C ₁₄	10	10	5	7	34	27	10	15	n.d	39	35	30	12	14	56
C ₁₅	85	83	72	255	226	53	n.d	n.d	n.d	82	66	17	114	74	69
C ₁₆	47	39	37	67	65	62	64	60	56	113	111	88	41	32	28
C ₁₇	293	271	221	482	315	255	161	132	79	122	82	79	431	314	249
Pri	73	67	54	79	67	61	94	79	48	68	52	51	186	116	90
C ₁₈	83	75	63	86	72	68	309	264	187	164	150	129	474	259	210
Phy	67	61	49	70	60	57	271	245	173	152	141	119	372	216	170
C ₁₉	90	83	109	283	269	106	515	414	399	258	248	241	407	347	118
C ₂₀	389	329	400	409	392	347	566	507	693	368	363	332	468	372	321
C ₂₁	1135	994	1150	1221	1087	627	1833	1236	1678	989	723	494	1327	973	318
C ₂₂	4380	3673	3687	4168	3726	1844	3274	2998	1581	2571	1226	635	4742	3169	844
C ₂₃	3375	3166	2720	3409	3368	861	2876	2788	1446	2474	1689	676	3592	2632	601
C ₂₄	6373	5789	4708	5956	5734	1180	5582	4031	3899	4092	3735	2017	6381	3636	2974
C ₂₅	7975	7669	5761	7988	6942	1162	7053	5767	5241	4504	3177	642	8870	4778	1391
C ₂₆	8264	8152	6100	8116	8281	1948	8283	6166	6351	5208	3812	2481	9790	5145	1287
C ₂₇	13993	8552	7860	9569	9437	958	7576	7475	8169	7686	2777	2693	10726	5865	1369
C ₂₈	11277	9651	6532	10023	10084	336	7193	8947	7482	5274	1977	2191	8819	7426	1105
C ₂₉	10264	8612	7467	9850	9824	653	7189	7174	7281	4747	2450	1866	7168	7128	2039
C ₃₀	11479	8672	5300	10583	10091	191	6512	7464	6936	3984	1636	1081	7771	7646	1103
C ₃₁	8811	6865	4356	8039	7616	202	5804	4610	4291	2876	1532	1087	7430	4535	592
C ₃₂	6457	5182	4752	5655	4964	n.d	5807	4402	3914	1678	959	n.d	4693	4176	792
C ₃₃	4860	3676	2800	3972	3640	n.d	4253	3386	2983	1139	673	n.d	3590	3253	n.d
C ₃₄	1450	899	408	1253	1584	n.d	n.d	1684	1236	375	131	n.d	1379	357	n.d

Notes: A = 0-10 cm; C = 20-30 cm; D = 30-40 cm; E = 40-50 cm; F = 50-60 cm; pri = pristane; phy = phytane and n.d = not detected

Table 4.7: Concentrations of n-alkanes in core sediments from Sarawak River

n-alkane	Concentrations (ng/g dw)																					
	SSWK01			SSWK02			SSWK03			SSWK04		SSWK05			SSWK06		SSWK07		SSWK08		SSWK09	
	A	C	E	A	C	D	A	C	D	A	B	A	B	C	A	B	A	B	A	B	A	B
C ₁₂	36	15	n.d	n.d	n.d	29	87	5	n.d	n.d	n.d	n.d	n.d	n.d	n.d	n.d	n.d	n.d	n.d	n.d	n.d	n.d
C ₁₃	14	9	n.d	n.d	n.d	7	11	12	n.d	n.d	n.d	n.d	n.d	n.d	1	n.d	n.d	n.d	n.d	n.d	n.d	n.d
C ₁₄	42	25	24	83	22	38	40	71	16.2	n.d	n.d	n.d	n.d	13	2	n.d	3.7	n.d	n.d	n.d	n.d	1
C ₁₅	71	66	43	93	91	84	141	129	51	n.d	n.d	34	32	28	n.d	n.d	n.d	n.d	n.d	n.d	n.d	n.d
C ₁₆	101	97	89	113	95	90	258	257	155	22	21	33	31	26	13	11	25	12	12	12	22	20
C ₁₇	166	151	125	237	217	191	335	215	143	32	21	34	29	25	23	20	25	21	31	24	30	26
Pri	90	83	66	101	86	83	90	70	49	27	17	23	20	18	17	13	21	17	27	22	28	24
C ₁₈	426	337	244	434	372	280	230	192	138	117	71	129	122	99	98	76	112	85	112	97	124	113
Phy	117	110	85	116	100	96	86	69	50	107	67	97	93	83	80	63	101	73	101	85	115	101
C ₁₉	664	507	385	631	566	548	420	374	287	71	60	73	72	68	89	65	67	61	64	62	72	66
C ₂₀	380	390	498	563	586	429	257	599	207	275	399	386	360	438	345	499	756	238	311	425	442	384
C ₂₁	686	480	740	1324	1190	1113	920	691	386	364	89	115	127	138	103	105	239	95	187	102	144	99
C ₂₂	1469	1767	1037	2463	1549	1862	2382	1643	1223	1228	1034	2365	2353	1610	2087	1952	1762	934	1308	1029	1944	1142
C ₂₃	1455	1029	921	1847	2218	1041	2172	2200	421	1007	949	2400	1727	830	2240	2119	1776	764	1081	1072	2165	1262
C ₂₄	3422	1948	2999	2318	2977	2159	2759	4050	510	1189	719	2028	1387	1723	3495	1625	3448	763	792	1113	1906	1353
C ₂₅	4653	3697	2110	3245	2690	2434	4048	3509	723	896	617	1992	1839	1584	4475	1553	5527	1262	697	493	3244	1306
C ₂₆	6898	4594	3339	6553	4267	4930	4297	4491	1036	560	412	2415	1248	902	4255	4144	4023	994	562	280	2140	1788
C ₂₇	6568	3573	3666	5249	5287	3665	4472	3572	2891	575	535	6248	2924	921	4483	4053	4313	2045	658	368	1771	1575
C ₂₈	6243	5715	3558	6389	5879	4198	4654	3207	2046	252	322	2518	1265	529	4243	3652	3081	1140	478	279	1226	253
C ₂₉	5025	5176	3176	7061	5142	4359	4409	3461	2821	701	596	4277	1859	2340	4197	2979	4134	1325	777	574	1731	1623
C ₃₀	4278	5915	3030	7504	6783	4124	4386	2297	1855	297	238	2861	2094	1556	2557	396	2431	1099	333	302	651	221
C ₃₁	7868	5761	4073	5658	4537	4091	3257	2345	295	1345	984	8810	4706	2250	2547	1190	3022	2142	923	734	1824	908
C ₃₂	3100	4590	5375	4330	3308	4075	2431	1276	269	319	215	1511	650	463	657	234	827	720	144	148	382	159
C ₃₃	3138	3739	4642	3579	2945	2887	1973	944	n.d	434	245	2249	1760	899	532	494	755	425	221	142	650	305
C ₃₄	2368	5047	1684	2016	1837	1703	545	165	n.d	n.d	n.d	n.d	n.d	n.d	148	n.d	n.d	n.d	n.d	n.d	n.d	n.d

Notes: A = 0-10 cm; B = 10-20 cm; C = 20-30 cm; D = 30-40 cm; E = 40-50 cm; pri = pristane; phy = phytane and n.d = not detected

According to Jeng (2006), a trend of $C_{25} < C_{27} < C_{29} < C_{31}$ indicates a biogenic source which is typical for tropical sources. However, all samples from both Santubong River and Sarawak River did not exhibit $C_{25} < C_{27} < C_{29} < C_{31}$ trend and this indicates petrogenic sources of n-alkanes (Jeng, 2006). Based on the observations above, it can be assumed that n-alkanes in the core sediments from both rivers originated from a mixture of terrestrial and petrogenic sources.

The spatial distribution trend for high molecular weight (HMW) n-alkanes ($>C_{23}$) in the upper layer of sediments from Santubong River and Sarawak River are presented in Figures 4.9 and 4.10, respectively. The vertical distribution trend for HMW n-alkanes in core sediments from Santubong River and Sarawak River are shown in Figures 4.11 and 4.12, respectively.

The concentrations of HMW n-alkanes in sediments from Santubong River decreased with increasing distance from the estuary until station SSTB04, before increasing further upstream (SSTB05). The highest concentration of HMW n-alkanes was observed in the surficial sediment of SSTB01 and this indicates that SSTB01 can be considered as the point source for HMW n-alkanes. SSTB01 which located at the estuary may have received biogenic HMW n-alkanes inputs from the mangrove areas. The concentration of HMW n-alkanes in the surface sediment of SSTB05 is also relatively high, indicating other additional sources of HMW n-alkanes compared to those found in other sediments. SSTB05 which located at the Bako Causeway may have received inputs of HMW n-alkanes from wood processing industries.

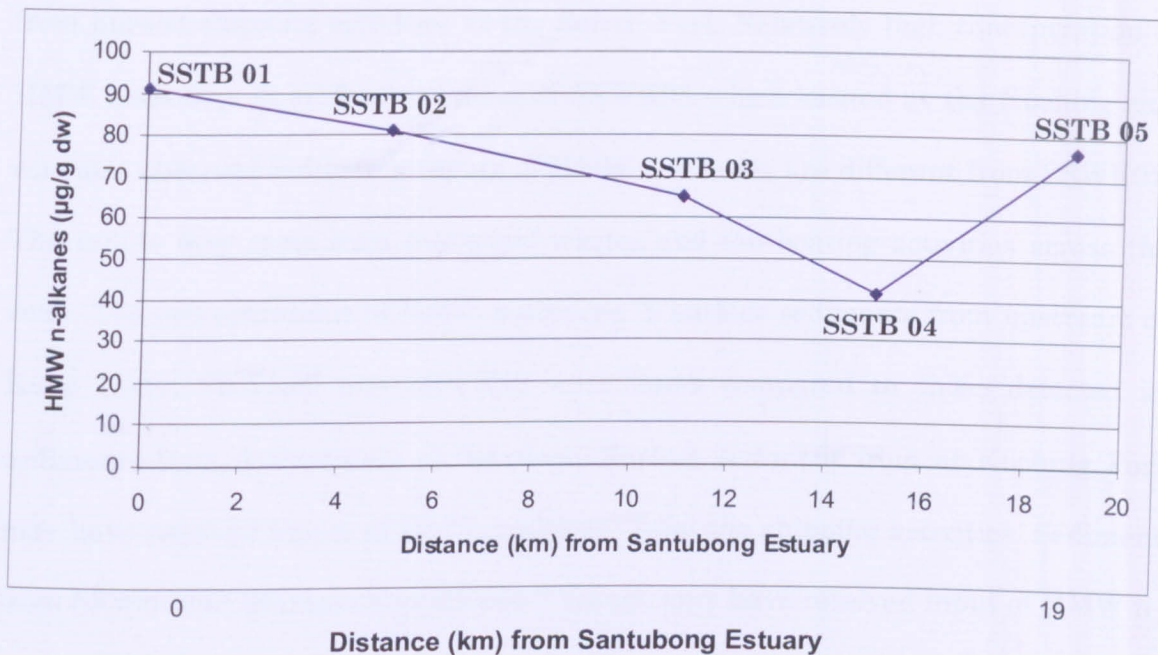


Figure 4.9: The spatial distribution of the HMW n-alkanes (>C₂₃) in the surficial sediments from Santubong River

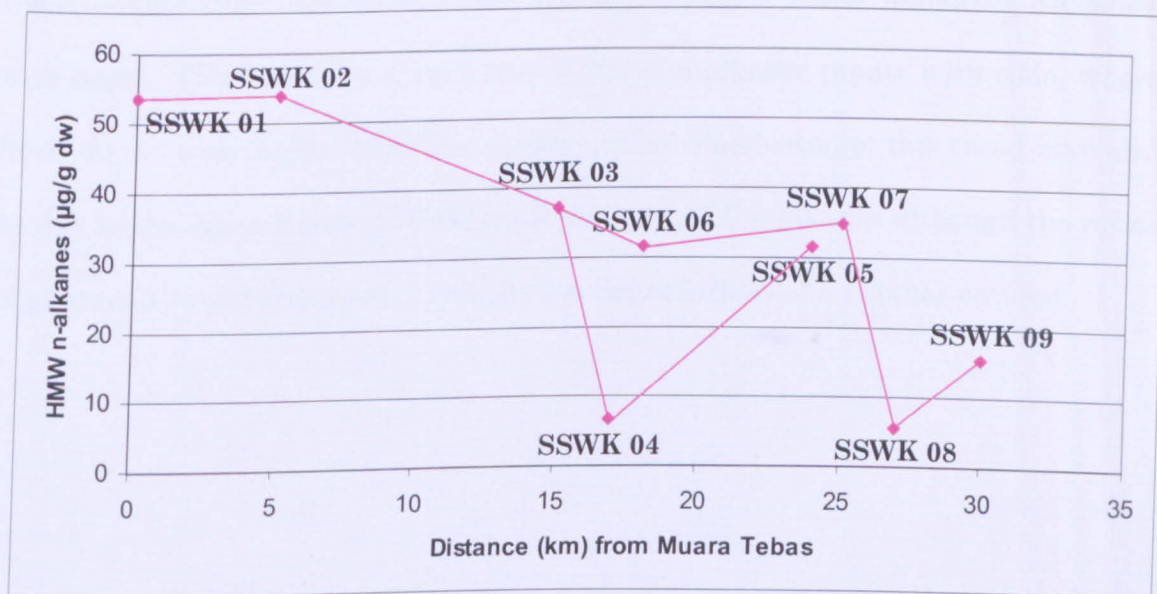


Figure 4.10: The spatial distribution of the HMW n-alkanes (>C₂₃) in the surficial sediments from Sarawak River

The concentrations of HMW n-alkanes in sediment from Sarawak River decreased toward upstream from SSWK01 and SSWK02 to SSWK04. Thus, SSWK02 can be considered as the point source for HMW n-alkanes in sediment particularly

from busiest shipping activities at the Senari Port. Relatively high concentration of HMW n-alkanes in surface sediment of SSWK05 which located at the Kuching city was also observed indicating inputs of HMW n-alkanes are different from SSWK02. The inputs may come from municipal wastes and the boating activities across the river. The concentrations of HMW n-alkanes in surface sediments from upstream of Kuap River, SSWK08 and SSWK09 were lower compared to those detected in sediments from downstream of the river. Surface sediment from at Kuching Port may have received inputs of HMW n-alkanes from the shipping activities. Sediment from SSWK09 at Stampin Resettlement Village may have received input of HMW n-alkanes from domestic wastes.

The vertical distributions of the HMW n-alkanes in core sediments from both rivers exhibit consistent trend where concentrations of HMW n-alkanes decreased with depth. This indicates a variation of HMW n-alkanes inputs with time, where fresh inputs were higher than the earlier inputs. Furthermore, this trend may also be due to the degradation of HMW n-alkanes to LMW n-alkanes although the ratios of pristane/C₁₇ and phytane/C₁₈ indicate low degradations of n-alkanes occurred.

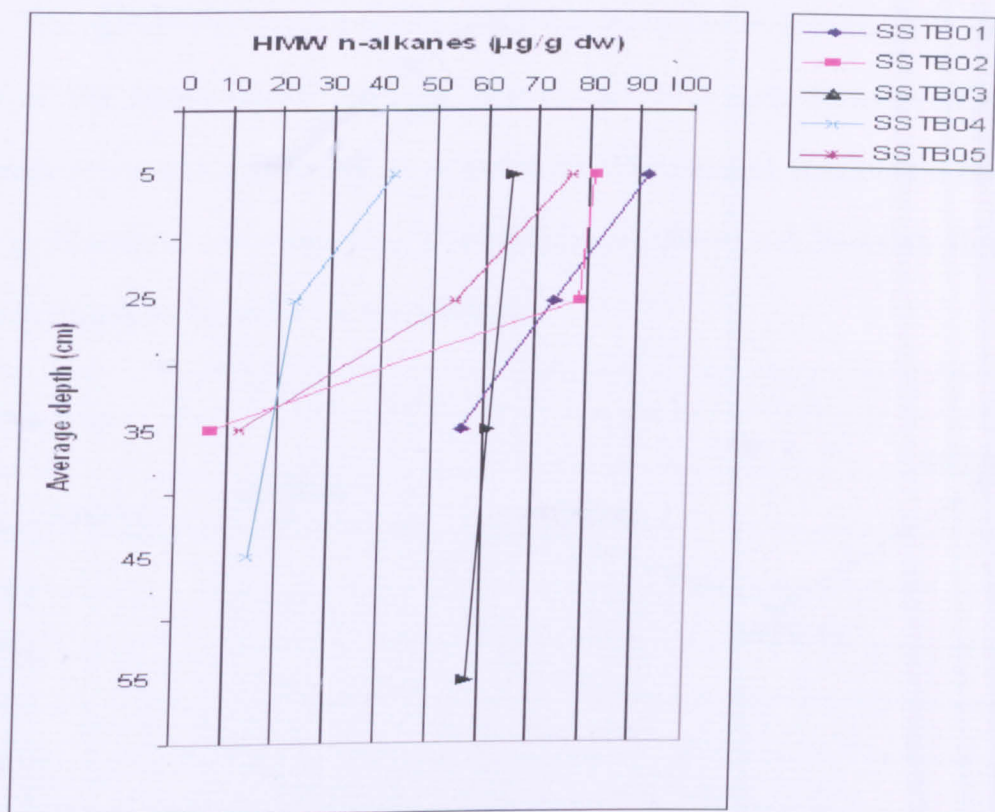


Figure 4.11: The vertical distribution of HMW n-alkanes ($>C_{23}$) in the core sediments from Santubong River

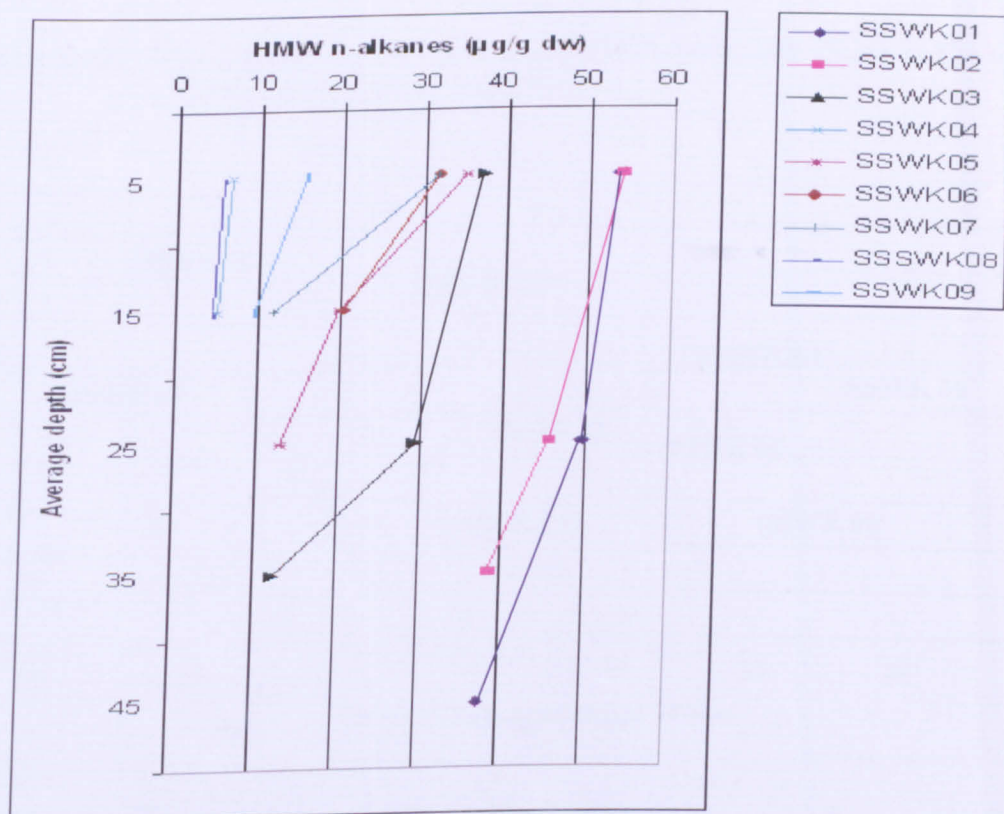


Figure 4.12: The vertical distribution of HMW n-alkanes ($>C_{23}$) in the core sediments from Sarawak River

The spatial distribution trends of the low molecular weight (LMW) n-alkanes ($\leq C_{23}$) in the upper sediments from Santubong River and Sarawak River are presented in Figures 4.13 and 4.14, respectively. The vertical distribution trends of LMW n-alkanes in core sediments from Santubong River and Sarawak River are shown in Figures 4.15 and 4.16, respectively.

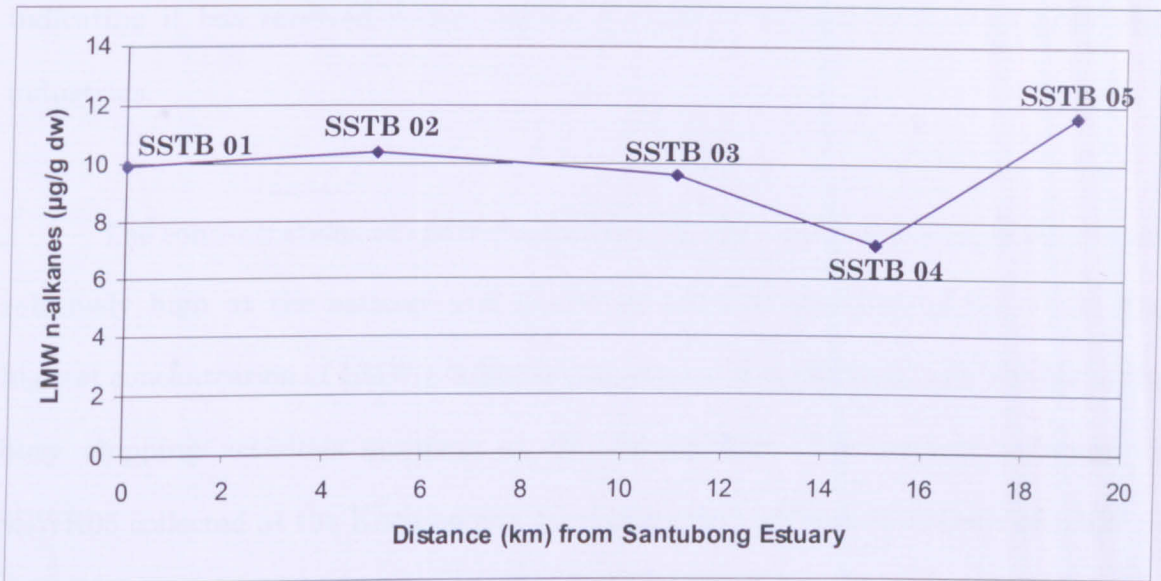


Figure 4.13: The spatial distribution of the LMW n-alkanes ($\leq C_{23}$) in the surficial sediments from Santubong River

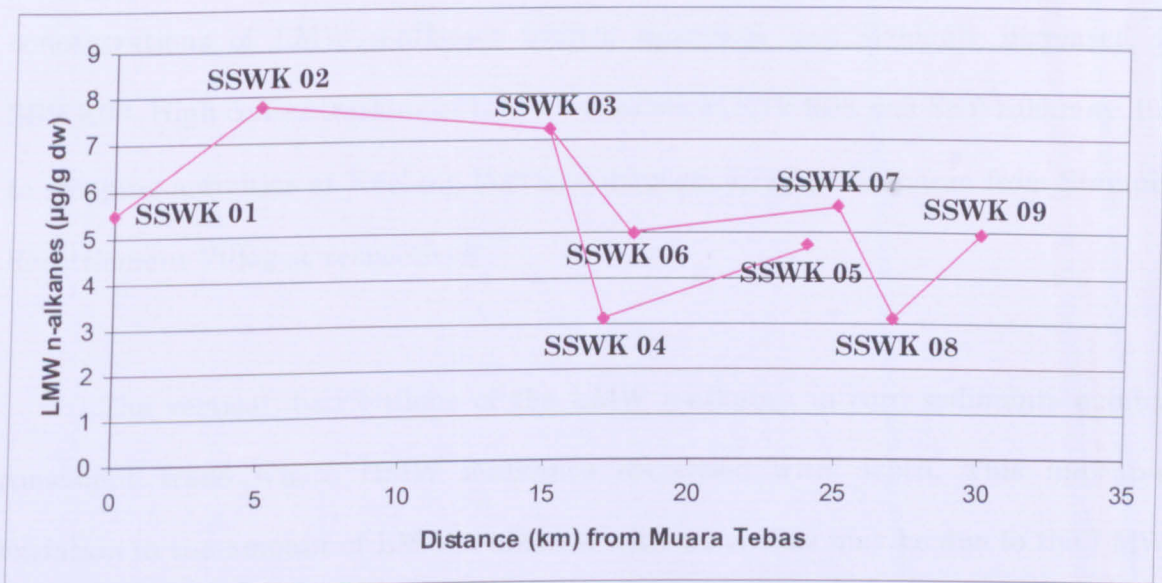


Figure 4.14: The spatial distribution of the LMW n-alkanes ($\leq C_{23}$) in the surficial sediments from Sarawak River

The concentrations of LMW n-alkanes in sediments from Santubong River decreased toward upstream from SSTB01 to SSTB04 and then increased at SSTB05. This may be due to different rate of n-alkanes degradation, where degradation of HMW n-alkanes caused high concentrations of LMW n-alkanes. The highest concentration of LMW n-alkanes was observed in the surface sediment of SSTB05 indicating it has received recent inputs of LMW n-alkanes from wood processing industries.

The concentrations of LMW n-alkanes in sediments from Sarawak River were relatively high at the estuary and decreased toward upstream of the river. The highest concentration of LMW n-alkanes was observed at SSWK02 may be due to the busy shipping activities occurring at the Senari Port. The surface sediment of SSWK05 collected at the Kuching city has relatively high concentrations of LMW n-alkanes indicating other inputs of LMW n-alkanes than those found in SSWK02 such as municipal sewage and from small boating activities across the river. The surficial sediments from Kuap River (Sarawak River tributary) showed a decrease in the concentrations of LMW n-alkanes toward upstream and suddenly increased at SSWK09. High concentrations of LMW n-alkanes at SSWK06 and SSWK09 may due to shipping activities at Kuching Port and domestic sewage discharge from Stampin Resettlement Villages, respectively.

The vertical distributions of the LMW n-alkanes in core sediments exhibit consistent trend where HMW n-alkanes decreased with depth. This indicates variation in the amount of LMW n-alkanes with time. This may be due to the LMW n-alkanes received and also due to degradation of LMW n-alkanes although low

degradations of n-alkanes occurred was observed as shown by the pristane/C₁₇ and phytane/C₁₈ ratios.

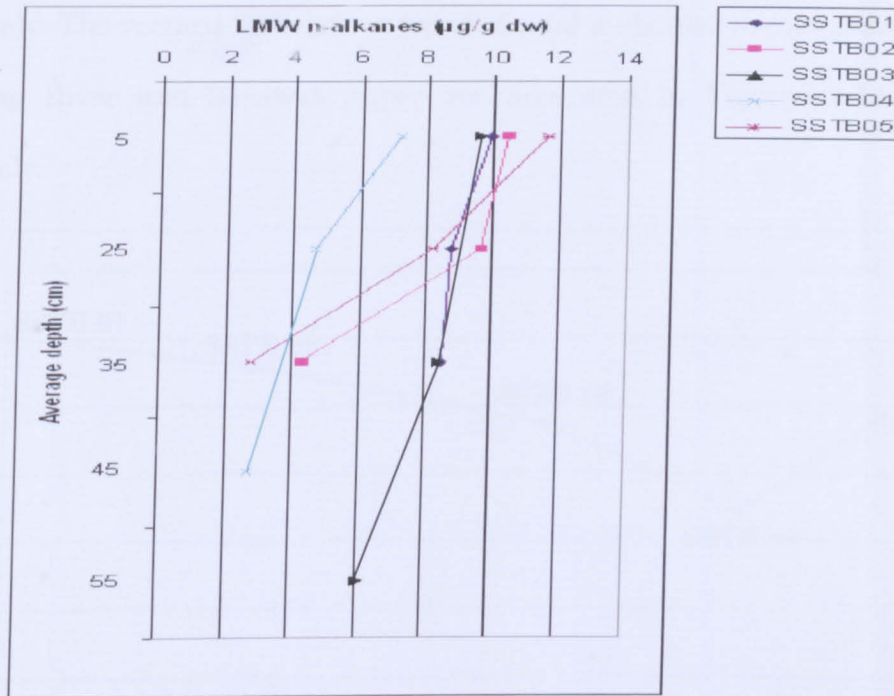


Figure 4.15: The vertical distribution of the LMW n-alkanes ($\leq C_{23}$) in the core sediments from Santubong River

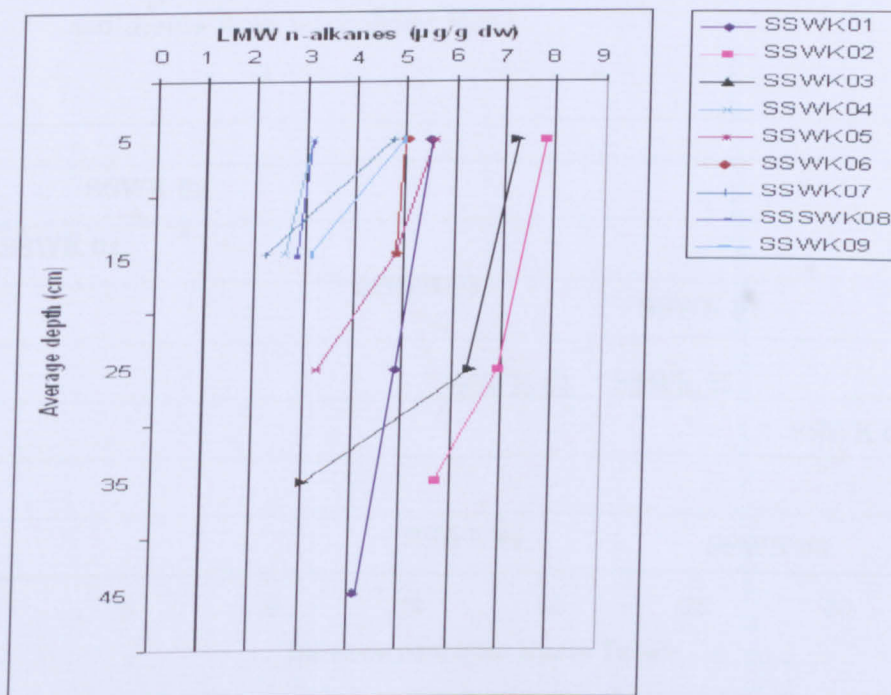


Figure 4.16: The vertical distribution of the LMW n-alkanes ($\leq C_{23}$) in the core sediments from Sarawak River

Figures 4.17 and 4.18 show the spatial distribution trends of the total n-alkanes in the surface sediments of Santubong River and Sarawak River, respectively. The vertical distribution trend of total n-alkanes in core sediments from Santubong River and Sarawak River are presented in Figures 4.19 and 4.20, respectively.

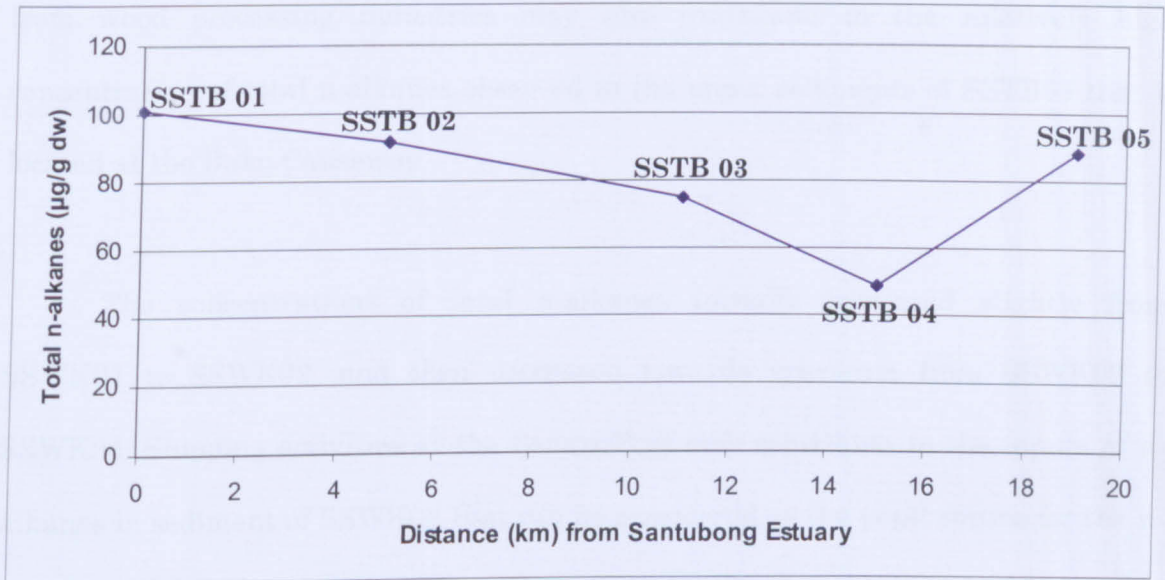


Figure 4.17: The spatial distribution of the total n-alkanes in the surficial sediments from Santubong River

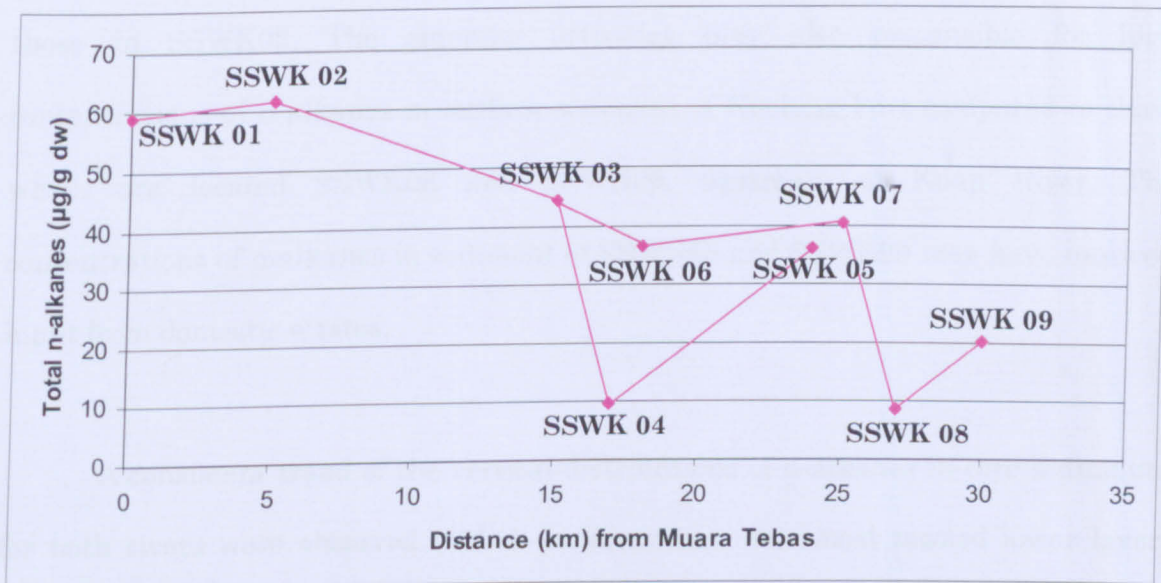


Figure 4.18: The spatial distribution of the total n-alkanes in the surficial sediments from Sarawak River

The concentrations of total n-alkanes in sediments from Santubong River show a decrease toward upstream and increased at SSTB05. SSTB01 can be considered as the point source for total n-alkanes especially of biogenic inputs from the mangrove areas as the highest concentration of total n-alkanes was observed in the estuarine sediment of SSTB01. Other additional inputs of n-alkanes such as from wood processing industries may also contribute to the relatively high concentration of total n-alkanes observed in the upper sediments of SSTB05 that is located at the Bako Causeway.

The concentrations of total n-alkanes initially increased slightly from SSWK01 to SSWK02, and then decreased towards upstream from SSWK02 to SSWK04. Shipping activities at the Senari Port may contribute to the inputs of n-alkanes in sediment of SSWK02 that can be considered as the point source for the n-alkanes in sediment from Sarawak River. Municipal wastes and the boating activities across the river are other additional sources of n-alkanes in the surface sediment of SSWK05 since concentration of total n-alkanes was higher compared to those in SSWK02. The shipping activities may also responsible for high concentrations of n-alkanes in surface sediment of Kuching Port compared to those which are located SSWK08 and SSWK09, upstream of Kuap River. The concentrations of n-alkanes in sediment of SSWK08 and SSWK09 may have received input from domestic wastes.

A consistent trend of the vertical distributions of n-alkanes in core sediments for both rivers were observed with it concentration decreased toward lower layer. This indicates a degradation of n-alkanes and also variation of n-alkanes sources with time, where amount of recent inputs were higher than older inputs.

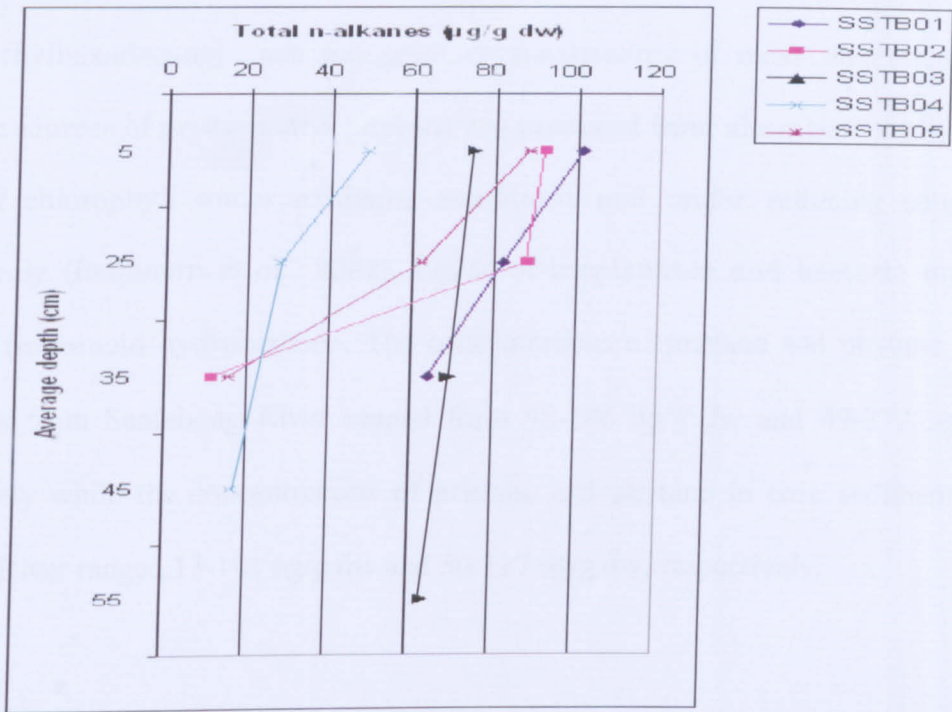


Figure 4.19: The vertical distribution of n-alkanes in the core sediments from Santubong River

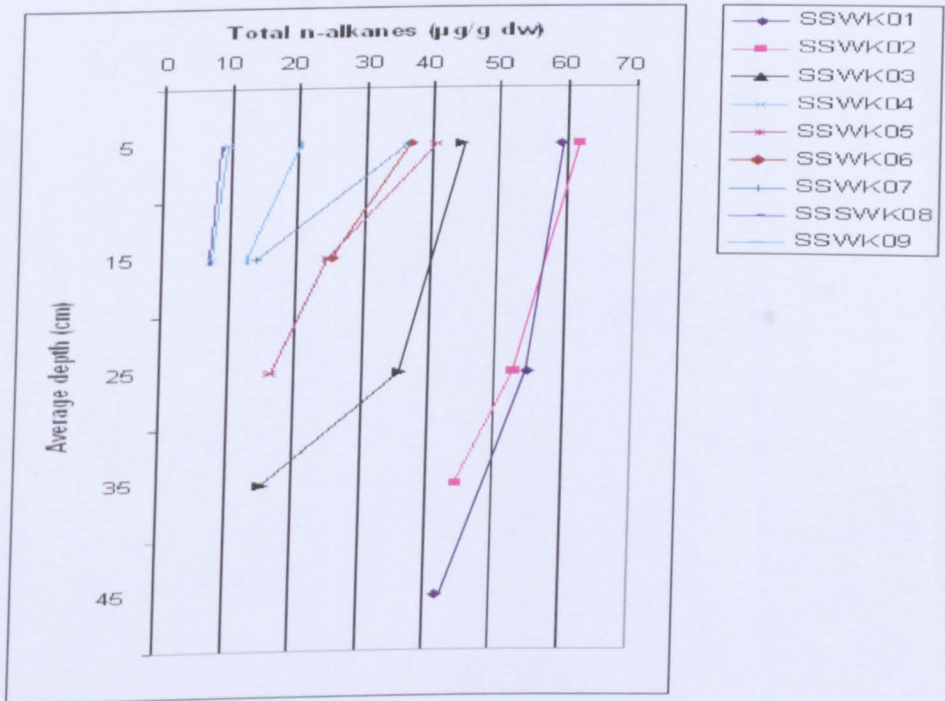


Figure 4.20: The vertical distribution of n-alkanes in the core sediments from Sarawak River

Pristane (2,6,10,14-tetramethylpentadecane) and phytane (2,6,10,14-tetramethylhexadecane) are not primary constituents of most terrestrial biota. Biogenic sources of pristane and phytane are produced from alteration of phytol side chain of chlorophyll under oxidising conditions and under reducing conditions, respectively (Readman *et al.*, 2002). Lipids of zooplankton and bacteria may also produce isoprenoid hydrocarbons. The concentrations of pristane and phytane in core sediments from Santubong River ranged from 48-186 ng/g dw and 49-372 ng/g dw, respectively while the concentrations of pristane and phytane in core sediments from Sarawak River ranged 13-101 ng/g dw and 50-117 ng/g dw, respectively.

4.4 Polycyclic Aromatic Hydrocarbons

4.4.1 PAHs Standard Mixture

The gas chromatogram obtained from GC/FID analysis of a mixture of authentic PAHs standard containing 16 individual PAHs is shown in Figure 4.21. The retention times for the 16 individual PAHs are presented in Table 4.8 while the RF values for the individual PAHs are shown in Table 4.9. Details on the molecular structures and molecular weights for the 16 individual PAHs are presented in Appendix B.

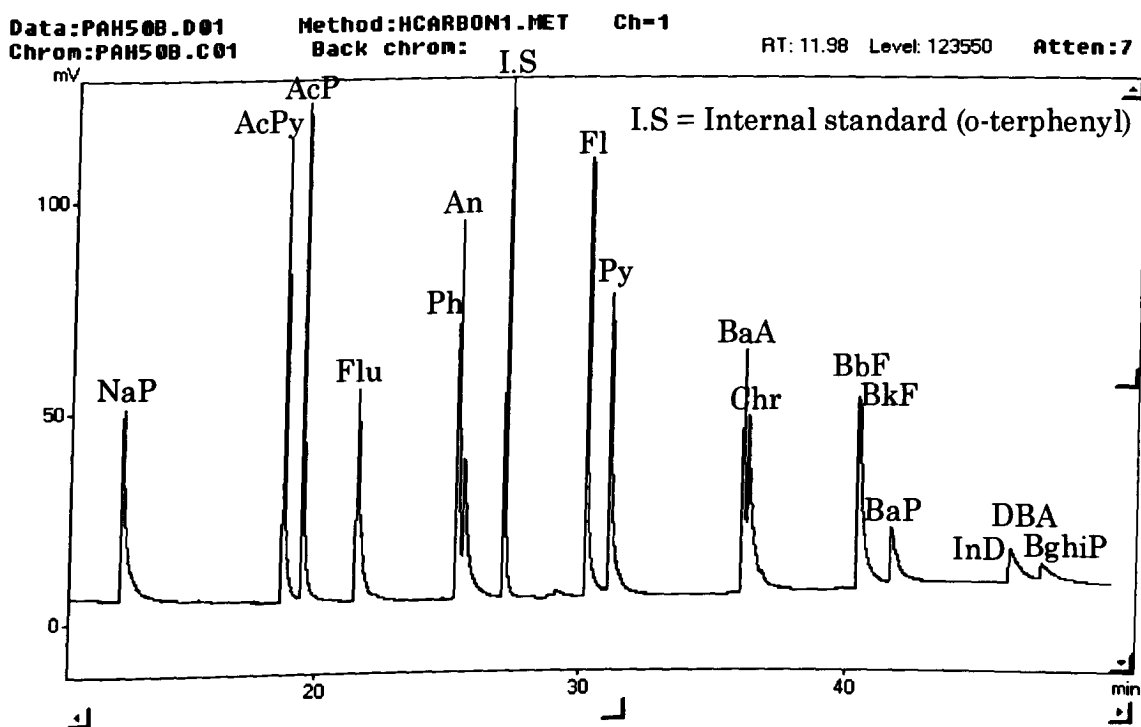


Figure 4.21: Gas chromatogram from GC/FID analysis of PAHs in a standard mixture

Table 4.8: Retention times for 16 individual PAHs

Compounds	Molecular formula	Retention Time (RT) (n=3)
Naphthalene	C ₁₀ H ₈	12.57 ± 0.01
Acenaphthylene	C ₁₂ H ₈	18.63 ± 0.01
Acenaphthene	C ₁₂ H ₁₀	19.34 ± 0.01
Fluorene	C ₁₃ H ₁₀	21.42 ± 0.02
Phenanthrene	C ₁₄ H ₁₀	25.20 ± 0.01
Anthracene	C ₁₄ H ₁₀	25.40 ± 0.07
O-terphenyl – Internal standard	C ₁₈ H ₁₄	26.99 ± 0.01
Fluoranthene	C ₁₆ H ₁₀	30.06 ± 0.01
Pyrene	C ₁₆ H ₁₀	30.93 ± 0.01
Benzo[a]anthracene	C ₁₈ H ₁₂	36.00 ± 0.01
Chrysene	C ₁₈ H ₁₂	36.18 ± 0.01
Benzo[b]fluoranthene	C ₂₀ H ₁₂	40.33 ± 0.01
Benzo[k]fluoranthene	C ₂₀ H ₁₂	40.40 ± 0.01
Benzo[a]pyrene	C ₂₀ H ₁₂	41.66 ± 0.08
Indeno[1,2,3-c,d]pyrene	C ₂₂ H ₁₂	46.13 ± 0.10
Dibenzo[a,h]anthracene	C ₂₂ H ₁₄	46.16 ± 0.11
Benzo[g,h,i]perylene	C ₂₂ H ₁₂	46.25 ± 0.12

Table 4.9: RF values for 16 individual PAHs using o-terphenyl as internal standard

Compounds	RF value (n=3)
Naphthalene (C ₁₀ H ₈)	1.63 ± 0.06
Acenaphthylene (C ₁₂ H ₈)	1.31 ± 0.06
Acenaphthene (C ₁₂ H ₁₀)	1.15 ± 0.03
Fluorene (C ₁₃ H ₁₀)	2.32 ± 0.04
Phenanthrene (C ₁₄ H ₁₀)	1.50 ± 0.05
Anthracene (C ₁₄ H ₁₀)	1.67 ± 0.05
Fluoranthene (C ₁₆ H ₁₀)	1.12 ± 0.01
Pyrene (C ₁₆ H ₁₀)	1.16 ± 0.01
Benzo[a]anthracene (C ₁₈ H ₁₂)	2.67 ± 0.05
Chrysene (C ₁₈ H ₁₂)	1.27 ± 0.05
Benzo[b]fluoranthene (C ₂₀ H ₁₂)	5.66 ± 0.06
Benzo[k]fluoranthene (C ₂₀ H ₁₂)	1.63 ± 0.06
Benzo[a]pyrene (C ₂₀ H ₁₂)	5.77 ± 0.07
Indeno[1,2,3-c,d]pyrene (C ₂₂ H ₁₂)	28.05 ± 0.08
Dibenzo[a,h]anthracene (C ₂₂ H ₁₄)	34.22 ± 0.08
Benzo[g,h,i]perylene (C ₂₂ H ₁₂)	31.70 ± 0.08

4.4.2 PAHs in Sediment Samples

The GC/FID chromatograms of PAHs fractions in core sediments from SSTB01 and SSWK01 stations are presented in Figures 4.22 and 4.23, respectively. Gas chromatograms for PAHs from other core sediments from Santubong River and Sarawak River are shown in Appendix C. Table 4.10 shows the effects-range low (ERL) and effects-range median (ERM) guideline values for PAHs (Long and Morgan, 1990). The concentrations of individual PAHs in core sediments from Santubong River and Sarawak River are shown in Tables 4.11 and 4.12, respectively.

Table 4.10: ERL and ERM guideline values for PAHs (ng/g dw) (Long and Morgan, 1990)

Compounds	ERL	ERM
Naphthalene	160	2100
Acenaphthylene	44	640
Acenaphthene	16	500
Fluorene	19	540
Phenanthrene	240	1500
Anthracene	85	1100
Fluoranthene	600	5100
Pyrene	665	2600
Benzo[a]anthracene	261	1600
Chrysene	384	2800
Benzo[a]pyrene	430	1600
Dibenzo[a,h]anthracene	63	260
Total PAHs	4022	44792

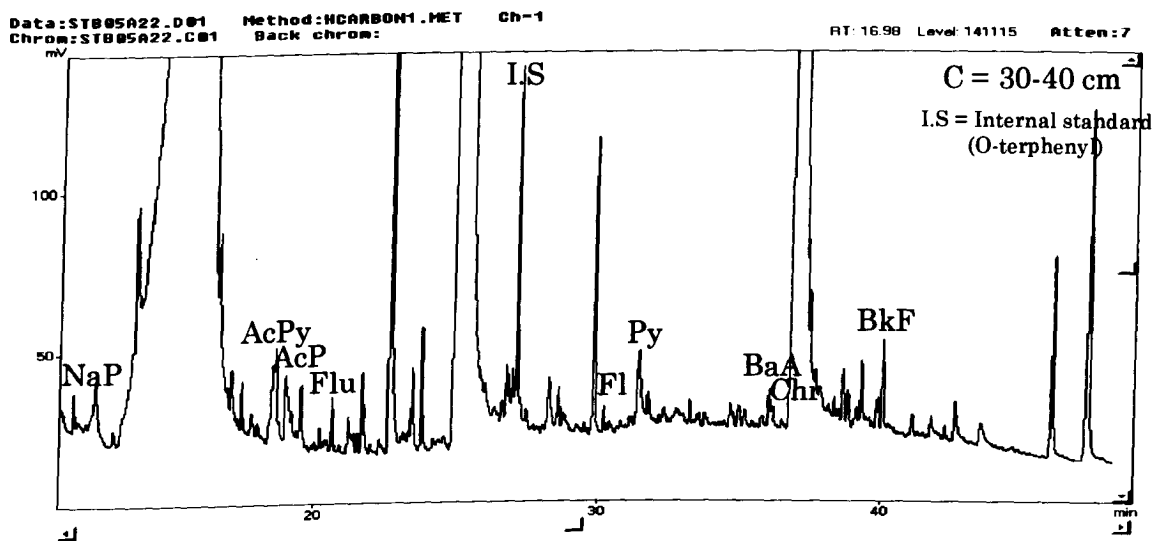
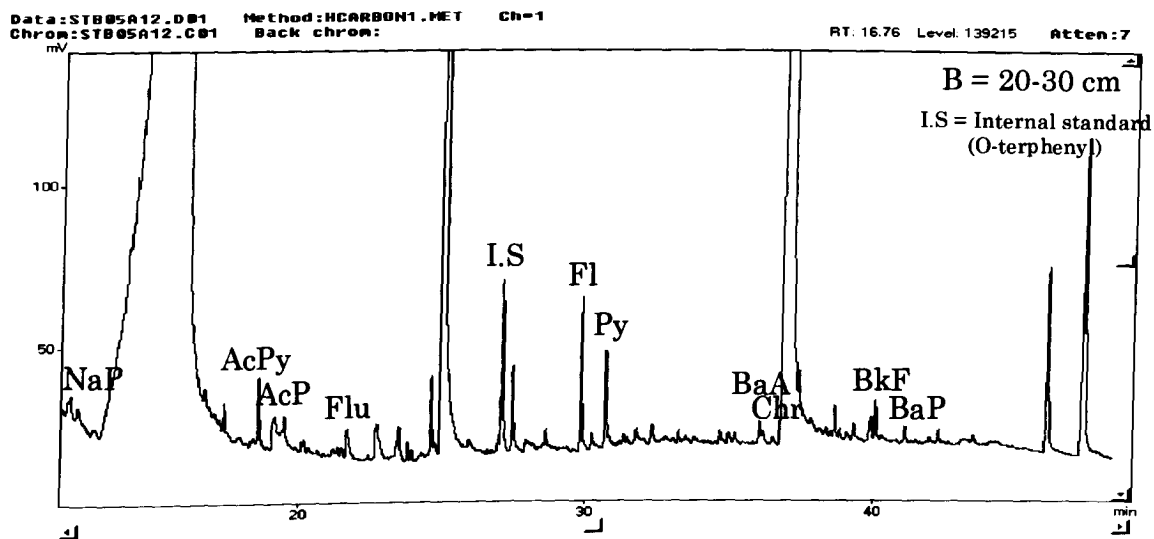
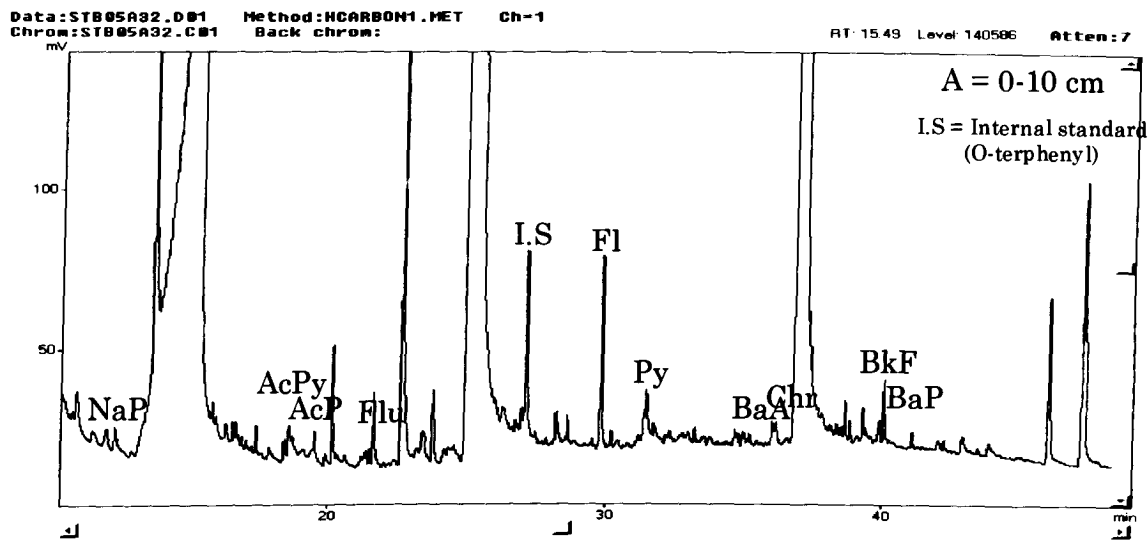


Figure 4.22: GC/FID chromatograms for PAHs fractions in core sediments from SSTB01 at three different layers

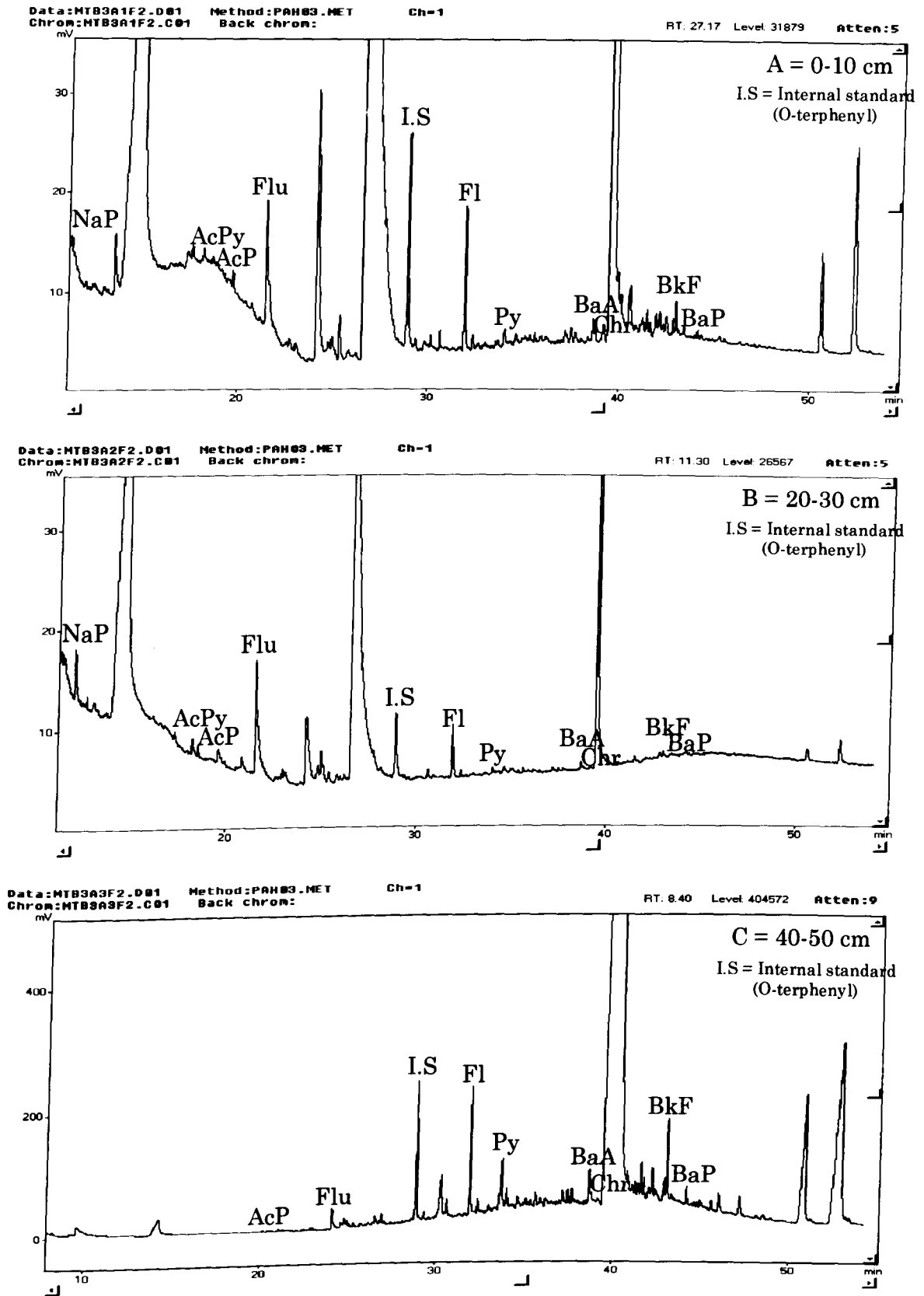


Figure 4.23: GC/FID chromatograms for PAHs fractions in core sediments from SSWK01 at three different layers

Table 4.11: Concentrations of PAHs in core sediments from Santubong River

PAHs	Concentrations (ng/g dw)														
	SSTB01			SSTB02			SSTB03			SSTB04			SSTB05		
	A	C	D	A	C	D	A	D	F	A	C	E	A	C	D
NaP	156	40	43	n.d	n.d	n.d	n.d	n.d	n.d	532	141	74	277	74	n.d
AcPy	191	104	47	80	66	n.d	109	100	57	176	63	81	144	110	n.d
AcP	52	58	101	103	88	n.d	92	106	50	20	66	46	208	186	157
Flu	180	143	46	74	52	n.d	300	237	253	54	225	90	175	82	n.d
Ph	n.d	n.d	n.d	n.d	n.d	93	n.d	n.d	n.d	n.d	n.d	n.d	n.d	n.d	61
An	n.d	n.d	n.d	n.d	n.d	96	n.d	n.d	n.d	n.d	n.d	n.d	n.d	n.d	28
Fl	46	35	29	36	25	17	370	244	47	436	272	35	94	78	25
Py	28	24	21	27	21	16	51	45	35	39	41	26	59	54	19
BaA	240	165	129	262	173	171	286	256	214	262	239	168	274	98	87
Chr	49	40	33	74	65	69	62	59	51	61	63	61	159	75	74
BbF	456	309	221	312	339	284	442	451	423	432	312	261	405	303	96
BkF	226	137	131	218	188	247	199	179	181	48	199	78	329	77	n.d
BaP	406	191	n.d	483	364	231	207	192	198	219	166	164	396	266	239
InD	n.d	n.d	n.d	n.d	n.d	n.d	n.d	n.d	n.d	146	n.d	n.d	n.d	n.d	n.d
DBA	n.d	n.d	n.d	n.d	n.d	n.d	n.d	n.d	n.d	n.d	n.d	n.d	n.d	n.d	n.d
BghiP	n.d	n.d	n.d	n.d	n.d	n.d	n.d	n.d	n.d	n.d	n.d	n.d	n.d	n.d	n.d

Notes: A = 0-10 cm; C = 20-30 cm; D = 30-40 cm; E = 40-50 cm; F= 50-60 cm and n.d = not detected

Table 4.12: Concentrations of PAHs in core sediments from Sarawak River

PAHs	Concentrations (ng/g dw)																					
	SSWK01			SSWK02			SSWK03			SSWK04		SSWK05			SSWK06		SSWK07		SSWK08		SSWK09	
	A	C	E	A	C	D	A	C	D	A	B	A	B	C	A	B	A	B	A	B	A	B
NaP	7	30	n.d	3	9	6	209	203	111	n.d	n.d	300	161	n.d	698	137	n.d	n.d	n.d	n.d	n.d	113
AcPy	18	3	n.d	1030	61	12	325	127	24	317	166	1173	n.d	n.d	462	102	244	40	256	n.d	312	271
AcP	73	19	3	126	249	68	275	139	191	301	157	n.d	280	222	120	86	419	294	n.d	189	n.d	168
Flu	74	40	13	325	297	151	126	27	16	227	158	714	446	203	469	216	526	576	705	257	194	241
Ph	736	579	332	n.d	6	23	212	123	28	n.d	n.d	n.d	307	212	n.d	203	n.d	n.d	n.d	115	652	n.d
An	325	324	86	n.d	12	5	18	24	15	n.d	n.d	n.d	n.d	n.d	n.d	136	n.d	n.d	n.d	n.d	n.d	n.d
Fl	50	30	20	100	49	36	88	81	70	168	82	283	239	209	193	104	284	153	164	142	325	198
Py	26	23	19	22	11	10	68	65	62	127	79	157	147	135	65	58	252	152	111	104	217	167
BaA	133	74	60	619	141	25	231	168	53	175	114	1178	723	504	324	297	562	353	408	313	540	474
Chr	20	12	11	125	35	16	92	70	34	125	93	634	429	383	291	288	455	351	310	280	320	299
BbF	14	21	22	111	4	12	61	21	5	496	491	1012	n.d	n.d	517	n.d	n.d	100	440	n.d	468	n.d
BkF	41	506	295	855	320	128	659	299	95	249	n.d	1230	1062	n.d	566	127	n.d	38	n.d	n.d	193	195
BaP	25	513	141	555	420	190	n.d	147	179	142	n.d	n.d	n.d	n.d	n.d	109	n.d	60	n.d	n.d	n.d	n.d
InD	944	n.d	n.d	42	n.d	n.d	n.d	n.d	n.d	n.d	n.d	n.d	n.d	n.d	n.d	n.d	n.d	n.d	n.d	n.d	n.d	n.d
DBA	42	n.d	n.d	n.d	n.d	n.d	n.d	n.d	n.d	n.d	n.d	n.d	n.d	n.d	n.d	n.d	n.d	n.d	n.d	n.d	n.d	n.d
BghiP	164	n.d	n.d	n.d	n.d	n.d	321	n.d	n.d	n.d	n.d	n.d	n.d	n.d	n.d	n.d	n.d	n.d	n.d	n.d	n.d	n.d

Notes: A = 0-10 cm; B = 10-20 cm; C = 20-30 cm; D = 30-40 cm; E = 40-50 cm and n.d = not detected

Three most abundant PAHs detected in core sediments from Santubong River were benzo[k]fluoranthene, benzo[a]pyrene and benzo[a]anthracene with concentrations ranging from n.d-328.5, n.d-483.4 and 86.6-285.5 ng/g dw, respectively. Dibenzo[a,h]anthracene and benzo[g,h,i]perylene were not detected in core sediments from Santubong River while three most abundant PAHs identified in core sediments from Sarawak River were benzo[a]anthracene, benzo[k]fluoranthene and fluorene with concentrations ranging from 24.7-1178.4, n.d-1229.8 and 12.7-714.0 ng/g dw, respectively. Indeno[1,2,3-c,d]pyrene, dibenzo[a,h]anthracene and benzo[g,h,i]perylene were not detected in most of Sarawak River core sediments except in surface sediment of SSWK01. Indeno[1,2,3-c,d]pyrene and benzo[g,h,i]perylene were detected in core sediments from SSWK02 and SSWK03, respectively.

The core sediments from Santubong River and Sarawak were assessed by comparing the PAHs concentrations with ERL and ERM values (Table 4.11). There was at least one individual PAH with concentration higher than the ERL value observed for all sediment from both rivers and this may pose biological impairments (Long and Morgan, 1990). However, there was no core sediments from Santubong River with the concentrations of individual PAHs higher than the ERM value. Five PAHs with concentrations higher than the ERL were detected in surface sediments from SSTB02, SSTB04 and SSTB05. The concentrations of acenaphthylene, acenaphthene, fluorene, benzo[a]anthracene and benzo[a]pyrene exceeded the ERL in surface sediment of SSTB02 while the concentrations of naphthalene, acenaphthylene, acenaphthene, fluorene and benzo[a]anthracene exceeded the ERL in surface sediments from SSTB04 and SSTB05.

A few PAHs with concentrations higher than the ERM value were observed in several of the Sarawak River core sediments. The concentrations of acenaphthylene in surface sediments from SSWK02 and SSWK05 and the concentrations of fluorene in surface sediments from SSWK05, SSWK07 and SSWK08 exceeded the ERM value. The PAHs concentrations higher than the ERM values indicate possibility of biological impairment (Long and Morgan, 1990). Six PAHs with concentrations higher than the ERL value were observed in lower layer of core sediments (10-20 cm) from SSWK05. The concentrations of naphthalene, acenaphthene, fluorene, phenanthrene, benzo[a]anthracene and chrysene exceeded the ERL value in lower layer of core sediment (10-20 cm) from SSWK05.

The spatial distribution of the HPAHs in the surface sediments of Santubong River and Sarawak River are presented in Figures 4.24 and 4.25, respectively. The vertical distribution trend of HPAHs in core sediments from Santubong River and Sarawak River are shown in Figures 4.26 and 4.27, respectively. The concentrations of HPAHs in core sediments from Santubong River were almost similar for all sampling stations with no obvious variation in their concentrations. The highest concentration of HPAHs was detected in the surface sediment of SSTB05 indicating that SSTB05 which located at the Bako Causeway is the point source for HPAHs. The sources of pyrolytic PAHs might be from wood processing industries located nearby.

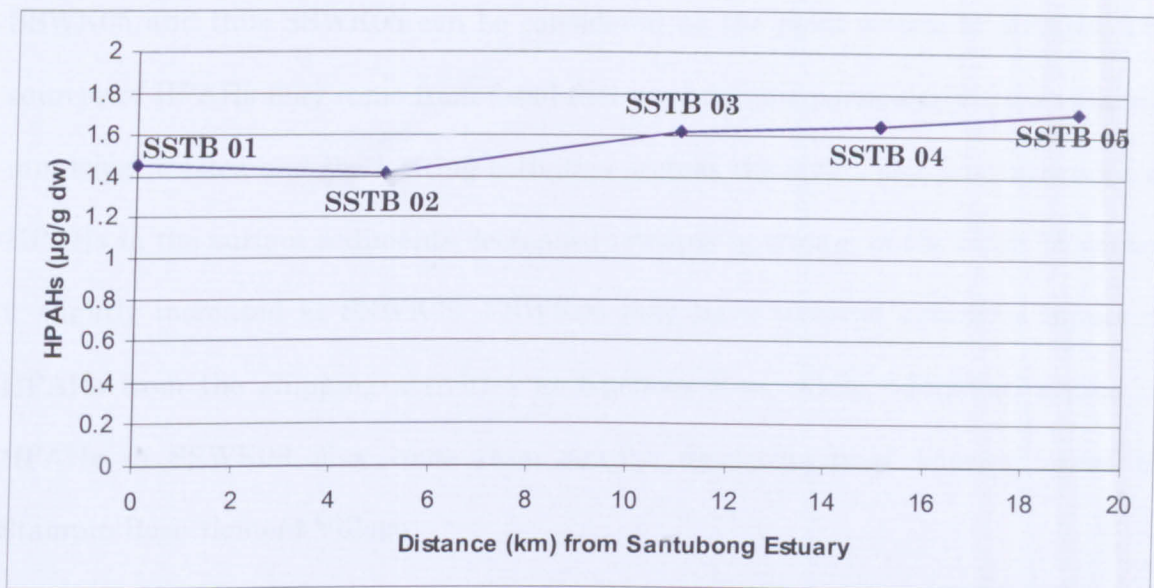


Figure 4.24: The spatial distribution of the HPAHs in the surface sediments from Santubong River

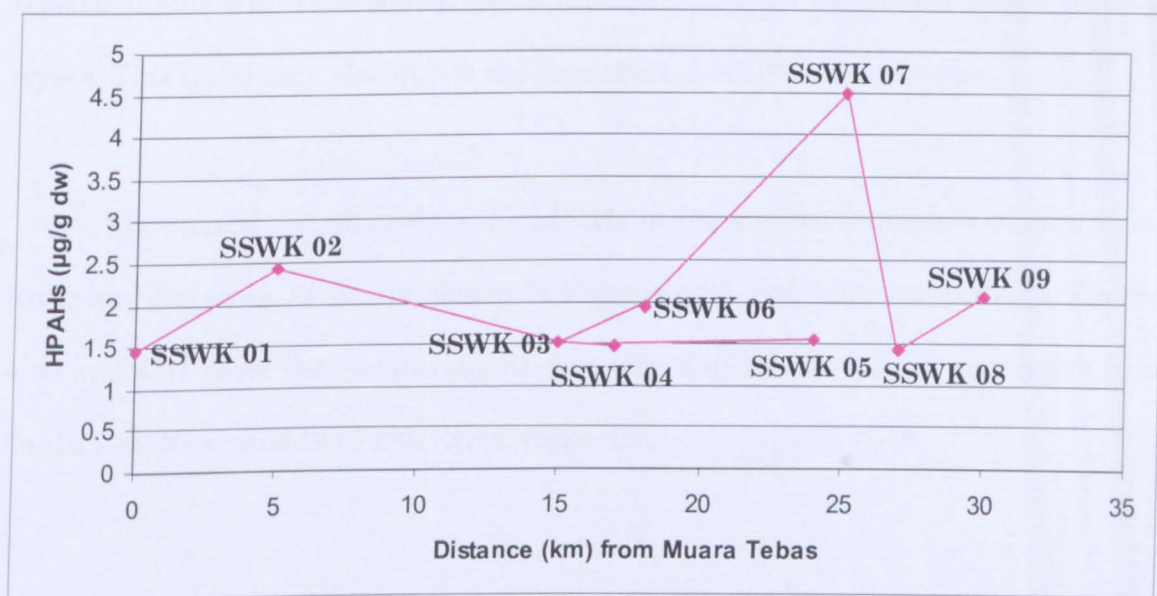


Figure 4.25: The spatial distribution of the HPAHs in the surface sediments from Sarawak River

The concentrations of HPAHs increased from SSWK01 to SSWK02, but subsequently decreased towards upstream suggesting that SSWK02 may be one of the point sources for HPAHs particularly from the shipping activities at the Senari Port. The highest concentration of HPAHs was detected in the surface sediment of

SSWK05 and thus SSWK05 can be considered as the point source of HPAHs. The sources of HPAHs may come from fossil fuel combustions particularly from vehicles, municipal wastes and the boating activities across the river. The concentrations of HPAHs in the surface sediments decreased towards upstream of the river. However, it slightly increased at SSWK09. SSWK06 may have received extensive inputs of HPAHs from the shipping activities at Kuching Port, while additional inputs of HPAHs in SSWK09 may come from sewage discharge from housing areas at Stampin Resettlement Village.

The vertical distributions of the HPAHs in the sediments exhibit consistent trend with decreasing HPAHs towards lower layers. This indicates a variation of HPAHs inputs with time where recent input were higher than older inputs at lower layers. This trend may also due to the degradation of HPAHs with time.

The spatial distribution of the LPAHs in the surface sediments of Santubong River and Sarawak River are shown in Figures 4.28 and 4.29, respectively. Figures 4.30 and 4.31 show the vertical distribution trend of LPAHs in core sediments from Santubong River and Sarawak River, respectively.

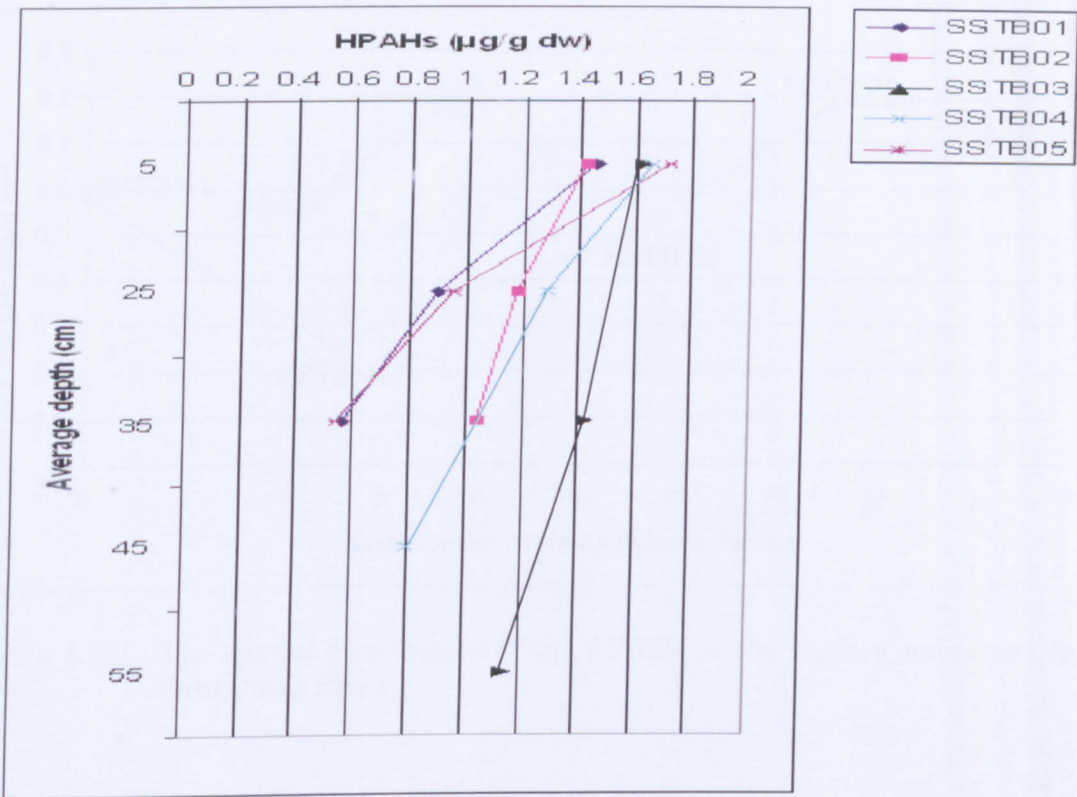


Figure 4.26: The vertical distribution of the HPAHs in core sediments from Santubong River

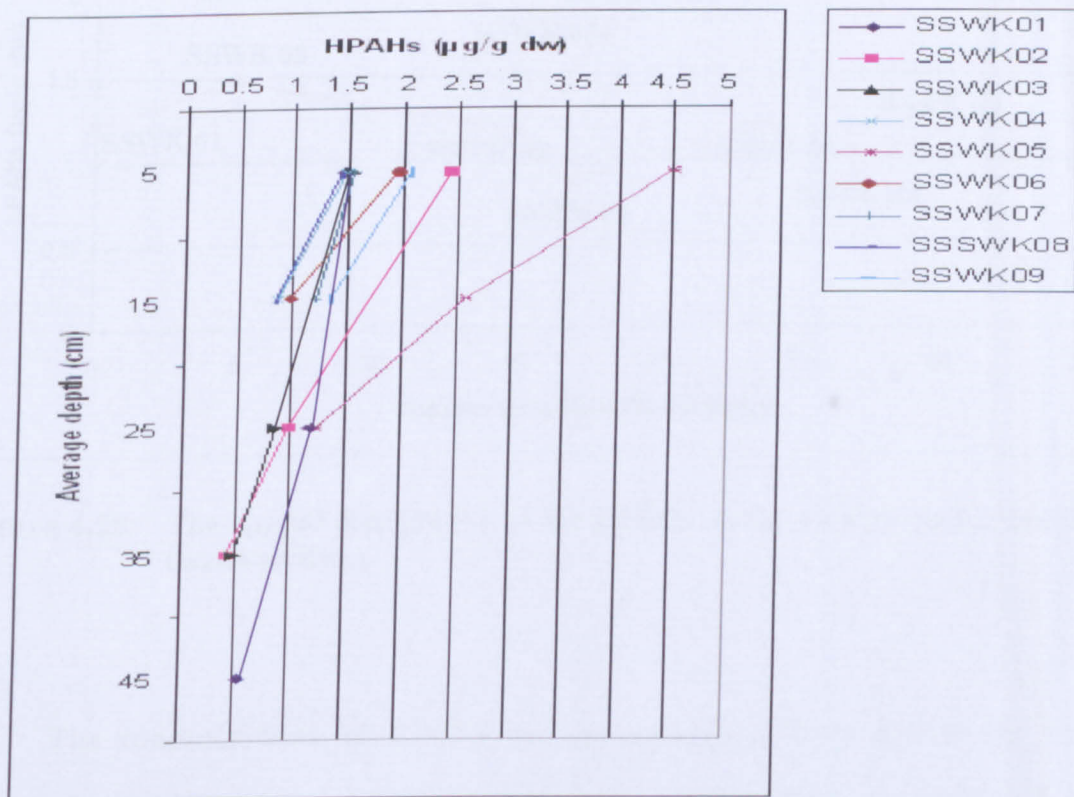


Figure 4.27: The vertical distribution of the HPAHs in core sediments from Sarawak River

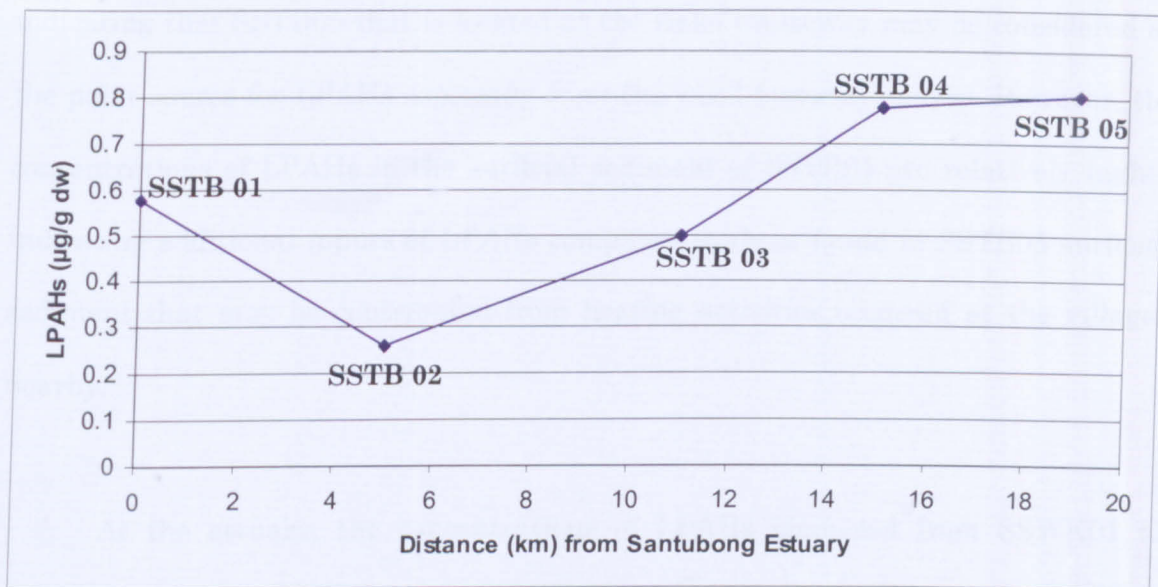


Figure 4.28: The spatial distribution of the LPAHs in the surface sediments from Santubong River

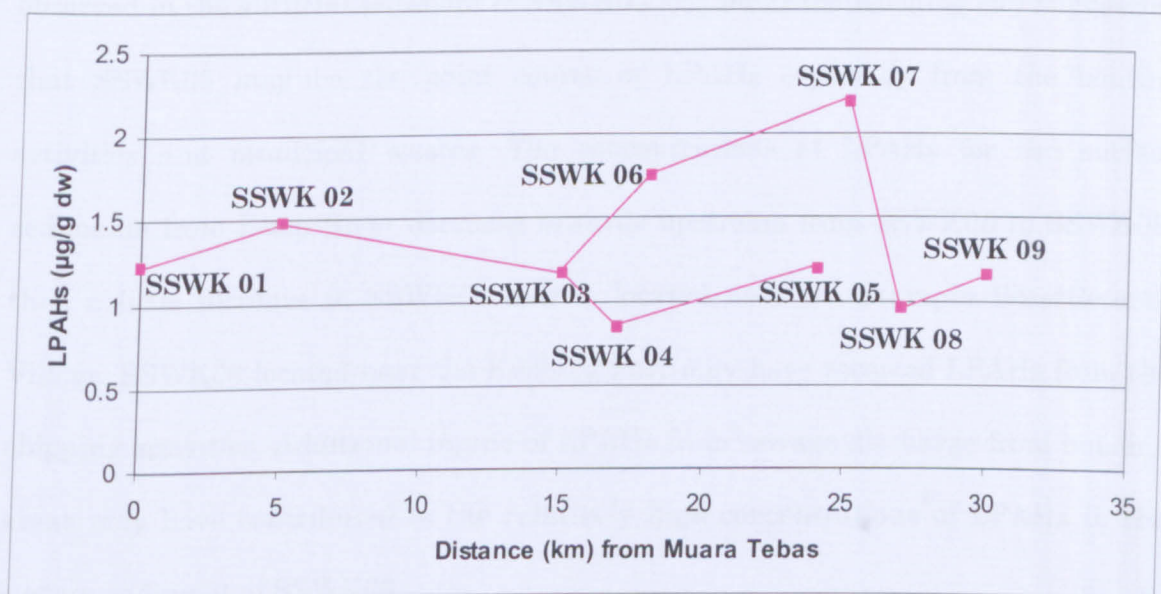


Figure 4.29: The spatial distribution of the LPAHs in the surface sediments from Sarawak River

The concentrations of LPAHs in core sediments from Santubong River decreased from SSTB01 to SSTB02 and increased from SSTB02 to SSTB05. The highest concentrations of LPAHs are found in the upper sediment of SSTB05

indicating that SSTB05 that is located at the Bako Causeway may be considered as the point source for LPAHs especially from the wood factories nearby. However, the concentrations of LPAHs in the surficial sediment of SSTB01 are relatively higher indicating additional inputs of LPAHs compared to those found in SSTB05 surficial sediment that may be contributed from boating activities occurred at the villages nearby.

At the estuary, the concentrations of LPAHs increased from SSWK01 to SSWK02, and decreased toward upstream from SSWK02 to SSWK04 indicating that SSWK02 may have additional inputs of LPAHs especially from the shipping activities that occur at the Senari Port. The highest concentrations of LPAHs was observed in the surficial sediment of SSWK05 located at the Kuching city suggesting that SSWK05 may be the point source of LPAHs especially from the boating activities and municipal wastes. The concentrations of LPAHs for the surface sediments from Kuap River decrease towards upstream from SSWK06 to SSWK08, then a little increase in SSWK09 that is located near the Stampin Resettlement Village. SSWK06 located near the Kuching Port may have received LPAHs from the shipping activities. Additional inputs of LPAHs from sewage discharge from housing areas may have contributed to the relatively high concentrations of LPAHs in the surface sediment of SSWK09.

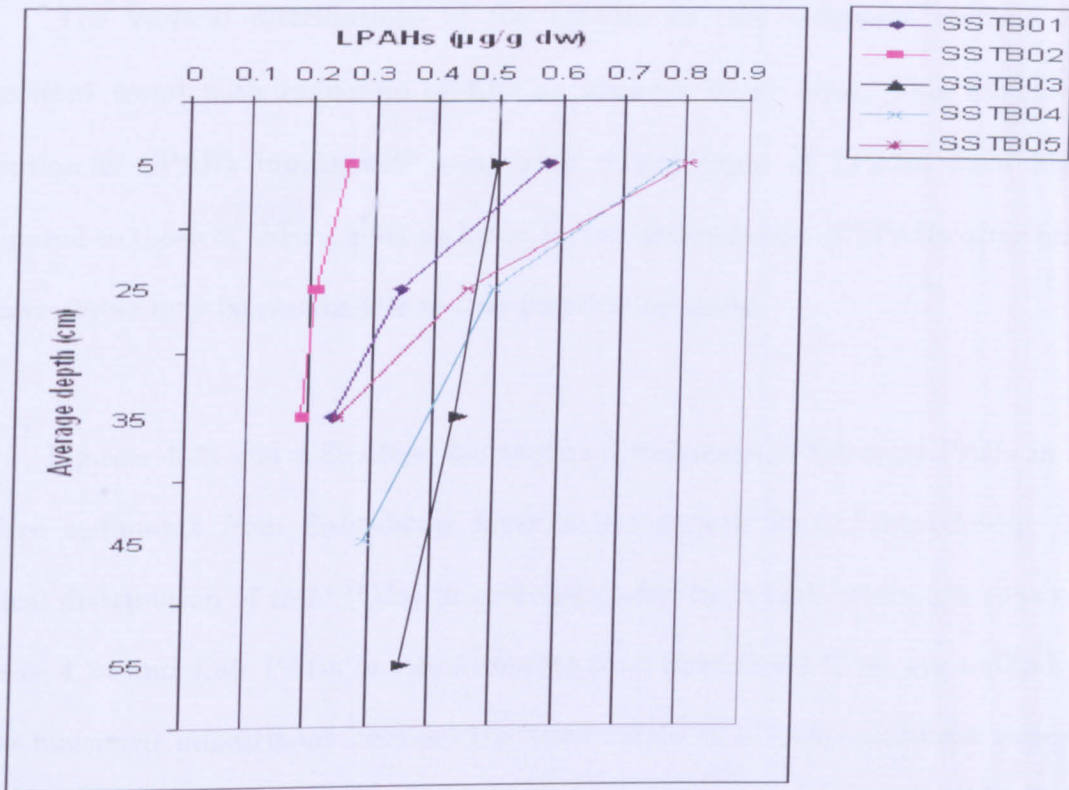


Figure 4.30: The vertical distribution of the LPAHs in core sediments from Santubong River

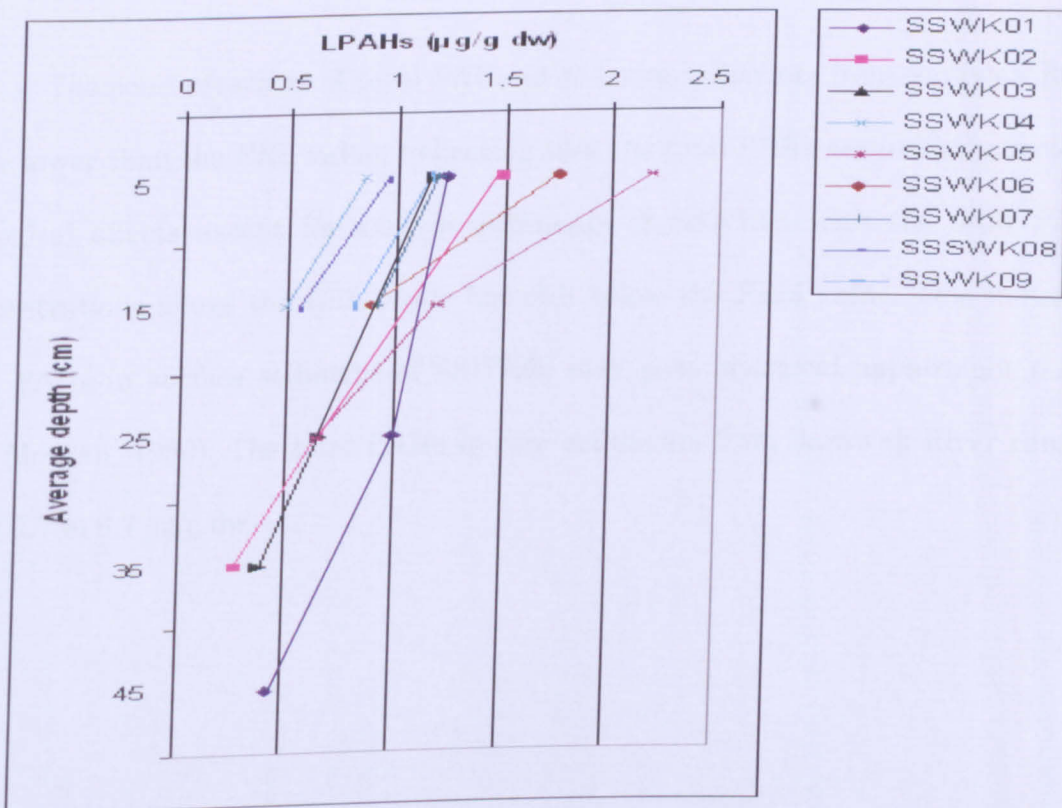


Figure 4.31: The vertical distribution of the LPAHs in core sediments from Sarawak River

The vertical distributions of the LPAHs in core sediment studied show consistent trend with reduction of LPAHs towards lower layer. This indicates a variation of LPAHs inputs with time with recent input of LPAHs were higher compared to those of older inputs at lower layers. Degradation of LPAHs after burial at lower layer may be responsible to this distribution trend.

Figures 4.32 and 4.33 show the spatial distribution of the total PAHs in the surface sediments from Santubong River and Sarawak River, respectively. The vertical distribution of total PAHs in core sediments from both rivers are shown in Figures 4.34 and 4.35. PAHs in core sediment from Santubong River are unlikely to cause biological impairment because the total PAHs in all core sediment samples were lower than the ERL value (4022 ng/g dry) see Table 4.11 with total PAHs in core sediments ranged from 0.8 to 2.5 $\mu\text{g/g dw}$.

The concentrations of total PAHs in the core sediments from Sarawak River were lower than the ERL value, indicating that the total PAHs are unlikely to cause biological effects except for surface sediments of SSWK05 with the total PAHs concentrations above the ERL value but still below the ERM value. This indicates that PAHs in surface sediment of SSWK05 may pose biological impairment (Long and Morgan, 1990). The total PAHs in core sediments from Sarawak River ranged from 0.7 to 6.7 $\mu\text{g/g dw}$.

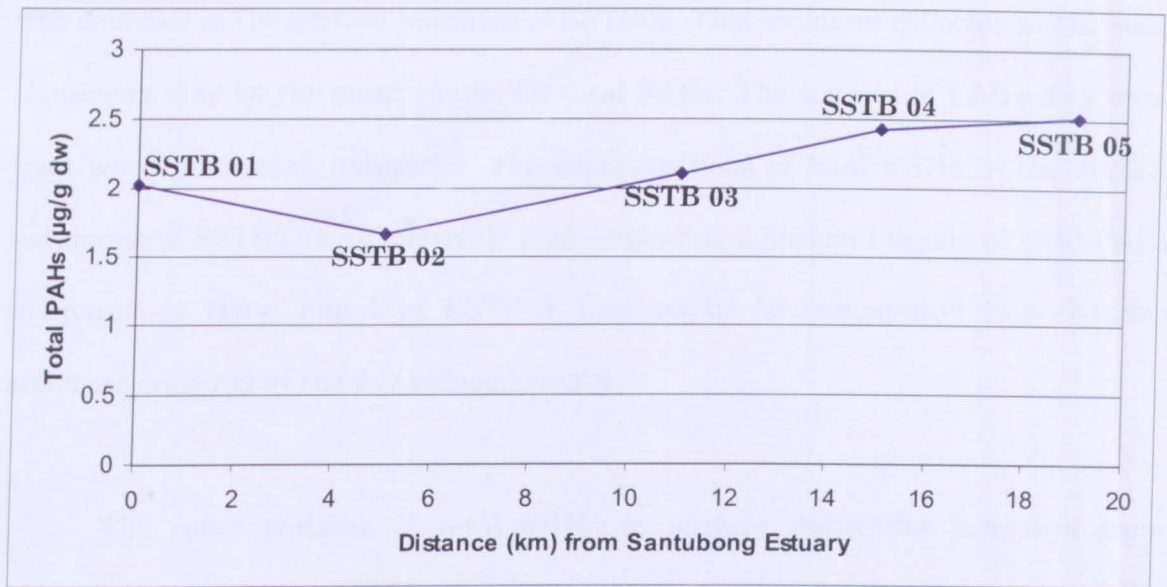


Figure 4.32: The spatial distribution of the total PAHs in the surface sediments from Santubong River

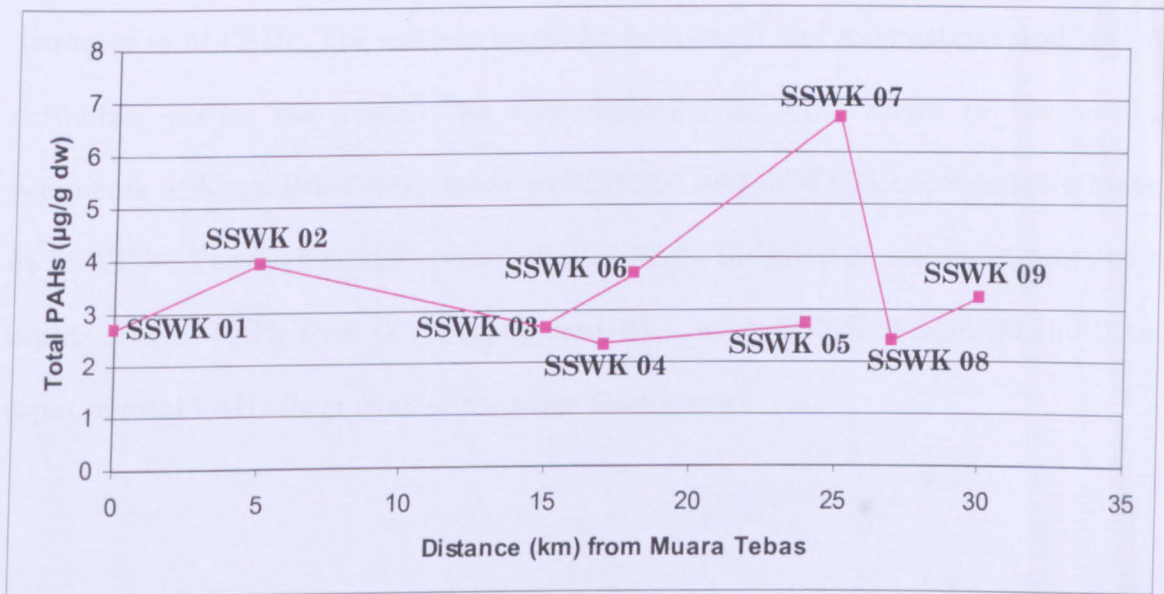


Figure 4.33: The spatial distribution of the total PAHs in the surface sediments from Sarawak River

The concentration of total PAHs in surface sediments from Santubong increased towards upstream of the river. The highest concentration of total PAHs

was detected in the surface sediment of SSTB05. This sediment collected at the Bako Causeway may be the point source for total PAHs. The sources of PAHs may come from wood processing industries. The concentrations of total PAHs in the surface sediments of SSTB01 was relatively high indicating additional inputs of total PAHs compared to those found in SSTB05 that might be contributed from boating activities occurred at the few villages nearby.

The concentrations of total PAHs in surface sediments increased from SSWK01 to SSWK02, and decreased from SSWK02 to SSWK04 indicating that SSWK02 may be one of the point sources for total PAHs particularly from the shipping activities at the Senari Port. The highest concentrations of total PAHs in the surface sediment of SSWK05 indicated that it can be considered as the point source of total PAHs. The sources might be from fossil fuel combustions and boating activities across the river. The concentrations of total PAHs in the surface sediments of Kuap River were lower at SSWK07 and SSWK08 but relatively higher at SSWK09. The high concentration of total PAHs in SSWK06 sediment was due to inputs of total PAHs from the shipping activities, while SSWK09 received additional input of total PAHs from domestic sewage discharges.

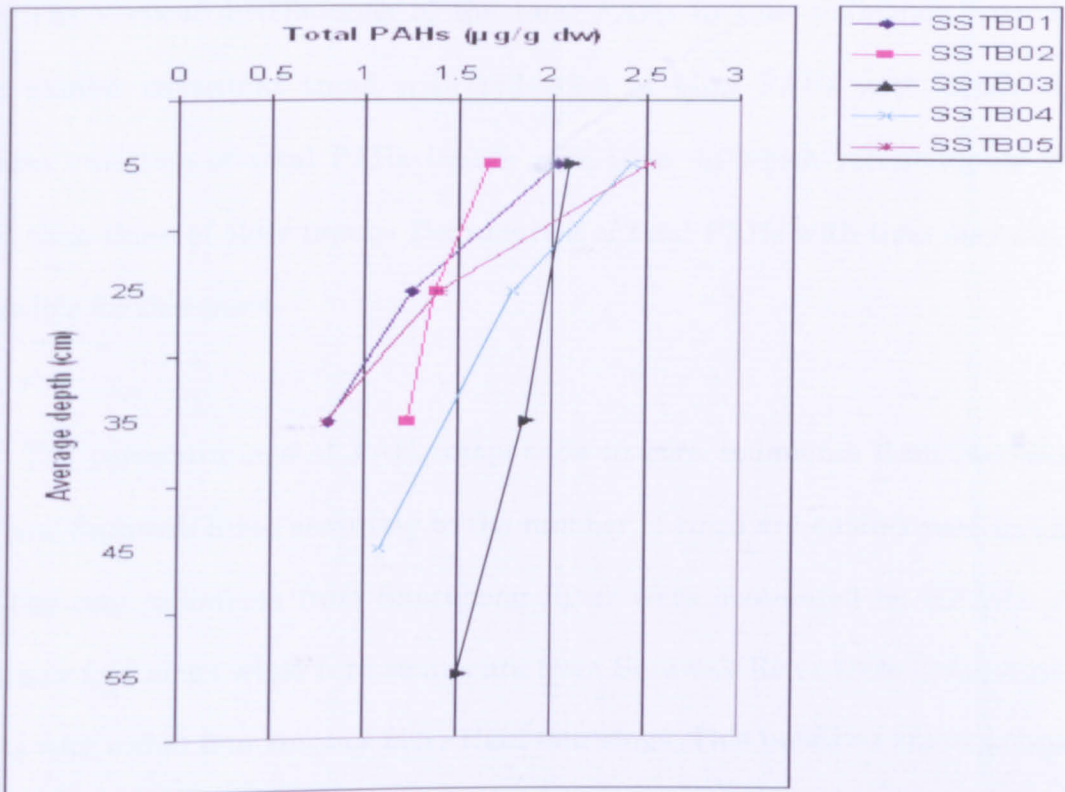


Figure 4.34: The vertical distribution of the total PAHs in core sediments from Santubong River

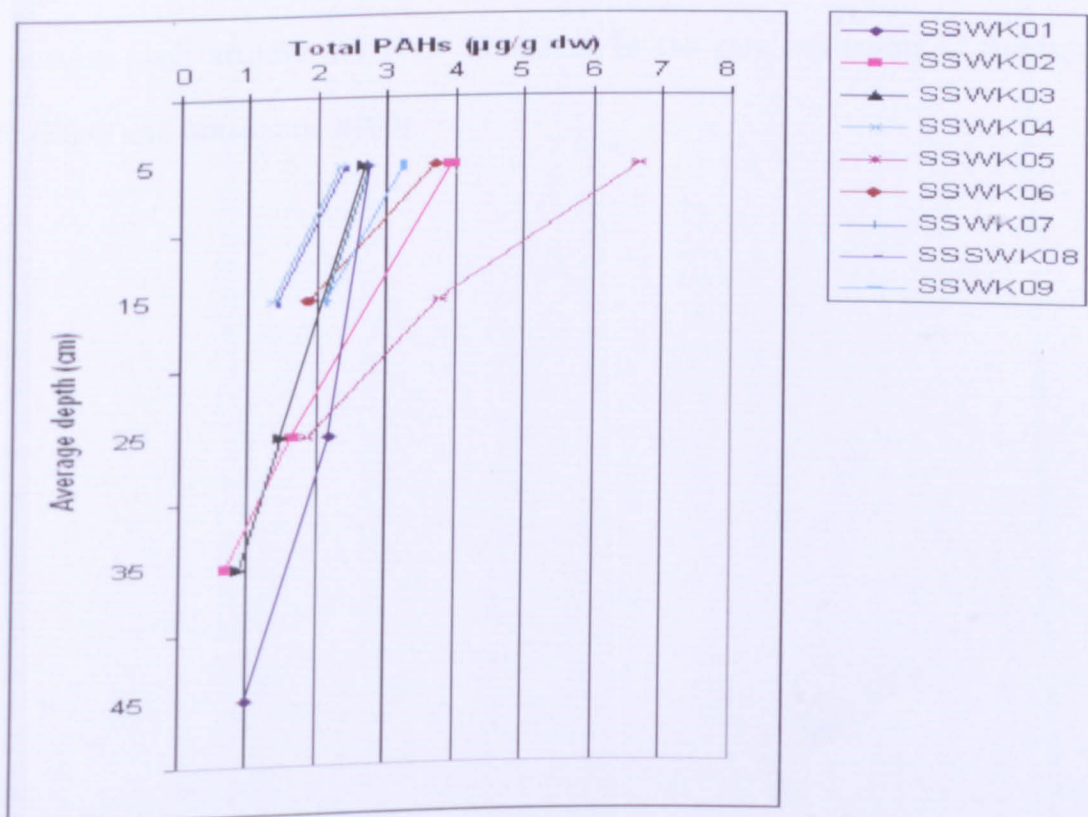


Figure 4.35: The vertical distribution of the total PAHs in core sediments from Sarawak River

The vertical distributions of the total PAHs in core sediments from both rivers exhibit consistent trend with reduction of total PAHs with depth. This indicates variation of total PAHs inputs with time, in which recent inputs were higher than those of older inputs. Degradation of total PAHs with time may also be responsible for this trend.

The concentrations of PAH compounds in core sediments from Santubong River and Sarawak River according to the number of rings are summarised in Table 4.13. The core sediments from Santubong River were dominated by HPAHs with more than four rings while core sediments from Sarawak River were dominated by HPAHs with either four rings or more than four rings. This indicates that the inputs of PAHs are more dominated by pyrolytic sources compared to petrogenic sources (Tolosa *et al.*, 2005). This may also due to the extensive biodegradation processes in sediments with PAHs resistant to degradation left undegraded. Thus, HPAHs that can sustain such attacks are more abundant in the core sediments of Santubong River (Zhou and Maskaoui, 2003).

Table 4.13: The concentrations of PAHs in core sediments from Santubong River and Sarawak River according to the number of rings

River	Samples	Depth (cm)	Concentrations (ng/g dry weight)			
			Two rings PAHs	Three rings PAHs	Four rings PAHs	> Four rings PAHs
Santubong	SSTB01	0-10	156.1	422.7	362.8	1088.5
		20-30	39.5	305.2	263.0	637.4
		30-40	43.3	193.5	211.8	352.2
	SSTB02	0-10	n.d	256.6	398.6	1013.6
		20-30	n.d	205.2	284.4	891.6
		30-40	n.d	189.0	272.2	761.2
	SSTB03	0-10	n.d	500.7	706.6	848.0
		30-40	n.d	441.7	604.4	822.0
		50-60	n.d	360.2	295.6	801.7
	SSTB04	0-10	531.5	248.9	798.6	845.3
		20-30	141.0	354.6	614.5	676.1
		40-50	74.3	216.2	290.6	503.4
	SSTB05	0-10	277.4	526.2	586.0	1129.5
		20-30	73.7	377.5	304.2	646.3
		30-40	n.d	246.2	204.3	334.8
Sarawak	SSWK01	0-10	7.0	1225.6	228.5	1229.6
		20-30	30.2	964.7	138.9	1039.4
		40-50	n.d	433.3	109.4	457.6
	SSWK02	0-10	3.0	1480.5	864.1	1561.9
		20-30	9.3	624.0	236.5	743.3
		30-40	6.1	258.0	86.9	329.7
	SSWK03	0-10	208.8	955.3	479.8	1040.6
		20-30	203.4	439.6	382.8	467.2
		30-40	110.8	273.1	219.6	277.9
	SSWK04	0-10	n.d	845.7	594.8	887.3
		10-20	n.d	480.7	368.7	491.1
	SSWK05	0-10	300.0	1887.1	2095.6	2241.3
		10-20	160.5	1032.1	1538.0	1062.0
		20-30	n.d	637.4	1231.2	n.d
	SSWK06	0-10	698.1	1050.4	872.6	1083.2
		10-20	137.4	741.9	746.7	236.3
	SSWK07	0-10	n.d	1189.4	1552.8	n.d
		10-20	n.d	910.1	1009.1	197.8
SSWK08	0-10	n.d	961.0	992.3	439.8	
	10-20	n.d	560.3	838.0	n.d	
SSWK09	0-10	n.d	1158.1	1184.9	660.7	
	10-20	113.4	679.8	1138.1	195.3	

Notes: Two rings PAHs = naphthalene; three rings PAHs = acenaphthylene, acenaphthene, fluorene, phenanthrene and anthracene; four rings PAHs = fluoranthene, pyrene, benzo[a]anthracene and chrysene; more than four rings PAHs = benzo[b]fluoranthene, benzo[k]fluoranthene, benzo[a]pyrene, indeno[1,2,3-c,d]pyrene, dibenzo[a,h]anthracene and benzo[g,h,i]perylene; n.d = not detected

4.5 Comparison of Hydrocarbons Data with Other Places

Total concentrations of n-alkanes and PAHs in core sediments from Sarawak and Santubong rivers were compared with those found in sediments from other places as shown in Table 4.14. The concentrations of total n-alkanes in sediments from Santubong and Sarawak rivers are relatively high as compared to those found in sediments from other places, but the highest total n-alkanes was reported in sediments from mangrove area of Cananeia, Brazil ranged from 4.37 to 157.90 $\mu\text{g/g dw}$ (Nishigima *et al.*, 2001). However, core sediments from Santubong River and Sarawak River could not be considered highly contaminated because the n-alkanes may originated from a mixture of biogenic and anthropogenic sources. The high concentration of n-alkanes in sediments from Cananeia, Brazil was originated from terrestrial plants with no indication of oil pollution or anthropogenic activities (Nishigima *et al.*, 2001).

The concentrations of total PAHs in sediments from both rivers studied are relatively higher compared to other places but still lower than those reported in sediments from Santos, Brazil (Nishigima *et al.*, 2001) and Arabian Gulf of Bahrain (Tolosa *et al.*, 2005). The PAHs in core sediments indicated that both rivers are moderately polluted compared to those found in sediments from Santos, Brazil (Nishigima *et al.*, 2001) and Arabian Gulf of Bahrain (Tolosa *et al.*, 2005).

Table 4.14: The concentrations of total n-alkanes and PAHs in sediments from marine environment in other countries and this study.

Location	Activities	TA ($\mu\text{g/g dw}$)	Total PAHs ($\mu\text{g/g dw}$)	References
Jiaozhou Bay, Qingdao (China)	Harbour and industrial regions	0.50 to 8.20	0.02 to 2.20	Wang <i>et al.</i> (2006)
Arabian Gulf (United Arab Emirates)	Oil refineries and industrial regions	0.04 to 1.10	<0.01	Tolosa <i>et al.</i> (2005)
Arabian Gulf (Qatar)	Harbour, oil refineries and industrial regions	0.07 to 3.30	<0.01 to 0.09	Tolosa <i>et al.</i> (2005)
Arabian Gulf (Bahrain)	Oil refineries	0.67 to 4.30	0.01 to 6.60	Tolosa <i>et al.</i> (2005)
Arabian Gulf (Oman)	Harbour and oil refineries	0.01 to 0.24	<0.01 to 0.03	Tolosa <i>et al.</i> (2005)
Sao Sebastiao (Brazil)	Oil refineries, harbour and sewage outfalls	0.03 to 4.77	0.02 to 0.20	Medeiros and Bicego (2004)
Black Sea (Turkey, Russia and Ukraine)	Harbour, industrial regions and urban areas	0.10 to 3.40	<0.01 to 0.64	Readman <i>et al.</i> (2002)
Santos (Brazil)	Harbour and industrial regions	1.05 to 4.29	0.08 to 42.39	Nishigima <i>et al.</i> (2001)
Cananeia (Brazil)	Mangrove region	4.37 to 157.90	n.d	Nishigima <i>et al.</i> (2001)
Hor Al-Hammar, Shatt Al-Arab (Northern Arabian Gulf)	Oil refineries, industrial regions and urban areas	2.20 to 16.89	n.d	Al-Saad and Al-Timari (1993)
Santubong River (Malaysia)	Mangrove region and industrial areas	10.80 to 101.10	0.80 to 2.50	This study
Sarawak River (Malaysia)	Port, industrial and urban areas	7.30 to 61.70	0.70 to 6.70	This study

4.6 Fatty Acid Methyl Esters (FAMEs)

The gas chromatograms of FAMEs in the core sediments from SSTB05 and SSWK03 sampling sites are shown in Figures 4.36 and 4.37, respectively. Gas chromatograms for FAMEs in other sediment samples studied are presented in Appendix D. FAMEs identified in core sediments from Santubong River and Sarawak River are presented in Tables 4.15 and 4.16, respectively. Details on the molecular structures and molecular weights for all FAMEs identified are presented in Appendix E.

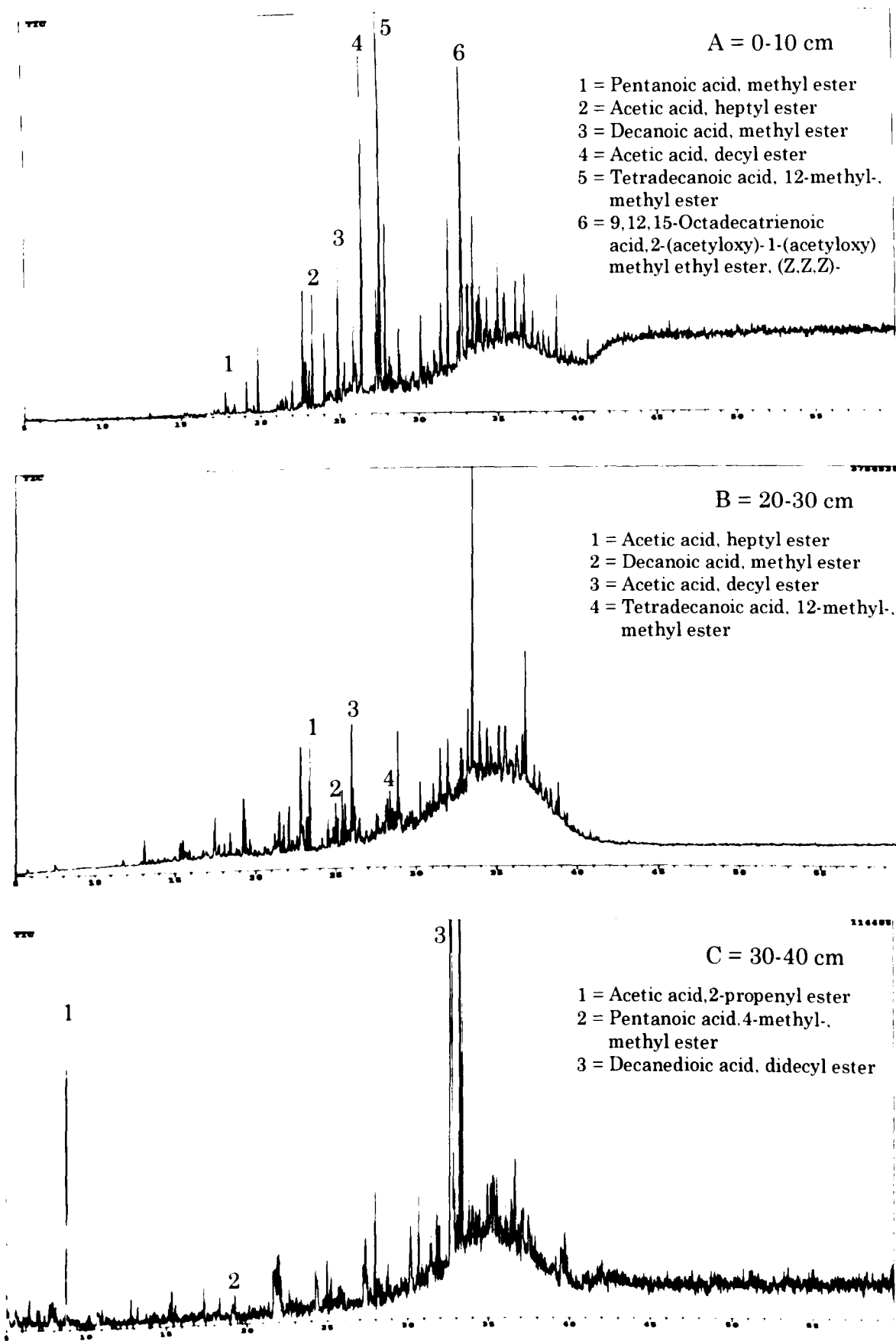


Figure 4.36: GC/MS chromatograms for FAMEs fractions in core sediments of SSTB05 at three different layers (A, B and C)

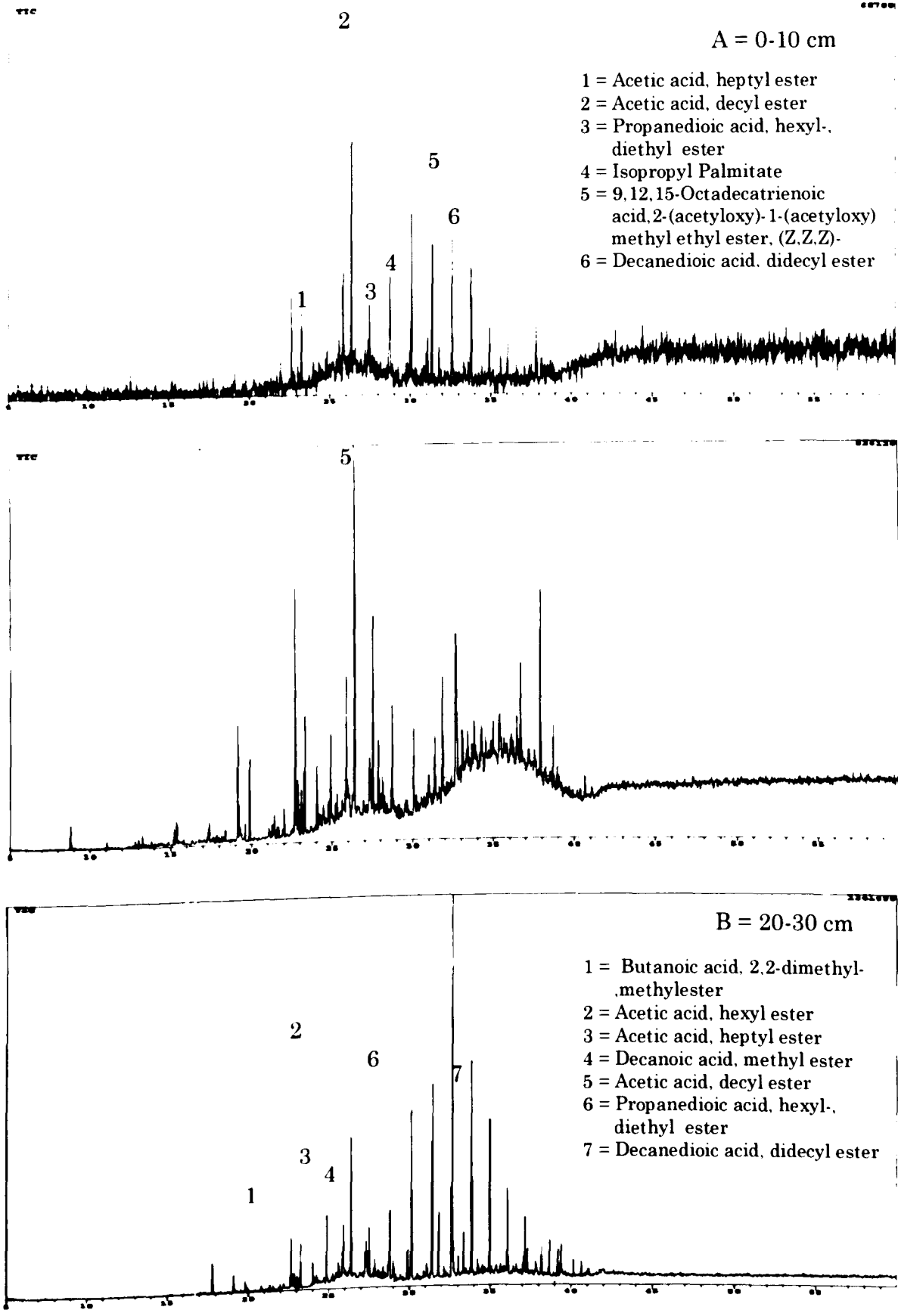


Figure 4.37: GC/MS chromatograms for FAMEs fractions in core sediments of SSWK03 at three different layers (A, B and C)

Table 4.15: Fatty acid methyl esters identified in Santubong River

Name of the compound	RT	SSTB01			SSTB02	SSTB03			SSTB04	SSTB05		
		A	C	D	A	A	D	F	A	A	C	D
Formic acid, ethenyl ester	6.108	x	x									
Acetic acid, 2-propenyl ester	8.000				x							x
Acetic acid, 2-methylpropyl ester	17.792					x						
Pentanoic acid, methyl ester	17.835									x		
Propanoic acid, 2-methyl-, 1-methylethyl ester	19.450				x	x						
Pentanoic acid, 4-methyl-, methyl ester	19.475	x	x						x			x
Butanoic acid, 2,2-dimethyl-, methylester	19.867									x		
Hexanoic acid, 5-methyl-, methyl ester	21.975								x	x		
Acetic acid, hexyl ester	22.567			x								
Acetic acid, 2-ethylbutyl ester	22.642							x				
Pentanoic acid, 1-methylethyl ester	22.983	x	x									
Acetic acid, heptyl ester	23.283			x		x	x	x		x	x	
Acetic acid, octyl ester	23.417	x	x		x		x	x				
Acetic acid, 2-ethylhexyl ester	24.042								x			
Decanoic acid, methyl ester	24.808	x	x	x	x					x	x	
Acetic acid, decyl ester	26.542	x	x		x	x	x	x	x	x	x	
Propanedioic acid, hexyl-, diethyl ester	27.267					x	x	x	x			
Tetradecanoic acid, 12-methyl-, methyl ester	27.867									x	x	
Hexadecanoic acid, 14-methyl-, methyl ester	28.233								x			
Isopropyl Palmitate	28.767					x	x					
Octadecanoic acid, 17-methyl-, methyl ester	29.375	x	x		x							
9-Octadecenoic acid, 12-(acetyloxy)-, methyl ester, R-(Z)-	29.758				x							
Nonanedioic acid, dihexyl ester	30.108					x	x					
9,12,15-Octadecatrienoic acid, 2-(acetyloxy)-1-(acetyloxy) methyl ethyl ester, (Z,Z,Z)-	31.839	x	x	x	x	x	x	x			x	
Decanedioic acid, didecyl ester	32.625					x	x	x	x			x

Notes: A = 0-10 cm; C = 20-30 cm; D = 30-40 cm; F = 50-60 cm and x = detected

Table 4.16: Fatty acid methyl esters identified in Sarawak River

Name of the compound	RT	SSWK01			SSWK02			SSWK03			SSWK04		SSWK05			SSWK06		SSWK07		SSWK08		SSWK09	
		A	C	E	A	C	D	A	C	D	A	B	A	B	C	A	B	A	B	A	B	A	B
Acetic acid,2-propenyl ester	8.000		x	x				x	x										x				
Acetic acid,2-methylpropyl ester	17.792																	x					
Propanoic acid,1,1-dimethylethyl ester	19.125							x															
Pentanoic acid,4-methyl-, methyl ester	19.475													x	x								
Butanoic acid, 2,2-dimethyl-, methylester	19.867								x	x		x					x			x		x	
Acetic acid, hexyl ester	22.567								x	x													
Pentanoic acid,1-methylethyl ester	22.983	x				x									x	x							
Heptanoic acid, ethyl ester	23.150										x												
Hexanoic acid,1-methylethyl ester	23.175										x	x	x				x		x	x	x	x	
Acetic acid, heptyl ester	23.283							x	x										x				
Acetic acid, octyl ester	23.417	x	x			x						x	x									x	
Acetic acid, 2-ethylhexyl ester	24.042		x	x											x								
Acetic acid, nonyl ester	24.775										x	x	x	x								x	
Decanoic acid, methyl ester	24.808	x	x			x	x		x	x					x		x			x	x		
Decanoic acid, ethyl ester	26.275										x	x		x	x		x					x	
Acetic acid, decyl ester	26.542	x	x			x	x	x	x	x					x		x	x	x	x	x	x	
Propanedioic acid, hexyl-, diethyl ester	27.267					x			x	x				x	x	x	x	x	x	x	x	x	
Tetradecanoic acid, 12-methyl-, methyl ester	27.867								x	x	x	x			x					x		x	
Hexadecanoic acid, 14-methyl-, methyl ester	28.233					x	x																
Isopropyl Palmitate	28.767							x	x											x			
Octadecanoic acid,17-methyl-,methyl ester	29.375	x	x			x	x				x				x							x	
9-Octadecenoic acid,12-(acetyloxy)-, methyl ester, R-(Z)-	29.758	x	x			x			x	x													
9,12,15-Octadecatrienoic acid,2-(acetyloxy)-1-(acetyloxy) methyl ethyl ester, (Z,Z,Z)-	31.839	x	x			x	x	x	x					x	x								
Decanedioic acid, didecyl ester	32.625					x	x	x	x	x	x		x									x	

Notes: A = 0-10 cm; B = 10-20 cm; C = 20-30 cm; D = 30-40 cm; E = 40-50 cm and x = detected

The fatty acids investigated consist of saturated, unsaturated and branched fatty acid methyl esters (FAMES). Even though various types of FAMES can be used to identify its sources, saturated C₁₄, C₁₆ and C₁₈ fatty acids are less source-specific compared to mono- and polyunsaturated fatty acids (Birgel *et al.*, 2004). So, their biomarker potential in marine geochemical investigation especially in deeper sediments are generally limited due to their ubiquity and probable additional derivation from biogeochemical reduction of unsaturated fatty acids.

The presence of short chain FAMES ($\leq C_{20}$) in core sediments from both rivers indicates planktonic sources of FAMES (Colombo *et al.*, 1997). The longest chain of esters observed in core sediments from both rivers is C₃₀ ester. The C₃ ester was the shortest chain ester detected in Santubong core sediment while C₅ ester was the shortest ester observed in Sarawak core sediments.

Most of the FAMES identified in the core sediments of Santubong River and Sarawak River were saturated FAMES with a limited number of unsaturated FAMES. Double bond in the unsaturated FAMES is easily hydrogenated and unsaturated FAMES are relatively more susceptible to bacterial degradation (Muri *et al.*, 2004). Saturated FAMES also have relatively higher melting point compared with the unsaturated FAMES (Solomons and Fryhle, 2004). Formic acid, ethenyl ester; acetic acid, 2-propenyl ester; 9-octadecenoic acid, 12-(acetyloxy)-, methyl ester, R-(Z)- and 9,12,15-octadecatrienoic acid, 2-(acetyloxy)-1-(acetyloxy) methyl ethyl ester, (Z,Z,Z)- are the unsaturated FAMES identified in the core sediments. Branched FAMES are also identified indicating inputs from sedimentary bacteria (Colombo *et al.*, 1997). Propanedioic acid, hexyl-, diethyl ester; 9-octadecenoic acid, 12-(acetyloxy)-, methyl ester, R-(Z)- and 9,12,15-octadecatrienoic acid, 2-

(acetyloxy)-1-(acetyloxy) methyl ethyl ester, (Z,Z,Z)- were among the branched FAMEs found in both rivers.

4.7 Phthalate Esters

The gas chromatograms of phthalate esters in the core sediments SSTB05 and SSWK03 are shown in Figures 4.38 and 4.39, respectively. Gas chromatograms for phthalate esters in other sediment samples studied are presented in Appendix F. Phthalate esters identified in core sediments from Santubong River and Sarawak River are presented in Tables 4.17 and 4.18, respectively. Details on the molecular structures and molecular weights for all phthalate esters identified are presented in Appendix G.

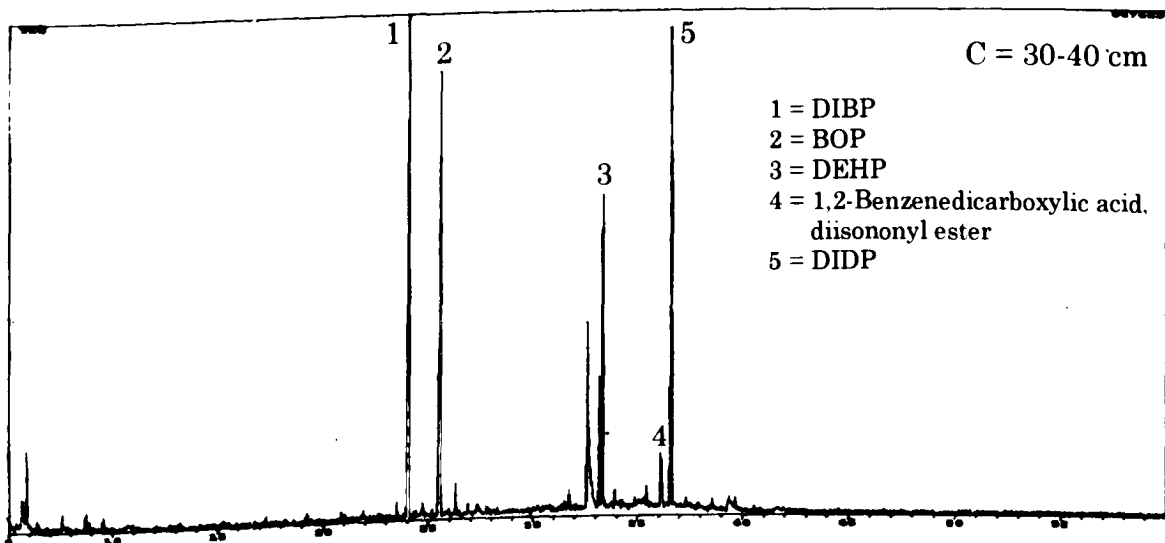
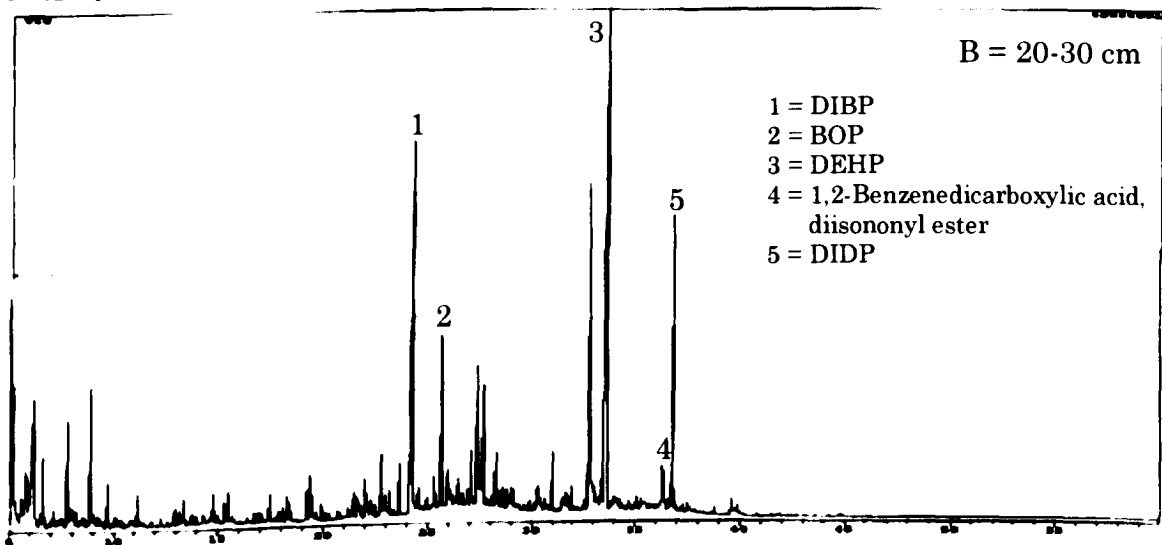
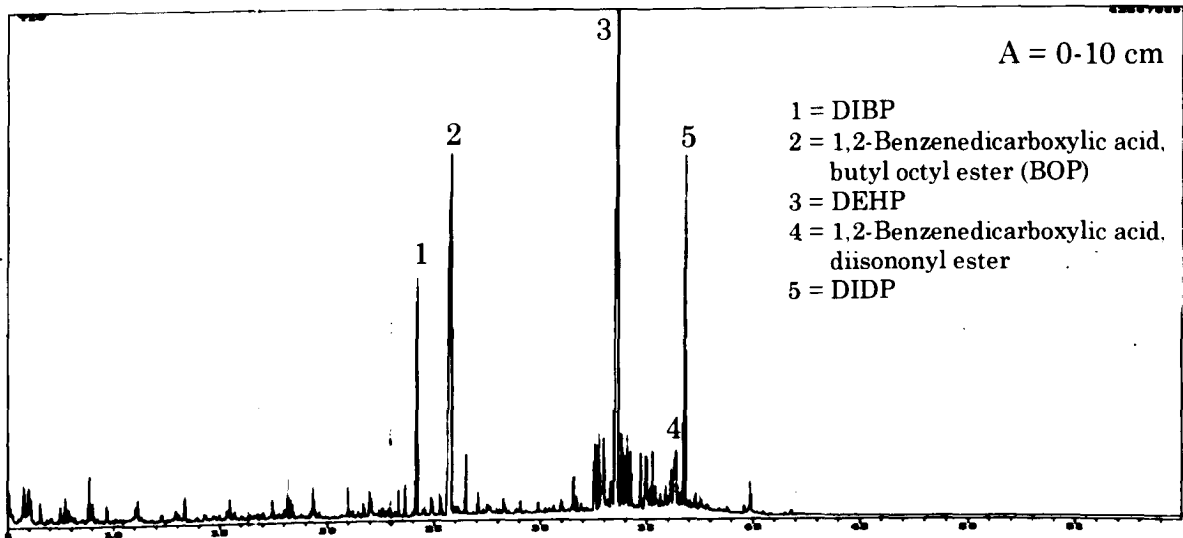


Figure 4.38: GC/MS chromatograms for phthalate ester fractions in core sediments of SSTB05 at three different layers (A, B and C)

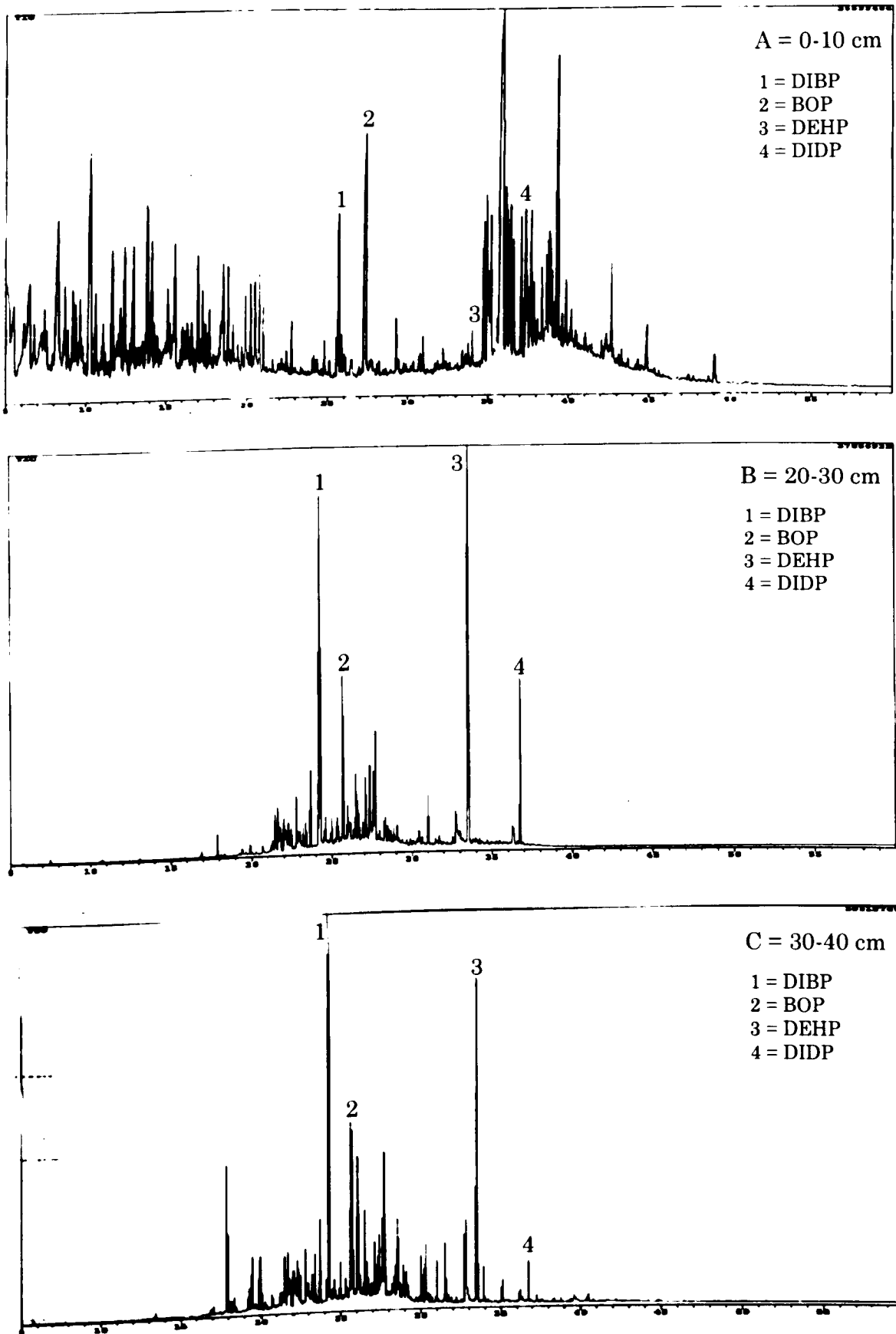


Figure 4.39: GC/MS chromatograms for phthalate esters fractions in core sediments of SSWK03 at three different layers (A, B and C)

Table 4.17: Phthalate esters identified in Santubong River

Name of the compound	RT	SSTB01			SSTB02		SSTB03			SSTB04		SSTB05	
		A	C	D	A	A	D	F	A	A	C	D	
DIBP	24.703	x	x	x	x	x	x	x	x	x	x	x	x
BOP	25.420	x	x	x	x	x	x	x	x	x	x	x	x
DEHP	33.907	x	x	x	x	x	x	x	x	x	x	x	x
1,2-Benzenedicarboxylic acid, diisononyl ester	36.326	x	x	x	x					x	x	x	x
DIDP	36.746	x	x	x	x	x	x			x	x	x	x

Notes: A = 0-10 cm; C = 20-30 cm; D = 30-40 cm; F = 50-60 cm and x = detected

Table 4.18: Phthalate esters identified in Sarawak River

Name of the compound	RT	SSWK01			SSWK02			SSWK03			SSWK04		SSWK05			SSWK06		SSWK07		SSWK08		SSWK09	
		A	C	E	A	C	D	A	C	D	A	B	A	B	C	A	B	A	B	A	B	A	B
DIBP	24.703	x	x	x	x	x	x	x	x	x	x	x	x	x	x	x	x	x	x	x	x	x	x
BOP	25.420	x	x	x	x	x	x	x	x	x	x	x	x	x	x	x	x	x	x	x	x	x	x
DEHP	33.907	x	x	x	x	x	x	x	x	x	x	x	x	x	x	x					x	x	x
1,2-Benzenedicarboxylic acid, diisononyl ester	36.326	x	x	x	x	x	x																
DIDP	36.746	x	x	x	x	x	x	x	x	x													

Notes: A = 0-10 cm; B = 10-20 cm; C = 20-30 cm; D = 30-40 cm; E = 40-50 cm and x = detected

Phthalate esters are one of the geochemical compounds detected in core sediments from Santubong and Sarawak Rivers. Phthalate esters are among the major compounds used in the production of plasticizers, which are formed by esterification of phthalic anhydride using alcohols (C₄ – C₁₂) (Brown *et al.*, 1996). The toxicity of phthalate esters to aquatic organisms increases with the decrease of alkyl chain length, though the toxicity effect is generally subtle (Turner and Rawling, 2000). Even though biotransformation of phthalates (that increases with trophic level) limited the bioaccumulation through the aquatic food chain, phthalate esters are still contaminants of concern as they are suspected to mimicking estrogen (Turner and Rawling, 2000).

The lowest molecular weight (278) of phthalate esters found was 1,2-benzenedicarboxylic acid, bis (2-methypropyl) ester (DIBP) while the highest (446) was 1,2-benzenedicarboxylic acid, diisodecyl ester (DIDP). The toxicity of phthalate esters to aquatic organisms increases with the decrease of alkyl chain length (Turner and Rawling, 2000). So, DIDP is considered to be more toxic compared to other phthalates esters detected, while DIBP is the least toxic. However, the toxicity effects of phthalate esters are generally subtle. DIDP was identified in every core sediments from Santubong River while in core sediments from Sarawak River, DIDP were only found in core sediments from Muara Tebas area (SSWK01, SSWK02 and SSWK03). As for DIBP, it was detected in all core sediments from both rivers. DIDP is mainly used for insulation of wires and cables, car undercoating, shoes, carpets and pool liners while DIBP is used in nitro cellulose plastic, nail polish, explosive material, lacquer manufacturing and used with methyl methacrylate applications (Kirby and Lewis, 2002).

1,2-benzenedicarboxylic acid, bis (2-ethylhexyl) ester (DEHP), which is a common phthalate esters found in environmental samples, were present in core sediments from Santubong and Sarawak rivers except for surficial sediment of SSWK07 and lower layer of core sediments (5-10 cm) from SSWK06 and SSWK07. DEHP is one of the most important and widely used phthalates for plasticizer productions in construction materials and medical devices and has been restricted for use in children's toys in the European Union (Turner and Rawling, 2000). Sediments may act as both a long-term sink and secondary source of DEHP due to the hydrophobicity of DEHP, adsorption followed by particle deposition (removal mechanisms from water) and slow degradation of DEHP in particle-bound forms under both aerobic and anaerobic conditions.

4.8 Alcohols and Sterols

The gas chromatograms of alcohols and sterols in the core sediments SSTB05 and SSWK03 are shown in Figures 4.40 and 4.41, respectively. Gas chromatograms for alcohols and sterols in other sediment samples studied are presented in Appendix H. Alcohols and sterols identified in core sediments from Santubong River and Sarawak River are presented in Tables 4.19 and 4.20, respectively. Details on the molecular structures and molecular weights for all alcohols and sterols identified are presented in Appendix I.

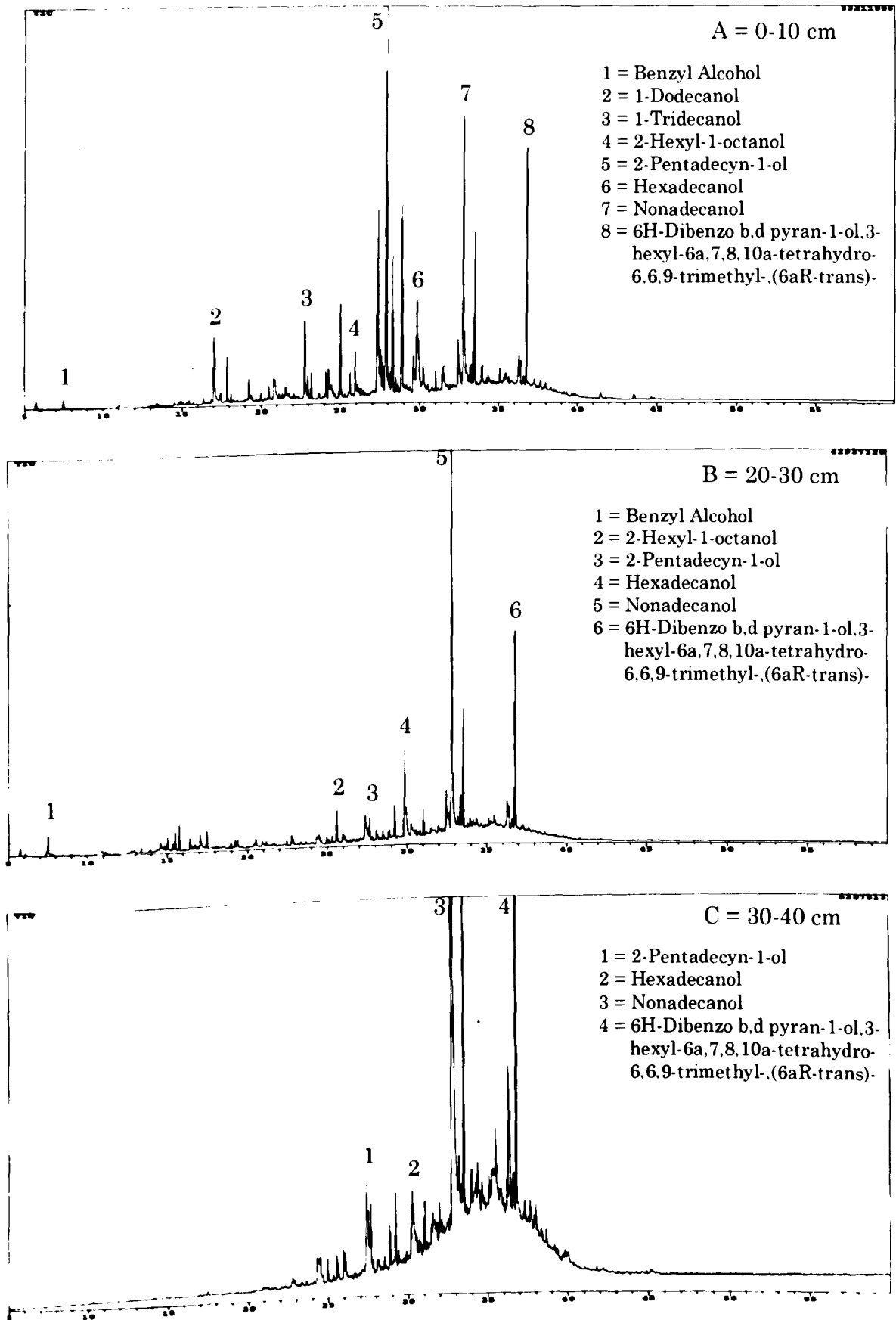


Figure 4.40: GC/MS chromatograms for alcohols and sterols fractions in core sediments of SSTB05 at three different layers (A, B and C)

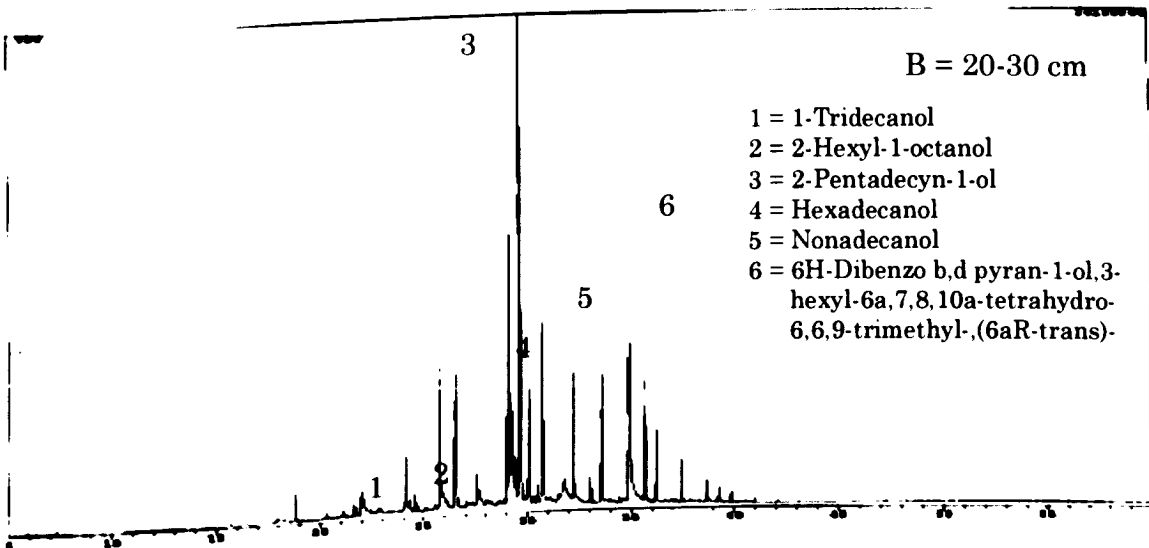
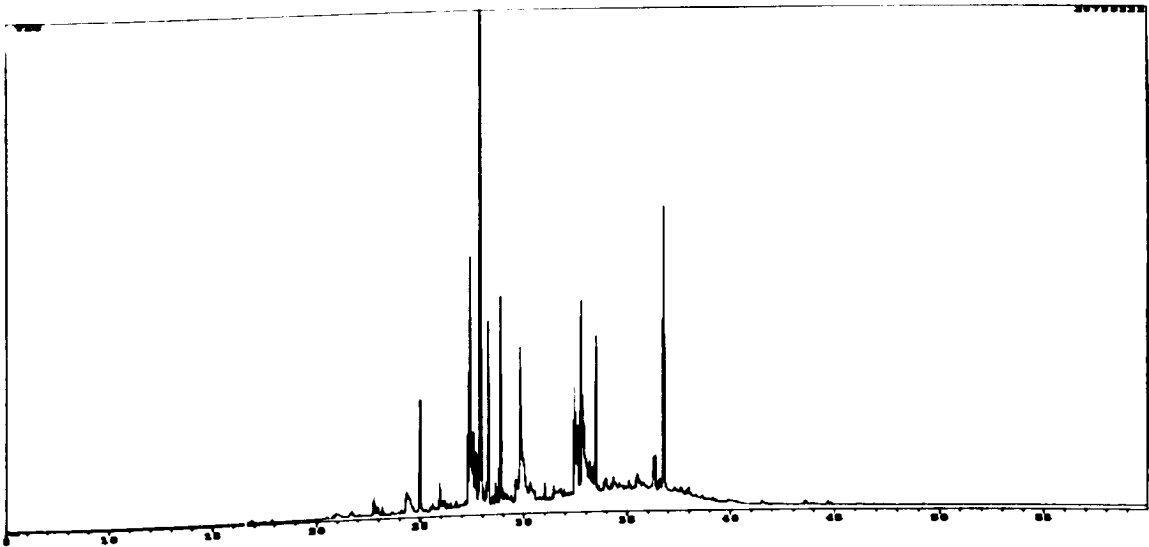
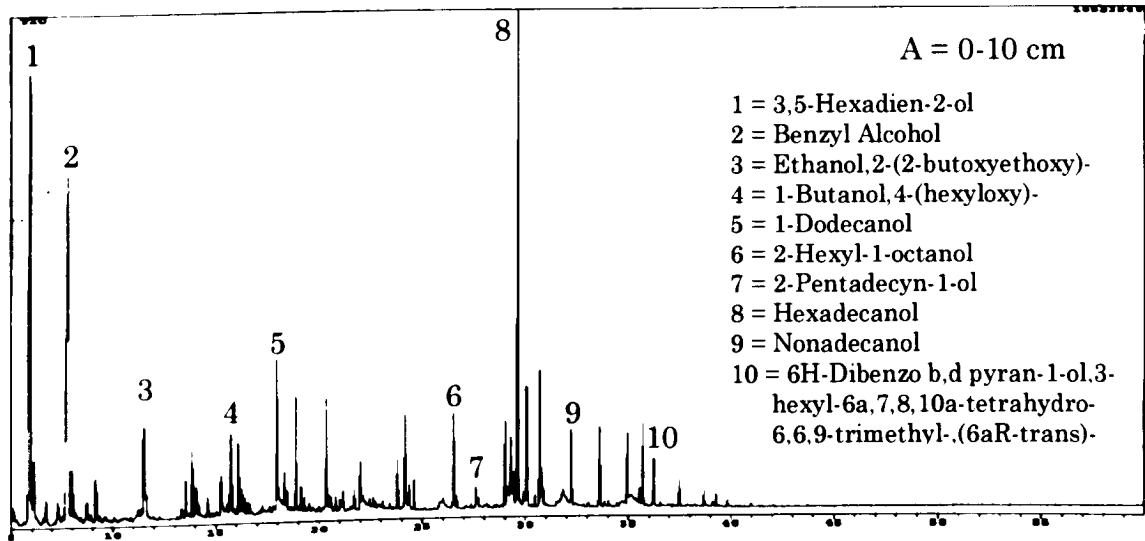


Figure 4.41: GC/MS chromatograms for alcohols and sterols fractions in core sediments of SSWK03 at three different layers (A, B and C)

Table 4.19: Alcohols and sterols identified in Santubong River

Name of the compound	RT	SSTB01			SSTB02		SSTB03			SSTB04		SSTB05	
		A	C	D	A	A	D	F	A	A	C	D	
Benzyl Alcohol	7.490	x	x			x	x			x	x		
Ethanol,2-(2-butoxyethoxy)-	11.049					x	x						
1-Butanol,4-(hexyloxy)-	15.008	x				x	x						
1-Dodecanol	17.035	x	x			x	x	x		x			
1-Tridecanol	22.770	x	x		x	x	x	x	x	x			
2-Hexyl-1-octanol	25.959	x	x		x					x	x		
2-Pentadecyn-1-ol	27.668	x	x	x	x	x	x	x	x	x	x	x	
Hexadecanol	29.848	x	x	x	x	x	x	x	x	x	x	x	
Nonadecanol	32.769	x	x	x	x	x	x	x	x	x	x	x	
6H-Dibenzo b,d pyran-1-ol,3-hexyl-6a,7,8,10a-tetrahydro-6,6,9-trimethyl-,(6aR-trans)-	36.808	x	x	x	x	x	x	x	x	x	x	x	
Stigmasterol	41.305									x			

Notes: A = 0-10 cm; C = 20-30 cm; D = 30-40 cm; F = 50-60 cm and x = detected

Table 4.20: Alcohols and sterols identified in Sarawak River

Name of the compound	RT	SSWK01			SSWK02			SSWK03			SSWK04		SSWK05			SSWK06		SSWK07		SSWK08		SSWK09	
		A	C	E	A	C	D	A	C	D	A	B	A	B	C	A	B	A	B	A	B	A	B
3,5-Hexadien-2-ol	6.319	x			x			x			x	x			x	x							
Benzyl Alcohol	7.490	x			x			x			x	x	x	x	x	x	x	x	x	x	x	x	x
Ethanol,2-(2-butoxyethoxy)-	11.049							x															
1-Butanol,4-(hexyloxy)-	15.008				x			x			x	x									x		x
1-Dodecanol	17.035				x	x		x			x	x	x	x	x	x	x	x	x	x	x	x	x
1-Tridecanol	22.770	x	x	x	x	x		x	x		x	x	x	x	x	x	x	x	x	x	x	x	x
2-Hexyl-1-octanol	25.959	x	x			x	x	x	x	x													
2-Pentadecyn-1-ol	27.668	x	x	x	x	x	x	x	x	x	x	x	x	x	x	x	x	x	x	x	x	x	x
Hexadecanol	29.848	x	x	x	x	x	x	x	x	x	x	x	x	x	x	x	x	x	x	x	x	x	x
Nonadecanol	32.769	x	x	x	x	x	x	x	x	x	x	x	x	x	x	x	x	x	x	x	x	x	x
6H-Dibenzo b,d pyran-1-ol,3-hexyl-6a,7,8,10a-tetrahydro-6,6,9-trimethyl-,(6aR-trans)-	36.808	x	x	x	x	x	x	x	x	x	x	x	x	x	x	x	x	x	x	x	x	x	x

Notes: A = 0-10 cm; B = 10-20 cm; C = 20-30 cm; D = 30-40 cm; E = 40-50 cm and x = detected

Alcohol and sterol biomarkers are used to identify whether the sources of organic matter in the environmental compartments originated from natural or anthropogenic sources. Cholesterol (marine markers), cholest-5,22-dien-ol, brassicasterol and dinosterol (phytoplankton origin), β -sitosterol and ergosterol (terrestrial sources) and 5 β -coprostanol (sewage sources) are the most common sterol biomarkers used (Mudge & Duce, 2005).

Short chain alcohols and sterols (≤ 22) were present in core sediments from both rivers and this indicates that inputs from unspecified marine, terrestrial and bacterial origins (Mudge and Duce, 2005). Stigmasterol (C₂₉) was identified in the surface sediment from SSTB04. This compound is a common steroid found in plant (Solomon and Fryhle, 2004) and usually detected in epicuticular waxes of vascular plants (Jeng *et al.*, 2003). C₂₂ was the longest chain of alcohol identified in Sarawak River sediments. The shortest chain of alcohol found in core sediments from Santubong River was C₇ while C₆ was the shortest alcohols identified in core sediments from Sarawak River.

4.9 Relationships Between Organic Matter, Particle Sizes, n-Alkanes and PAHs

The statistical analysis was performed in order to determine the inter-relationships between the organic matter, particle sizes, n-alkanes and PAHs. The statistical analyses were carried out using the Pearson's correlation coefficient and principal component analysis (PCA).

4.9.1 Correlation Coefficient

The Pearson's correlation coefficient was used to determine the inter-relationship between TOM, type of sediments, total n-alkanes and total PAHs. The graphs showing the relationship between percentages of TOM and percentages of sediments type are shown in Figures 4.42 to 4.44. The results of Pearson correlation analysis on organic matter content with three types of sediments are presented in Table 4.21.

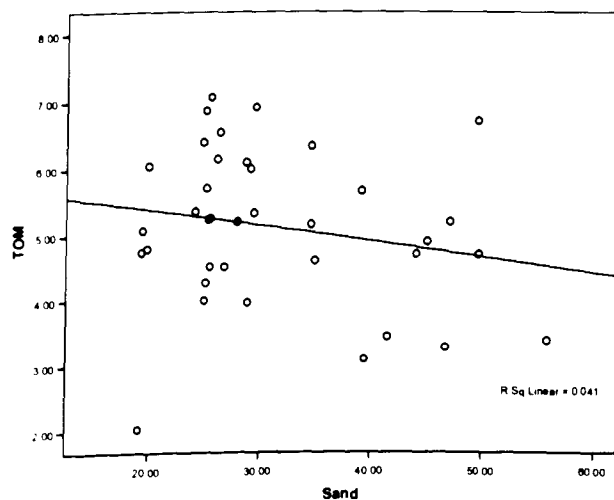


Figure 4.42: The correlation between the percentages of TOM (%) and sand (%)

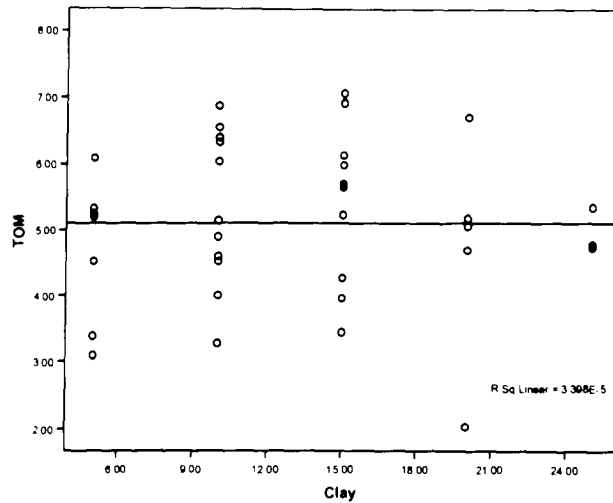


Figure 4.43: The correlation between the percentages of TOM (%) and clay (%)

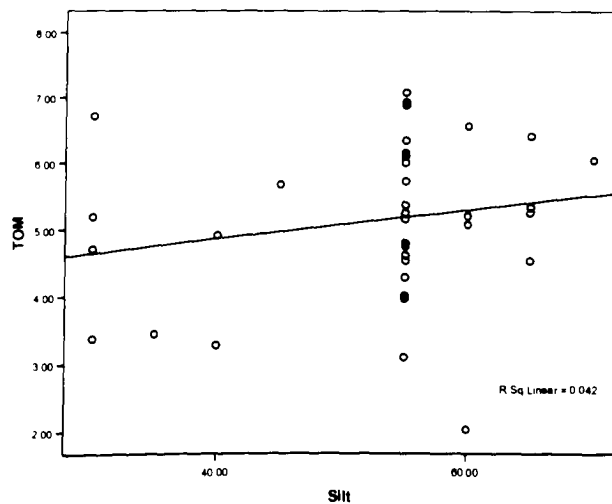


Figure 4.44: The correlation between the percentages of TOM (%) and silt (%)

There was no correlations between the percentages TOM with the types of sediments ($p > 0.05$). So, the percentages of TOM and the types of sediments were not affected by each other in Santubong River and Sarawak River. A study conducted by Commendatore and Esteves (2004) also found no correlation between percentages of organic matter and fine sediments.

Table 4.21: Pearson correlation matrices for type of sediments and TOM

		Type of sediments	TOM
Sand	Pearson Correlation	1	-.202
	Sig. (2-tailed)		.230
TOM	Pearson Correlation	-.202	1
	Sig. (2-tailed)	.230	
Clay	Pearson Correlation	1	.006
	Sig. (2-tailed)		.973
TOM	Pearson Correlation	.006	1
	Sig. (2-tailed)	.973	
Silt	Pearson Correlation	1	.206
	Sig. (2-tailed)		.222
TOM	Pearson Correlation	.206	1
	Sig. (2-tailed)	.222	

The graph showing the relationship between the concentrations of total n-alkanes ($\mu\text{g/g dw}$) and percentages of TOM is shown in Figure 4.45 while the results of Pearson correlation analysis on total n-alkanes with organic matter content are presented in Table 4.22.

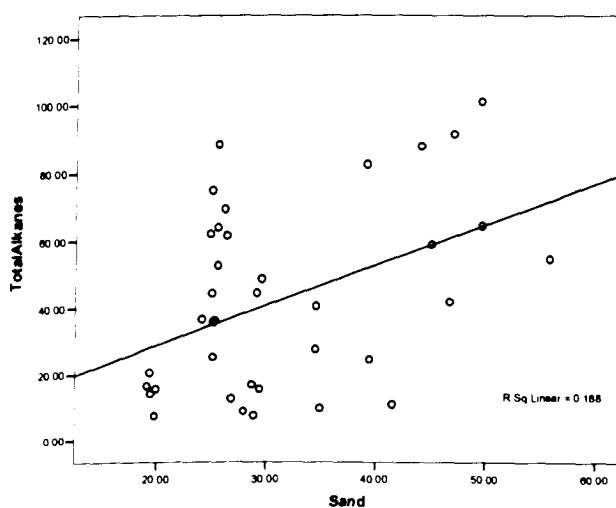


Figure 4.45: The correlation between the concentrations of total n-alkanes ($\mu\text{g/g dw}$) with percentages of TOM (%)

There was a weak positive correlation ($r = 0.428$) with confident intervals 99% between concentrations of total n-alkanes ($\mu\text{g/g dw}$) with percentages of TOM (%). This shows a significant contribution of the total n-alkanes by the organic matter content as their concentrations were relatively high in core sediments compared to the concentrations of total PAHs.

Table 4.22: Pearson correlation matrices for TOM and total n-alkanes

		TOM	Total n-alkanes
TOM	Pearson Correlation	1	.428(**)
	Sig. (2-tailed)		.008
	N	37	37
Total n-alkanes	Pearson Correlation	.428(**)	1
	Sig. (2-tailed)	.008	
	N	37	37

** Correlation is significant at the 0.01 level (2-tailed).

The graphs showing the relationship between concentrations of total n-alkanes ($\mu\text{g/g dw}$) and percentages of type of sediments (%) are shown in Figures 4.46 to 4.48 while the results of Pearson correlation analysis on total n-alkanes with type of sediments are presented in Table 4.23.

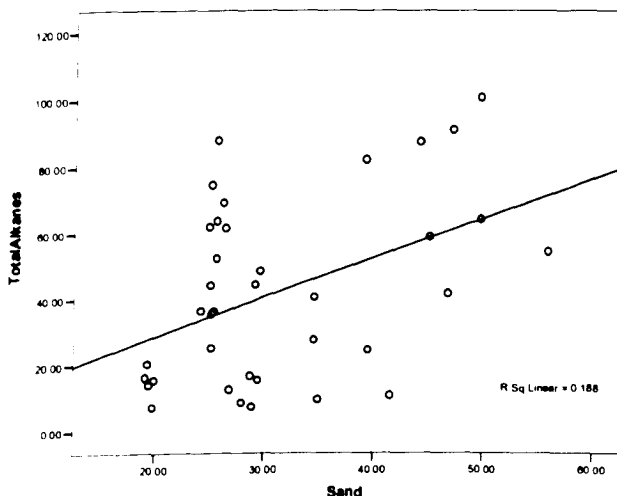


Figure 4.46: The correlation between the concentrations of total n-alkanes ($\mu\text{g/g dw}$) with percentages of sand (%)

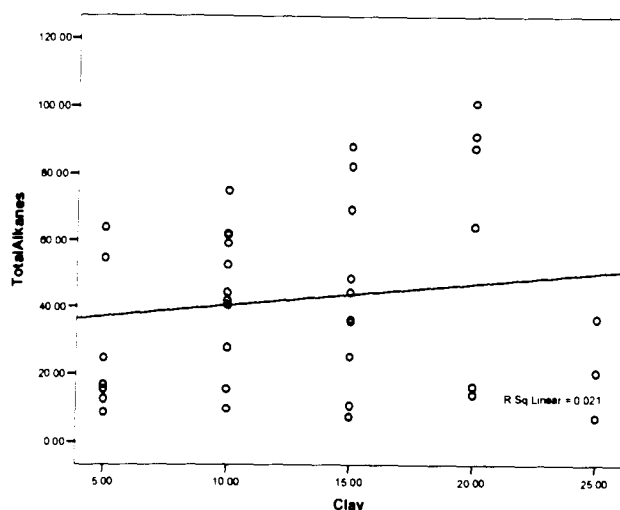


Figure 4.47: The correlation between the concentrations of total n-alkanes ($\mu\text{g/g dw}$) with percentages of clay (%)

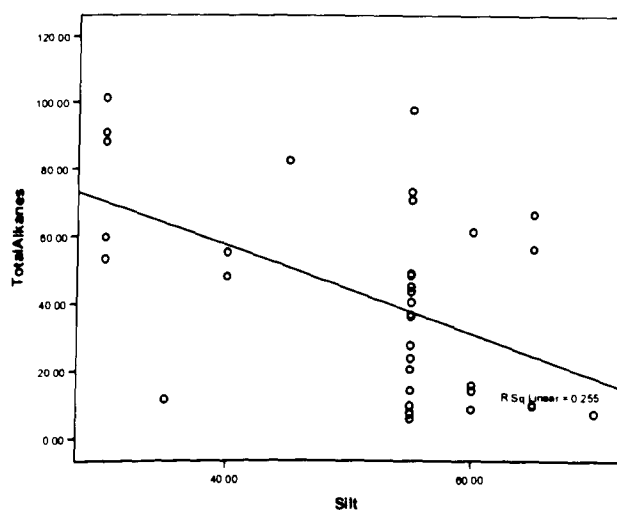


Figure 4.48: The correlation between the concentrations of total n-alkanes ($\mu\text{g/g dw}$) with percentages of silt (%)

There was a weak positive correlation ($r = 0.434$) with confident intervals 99% between concentrations of total n-alkanes with percentages of sand, while a weak negative correlation ($r = -0.505$) with 99% confident intervals was found between total alkanes and silt. However, no correlation ($p > 0.05$) was observed between concentrations of total n-alkanes with percentages of clay. These observations may be due to their different physical and chemical properties of sediments.

Table 4.23: Pearson correlation matrices for type of sediments and total n-alkanes

		Type of sediments	Total n-alkanes
Sand	Pearson Correlation	1	.434(**)
	Sig. (2-tailed)		.007
Total alkanes	Pearson Correlation	.434(**)	1
	Sig. (2-tailed)	.007	
Clay	Pearson Correlation	1	.146
	Sig. (2-tailed)		.389
Total alkanes	Pearson Correlation	.146	1
	Sig. (2-tailed)	.389	
Silt	Pearson Correlation	1	-.505(**)
	Sig. (2-tailed)		.001
Total alkanes	Pearson Correlation	-.505(**)	1
	Sig. (2-tailed)	.001	

** Correlation is significant at the 0.01 level (2-tailed).

The graph showing the relationship between concentrations of total PAHs ($\mu\text{g/g dw}$) and percentages of TOM (%) is shown in Figure 4.49, while the results of Pearson correlation analysis on total PAHs with TOM are presented in Table 4.24.

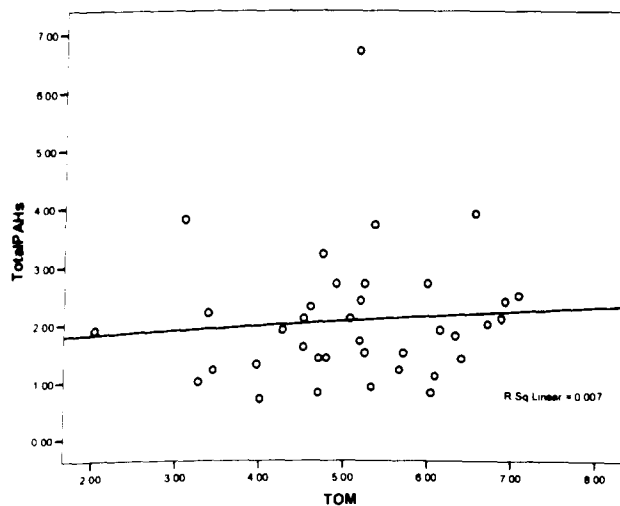


Figure 4.49: The correlation between the concentrations of total PAHs ($\mu\text{g/g dw}$) with percentages of TOM (%)

There was no correlation ($p > 0.05$) between concentrations of total PAHs ($\mu\text{g/g dw}$) with percentages of TOM (%). The concentrations of total PAHs were relatively lower compared to the concentrations of total n-alkanes in core sediments from both rivers, so the contribution of the total PAHs by the organic matter content can be considered minimal. This also may due to the complex input of pyrolytic sources of PAHs in core sediments of both rivers.

Table 4.24: Pearson correlation matrices for TOM and PAHs

		TOM	PAHs
TOM	Pearson Correlation	1	.082
	Sig. (2-tailed)		.629
PAHs	Pearson Correlation	.082	1
	Sig. (2-tailed)	.629	

The graphs showing the relationship between concentrations of total PAHs ($\mu\text{g/g dw}$) and percentages of type of sediments (%) are shown in Figures 4.50 to 4.52 while the results of Pearson correlation analysis on total PAHs with type of sediments are presented in Table 4.25.

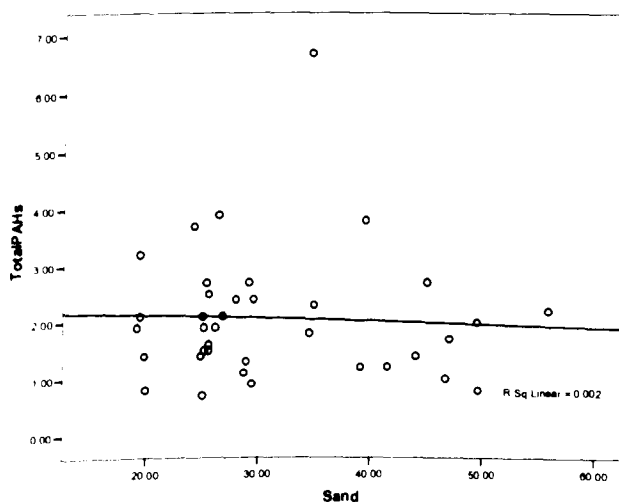


Figure 4.50: The correlation between the concentrations of total PAHs ($\mu\text{g/g dw}$) with percentages of sand (%)

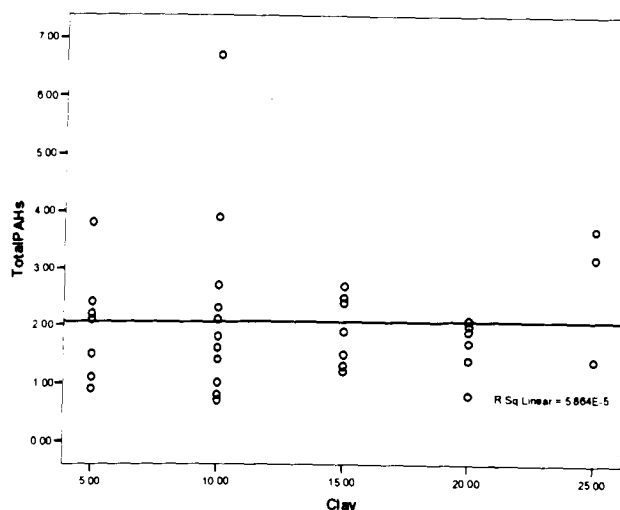


Figure 4.51: The correlation between the concentrations of total PAHs ($\mu\text{g/g dw}$) with percentages of clay (%)

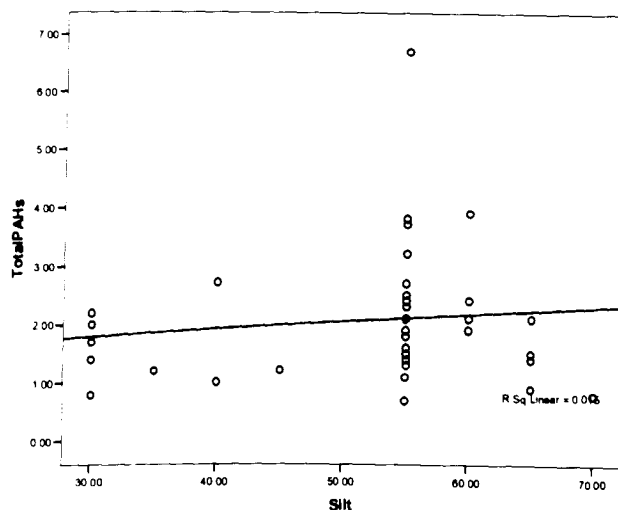


Figure 4.52: The correlation between the concentrations of total PAHs ($\mu\text{g/g dw}$) with percentages of silt (%)

There was no significance correlation ($p > 0.05$) between concentrations of total PAHs ($\mu\text{g/g dw}$) with percentages of sand, clay and silt (%). So, the concentrations of total PAHs were not affected by the type of sediments from Santubong River and Sarawak River.

Table 4.25: Pearson correlation matrices for type of sediments and total PAHs

		Type of soil	Total PAHs
Sand	Pearson Correlation	1	-.048
	Sig. (2-tailed)		.778
Total PAHs	Pearson Correlation	-.048	1
	Sig. (2-tailed)	.778	
Clay	Pearson Correlation	1	.008
	Sig. (2-tailed)		.964
Total PAHs	Pearson Correlation	.008	1
	Sig. (2-tailed)	.964	
Silt	Pearson Correlation	1	.123
	Sig. (2-tailed)		.470
Total PAHs	Pearson Correlation	.123	1
	Sig. (2-tailed)	.470	

The graph showing the relationship between concentrations of total n-alkanes ($\mu\text{g/g dw}$) with total PAHs ($\mu\text{g/g dw}$) is shown in Figure 4.53 while the results of Pearson correlation analysis on total n-alkanes with total PAHs are presented in Table 4.26. There was no significance correlation ($p > 0.05$) between concentrations of total n-alkanes ($\mu\text{g/g dw}$) with concentrations of total PAHs ($\mu\text{g/g dw}$) indicating different primary sources and/or varied transport processes for both compounds.

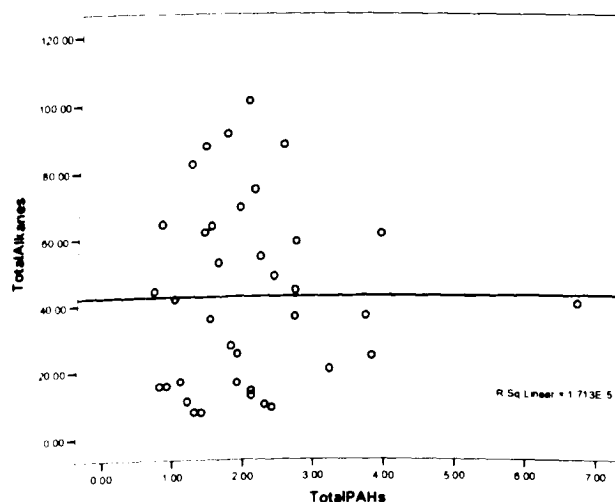


Figure 4.53: The correlation between the concentrations of total n-alkanes ($\mu\text{g/g dw}$) with concentrations of total PAHs ($\mu\text{g/g dw}$)

Table 4.26: Pearson correlation matrices for total n-alkanes and total PAHs

		Total alkanes	Total PAHs
Total alkanes	Pearson Correlation	1	.004
	Sig. (2-tailed)		.981
	N	37	37
Total PAHs	Pearson Correlation	.004	1
	Sig. (2-tailed)	.981	
	N	37	37

4.9.2 Principal Component Analysis (PCA)

The PCA was performed in order to summarize the available data and to analyze the inter-relationships among a large number of variables (Hair *et al.*, 1995). The eigenvalues of the extracted factors, the eigenvalues difference among factors and the proportion of total sample variance explained by the factors for the rotated factor loadings (Varimax with Kaiser Normalization) are shown in Table 4.27. The PCA has reduced the dimensionality of the problem of twelve original variables into four new factors for every core sediments studied. The four factors were selected to represent the geochemical parameters namely TOM, particle sizes, total n-alkanes and total PAHs without losing significant information.

The first factor explains the largest proportions of total variance, which is 33.442%, while the second, third and fourth factors explain 23.882%, 21.489% and 10.454% of total variance, respectively.

Table 4.27: Eigenvalues, percentage of variance and cumulative of variance in the factor analysis for core sediments from Santubong River and Sarawak River

Component	Rotation Sums of Squared Loadings		
	Total	% of Variance	Cumulative %
1	4.013	33.442	33.442
2	2.866	23.882	57.324
3	2.579	21.489	78.813
4	1.255	10.454	89.267

Extraction Method: Principal Component Analysis

Table 4.28 shows the PCA loading of TOM, particle sizes, total n-alkanes, total PAHs and other parameters using varimax rotation while Figure 4.54 presents the PCA score plot of the four factors that represent 89.267% of the total variance. In the first factor, TOM, total n-alkanes, LMW n-alkanes, HMW n-alkanes, pristane and phytane are very high in the positive direction. Total PAHs, LPAHs and HPAHs show high positive loadings on Factor 2. Silt shows positive loading while sand shows high negative loading on factor 3. Clay is very high in the negative direction on Factor 4. Thus, factor 1 represents the concentrations of n-alkanes where there are positive correlations between n-alkanes and TOM. Factor 2 represents the PAHs concentrations where there is no correlations between PAHs concentrations with other variables. Factor 3 represents particle sizes ≥ 0.002 mm while factor 4 represents particle sizes < 0.002 mm. There is a negative correlation between sand and silt as shown in factor 3. However, no correlation with other variables was observed for clay.

Table 4.28: PCA loading of TOM, particle sizes, total n-alkanes, total PAHs and concentrations of LMW n-alkanes, HMW n-alkanes, LPAHs, HPAHs, pristane and phytane using varimax rotation.

Parameter	Component			
	1	2	3	4
TOM	.715	.076	-.365	.035
Sand	.084	-.018	.949	-.170
Clay	.034	.004	.036	.976
Silt	-.136	.100	-.915	-.243
TotalAlkanes	.852	.038	.440	.154
TotalPAHs	.011	.998	-.031	-.001
LMWalkanes	.889	.043	.306	.219
HMWalkanes	.841	.011	.455	.131
LPAHs	-.126	.936	-.097	.023
HPAHs	.098	.966	.010	-.011
Pristane	.847	-.202	.018	-.222
Phytane	.713	.040	-.447	-.271

Extraction Method: Principal Component Analysis.
 Rotation Method: Varimax with Kaiser Normalization.

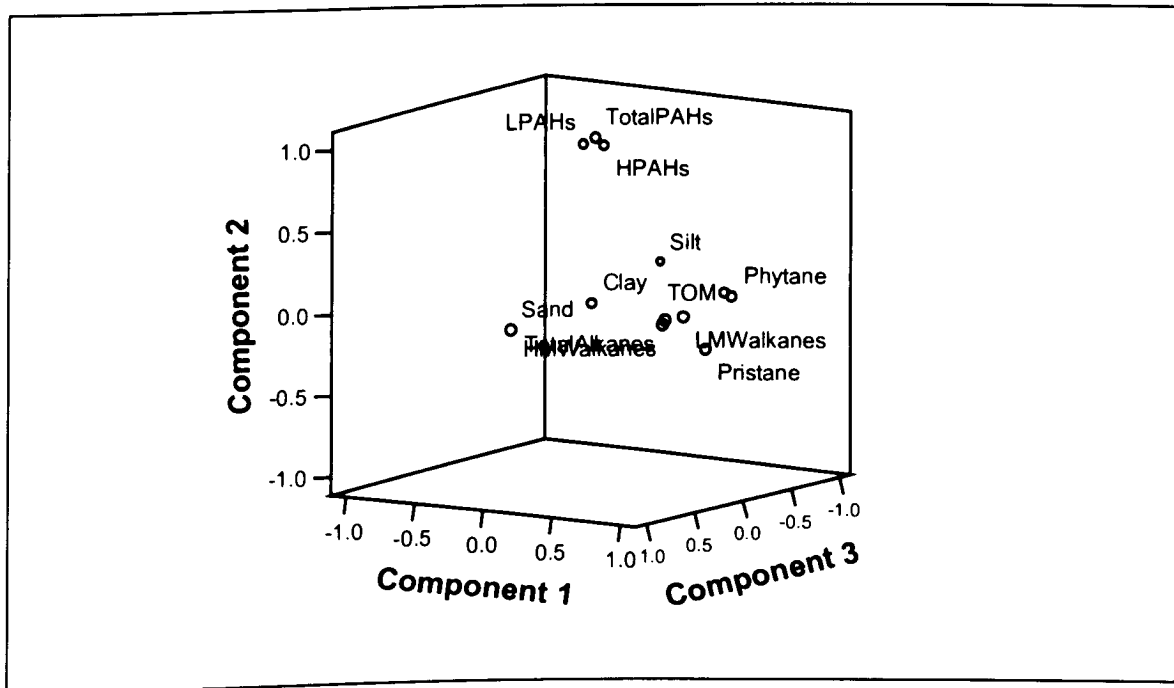


Figure 4.54: PCA score plot of first, second, third and fourth factors accounting for 89.267% of variance for core sediments from Santubong River and Sarawak River

4.10 Sources of Organic Matter in Sediments

The bioindicators of both n-alkanes and PAHs were used to identify the sources of organic matter from Santubong and Sarawak Rivers. The ratios and indices for saturated aliphatic hydrocarbons such as pristane/phytane, isoprenoid/n-alkanes, CPI and total n-alkanes in core sediments from Santubong River and Sarawak River are given in Tables 4.29 and 4.30, respectively while the PAHs ratios of fluoranthene/pyrene, benzo[a]anthracene/chrysene, total LPAHs/total HPAHs and total PAHs in core sediments from both rivers are given in Table 4.31. The total n-alkanes ranging from 10.8 to 101.1 $\mu\text{g/g dw}$ and 7.3 to 61.7 $\mu\text{g/g dw}$ were observed in core sediments from Santubong River and Sarawak River, respectively. The total PAHs in core sediments from Santubong River ranged from 0.8 to 2.5 $\mu\text{g/g dw}$ while 0.7 to 6.7 $\mu\text{g/g dw}$ of total PAHs were observed in Sarawak River.

Table 4.29: Hydrocarbon indices of core sediments from Santubong River

Biomarker Indices	SSTB01			SSTB02			SSTB03			SSTB04			SSTB05		
	A	C	D	A	C	D	A	D	F	A	C	E	A	C	D
Pristane/phytane	1.1	1.1	1.1	1.1	1.1	1.1	0.3	0.3	0.3	0.4	0.4	0.4	0.5	0.5	0.5
Pristane/C ₁₇	0.2	0.2	0.2	0.2	0.2	0.2	0.6	0.6	0.6	0.6	0.6	0.6	0.4	0.4	0.4
Phytane/C ₁₈	0.8	0.8	0.8	0.8	0.8	0.8	0.9	0.9	0.9	0.9	0.9	0.9	0.8	0.8	0.8
nC ₂₅ /nC ₁₅	93.8	92.4	80.0	31.3	30.7	21.9	0.0	0.0	0.0	54.9	48.1	37.8	77.8	64.6	20.2
nC ₃₁ /nC ₁₉	97.9	82.7	40.0	28.4	28.3	1.9	11.3	11.1	10.8	11.4	6.2	4.5	18.3	13.1	6.7
CPI	1.1	1.0	1.1	1.0	1.0	1.0	1.1	1.0	1.0	1.2	1.1	1.0	1.1	1.0	1.0
LMW/HWM	0.1	0.1	0.2	0.1	0.1	0.7	0.1	0.1	0.1	0.2	0.2	0.2	0.2	0.2	0.2
Even/odd	1.0	1.1	1.0	1.0	1.1	1.2	1.0	1.1	1.0	1.0	1.1	1.1	1.0	1.1	1.3
TA/nC ₁₆	2150.9	2113.9	1743.5	1364.0	1350.4	174.8	1169.7	1158.7	1141.1	431.4	248.2	191.0	2151.8	1941.6	552.4
TA (µg/g dw)	101.1	82.4	64.5	91.4	87.8	10.8	74.9	69.5	63.9	48.7	27.6	16.8	88.2	62.1	15.5

Notes: A = 0-10 cm; C = 20-30 cm; D = 30-40 cm; E = 40-50 cm; F = 50-60 cm; pri = pristane and phy = phytane

Table 4.30: Hydrocarbon indices of core sediments from Sarawak River

Biomarker Indices	Concentrations (ng/g dry weight)																					
	SSWK01			SSWK02			SSWK03			SSWK04		SSWK05			SSWK06		SSWK07		SSWK08		SSWK09	
	A	C	E	A	C	D	A	C	D	A	B	A	B	C	A	B	A	B	A	B	A	B
Pristane/ phytane	0.8	0.8	0.8	0.9	0.9	0.9	1.0	1.0	1.0	0.3	0.3	0.2	0.2	0.2	0.2	0.2	0.2	0.2	0.3	0.3	0.2	0.2
Pristane/ C ₁₇	0.5	0.5	0.5	0.4	0.4	0.4	0.3	0.3	0.3	0.8	0.8	0.7	0.7	0.7	0.7	0.7	0.8	0.8	0.9	0.9	0.9	0.9
Phytane/ C ₁₈	0.3	0.3	0.3	0.3	0.3	0.3	0.4	0.4	0.4	0.9	0.9	0.8	0.8	0.8	0.8	0.8	0.9	0.9	0.9	0.9	0.9	0.9
nC ₂₇ /nC ₁₅	65.5	56.0	49.1	34.9	29.6	29.0	28.7	27.2	14.2	0.0	0.0	58.6	57.5	56.6	0.0	0.0	0.0	0.0	0.0	0.0	0.0	0.0
nC ₃₁ /nC ₁₉	11.8	11.4	10.6	9.0	8.0	7.5	7.8	6.3	1.0	18.9	16.4	120.7	65.4	33.1	28.6	18.3	45.1	35.1	14.4	11.8	25.3	13.8
CPI	1.2	0.9	1.0	0.9	0.9	0.9	1.0	1.1	1.2	2.1	2.0	2.3	2.2	1.9	1.2	1.1	1.5	1.7	1.8	1.7	1.8	1.9
LMW/ HMW	0.1	0.1	0.1	0.1	0.1	0.1	0.2	0.2	0.2	0.5	0.5	0.2	0.2	0.2	0.2	0.2	0.2	0.2	0.6	0.6	0.3	0.3
Even/odd	0.9	1.3	1.1	1.1	1.1	1.2	1.0	1.0	0.9	0.8	0.8	0.5	0.66	0.8	1.0	1.0	0.8	0.7	0.9	1.0	0.8	0.8
TA/ nC ₁₆	584.9	563.2	469.1	545.9	553.2	492.6	172.4	138.9	99.8	440.2	358.4	1226.6	793.1	632.4	2814.6	2287.9	1453.1	1177.1	724.3	604.7	930.4	630.2
TA (µg/g dw)	59.1	54.6	41.8	61.7	52.6	44.3	44.5	35.7	15.5	9.7	7.5	40.5	24.6	16.4	36.6	25.2	36.3	14.1	8.7	7.3	20.5	12.6

Notes: A = 0-10 cm; B = 10-20 cm; C = 20-30 cm; D = 30-40 cm and E = 40-50 cm

Table 4.31: PAHs ratios and total PAHs in the core sediments from Santubong River and Sarawak River

River	Samples	Depth (cm)	Fl/Py	BaA/Chr	Σ LPAHs/ Σ HPAHs	Total PAHs (μ g/g dw)
Santubong	SSTB01	0-10	1.6	4.9	0.4	2.0
		20-30	1.5	4.2	0.4	1.2
		30-40	1.4	3.9	0.4	0.8
	SSTB02	0-10	1.3	3.5	0.2	1.7
		20-30	1.2	2.7	0.2	1.4
		30-40	1.1	2.5	0.2	1.2
	SSTB03	0-10	7.2	4.6	0.3	2.1
		30-40	5.5	4.3	0.3	1.9
		50-60	1.4	4.2	0.3	1.5
	SSTB04	0-10	11.1	4.3	0.5	2.4
		20-30	6.7	3.8	0.5	1.8
		40-50	1.3	2.7	0.5	1.1
	SSTB05	0-10	1.6	1.7	0.5	2.5
		20-30	1.5	1.3	0.5	1.4
		30-40	1.3	1.2	0.5	0.8
Sarawak	SSWK01	0-10	1.9	6.8	0.8	2.7
		20-30	1.3	6.1	0.8	2.2
		40-50	1.0	5.2	0.8	1.0
	SSWK02	0-10	4.5	5.0	0.6	3.9
		20-30	4.4	4.0	0.6	1.6
		30-40	3.5	1.6	0.6	0.7
	SSWK03	0-10	1.3	2.5	0.8	2.7
		20-30	1.2	2.4	0.8	1.5
		30-40	1.1	1.6	0.8	0.9
	SSWK04	0-10	1.3	1.4	0.6	2.3
		10-20	1.0	1.2	0.6	1.3
	SSWK05	0-10	1.8	1.9	0.5	6.7
		10-20	1.6	1.7	0.5	3.8
		20-30	1.5	1.3	0.5	1.9
	SSWK06	0-10	3.0	1.1	0.9	3.7
10-20		1.8	1.0	0.9	1.9	
SSWK07	0-10	1.1	1.2	0.8	2.7	
	10-20	1.0	1.0	0.8	2.1	
SSWK08	0-10	1.5	1.3	0.7	2.4	
	10-20	1.4	1.1	0.7	1.4	
SSWK09	0-10	1.5	1.7	0.6	3.2	
	10-20	1.2	1.6	0.6	2.1	

Carbon preference index (CPI) can be used to differentiate between biogenic and petrogenic sources of hydrocarbons (Medeiros and Bicego, 2004). The values of CPI obtained for all core sediments from Santubong River were around 1. CPI values observed in core sediments from Sarawak River were around 1 for SSWK01, SSWK02, SSWK03 and SSWK05 stations. This indicates that the sediments have received organic matter from petrogenic sources. Although CPI values for the other core sediments from Sarawak River were above 1, it was still considered as contaminated as CPI values for the uncontaminated sediments are between 3-6 (Commendatore and Esteves, 2004).

However, the LMW/HMW for all core sediments from both rivers were < 1 indicating biogenic sources (Commendatore and Esteves, 2004). $C_{25}/C_{15} > 0.8$ for most of the samples from Santubong River and Sarawak River indicating sediment received organic matter with high amount of waxes originated from high terrestrial plants (Copper, 1990). Other core sediments from SSTB03, SSWK04 and upstream of Kuap rivers have the C_{25}/C_{15} ratio values 0.0 indicating anthropogenic inputs of hydrocarbons.

The relative proportions of allochthonous and autochthonous hydrocarbon inputs can be determined using ratios of C_{31}/C_{19} . The ratios of $C_{31}/C_{19} > 0.4$ indicating non-marine sources of organic matter (Gao *et al.*, 2007). The ratios of C_{25}/C_{15} and C_{31}/C_{19} exhibit consistent trend where they decrease with depth. This is due to the increase in concentrations of short chain hydrocarbon (C_{15} and C_{19}) and the decrease of long chain hydrocarbon (C_{25} and C_{31}) with depths. This observation also supports the degradation of HMW n-alkanes to LMW n-alkanes as suggested by the vertical distribution of HMW n-alkanes.

Core sediments from Santubong River and Sarawak River show no predominance of even/odd ratio indicating petrogenic sources because biogenic sources (plant waxes) usually show odd-numbered carbon alkanes that were 8-10 times more abundant than even-numbered carbon alkanes (Commendatore and Esteves, 2004). Total n-alkanes/C₁₆ ratio are higher than 50 for all core sediments from both rivers indicating biogenic sources of n-alkanes (Commendatore and Esteves, 2004). Based on the observations above, it can be assumed that n-alkanes in all core sediments from Santubong River and Sarawak River were originated from a mixture of terrestrial and petrogenic sources.

The pristane/phytane ratios for Santubong River and Sarawak River sediments are below 1 for most samples indicating petrogenic sources (Aboul Kassim & Simoneit, 1996). Estuarine sediments from Santubong River have pristane/phytane ratios slightly above 1 but still lower than 3, which is a typical value for biogenic sources.

Pri/C₁₇ and phy/C₁₈ are relatively low (≤ 1.0) in all core sediments indicating low degradation of aliphatic hydrocarbons (Aboul Kassim & Simoneit, 1996). No significant variation on the ratios of the isoprenoid hydrocarbons with depth was observed for core sediments from both rivers.

The ratios of Fl/Py > 1 (Zhou and Maskaoui, 2003) and BaA/Chr > 0.4 (Medeiros and Bicego, 2004) in all core sediments from both rivers showed that PAHs originated from pyrolytic sources. Fl/Py and BaA/Chr ratios also exhibit consistent trend in core sediments from both rivers where it decreased toward the

lower layers. All core sediment from both rivers exhibited $\Sigma\text{LPAHs}/\Sigma\text{HPAHs} < 1$ indicating PAHs were originated from pyrolytic sources (Wang *et al.*, 2006).

The overall sources of the organic matter in the core sediments of Santubong and Sarawak Rivers are summarized in Table 4.32.

Table 4.32: Sources of organic matter as indicated by the bioindicators

River	Biomarkers	Bio	Ter	Ant	Pet	Pyr	Mar	Non-Mar
Santubong	n-Alkanes	X	X		X			X
	Isoprenoid				X			
	PAHs					X		
	FAMEs	X						
	Phthalate esters			X				
	Alcohols & sterols	X						
Sarawak	n-Alkanes	X	X		X			X
	Isoprenoid				X			
	PAHs					X		
	FAMEs	X						
	Phthalate esters			X				
	Alcohols & sterols	X	X				X	

Notes: Bio = biogenic; ter = terrestrial; ant = anthropogenic; pet = petrogenic; pyr = pyrolytic; mar = marine and non-mar = non-marine

CHAPTER FIVE

CONCLUSIONS AND RECOMMENDATIONS

The distributions of aliphatic hydrocarbons, PAHs, FAMEs, phthalate esters and sterols in the core sediments of Santubong and Sarawak rivers were analyzed using gas chromatography techniques. The TOM contents and particle sizes in the core sediments from both rivers were also determined. Santubong and Sarawak rivers sediments can be classified into loam and silt loam according to USDA soil textural triangle. TOM in the core sediments from Santubong and Sarawak rivers were in the range of 3.44 - 7.07 % and 2.03 - 6.55 %, respectively. Distribution of TOM in the core sediments from both rivers showed a consistent trend with reduction of TOM toward the lower layers.

The core sediments studied showed dominance of long-chain n-alkanes ($>C_{23}$) such as C_{23} , C_{25} , C_{27} , C_{29} and C_{31} indicating the sources of aliphatic hydrocarbons are from vascular terrestrial plants. The total n-alkanes in the core sediments from Santubong and Sarawak rivers ranged from 10.8 to 101.1 $\mu\text{g/g dw}$ and 7.3 to 61.7 $\mu\text{g/g dw}$, respectively. Both rivers are considered moderately polluted with n-alkanes compared to those reported in other places. The spatial distribution of total n-alkanes suggests a mixture of inputs from both biogenic and petrogenic sources, particularly from anthropogenic activities at Kuching City, Pending and Sejingkat Barrage and shipping activities at the estuary and Senari Harbour.

At least one individual PAH with concentration higher than the ERL value was identified in the core sediments studied which may pose biological impairments. The concentrations of acenaphthylene and fluorine were higher than the ERM value

in some of the core sediments from Sarawak River. Total PAHs in the core sediments ranged from 0.8 to 2.5 $\mu\text{g/g dw}$ and 0.7 to 6.7 $\mu\text{g/g dw}$ for Santubong and Sarawak rivers, respectively. The concentration levels of PAHs in the core sediments from both rivers are comparable to those reported in the core sediments from other places. However, this level of total PAHs concentration is unlikely to cause biological impairment as it was lower than the ERL. There was a few core sediments from Sarawak River with the total PAHs concentrations greater than the ERL value but still below the effects-range median (ERM) indicating that it may occasionally pose biological impairment.

The FAMEs fractions from the core sediments for both rivers were dominated by short chain FAMEs ($\leq C_{20}$) and this indicates planktonic origins of FAMEs. The alcohols fractions from core sediments of both rivers were dominated by short chain alcohols and sterols ($\leq C_{22}$). This indicates inputs from unspecified marine, terrestrial and bacterial origins. DEHP, which is a common phthalate esters found in environmental samples, was detected in almost all core sediments from both rivers.

CPI values for n-alkanes in the core sediments from both rivers indicated it was originated from petrogenic sources. However, biomarker indices indicated that the input of aliphatic hydrocarbons in the core sediments were originated from a mixture of terrestrial and petrogenic sources. Ratios of pri/C_{17} and phy/C_{18} (< 1.0) indicate low degradation of aliphatic hydrocarbons in the core sediments from both rivers. The spatial distribution of PAHs and data of PAHs ratios showed pyrolytic inputs originated from several anthropogenic activities including shipping activities at Senari Port, boating activities and municipal wastes at Kuching City and also industrial wastes near the Pending area and Sejingkat Barrage.

The Pearson correlation and PCA analyses showed a weak positive correlation between concentrations of total n-alkanes with percentages of TOM and sand at 99% level of significance but showed a weak negative correlation with silt at 99% confident intervals. No significance correlation was observed between concentrations of total n-alkanes with concentrations of total PAHs indicating different primary sources and/or varied transport processes for both compounds.

There are few aspects need to be considered in order to provide a more complete information on the status of distribution of organic compounds in the core sediments from Santubong and Sarawak rivers. Future studies should include analysis on the regular hydrocarbon biomarkers including hopanoid and triterpenoid hydrocarbons. A comprehensive quantitative analysis should be carried out on polar compounds (FAMEs, phthalate esters and alcohols) so that a better understanding of the sources and depositional environment of organic matter in the core sediments can be obtained. Carbon dating analysis of core sediments should also be performed in future studies in order to determine the accurate history of aliphatic and PAHs inputs with time in the core sediments.

REFERENCES

- Aboul-Kassim, T.A.T. and Simoneit, B.R.T. 1996. Lipid geochemistry of surficial sediments from the coastal environment of Egypt 1. Aliphatic hydrocarbons-characterization and sources. *Marine Chemistry*, **54**: 135-158
- Al-Saad, H.T. and Al-Timari, A. 1993. Sources of hydrocarbon and fatty acids in sediments from Hor Al-Hammar Marsh, Shatt Al-Arab, and north-west Arabian Gulf. *Marine Pollution Bulletin*, **26**: 559-564
- Berthod, A., Wang, X., Gahm, K.H. and Armstrong, D.W. 1998. Quantitative & stereoisomeric determination of light biomarkers in crude oil and coal samples. *Geochimica et Cosmochimica Acta*, **62**: 1619-1630
- Birgel, D., Stein, R. and Hefter, J. 2004. Aliphatic lipids in recent sediments of the Fram Strait/ Yermak Plateau (Arctic Ocean): composition, sources and transport processes. *Marine Chemistry*, **88**: 127-160
- Blumer, M. 1957. Removal of elemental sulfur from hydrocarbon fractions. *Analytical Chemistry*, **29**: 1039-1041
- Bouloubassi, I. and Saliot, A. 1993. Investigation of anthropogenic and natural organic inputs in estuarine sediments using hydrocarbon markers (NAH, LAB, PAH). *Oceanologica Acta*, **16**: 145-161
- Bray, E.E. and Evans, E.D. 1961. Distribution of n-paraffins as a clue to recognition of source beds. *Geochimica et Cosmochimica Acta*, **22**: 2 – 15
- Brown, D., Thompson, R.S., Stewart, K.M., Croudace, C.P. and Gillings, E. 1996. The effect of phthalate ester plasticisers on the emergence of the midge (*Chironomus riparius*) from treated sediments. *Chemosphere*, **32**: 2177-2187
- Brown, R.B. 2003. *Soil Texture*. Fact Sheet SL-29, Soil and Water Science Department, Institute of Food and Agricultural Sciences, University of Florida, Gainesville. pp. 1-8
- Colombo, J.C., Barreda, A., Bilos, C., Cappelletti, N., Demichelis, S., Lombardi, P., Migoya, M.C., Skorupka, C. and Suarez, G. 2005. Oil spill in the Rio de la Plata Estuary, Argentina: 1. Biogeochemical assessment of waters, sediments, soils and biota. *Environmental Pollution*, **134**: 277-289
- Colombo, J.C., Silverberg, N. and Gearing, J.N. 1997. Lipid biogeochemistry in the Laurentian Trough-II. Changes in composition of fatty acids, sterols and aliphatic hydrocarbons during early diagenesis. *Organic Geochemistry*, **26**: 257-274
- Commendatore, M.G. and Esteves, J.L. 2004. Natural and anthropogenic hydrocarbons in sediments from the Chubut River (Patagonia, Argentina). *Marine Pollution Bulletin*, **48**: 910-918

- Commendatore, M.G., Esteves, J.L. and Colombo J.C. 2000. Hydrocarbons in coastal sediments of Patagonia, Argentina: levels and probable sources. *Marine Pollution Bulletin*, **40**: 989-998
- Copper, B.S. 1990. Oil generating coals. In: Thomas, B.M. (ed.). *Petroleum Geochemistry in Exploration of the Norwegian Shelf*. Lancaster: Graham & Trotman Ltd. pp. 59-74
- Dyer, K.R. 1994. Estuarine sediment transport and deposition. In: K. Pye, (ed.). *Sediment Transport and Depositional Processes*. Oxford: Blackwell Scientific Publications. pp. 193-196
- Esteves, J.L., Commendatore, M.G., Nievas, M.L., Paletto, V.M. and Amin, O. 2006. Hydrocarbon pollution in coastal sediments of Tierra del Fuego Islands, Patagonia Argentina. *Marine Pollution Bulletin*, **52**: 572-597
- Franco, M.A., Vinas, L., Soriano, J.A., de Armas, D., Gonzalez, J.J., Beiras, R., Salas, N., Bayona, J.M. and Albaiges, J. 2006. Spatial distribution and ecotoxicity of petroleum hydrocarbons in sediments from the Galicia Continental Shelf (NW Spain) after the *Prestige* oil spill. *Marine Pollution Bulletin*, **53**: 260-271
- Fromme, H., Kuchler, T., Otto, T., Pilz, K., Muller, J. And Wenzel, A. 2002. Occurrence of phthalates and bisphenol A and F in the environment. *Water Research*, **36**: 1429-1438
- Gao, X., Chen S., Xie, X., Long, A. and Ma, F. 2007. Non-aromatic hydrocarbons in surface sediments near the Pearl River Estuary in the South China Sea. *Environmental Pollution*, **148**: 40-47
- Giger, W. and Blumer, M. 1974. Polycyclic aromatic hydrocarbons in the environment: Isolation and characterization by chromatography, visible, ultraviolet and mass spectrometry. *Analytical Chemistry*, **46**: 1663-1671
- Gogou, A. and Stephanou, E.G. 2004. Marine organic geochemistry of the Eastern Mediterranean: 2. Polar biomarkers in Cretan Sea surficial sediments. *Marine Chemistry*, **85**: 1-25
- Hair, J.F., Anderson, R.E., Tatham, R.L. and William, C.B. 1995. *Multivariate Data Analysis*. New Jersey: Prentice Hall. pp. 364 – 455
- Hostettler, F.D., Pereira, W.E., Kvenvolden, K.A., van Geen, A., Luoma, S.N., Fuller, C.C. and Anima, R. 1999. A record of hydrocarbon input to San Francisco Bay as traced by biomarker profiles in surface sediment and sediment cores. *Marine Chemistry*, **64**: 115-127
- Jaffe, R., Gardinali, P.R., Cai, Y., Sudburry, A., Fernandez, A. and Hay, B.J. 2003. Organic compounds and trace metals of anthropogenic origin in sediments from Montego Bay, Jamaica: Assessment of sources and distribution pathways. *Environmental Pollution*, **123**: 291-299

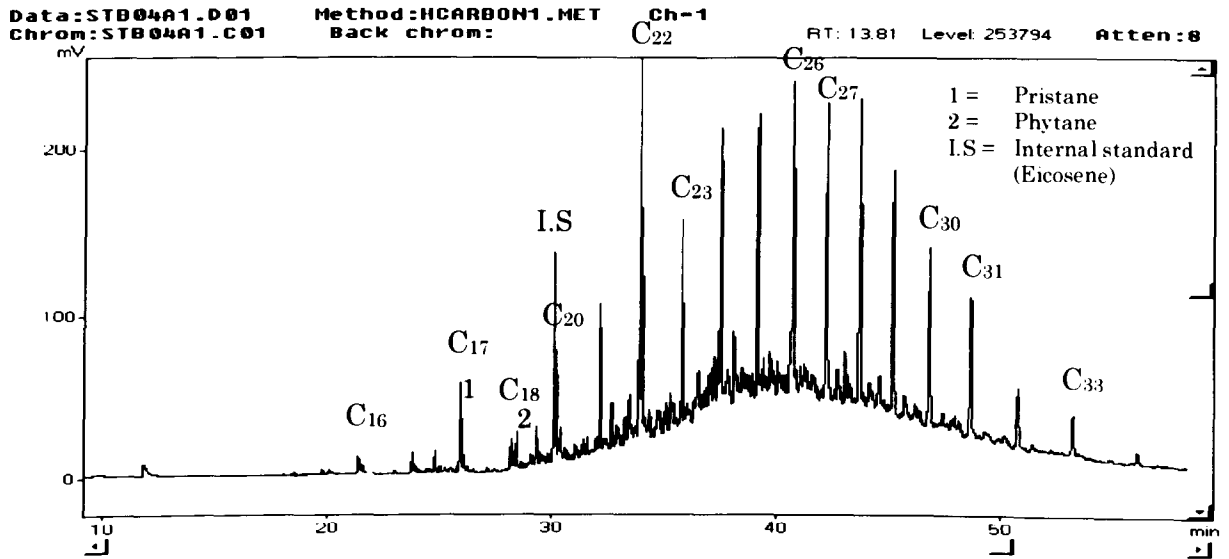
- Jeng, W.L. 2006. Higher plant n-alkane average chain length as an indicator of petrogenic hydrocarbon contamination in marine sediments. *Marine Chemistry*, **102**: 242-251
- Jeng, W.L., Lin, S. and Kao, S.J. 2003. Distribution of terrigenous lipids in marine sediments of northeastern Taiwan. *Deep-Sea Research II*, **50**: 1179-1201
- Jeng, W.L., Wang, J. and Han, B.C. 1996. Coprostanol distribution in marine sediments of Southwestern Taiwan. *Environmental Pollution*, **94**: 47-52
- Kanaly, R.A. and Harayama, S. 2000. Biodegradation of high-molecular-weight polycyclic aromatic hydrocarbons by bacteria. *American Society for Microbiology*, **182**: 2059-2067
- Kirby, G.H. and Lewis, J.A. 2002. Rheological property evolution in concentrated cement-polyelectrolyte suspensions. *Journal of the American Ceramic Society*, **85**: 2989-2994
- Leeder, M.R. 1982. *Sedimentology: Process and Product*. London: G.Alden & Unwin Press Ltd. pp. 192-194
- Levin, H.L. 1985. *Essentials of Earth Science*. Philadelphia: Saunders College Publication. pp. 70-73
- Li, G., Xia, X., Yang, Z., Wang, R. and Voulvoulis, N. 2006. Distribution and sources of polycyclic aromatic hydrocarbons in the Middle and Lower reaches of the Yellow River, China. *Environmental Pollution*, **144**: 985-993
- Liu, M., Baugh, P.J., Hutchinson, S.M., Yu, L. and Xu, S. 2000. Historical record and sources of polycyclic aromatic hydrocarbons in core sediments from the Yangtze Estuary, China. *Environmental Pollution*, **110**: 357-365
- Long, E.R. and Morgan, L.G. 1990. *The Potential for biological effects of sediment-sorbed contaminants tested in the National Status and Trends Program*. NOAA Technical Memorandum NOS OMA 52. Seattle, Washington. pp. 173 and appendices
- Mai, B., Fu, J., Sheng, G., Kang, Y., Lin, Z., Zhang, G., Min, Y. and Zeng, E.Y. 2002. Chlorinated and polycyclic aromatic hydrocarbons in riverine and estuarine sediments from Pearl River Delta, China. *Environmental Pollution*, **117**: 457-474
- Maldonado, C., Venkatesan, M.I., Phillips, C.R. and Bayona, J.M. 2000. Distribution of trialkylamines and coprostanol in San Pedro shelf sediments adjacent to a sewage outfall. *Marine Pollution Bulletin*, **40**: 680-687
- Maskaoui, K., Zhou, J.L., Hong, H.S. and Zhang, Z.L. 2002. Contamination by polycyclic aromatic hydrocarbons in the Jiulong River Estuary and Western Xiamen Sea, China. *Environmental Pollution*, **118**: 109-122

- Medeiros, P.M. and Bicego, M.C. 2004. Investigation of natural and anthropogenic hydrocarbon inputs in sediments using geochemical markers. II. Sao Sebastiao, SP-Brazil. *Marine Pollution Bulletin*, **49**: 892-899
- Mudge, S.M. and Duce, C.E. 2005. Identifying the source, transport path and sinks of sewage derived organic matter. *Environmental Pollution*, **136**: 209-220
- Muri, G., Wakeham, S.G., Pease, T.K. and Faganeli, J. 2004. Evaluation of lipid biomarkers as indicators of changes in organic matter delivery to sediments from Lake Planina, a remote mountain lake in NW Slovenia. *Organic Geochemistry*, **35**: 1083-1093
- Nishigima, F.N., Weber, R.R. and Bicego, M.C. 2001. Aliphatic and aromatic hydrocarbons in sediments of Santos and Cananea, SP, Brazil. *Marine Pollution Bulletin*, **42**: 1064-1072
- Peijnenburg, W.J.G.M. and Struijs, J. 2006. Occurrence of phthalate esters in the environment of the Netherlands. *Ecotoxicology and Environmental Safety*, **63**: 204-215
- Peng, X., Zhang, G., Mai, B., Hu, J., Li, K. and Wang, Z. 2005. Tracing anthropogenic contamination in the Pearl River estuarine and marine environment of South China Sea using sterols and other organic molecular markers. *Marine Pollution Bulletin*, **50**: 856-865
- Peng, X., Zhang, G., Mai, B., Min, Y. and Wang, Z. 2002. Spatial and temporal trend of sewage pollution indicated by coprostanol in Macao Estuary, Southern China. *Marine Pollution Bulletin*, **45**: 295-299
- Peters, K.E. and Moldowan, J.M. 1993. *The Biomarker Guide: Interpreting Molecular Fossils in Petroleum and Ancient Sediments*. New Jersey: Prentice Hall. pp. 1-9, 140-250
- Preston, M.R. 1989. Phthalate ester speciation in estuarine water, suspended particulates and sediments. *Environmental Pollution*, **62**: 183-193
- Readman, J.W., Fillmann, G., Tolosa, I., Bartocci, J., Villeneuve, J.P., Catinni, C. and Mee, L.D. 2002. Petroleum and PAH contamination of the Black Sea. *Marine Pollution Bulletin*, **44**: 48-62
- Reineck, H.E. and Singh, I.B. 1980. *Depositional Sedimentary Environments*. Berlin: Springer-Verlag. pp. 315-320
- Shao, L., Jones, T., Gayer, R., Dai, S., Li, S., Jiang, Y. and Zhang, P. 2003. Petrology and geochemistry of the high-sulphur coals from the upper Permian carbonate coal measures in the Heshan coalfield, Southern China. *International Journal of Coal Geology*, **1**: 1-26

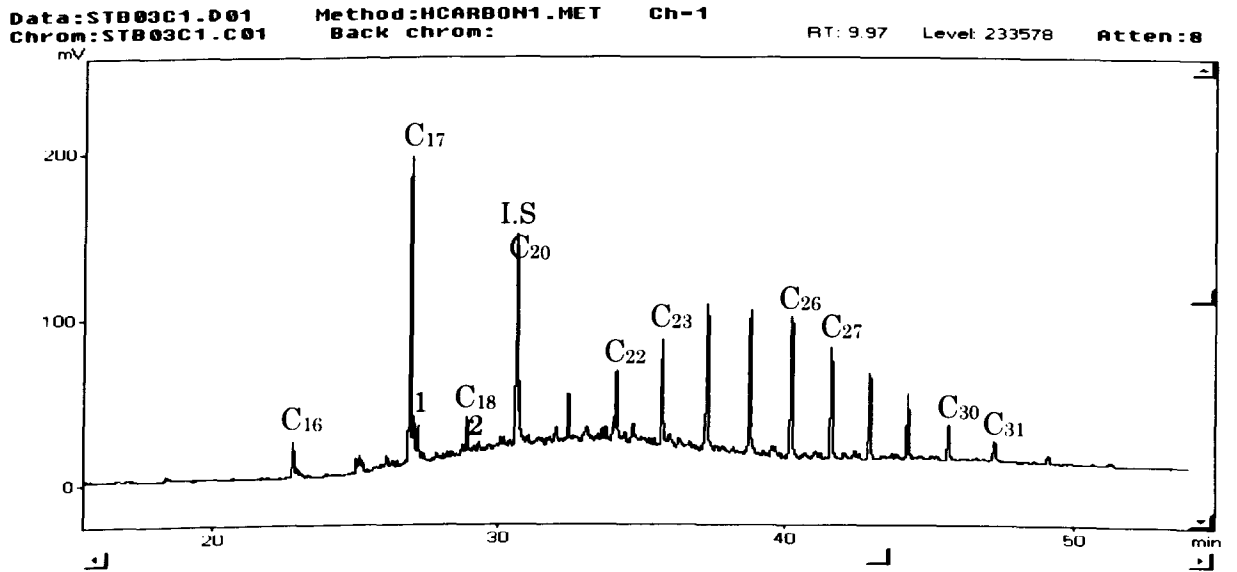
- Shi, Z., Tao, S., Pan, B., Fan, W., He, X.C., Zuo, Q., Wu, S.P., Li, B.G., Cao, J., Liu, W.X., Xu, F.L., Wang, X.J., Shen, W.R. and Wong, P.K. 2005. Contamination of rivers in Tianjin, China by polycyclic aromatic hydrocarbons. *Environmental Pollution*, **134**: 97-111
- Solomons, T.W.G. and Fryhle, C.B. 2004. *Organic Chemistry 8th Ed.* New York: John Wiley & Sons Inc. pp. 63-64, 135, 929, 1130-1131
- Starr, G.C., Barak, P., Lowery, B. and Avila-Segura, M. 2000. Soil particle concentrations and size analysis using a dielectric method. *Soil Science Society of America Journal*, **64**: 858-866
- Tolosa, I., de Mora, S.J., Fowler, S.W., Villeneuve, J.P., Bartocci, J. and Cattini, C. 2005. Aliphatic and aromatic hydrocarbons in marine biota and coastal sediments from the Gulf and the Gulf of Oman. *Marine Pollution Bulletin*, **50**: 1619-1633
- Tolosa, I., Vescovali, I., LeBlond, N., Marty, J., de Mora, S. and Prieur, L. 2004a. Distribution of pigments and fatty acid biomarkers in particulate matter from the frontal structure of the Alboran Sea (SW Mediterranean Sea). *Marine Chemistry*, **88**: 103-125
- Tolosa, I., de Mora, S.J., Sheikholeslami, M.R., Villeneuve, J.P., Bartocci, J. and Cattini, C. 2004b. Aliphatic and aromatic hydrocarbons in coastal Caspian Sea sediments. *Marine Pollution Bulletin*, **48**: 44-60
- Turner, A. and Rawling, M.C. 2000. The Behaviour of di-(2-ethylhexyl) phthalate in estuaries. *Marine Chemistry*, **68**: 203-217
- Wang, X.C., Sun, S., Ma, H.Q. and Liu, Y. 2006. Sources and distribution of aliphatic and polyaromatic hydrocarbons in sediments of Jiaozhou Bay, Qingdao, China. *Marine Pollution Bulletin*, **52**: 129-138
- Xu, S., Tao, J., Chen, Z. and Lu, Q. 1997. Dynamic accumulation of heavy metals in tidal flat sediments of Shanghai. *Oceanologia et Limnologia Sinica*, **28**: 509-515
- Yuan, D., Yang, D., Wade, T.L. and Qian, Y. 2001. Status of persistent organic pollutants in the sediment from several estuaries in China. *Environmental Pollution*, **114**: 101-111
- Zhou, J.L. and Maskaoui, K. 2003. Distribution of polycyclic aromatic hydrocarbons in water and surface sediments from Daya Bay, China. *Environmental Pollution*, **121**: 269-281

APPENDICES

Appendix 1: GC/FID chromatograms of aliphatic fractions of core sediments from Santubong River and Sarawak River

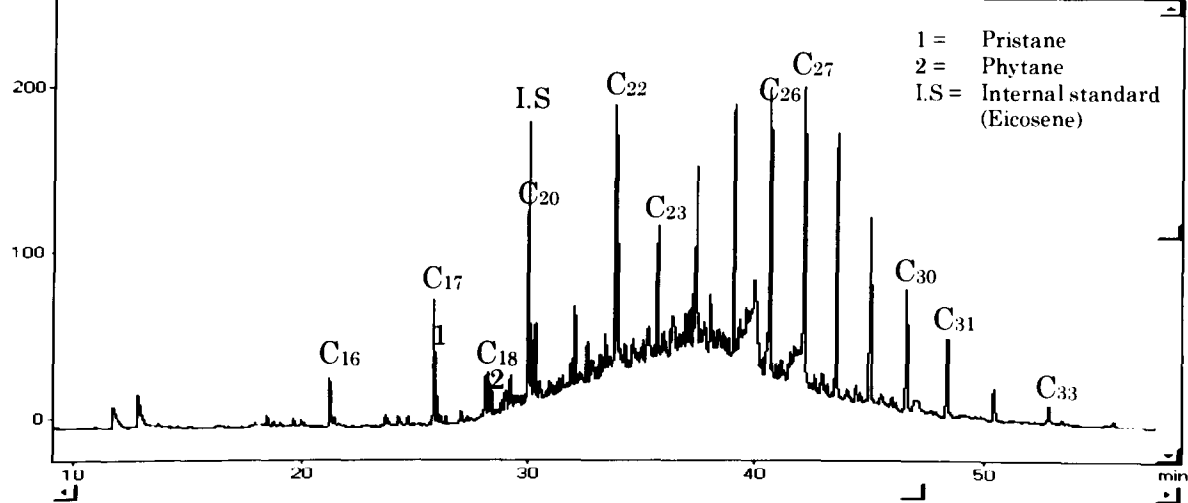


(a) SSTB02 (0-10cm)



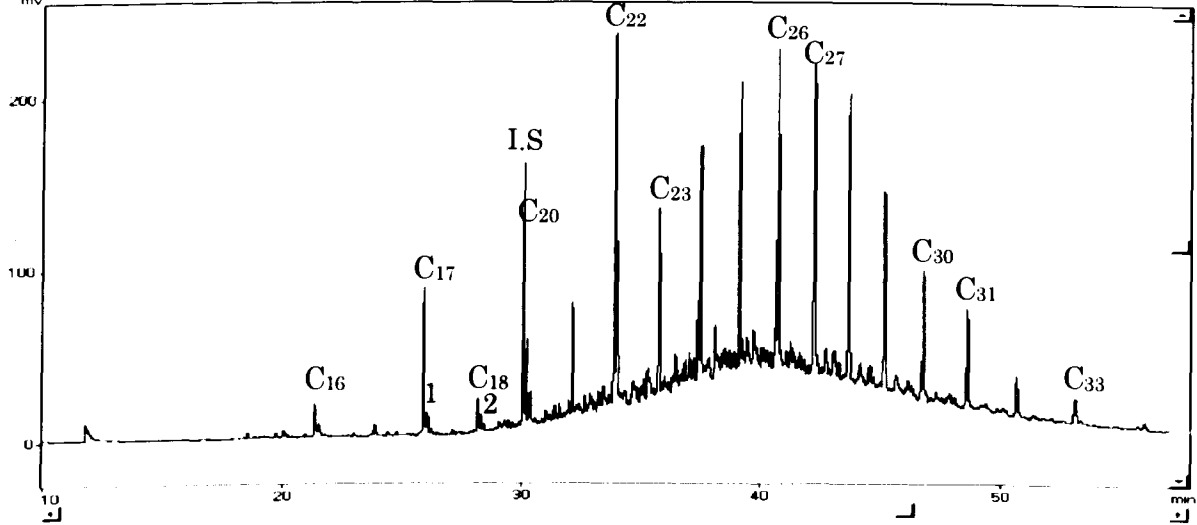
(b) SSTB03 (0-10cm)

Data: STB02C1.D01 Method: HCARBON1.MET Ch-1 RT: 14.31 Level: 247884 Atten: 8
Chrom: STB02C1.C01 Back chrom:

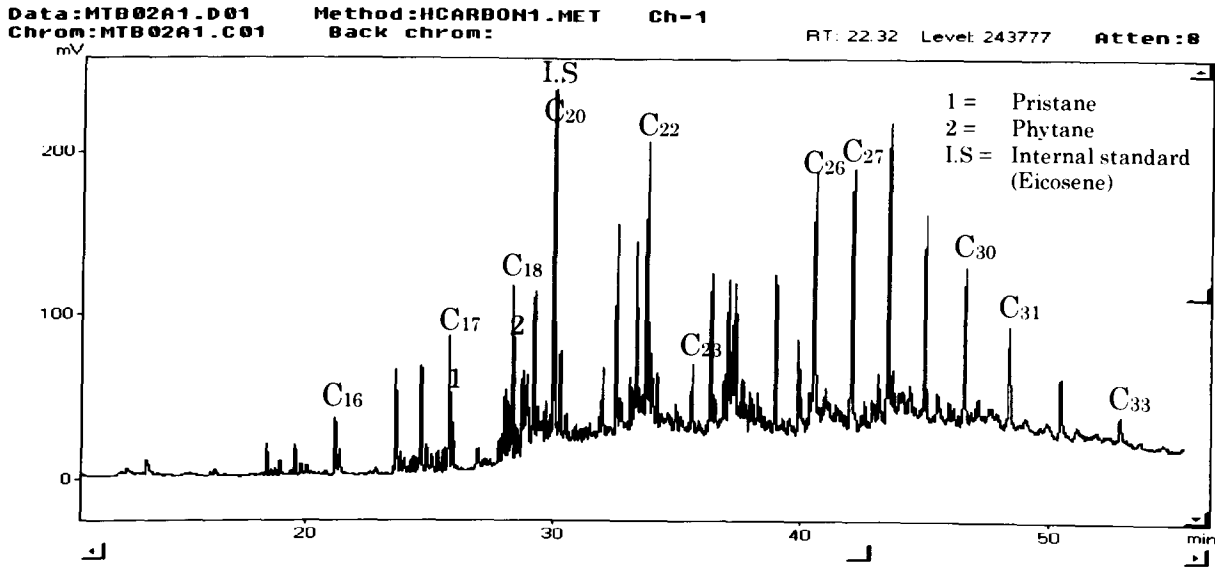


(c) SSTB04 (0-10cm)

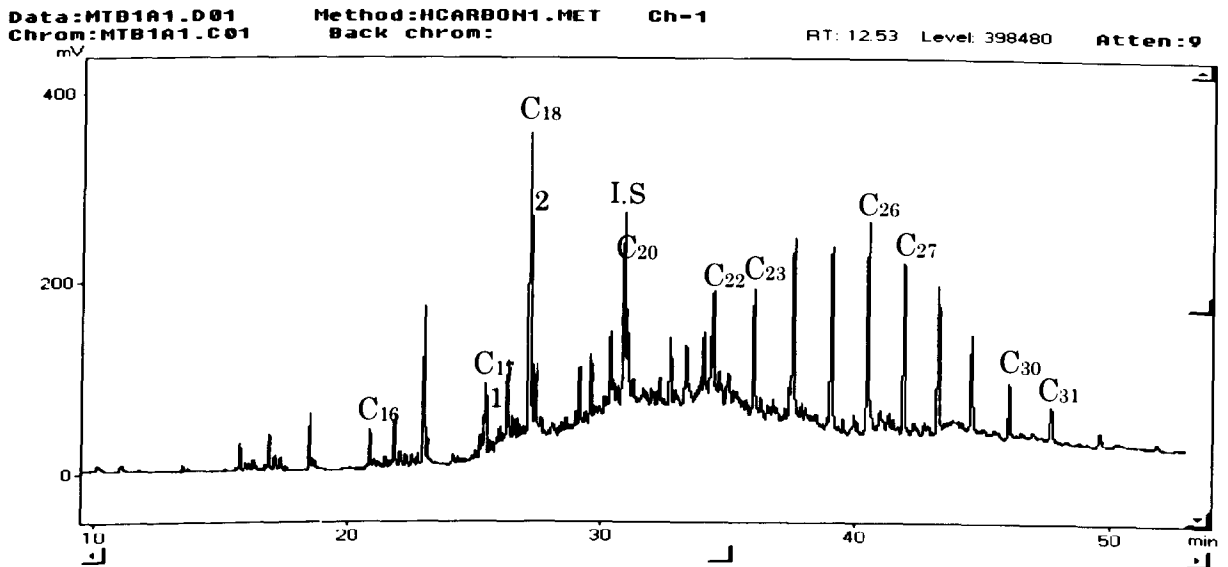
Data: STB0101.D01 Method: HCARBON1.MET Ch-1 RT: 12.78 Level: 252690 Atten: 8
Chrom: STB0101.C01 Back chrom:



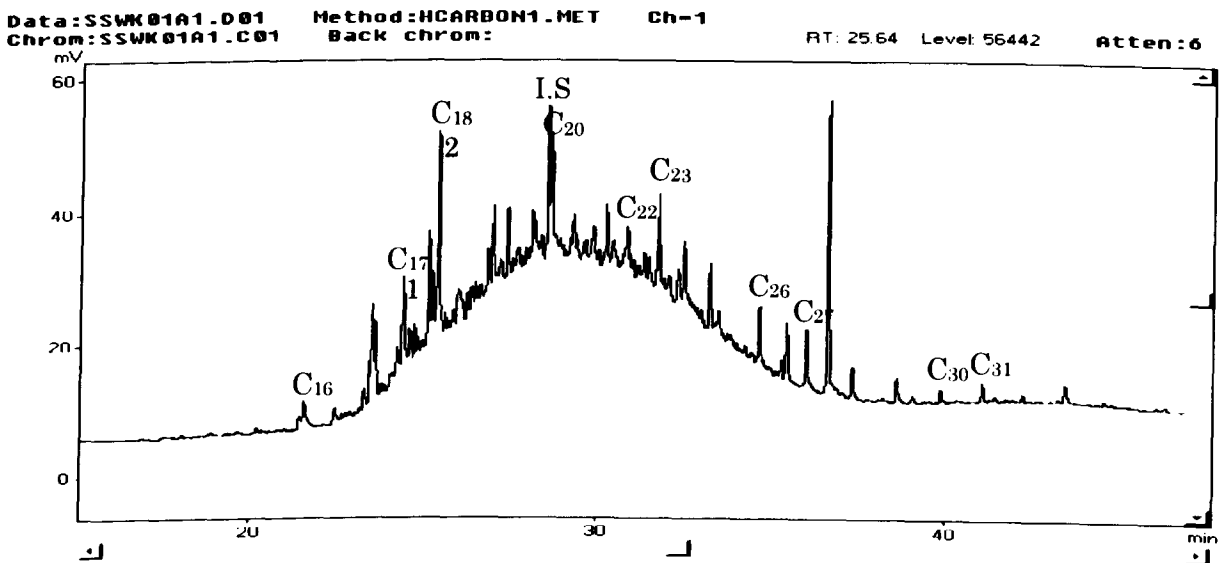
(d) SSTB05 (0-10cm)



(e) SSWK02 (0-10cm)

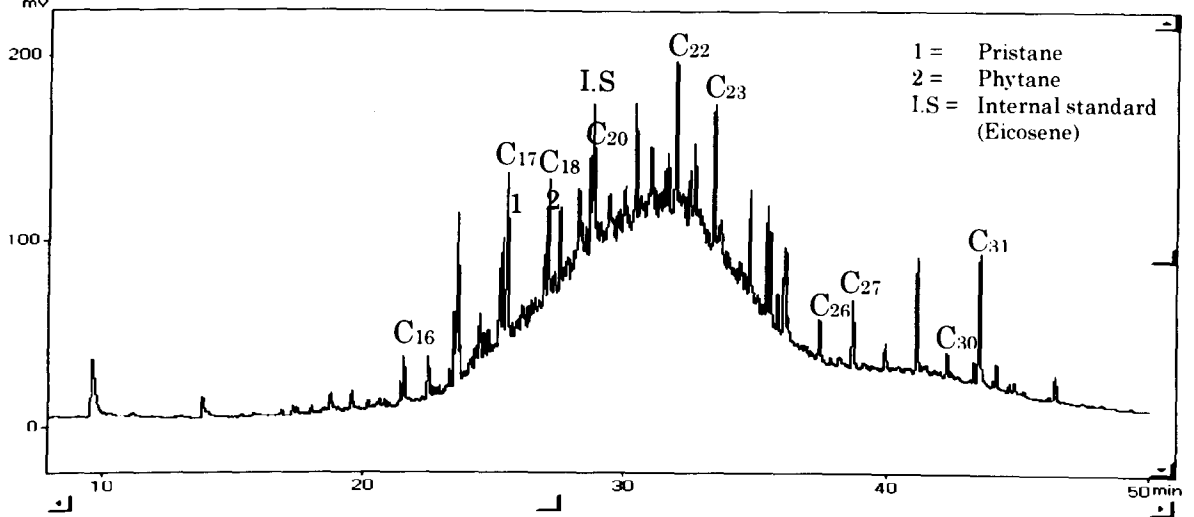


(f) SSWK03 (0-10cm)



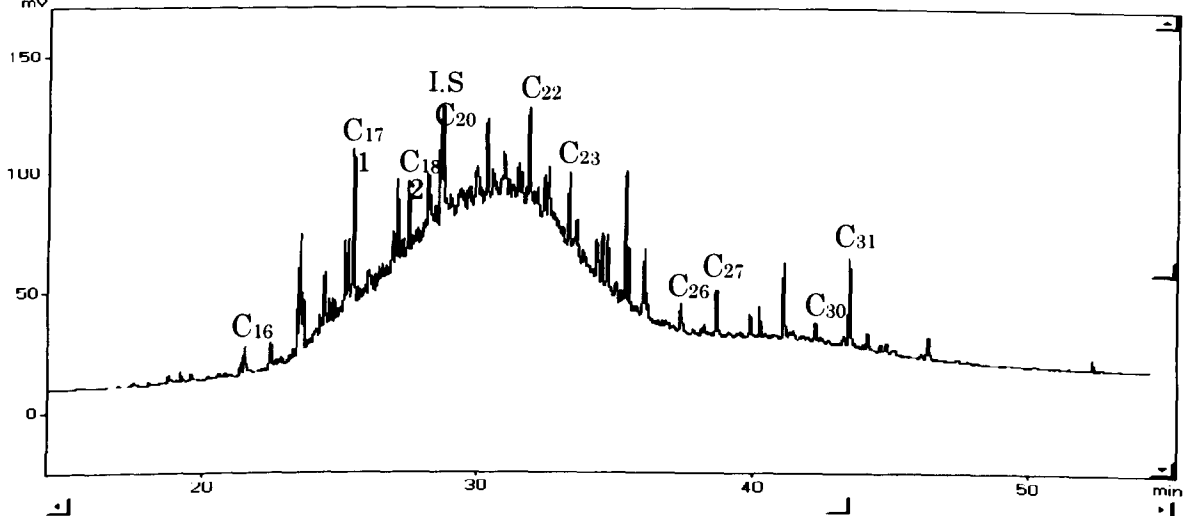
(g) SSWK04 (0-10cm)

Data:SSWK02A1.D01 Method:H-CARBON1.MET Ch-1
Chrom:SSWK02A1.C01 Back chrom: RT: 8.84 Level: 219406 Atten:8



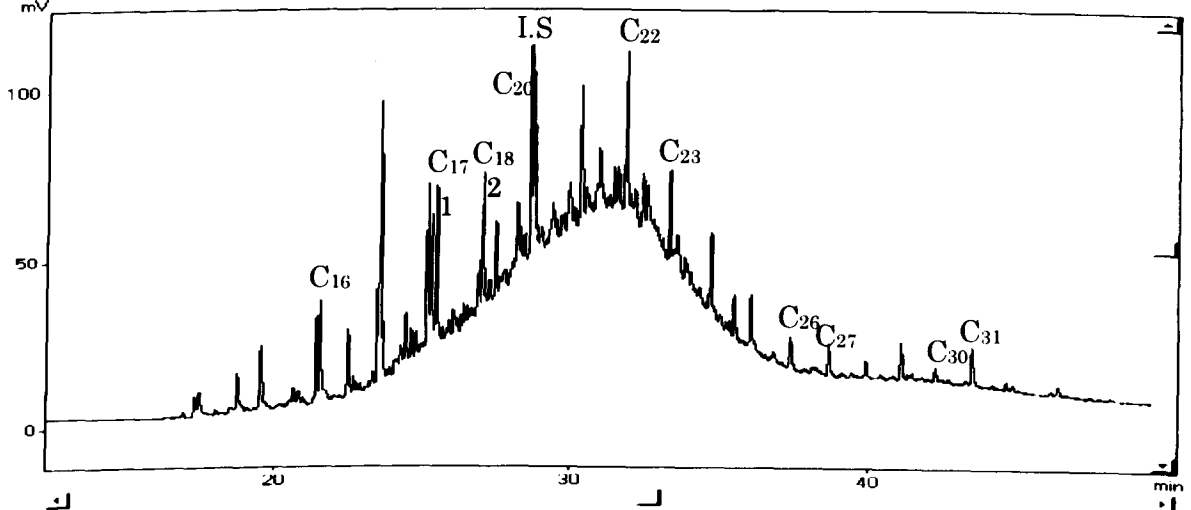
(h) SSWK05 (0-10cm)

Data:SSWK02A2.D01 Method:H-CARBON1.MET Ch-1
Chrom:SSWK02A2.C01 Back chrom: RT: 10.80 Level: 253929 Atten:8



(i) SSWK05 (10-20cm)

Data:SSWK02A3.D01 Method:H-CARBON1.MET Ch-1
Chrom:SSWK02A3.C01 Back chrom: RT: 12.89 Level: 118652 Atten:7

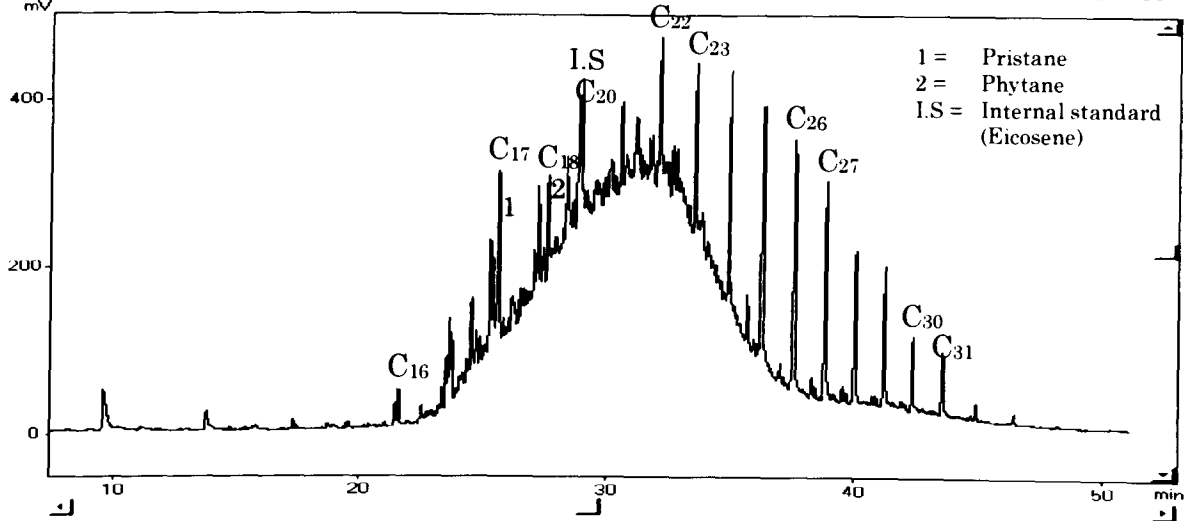


(j) SSWK05 (20-30cm)

Data: KUAP0A1.D01
Chrom: KUAP0A1.C01

Method: HCARBON1.MET Ch-1
Back chrom:

RT: 11.42 Level: 491572 Atten: 9

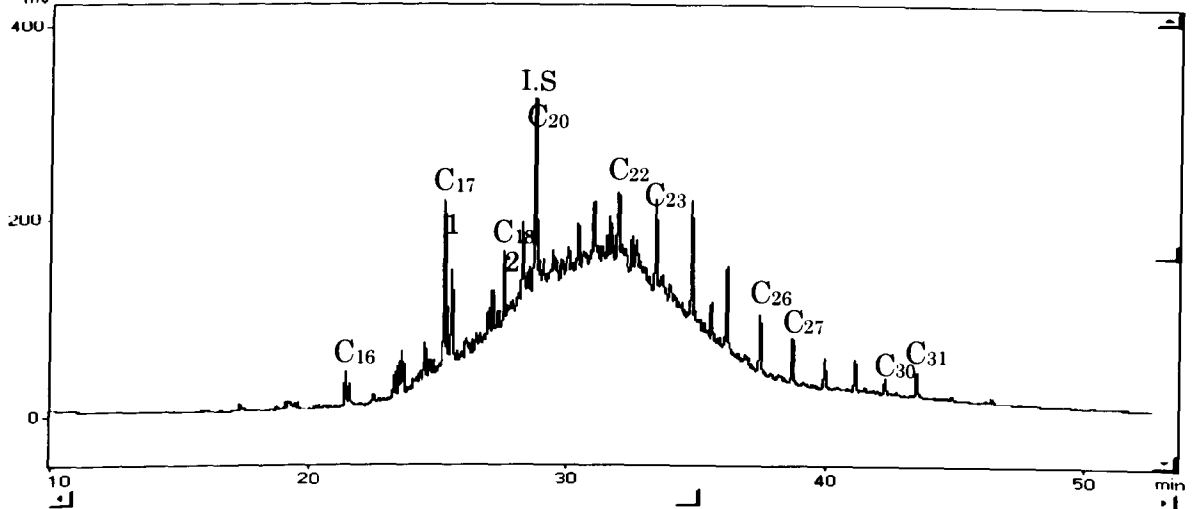


(k) SSWK06 (0-10cm)

Data: KUAP02A1.D01
Chrom: KUAP02A1.C01

Method: HCARBON1.MET Ch-1
Back chrom:

RT: 15.15 Level: 450795 Atten: 9

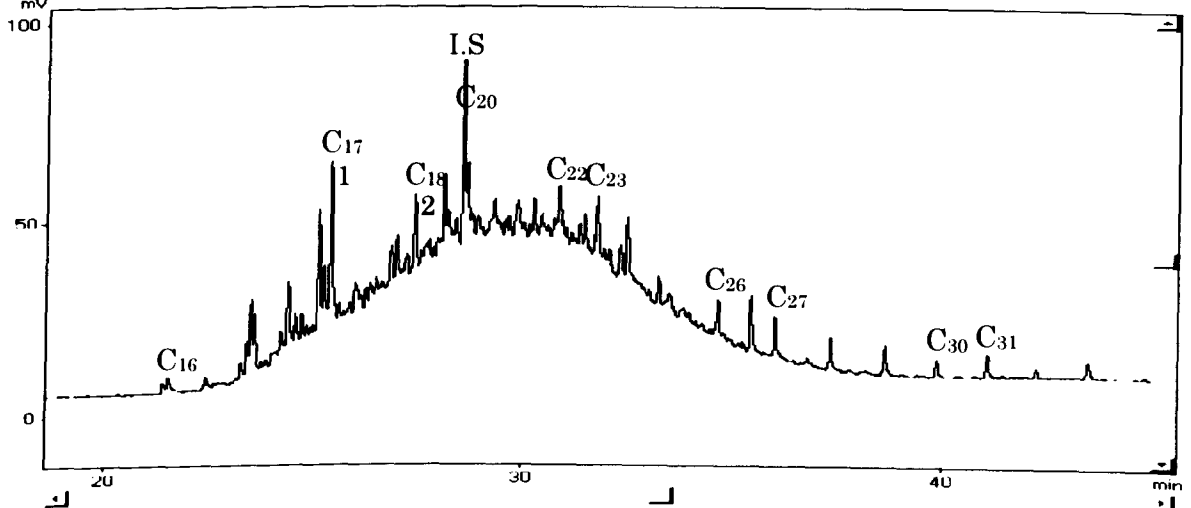


(l) SSWK07 (0-10cm)

Data: KUAP03A1.D01
Chrom: KUAP03A1.C01

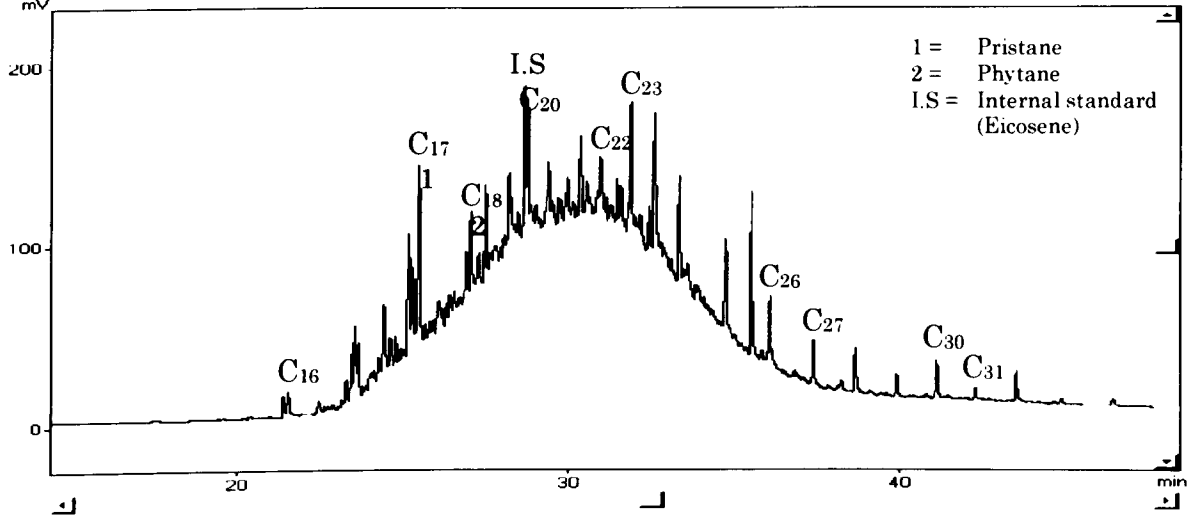
Method: HCARBON1.MET Ch-1
Back chrom:

RT: 27.34 Level: 22781 Atten: 7



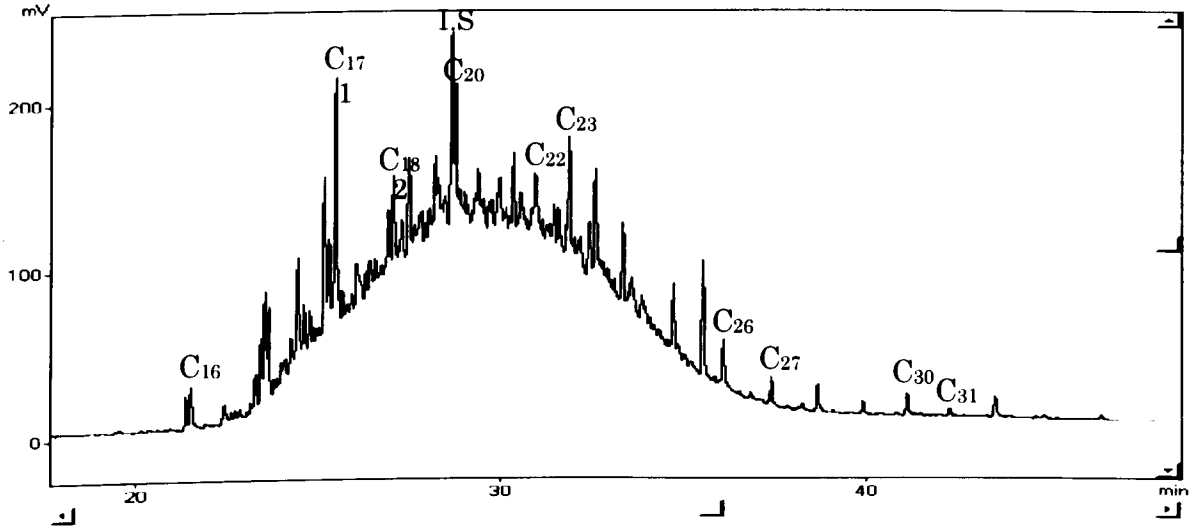
(m) SSWK08 (0-10cm)

Data: KUAP04A1.D01 Method: HCARBON1.MET Ch-1 RT: 14.61 Level: 226080 Atten: 8
Chrom: KUAP04A1.C01 Back chrom:



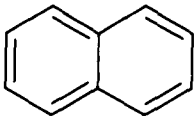
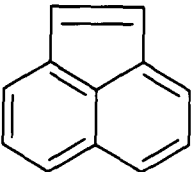
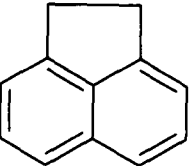
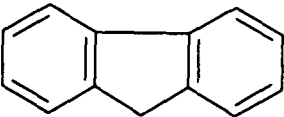
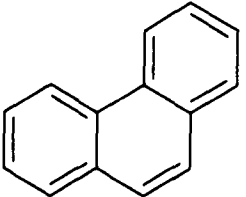
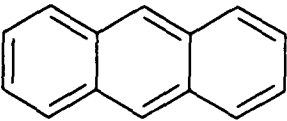
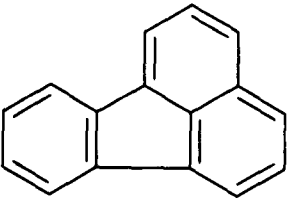
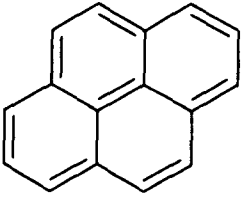
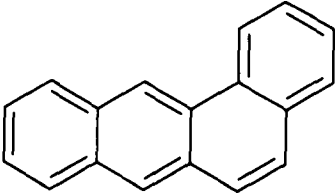
(n) SSWK09 (0-10cm)

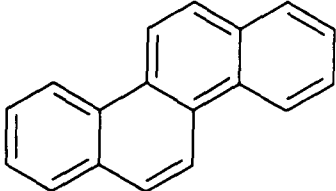
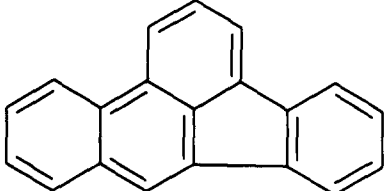
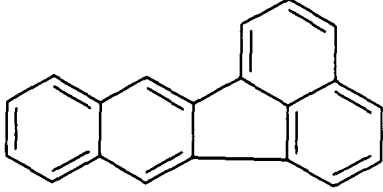
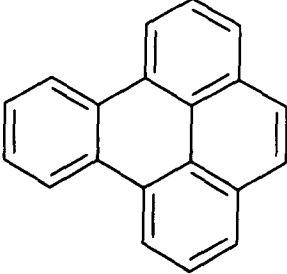
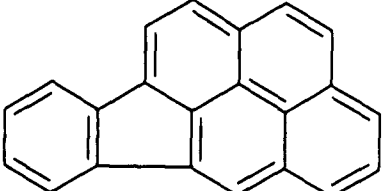
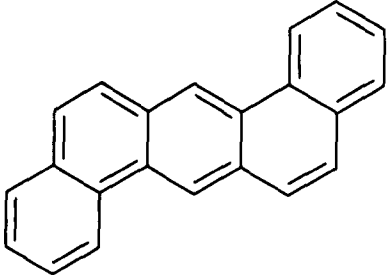
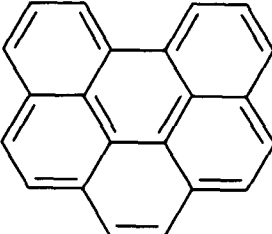
Data: KUAP04A2.D01 Method: HCARBON1.MET Ch-1 RT: 28.44 Level: 184576 Atten: 8
Chrom: KUAP04A2.C01 Back chrom:



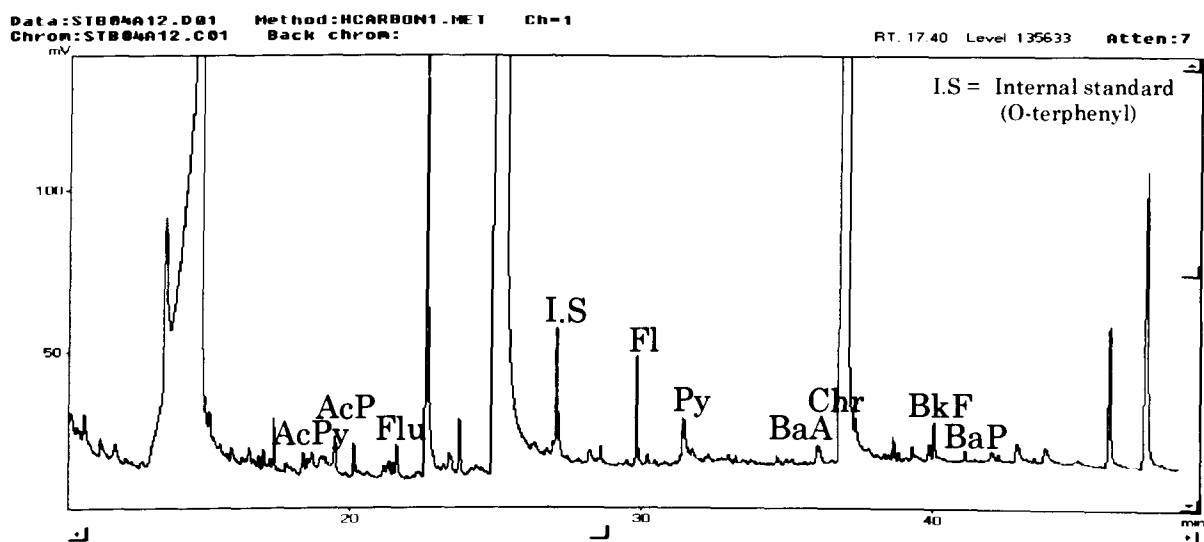
(o) SSWK09 (10-20cm)

Appendix 2: Polycyclic aromatic hydrocarbons structures

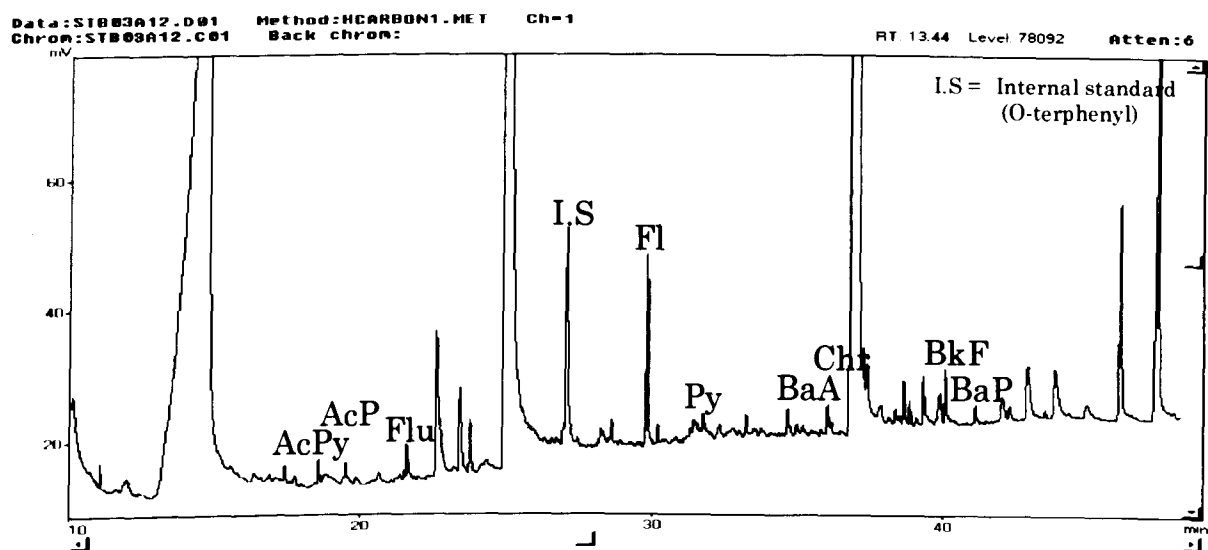
Compounds	Molecular weight (g/mol)	Structure
Napthalene	128	
Acenaphthylene	152	
Acenaphthene	154	
Fluorene	166	
Phenanthrene	178	
Anthracene	178	
Fluoranthene	202	
Pyrene	202	
Benzo(a)anthracene	228	

Compounds	Molecular weight (g/mol)	Structure
Chrysene	228	
Benzo(b)fluoranthene	252	
Benzo(k)fluoranthene	252	
Benzo(a)pyrene	252	
Indeno(1,2,3-c,d)pyrene	276	
Dibenzo(a,h)anthracene	278	
Benzo(g,h,i)perylene	276	

Appendix 3: GC/FID chromatograms of PAHs fractions of core sediments from Santubong River and Sarawak River



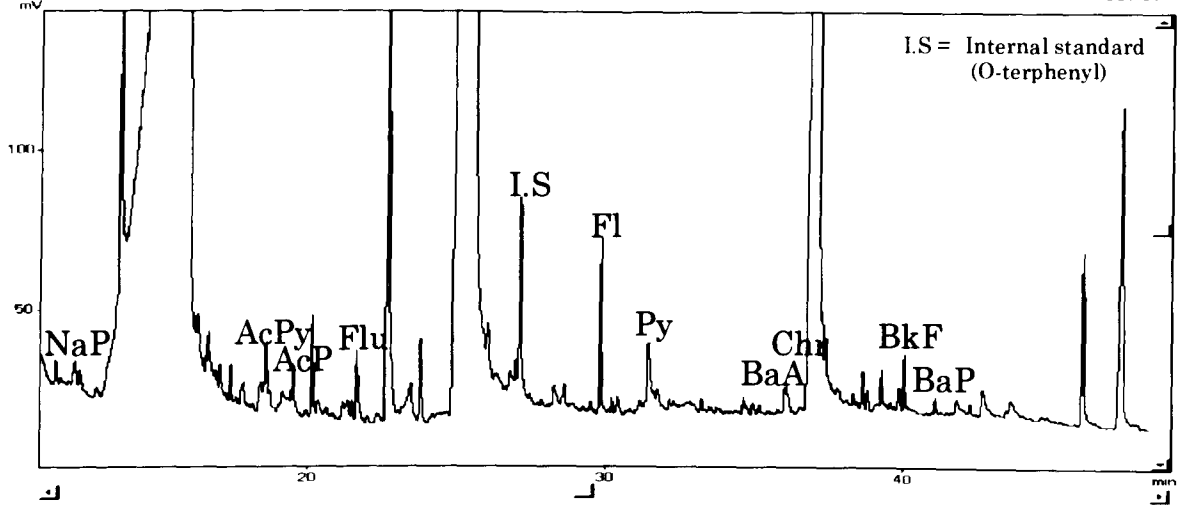
(a) SSTB02 (0-10cm)



(b) SSTB03 (0-10cm)

Data: STB02A12.D01 Method: NCARBON1.MET Ch-1
Chrom: STB02A12.C01 Back chrom:

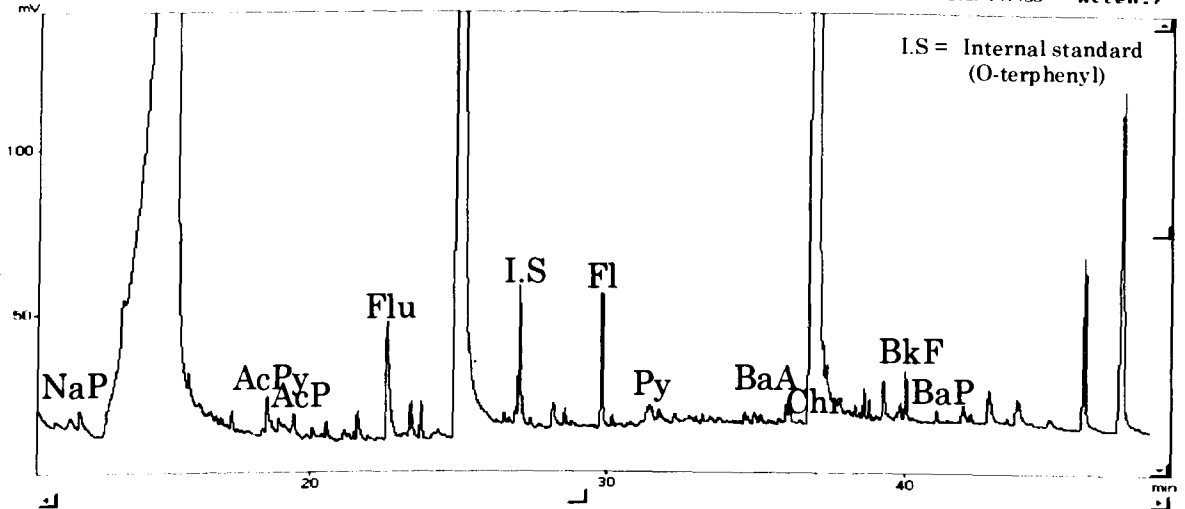
RT: 11.73 Level: 109685 Atten: 7



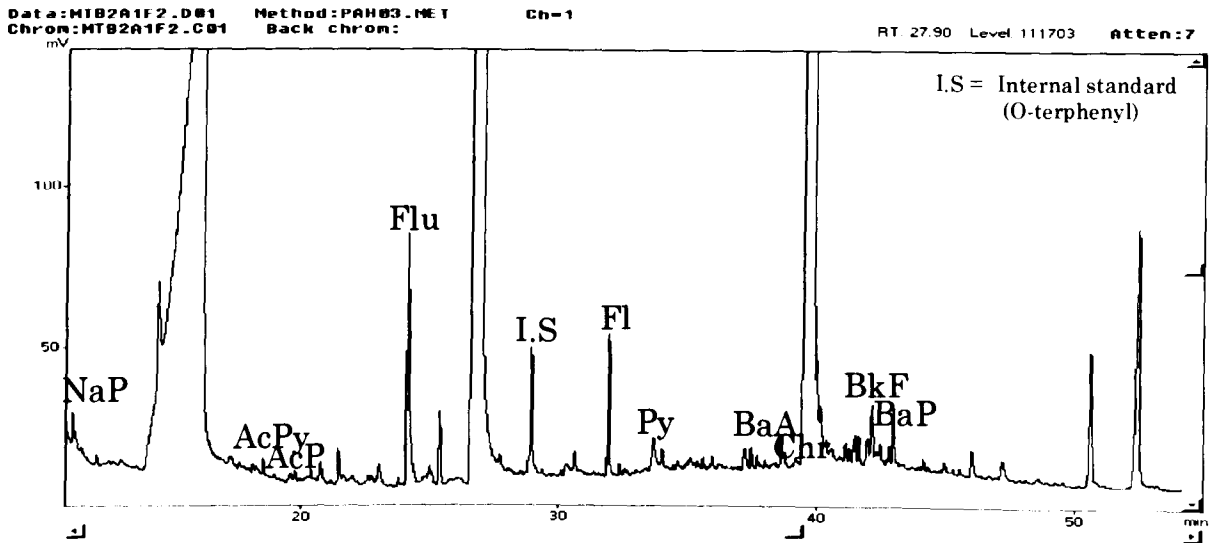
(c) SSTB04 (0-10cm)

Data: STB01A12.D01 Method: NCARBON1.MET Ch-1
Chrom: STB01A12.C01 Back chrom:

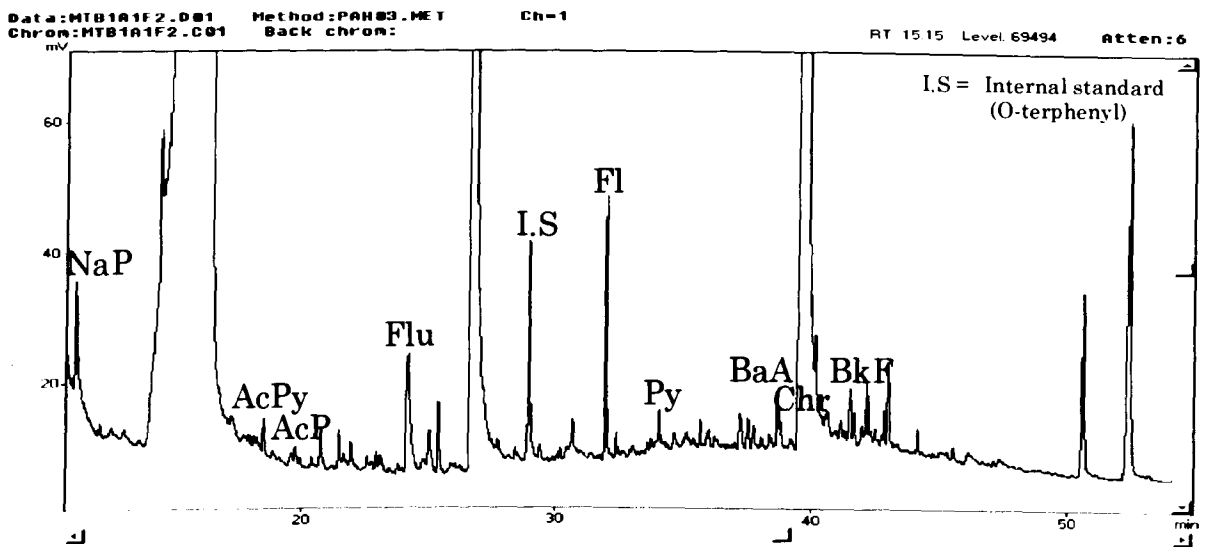
RT: 12.34 Level: 141458 Atten: 7



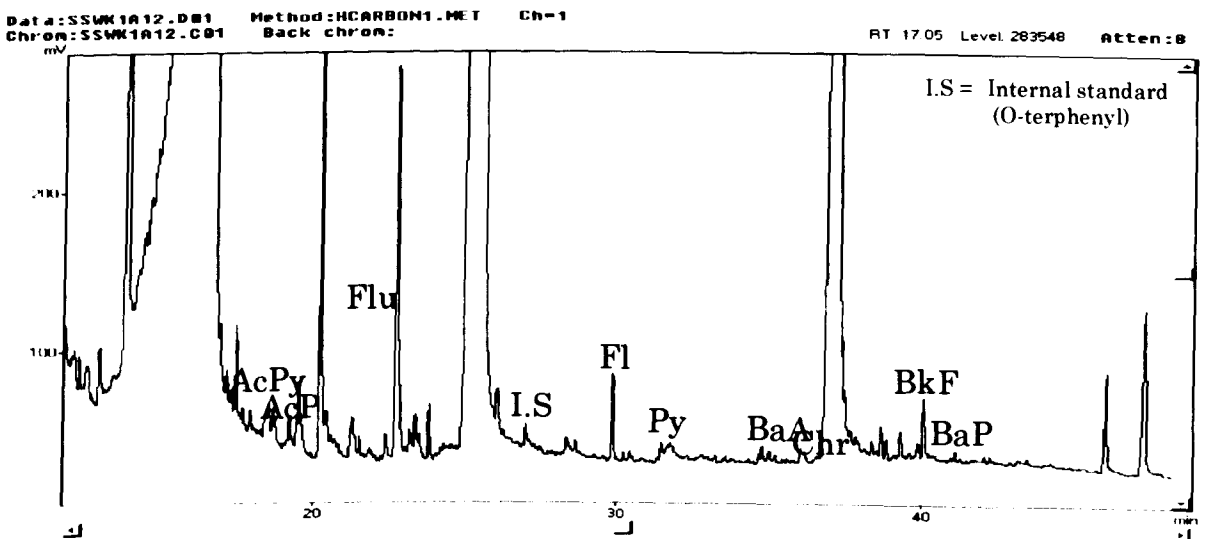
(d) SSTB05 (0-10cm)



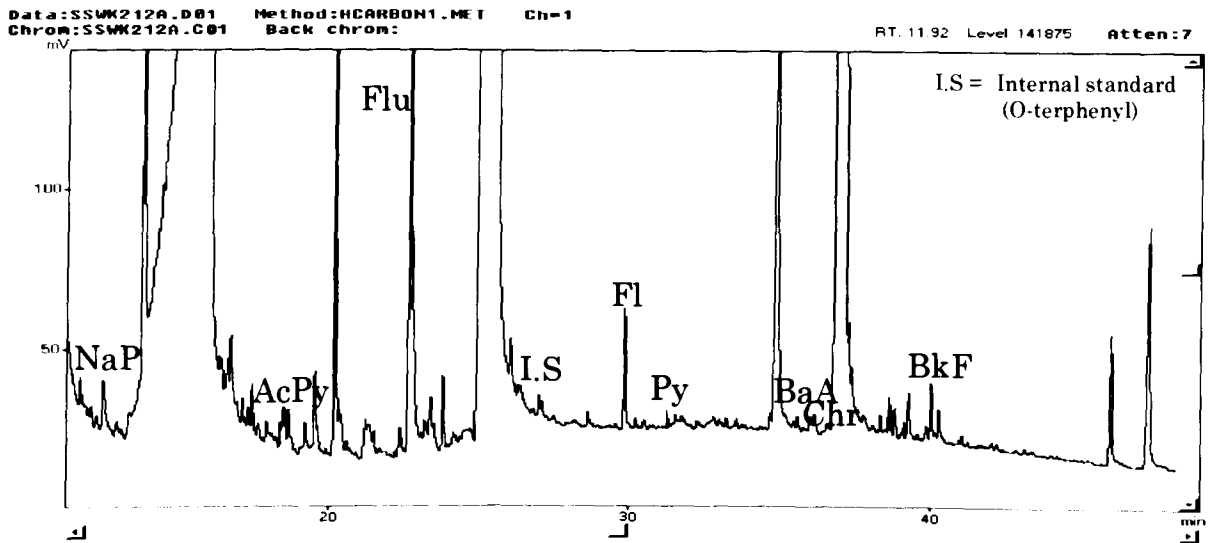
(e) SSWK02 (0-10cm)



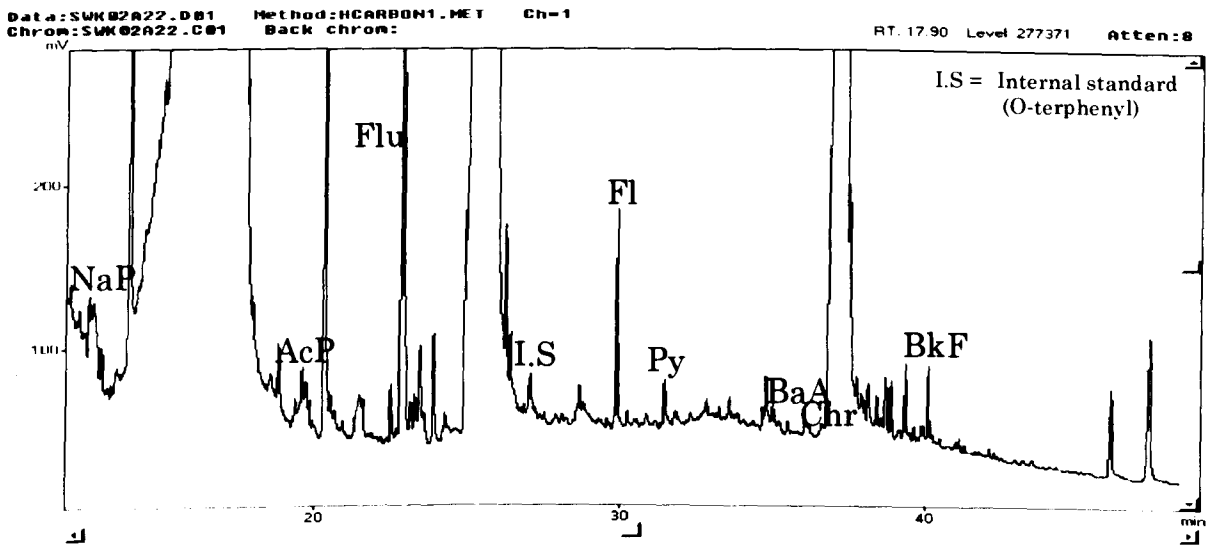
(f) SSWK03 (0-10cm)



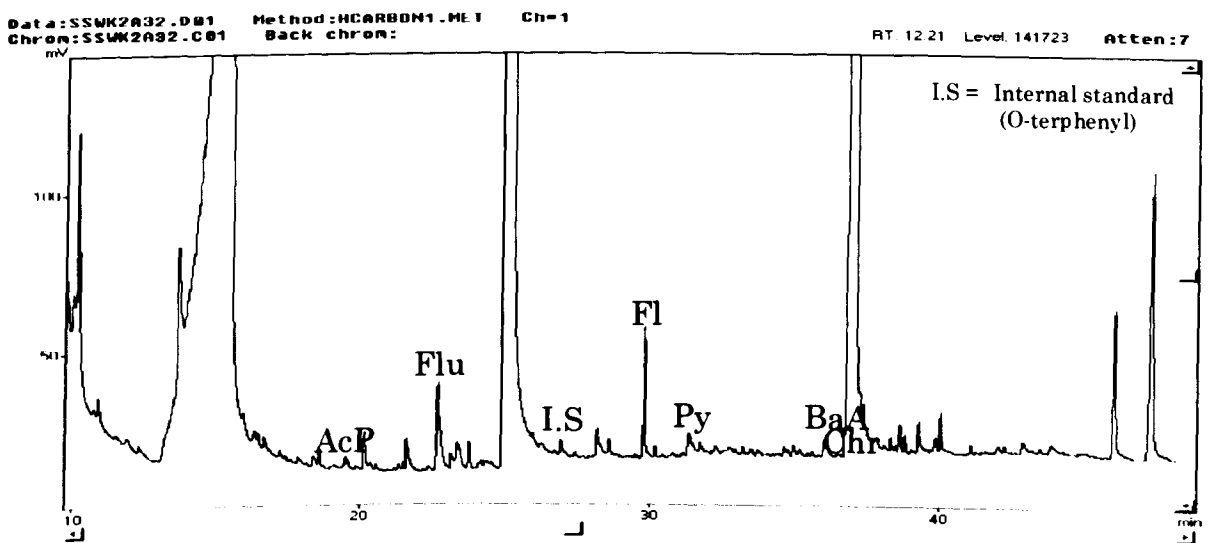
(g) SSWK04 (0-10cm)



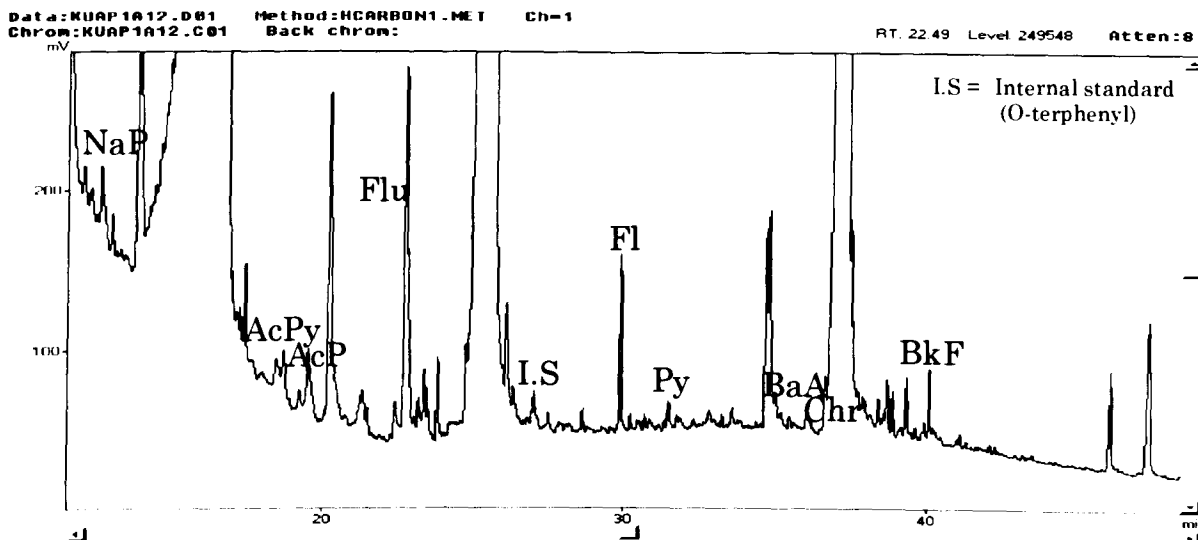
(h) SSWK05 (0-10cm)



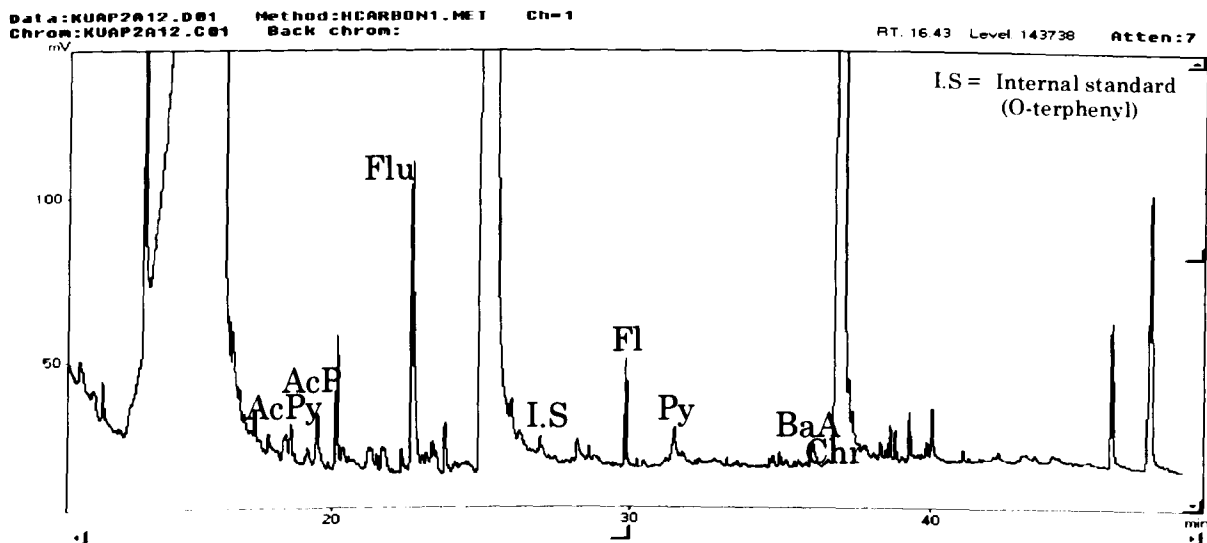
(i) SSWK05 (10-20cm)



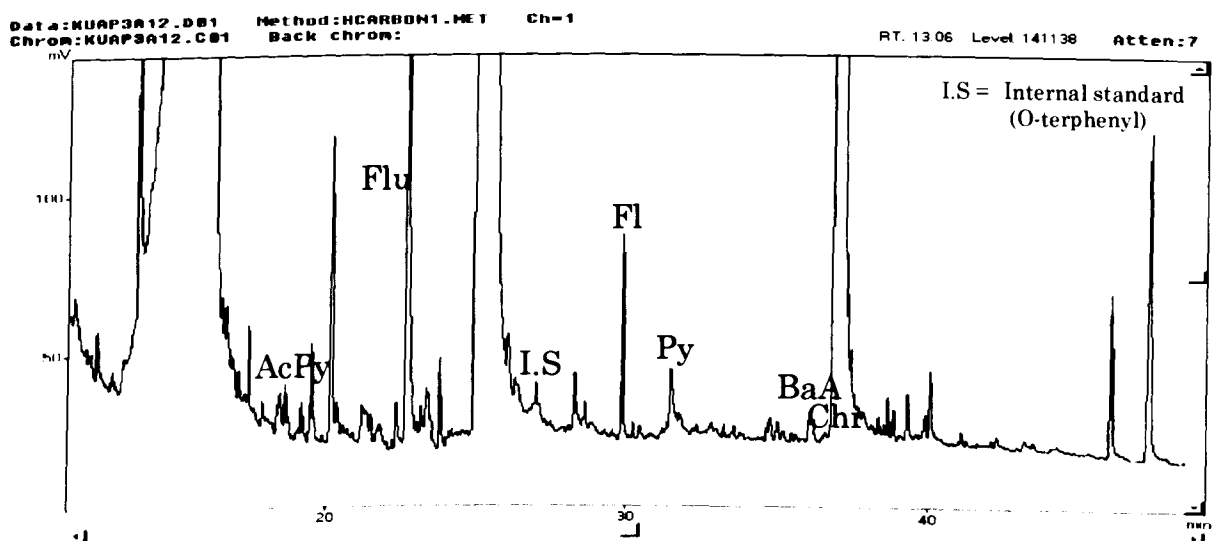
(j) SSWK05 (20-30cm)



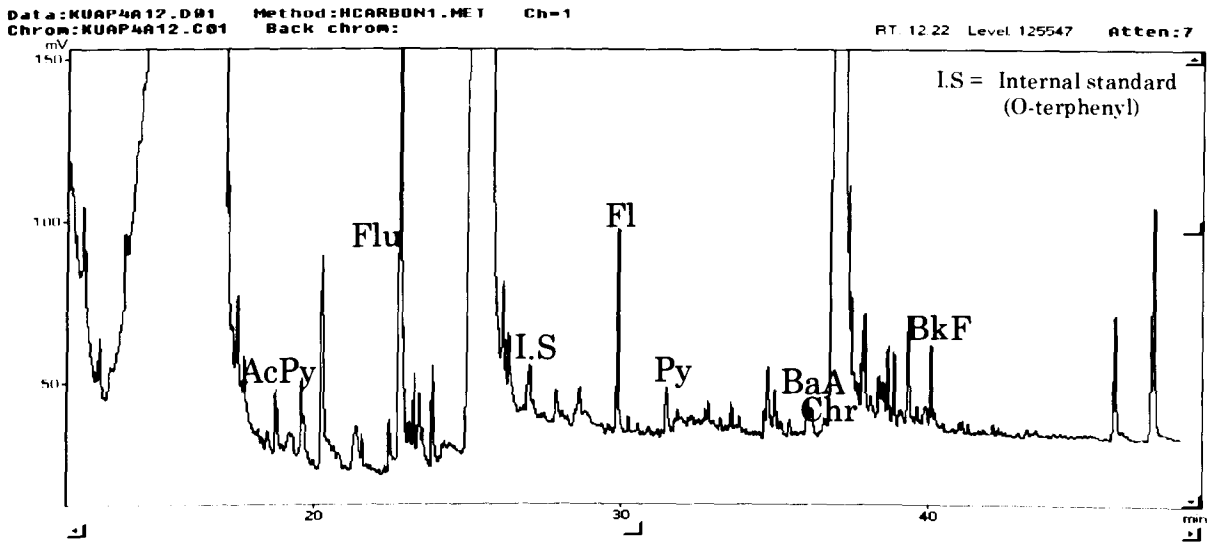
(k) SSWK06 (0-10cm)



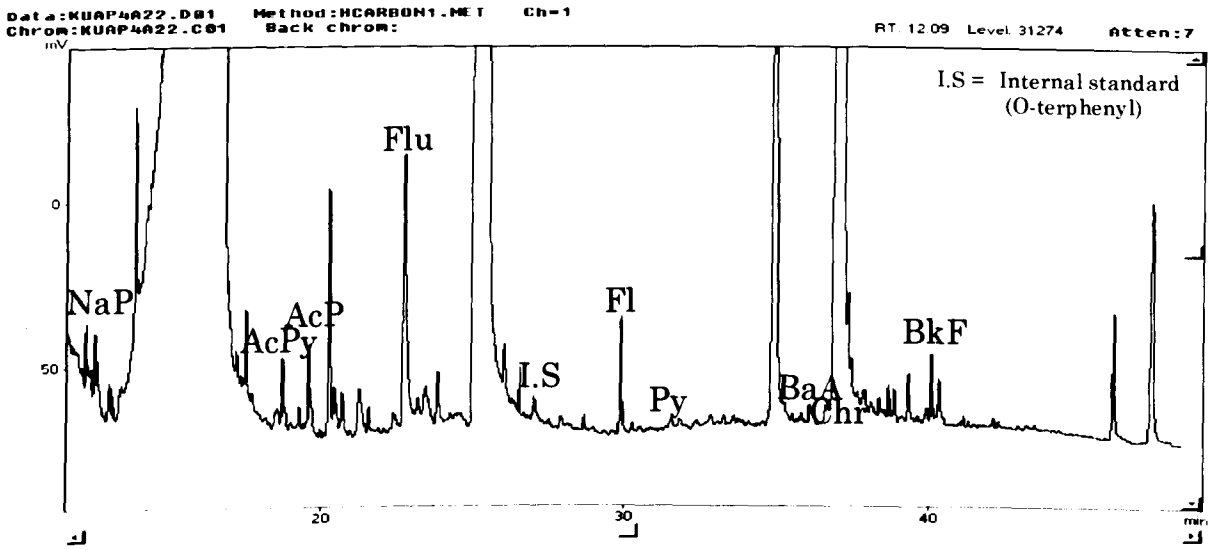
(l) SSWK07 (0-10cm)



(m) SSWK08 (0-10cm)

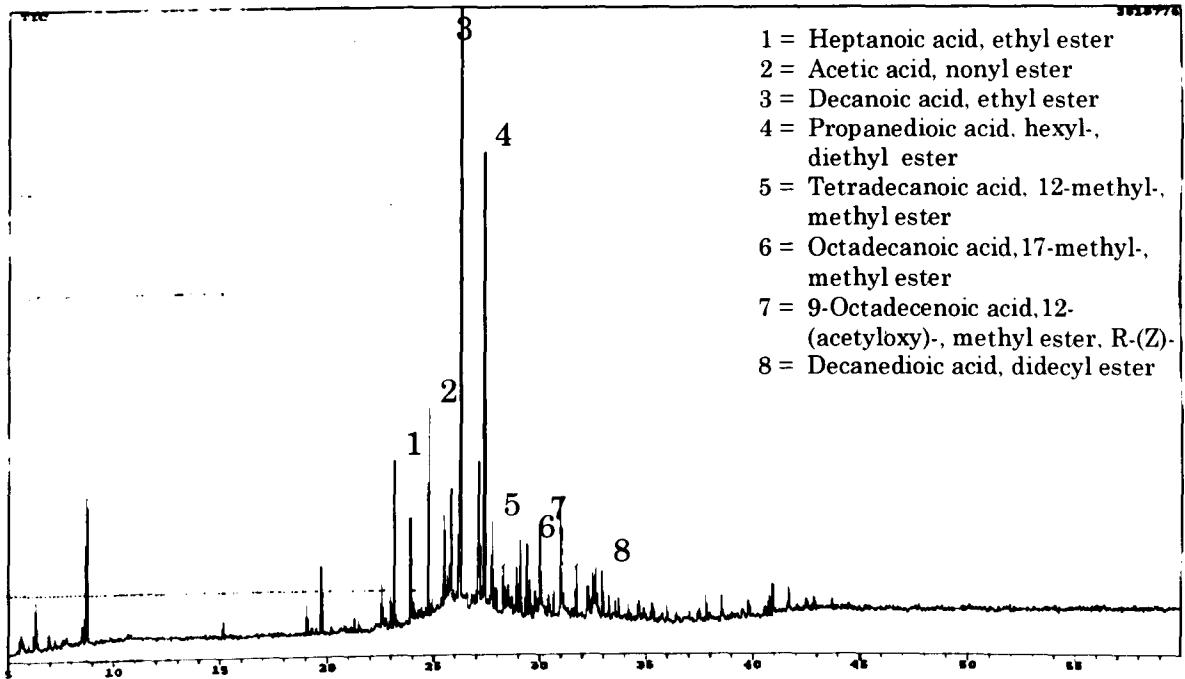


(n) SSWK09 (0-10cm)

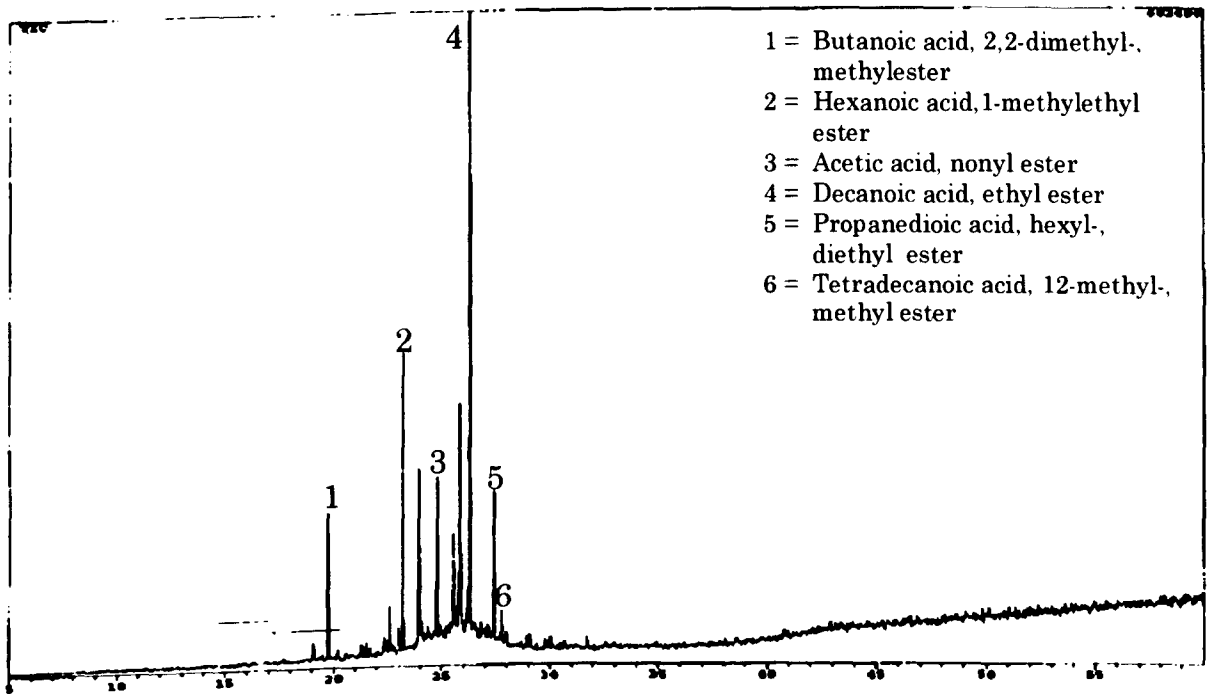


(o) SSWK09 (10-20cm)

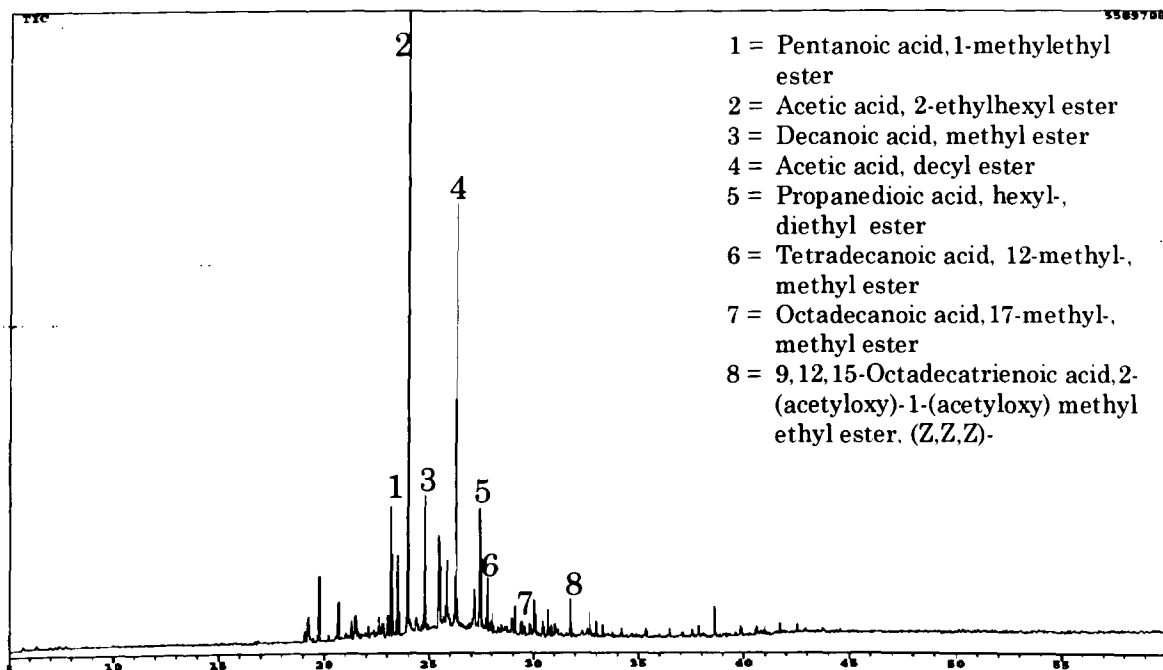
Appendix 4: GC/MS chromatograms of FAMEs fraction in core sediments from Sarawak River



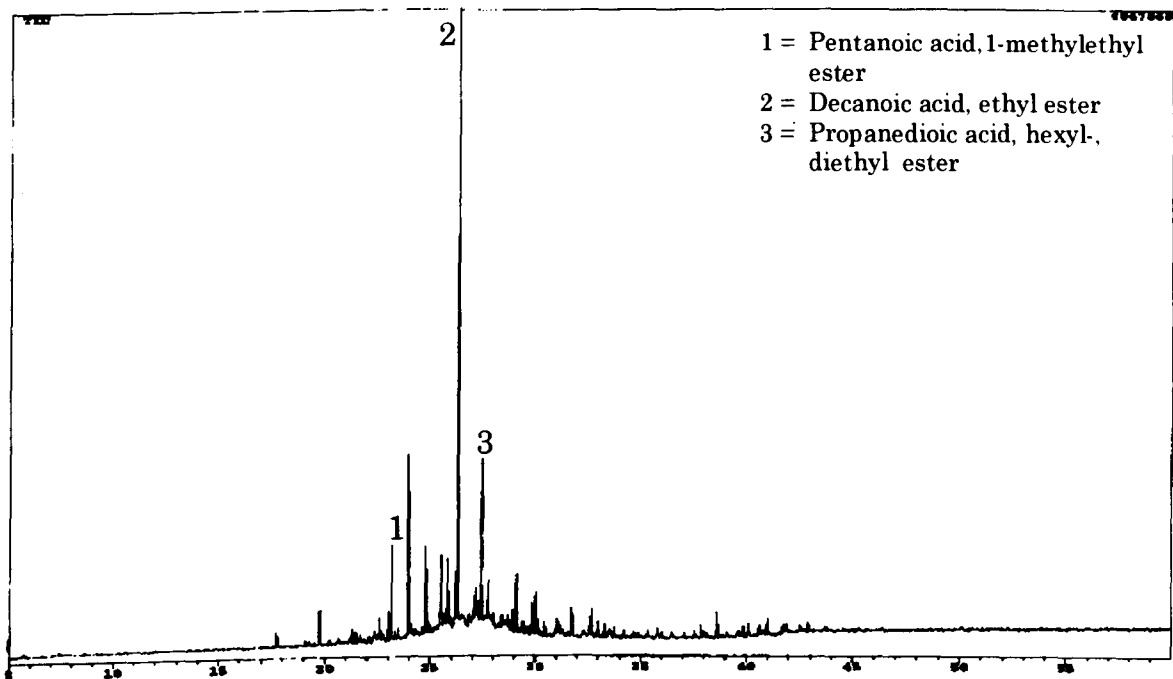
(a) SSWK04 (0-10cm)



(b) SSWK04 (10-20cm)

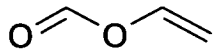
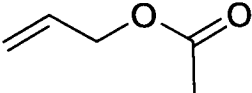
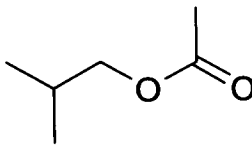
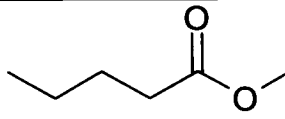
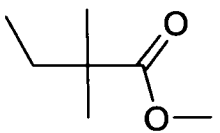
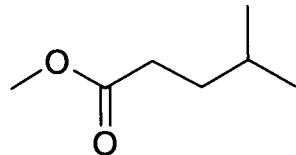
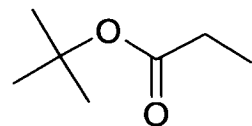


(c) SSWK06 (0-10cm)

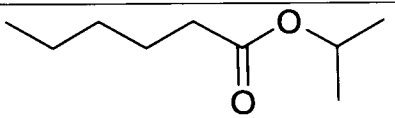
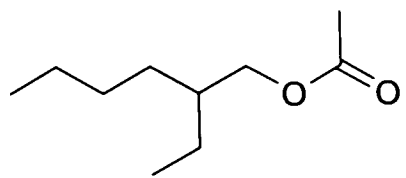
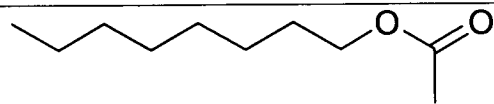
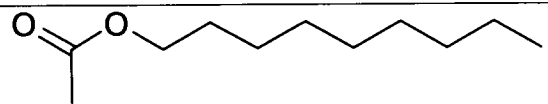
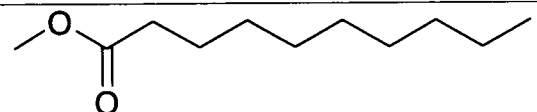
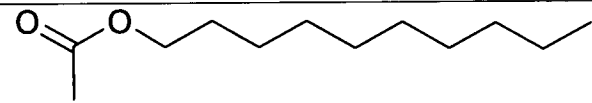
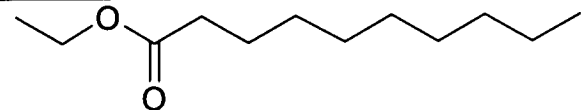


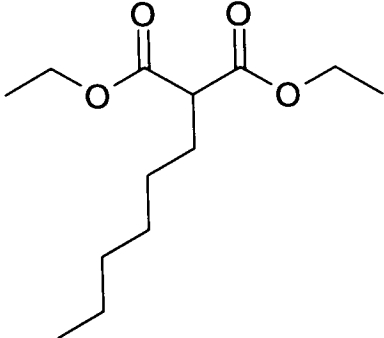
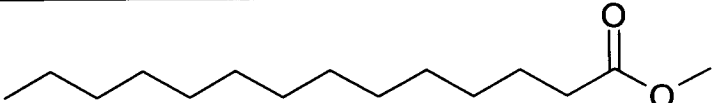
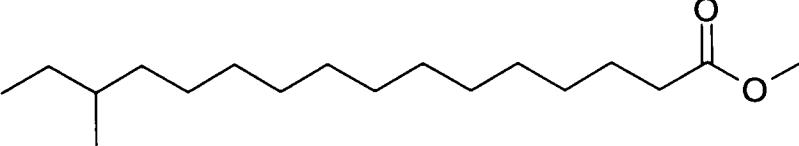
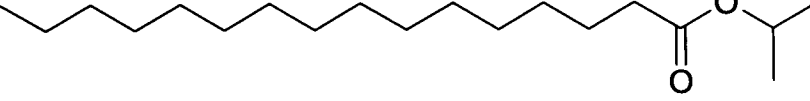
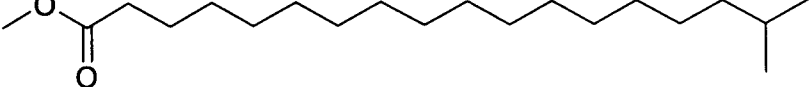
(d) SSWK06 (10-20cm)

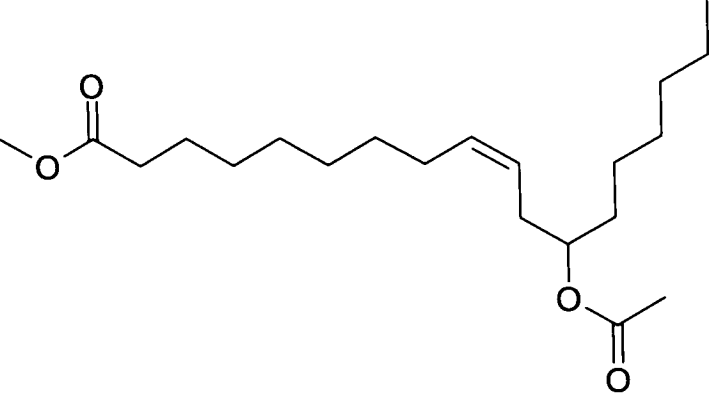
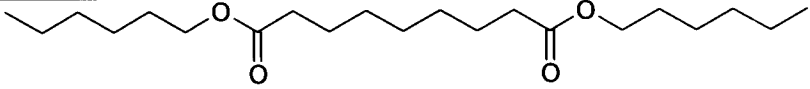
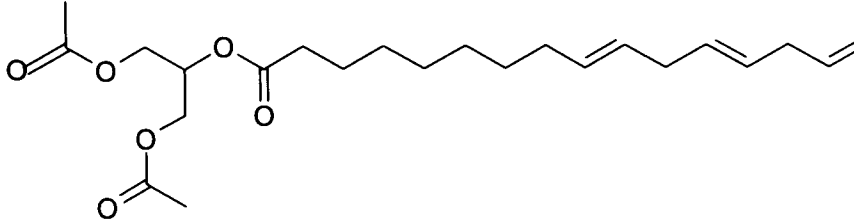
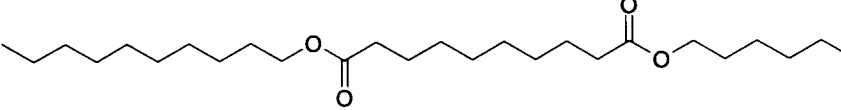
Appendix 5: Fatty acid methyl esters structures

Compounds	Molecular Formula	Molecular weight (g/mol)	Structure
Formic acid, ethenyl ester	$C_3H_4O_2$	72	
Acetic acid, 2-propenyl ester	$C_5H_8O_2$	100	
Acetic acid, 2-methylpropyl ester	$C_6H_{12}O_2$	116	
Pentanoic acid, methyl ester	$C_6H_{12}O_2$	116	
Butanoic acid, 2,2-dimethyl-, methyl ester	$C_7H_{14}O_2$	130	
Pentanoic acid, 4-methyl-, methyl ester	$C_7H_{14}O_2$	130	
Propanoic acid, 1,1-dimethylethyl ester	$C_7H_{14}O_2$	130	

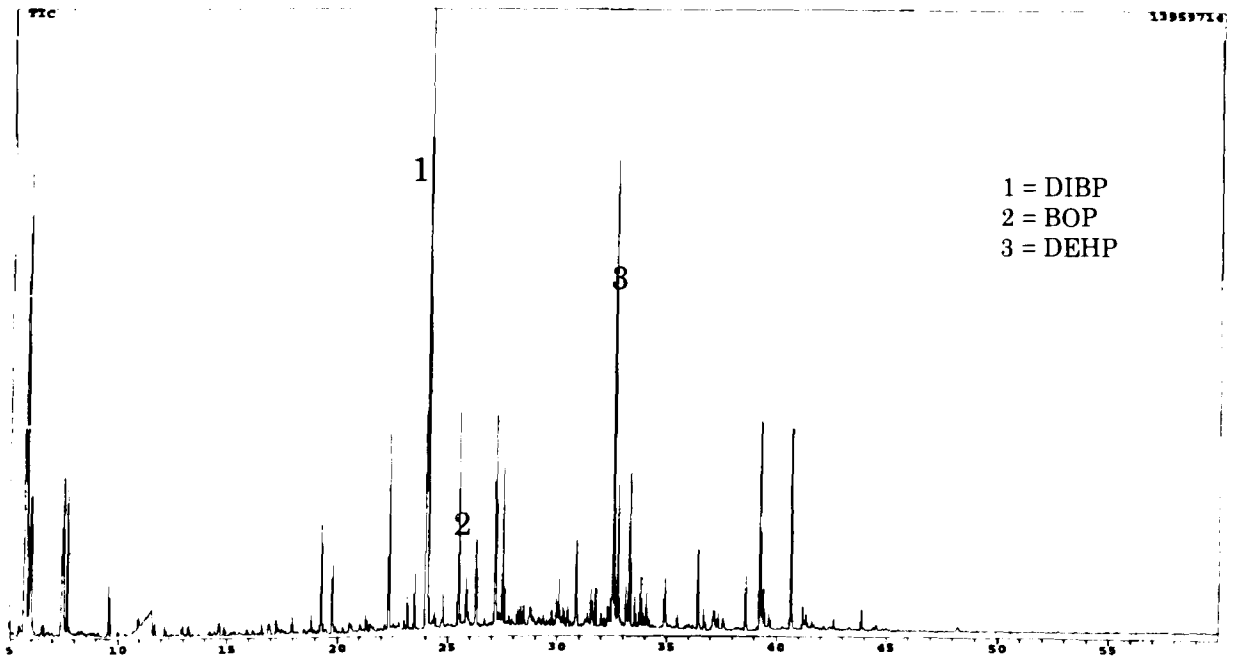
Compounds	Molecular Formula	Molecular weight (g/mol)	Structure
Propanoic acid, 2-methyl-, 1-methylethyl ester	$C_7H_{14}O_2$	130	
Acetic acid, 2-ethylbutyl ester	$C_8H_{16}O_2$	144	
Acetic acid, hexyl ester	$C_8H_{16}O_2$	144	
Hexanoic acid, 5-methyl-, methyl ester	$C_8H_{16}O_2$	144	
Pentanoic acid, 1-methylethyl ester	$C_8H_{16}O_2$	144	
Acetic acid, heptyl ester	$C_9H_{18}O_2$	158	
Heptanoic acid, ethyl ester	$C_9H_{18}O_2$	158	

Compounds	Molecular Formula	Molecular weight (g/mol)	Structure
Hexanoic acid, 1-methylethyl ester	$C_9H_{18}O_2$	158	
Acetic acid, 2-ethylhexyl ester	$C_{10}H_{20}O_2$	172	
Acetic acid, octyl ester	$C_{10}H_{20}O_2$	172	
Acetic acid, nonyl ester	$C_{11}H_{22}O_2$	186	
Decanoic acid, methyl ester	$C_{11}H_{22}O_2$	186	
Acetic acid, decyl ester	$C_{12}H_{24}O_2$	200	
Decanoic acid, ethyl ester	$C_{12}H_{24}O_2$	200	

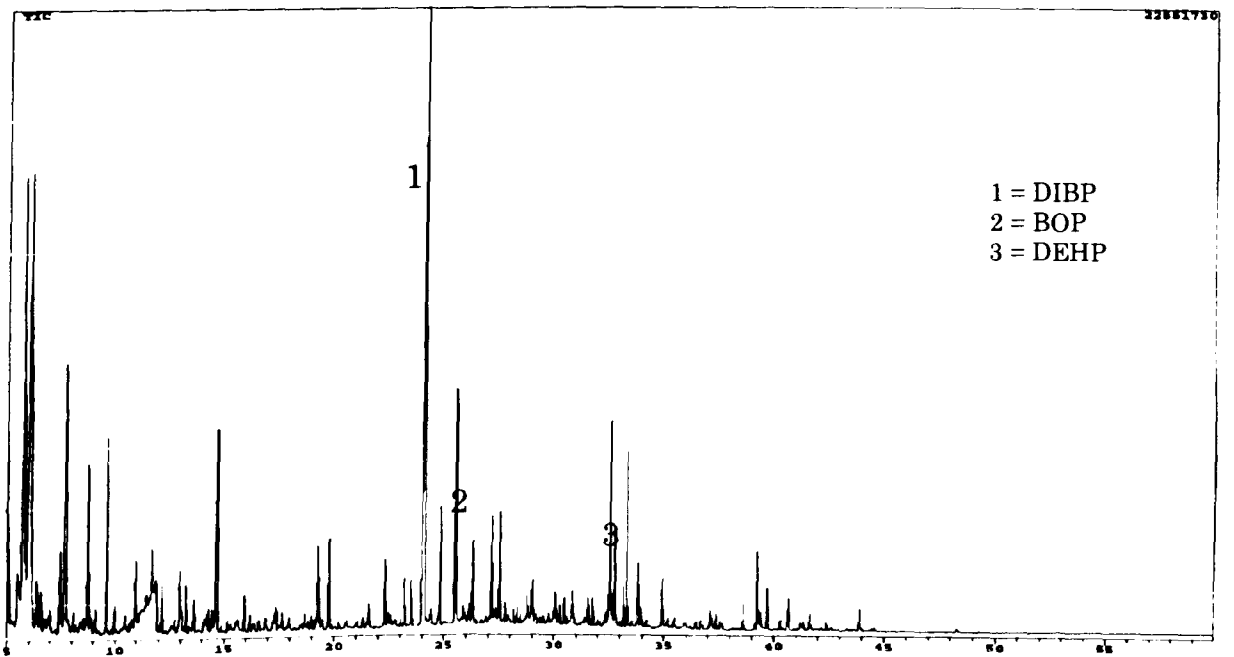
Compounds	Molecular Formula	Molecular weight (g/mol)	Structure
Propanedioic acid, hexyl-, diethyl ester	$C_{13}H_{24}O_4$	244	
Tetradecanoic acid, 12-methyl-, methyl ester	$C_{16}H_{32}O_2$	256	
Hexadecanoic acid, 14-methyl-, methyl ester	$C_{18}H_{36}O_2$	284	
Isopropyl Palmitate	$C_{19}H_{38}O_2$	298	
Octadecanoic acid, 17-methyl-, methyl ester	$C_{20}H_{40}O_2$	312	

Compounds	Molecular Formula	Molecular weight (g/mol)	Structure
9-Octadecenoic acid, 12-(acetyloxy)-, methyl ester, R-(Z)-	$C_{21}H_{38}O_4$	354	
Nonanedioic acid, dihexyl ester	$C_{21}H_{40}O_4$	356	
9, 12, 15-Octadecatrienoic acid, 2-(acetyloxy)-1-(acetyloxy) methyl ethyl ester, (Z,Z,Z)-	$C_{25}H_{40}O_6$	436	
Decanedioic acid, didecyl ester	$C_{30}H_{58}O_4$	482	

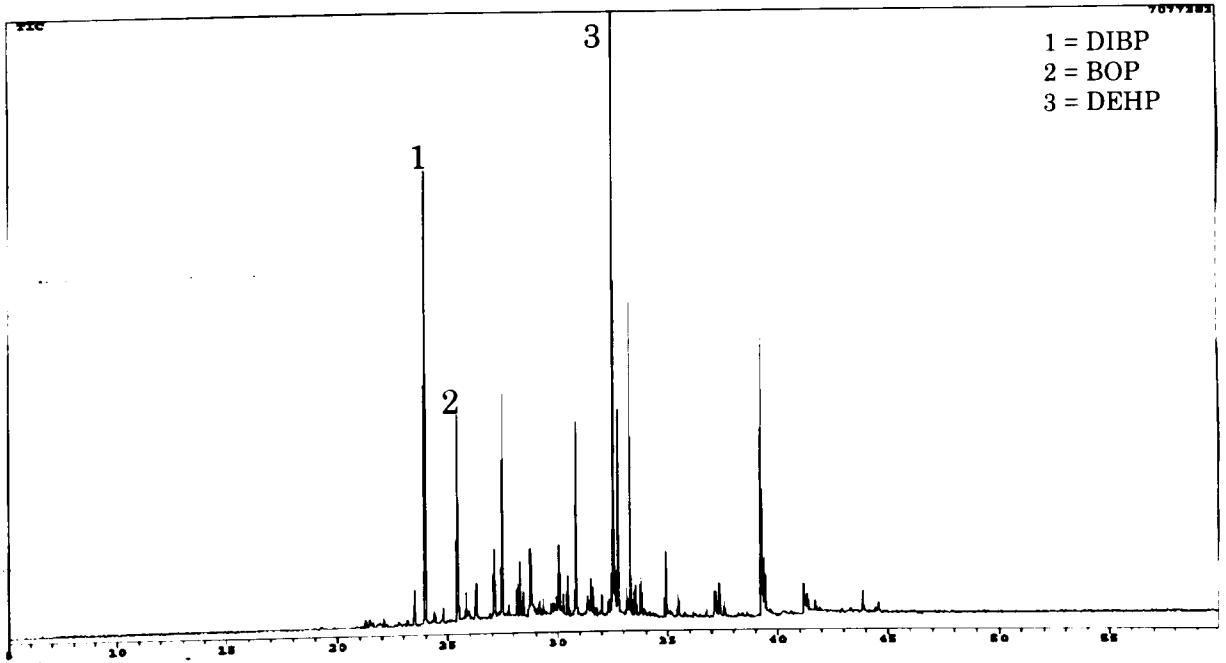
Appendix 6: GC/MS chromatograms of phthalate esters fractions in core sediments from Sarawak River



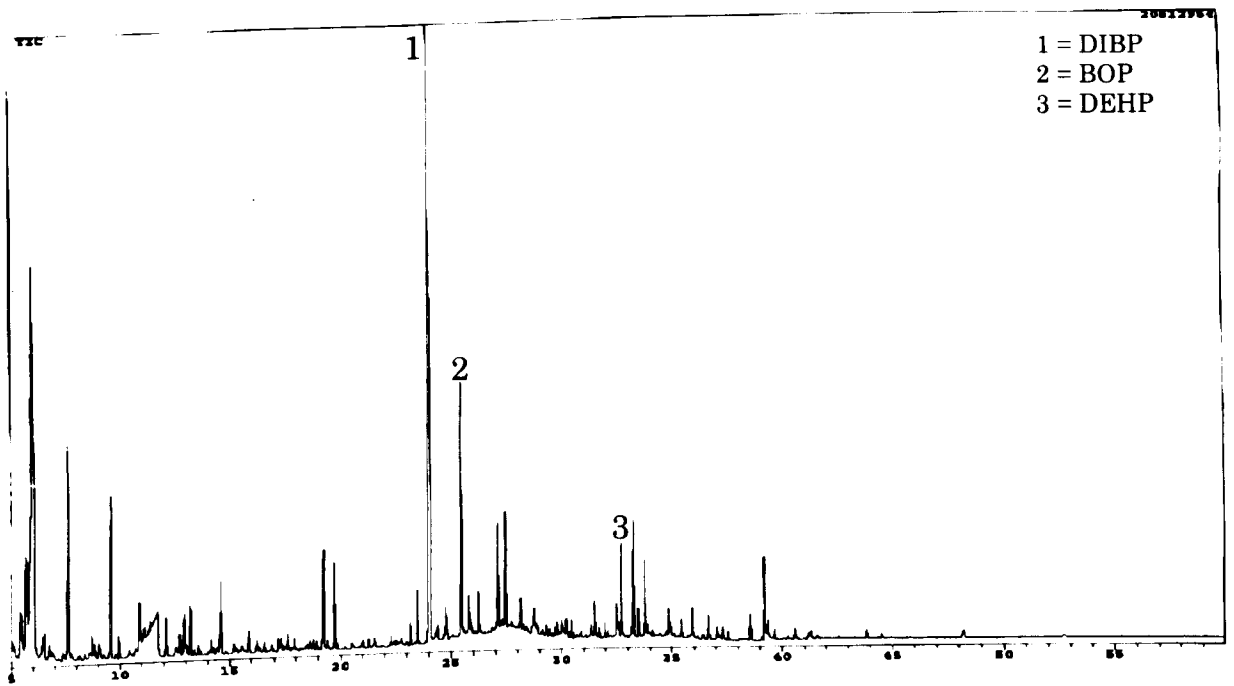
(a) SSWK04 (0-10cm)



(b) SSWK04 (10-20cm)

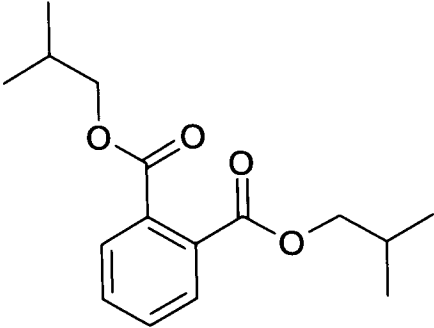
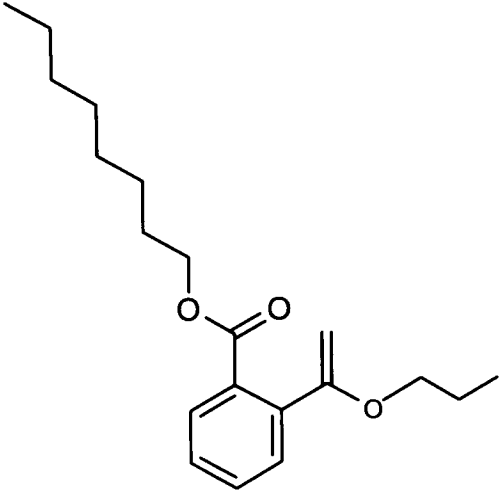


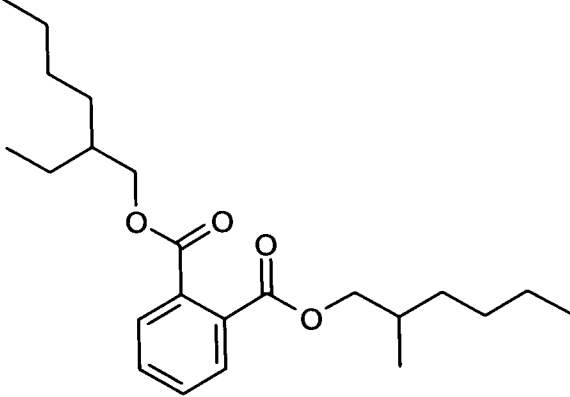
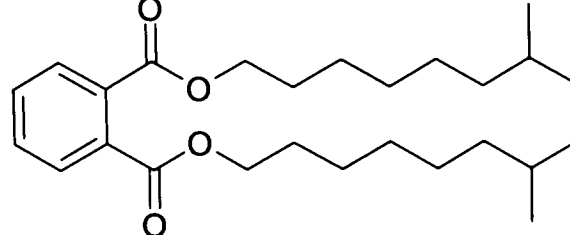
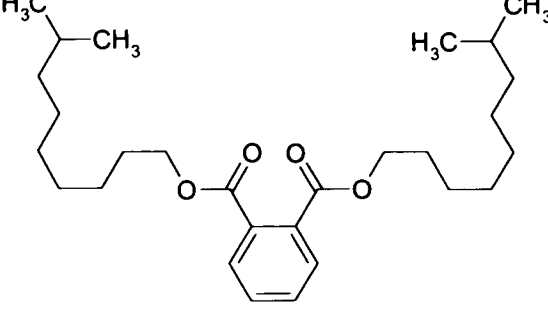
(c) SSWK06 (0-10cm)



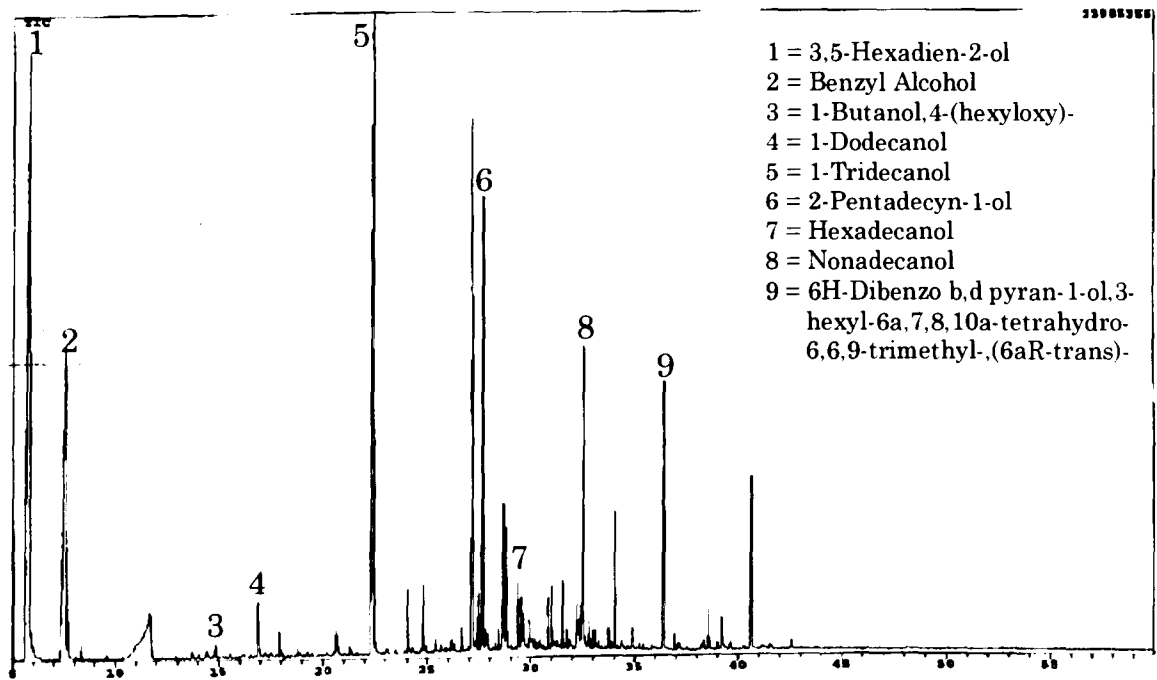
(d) SSWK06 (10-20cm)

Appendix 7: Phthalate esters structures

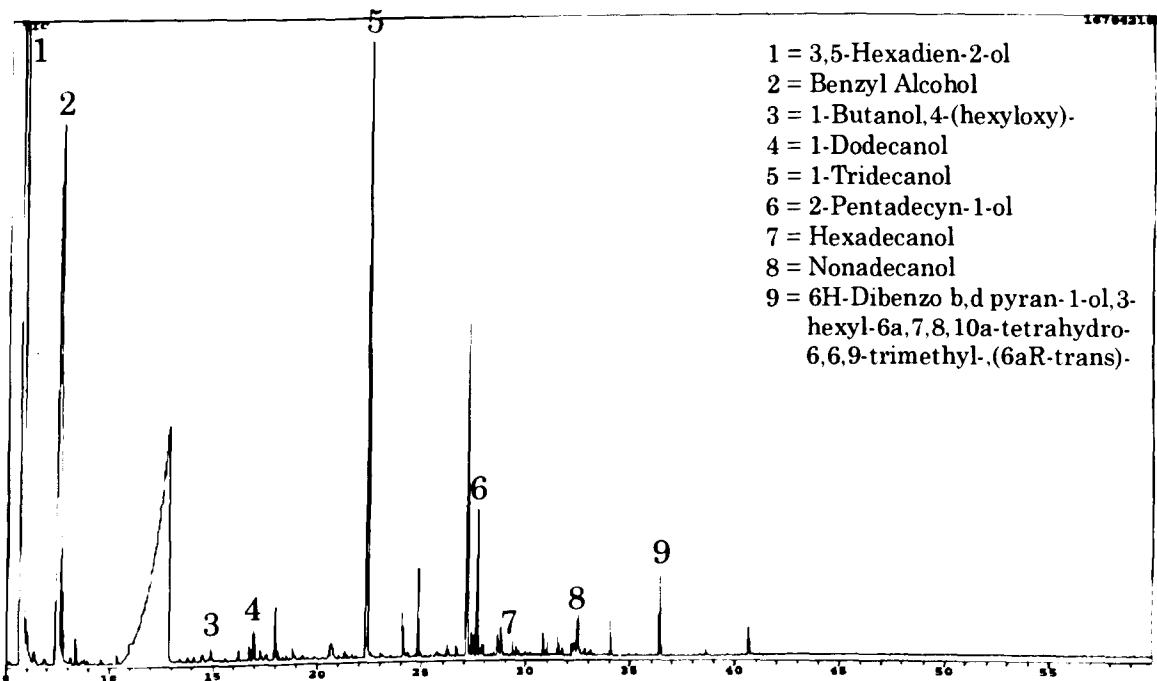
Compounds	Molecular Formula	Molecular weight (g/mol)	Structure
1,2-Benzenedicarboxylic acid, bis (2-methypropyl) ester (DIBP)	$C_{16}H_{22}O_4$	278	
1,2-Benzenedicarboxylic acid, butyl octyl ester (BOP)	$C_{20}H_{30}O_4$	334	

Compounds	Molecular Formula	Molecular weight (g/mol)	Structure
1,2-Benzenedicarboxylic acid, bis (2-ethylhexyl) ester (DEHP)	$C_{24}H_{38}O_4$	390	
1,2-Benzenedicarboxylic acid, diisononyl ester	$C_{26}H_{42}O_4$	418	
1,2-Benzenedicarboxylic acid, diisodecyl ester (DIDP)	$C_{28}H_{46}O_4$	446	

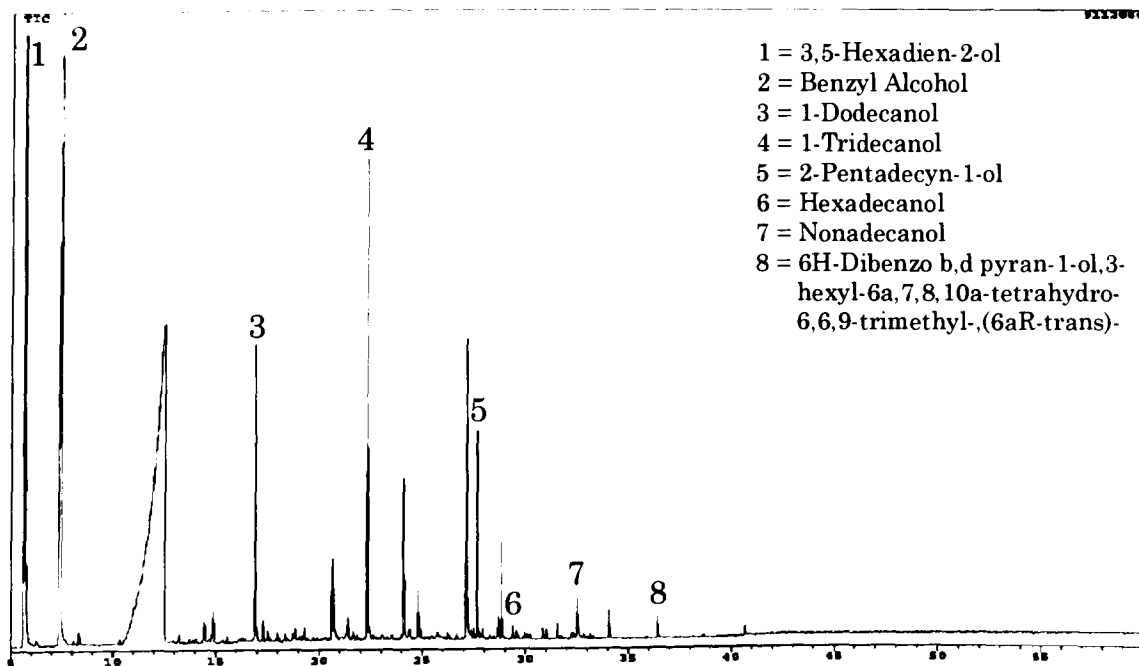
Appendix 8: GC/MS chromatograms for alcohols fractions in core sediments from Sarawak River



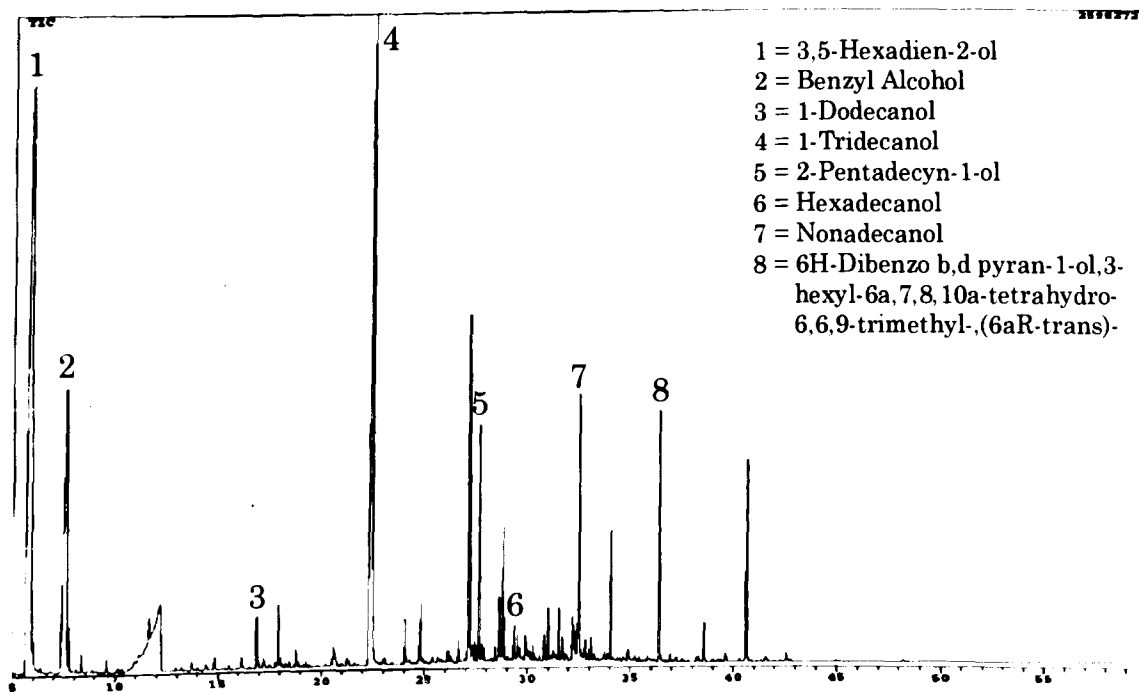
(a) SSWK04 (0-10cm)



(b) SSWK04 (10-20cm)

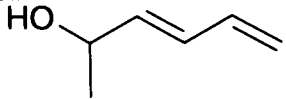
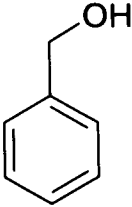
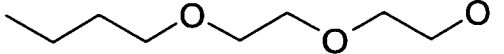
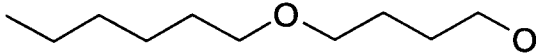
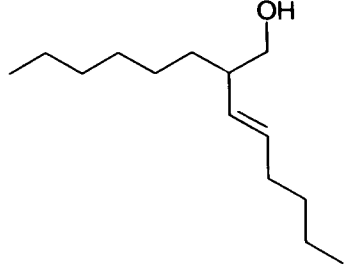


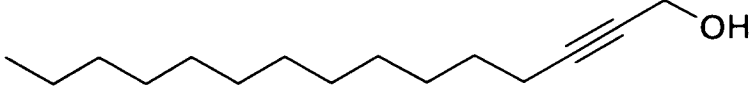
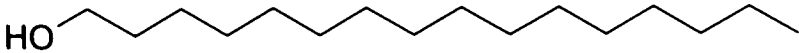
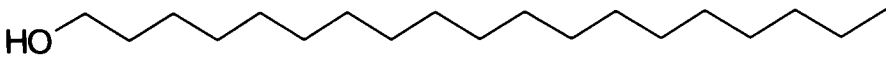
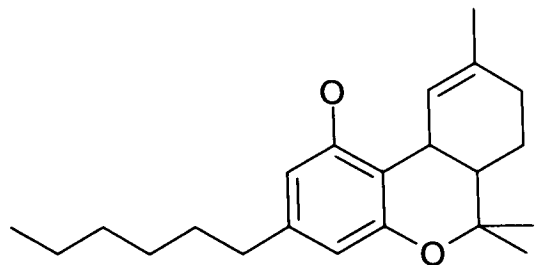
(c) SSWK06 (0-10cm)



(d) SSWK06 (10-20cm)

Appendix 9: Alcohols and sterols structures

Compounds	Molecular Formula	Molecular weight (g/mol)	Structure
3,5-Hexadien-2-ol	$C_6H_{10}O$	98	
Benzyl Alcohol	C_7H_8O	108	
Ethanol,2-(2-butoxyethoxy)-	$C_8H_{18}O_3$	162	
1-Butanol,4-(hexyloxy)-	$C_{10}H_{22}O_2$	174	
1-Dodecanol	$C_{12}H_{26}O$	186	
1-Tridecanol	$C_{13}H_{28}O$	200	
2-Hexyl-1-octanol	$C_{14}H_{30}O$	214	

Compounds	Molecular Formula	Molecular weight (g/mol)	Structure
2-Pentadecyn-1-ol	$C_{15}H_{28}O$	224	
Hexadecanol	$C_{16}H_{34}O$	242	
Nonadecanol	$C_{19}H_{40}O$	284	
6H-Dibenzo b,d pyran-1-ol,3-hexyl-6a,7,8,10a-tetrahydro-6,6,9-trimethyl-,(6aR-trans)-	$C_{22}H_{32}O_2$	328	
Stigmasterol	$C_{29}H_{48}O$	412	